1

The Potential of Zero Charge

Sergio Trasatti

Department of Physical Chemistry and Electrochemistry, University of Milan, 20133 Milan, Italy

Enn Lust

Institute of Physical Chemistry, University of Tartu, 2400 Tartu, Estonia

I. INTRODUCTORY CONCEPTS

1. Potential of Zero Charge

An electrode is customarily thought of as an ensemble of an electronic conductor (most frequently a metal) in contact with an ionic conductor (electrolyte solution, solid electrolyte, or molten salt). It is the change of charge carriers from ions to electrons across the interface that makes it possible to convert chemical into electrical energy (and vice versa) because of the vanishingly small solubility of metals in most solvents (apart from the instability of electrons in liquids). In some organic solvents the solubility of specific metals is such that they behave as sparingly soluble salts. In these cases a metal in solution is no longer an electrode; it is a system in chemical equilibrium and as such is unable to perform work.

As a metal is brought in contact with an electrolyte, various phenomena occur that result in the onset of an electric potential difference $(\phi^M - \phi^S)$, where M and S stand for metal and solution (the most usual electrolyte), respectively. The kind of phenomenon depends on the nature of the

Modern Aspects of Electrochemistry, Number 33, edited by Ralph E. White *et al.* Kluwer Academic / Plenum Publishers, New York, 1999.

interface. In this respect, two limiting categories are considered[1]: polarizable and nonpolarizable interfaces, respectively, depending on whether the phase boundary is permeable to charged species (of any kind, electrons or ions). These limiting cases describe *ideal* situations. Real interfaces behave intermediately, approaching one of the two best.

Thermodynamically, all metal/solution interfaces are nonpolarizable, i.e., they can exchange electrical charges freely across the phase boundary. It is the extreme slowness of these exchanges that turns a nonpolarizable into a polarizable interface. Therefore polarizable interfaces are a limiting case of nonpolarizable interfaces.[2]

(i) Nonpolarizable Interfaces

Nonpolarizable interfaces correspond to interfaces on which a reversible reaction takes place. An Ag wire in a solution containing Ag^+ ions is a classic example of a nonpolarizable interface. As the metal is immersed in solution, the following phenomena occur[3]: (1) solvent molecules at the metal surface are reoriented and polarized; (2) the electron cloud of the metal surface is redistributed (retreats or spills over); (3) Ag^+ ions cross the phase boundary (the net direction depends on the solution composition). At equilibrium, an electric potential drop occurs so that the following electrochemical equilibrium is established:

$$\tilde{\mu}^{M}_{Ag^+} = \tilde{\mu}^{S}_{Ag^+} \tag{1}$$

from which

$$(\phi^M - \phi^S) = \mu^{S}_{Ag^+} - \mu^{M}_{Ag^+} \tag{2}$$

Equation (2) is nothing but the well-known Nernst equation. It shows that $(\phi^M - \phi^S)$ is governed by the composition of the solution and cannot be changed without changing the latter.

The redistribution of charges leading to Eq. (1) involves both free charges and dipolar layers. Therefore $(\phi^M - \phi^S)$ can be split into two terms[4]:

$$(\phi^M - \phi^S) = g(\text{ion}) + g(\text{dip}) \tag{3}$$

where ion stands for free charges. Therefore, from Eq. (2):

$$\mu^{S}_{Ag^+} - \mu^{M}_{Ag^+} = g(\text{ion}) + g(\text{dip}) \tag{4}$$

In Eq. (4) the left-hand side (l.h.s.) expresses the thermodynamic driving force, while the right-hand side (r.h.s.) gives a structural, physical description of the interfacial region.[5]

Since $\mu^{M}_{Ag^+}$ is a constant while $\mu^{S}_{Ag^+}$ can be varied, there exists a composition of the solution at which the charge located at the interface vanishes. Under these circumstances $g(\text{ion}) = 0$ and

$$(\phi^{M} - \phi^{S})_0 = g(\text{dip})_0 \qquad (5)$$

Equation (5) shows that the electric potential drop consists only of dipolar contributions. The corresponding electrode potential is what is termed the *potential of zero charge* (pzc).

If the concentration of the metal ion is not negligible at the potential of zero charge, the electrode potential varies linearly with log c according to Eq. (2) and there is no distinctive sign of the situation where the charge at the interface vanishes. The Nernst approach is obviously unsuitable for defining the nature and the amount of the charge at an interface. If the concentration of the metal ion at the pzc is small or very small, the behavior of the interface becomes that of a polarizable electrode.

(ii) Polarizable Interfaces

Since a metal is immersed in a solution of an inactive electrolyte and no charge transfer across the interface is possible, the only phenomena occurring are the reorientation of solvent molecules at the metal surface and the redistribution of surface metal electrons.[6,7] The potential drop thus consists only of dipolar contributions, so that Eq. (5) applies. Therefore the potential of zero charge is directly established at such an interface.[3,8–10] Experimentally, difficulties may arise because of impurities and local microreactions,[9] but this is irrelevant from the ideal point of view.

(iii) Total and Surface Charge

Equation (5) tells us that the potential of zero charge is the same for the same metal under both nonpolarizable and polarizable conditions (provided no other effects are present). This is true from a structural point of view in that the presence of metal ions in solution only provides surface charging conditions. However, the charge referred to earlier as the one governing the magnitude of g(ion) is the charge physically residing on either side of the metal/solution interface. This is not the charge thermo-

dynamically defined by the Gibbs equation and therefore the one experimentally determinable. This aspect has been emphasized by Frumkin[2] and discussed several times in the literature.[1,8,11]

At constant p and T, the Gibbs adsorption equation for an electrode interface leads to the well-known Lippmann equation[12]:

$$q = -(\partial\gamma/\partial E)_{T,p,\mu} \tag{6}$$

where γ is the surface tension of the metal, E is the electrode potential, μ includes all independent components of the solution, and q is the electric charge per unit area of the interface. For an ideal polarizable electrode, q has a unique value for a given set of conditions.[1] It measures the electric charge residing on either side of the interface; in this case it is replaced by the symbol σ (surface charge density). On the metal it is determined by the surface excess or deficiency of electrons.

For an ideally polarizable electrode, q has a unique value for a given set of conditions.[1] For a nonpolarizable electrode, q does not have a unique value. It depends on the choice of the set of chemical potentials as independent variables[1] and does not coincide with the physical charge residing at the interface. This can be easily understood if one considers that q measures the electric charge that must be supplied to the electrode as its surface area is increased by a unit at a constant potential.[11] Clearly, with a nonpolarizable interface, only part of the charge exchanged between the phases remains localized at the interface to form the electrical double layer.

As an alternative view,[8,13] in the case of a metal in a solution containing ions of the same metal, the charge is defined by

$$(\partial\gamma/\partial E)_{\mu} = -q = -\Gamma_{M^+} \tag{7}$$

where Γ_{M^+} is the amount of metal ions that must be supplied to the solution to keep its composition constant. Thermodynamically this is the only charge that can be determined experimentally. q includes the free charge at the interface:

$$q = \sigma + A_{M^+} \tag{8}$$

where A_{M^+} (the symbol has been introduced by Frumkin)[11] is the fraction of charge that has crossed the interface moving from one phase to the other. This charge is not found at the interface.

A nonpolarizable interface behaves as a capacitor C and a resistor R in parallel; a polarizable interface responds as a pure capacitor. The higher the resistance R, the closer the behavior of the former to the latter. For $R \rightarrow \infty$, a nonpolarizable interface becomes polarizable. The condition $R \rightarrow \infty$ corresponds to $A_{M^+} \rightarrow 0$. This condition is met when the amount of M^+ in the null solution is negligibly small.

As a consequence of the thermodynamic analysis sketched above, it has been proposed[14] to call the potential at which $q = 0$, the *potential of zero total charge* (pztc), and the potential at which $q = \sigma = 0$, the *potentia of zerofree charge* (pzfc). The latter definition is rigorous only if phenomena of partial charge transfer in chemisorbed species are absent. A potential of zero total charge has been observed and measured only for the Pt group metals due to chemisorption of H atoms. In all other cases, the pzfc is usually observed and measured. The latter will be termed for simplicity *potential of zero charge* (pzc), and denoted by $E_{\sigma=0}$.

(iv) Importance of the Potential of Zero Charge

The most important quality of the pzc is that it contains information about the structural details of the metal/solution interface. In the absence of surface-active electrolytes, the pzc depends only on the nature of the metal and the solvent.[3,4,8] Conversely, the pztc is not exclusively relevant to the structure of the interface; this is truer the larger the value of A_{M^+} in Eq. (8) (or of A_i where i is the species to which the electrode is reversible; e.g., H^+ for the Pt group metals in the H adsorption region).

For a metal/solution interface, the pcz is as informative as the electron work function is for a metal/vacuum interface.[6,15] It is a property of the nature of the metal and of its surface structure (see later discussion); it is sensitive to the presence of impurities. Its value can be used to check the cleanliness and perfection of a metal surface. Its position determines the potential ranges of ionic and nonionic adsorption, and the region where double-layer effects are possible in electrode kinetics.[8,10,16]

Although the pzc contains all the essential structural information about the metal/solution interface, this information is not immediately apparent but must be appropriately decoded. This necessitates a description of $(\phi^M - \phi^S)_0$ in microscopic terms that require a minimum of model assumptions.[3] Another problem is that $(\phi^M - \phi^S)_0$ is not directly accessible to experimental determination. What is actually measured, usually de-

noted by $E_{\sigma=0}$, is $(\phi^M - \phi^S)_0$ plus additional terms.[17] A discussion of this point is necessary before examining the experimental data. Since the measured $E_{\sigma=0}$ is a quantity relative to a reference electrode, an analysis of the relationship between relative and "absolute" potential scales is also necessary.[5]

(v) Previous Reviews

The relevance of the pzc to the structure of the metal/solution interface and its relation to the metal/vacuum situation was first emphasized by Frumkin and Gorodetzkaya in 1928.[18] The first compilation of pzc values was prepared by Frumkin in 1933.[19]

The notion of pzc is absent in early textbooks. A table with pzc values for about 10 metals (but for only 5 are reliable values claimed) was given by Parsons in 1954 in the first volume of this series.[4] After a more complete attempt by Frumkin in 1965[20] to compare $E_{\sigma=0}$ and work function, extensive work on pzc was reported by Perkins and Andersen[9] in this series and by Frumkin *et al.*[8] in another series. Compilations of pzc values were also made by Campanella,[21] Trasatti,[6,22] Frumkin *et al.*,[23] and Frumkin and Petrii[14] up to 1979. A book by Frumkin[10] devoted entirely to the potential of zero charge was published posthumously in 1979.

It appears that no comprehensive review was published after Perkins and Andersen's work. Nevertheless, articles devoted to particular aspects have been written. Thus collections of data were compiled by Hamelin *et al.*[24] for single-crystal face electrodes (Cu, Ag, Au, Sn, Pb, Zn, and Bi) in 1983, by Trasatti[25,26] in 1986 and 1992, by Khrushcheva and Kazarinov[27] in 1986, and by Lust *et al.*[28] in 1996 for Bi, Sb, and Cd.

Owing to the rapid development of the field from an experimental point of view, and the persistence of discussions on some of the aspects outlined above, a chapter on the pzc that includes a discussion of the relation between the electrochemical and the ultrahigh vacuum (UHV) situation in reference to the conditions at the pzc seems timely. This review of the literature will not be exhaustive but selective, taking into account the compilations already existing. In any case, the objective is to evaluate the existing data in order to recommend the most reliable. Finally, the data on pzc will be discussed in comparison with electron work function values. The role and significance of work functions in electrochemistry were discussed by Trasatti[6] in 1976.

2. Electrode Potentials and Energy Scales

(i) Measurability of $(\phi^M - \phi^S)_0$

Drops in electric potential between dissimilar phases are not experimentally measurable.[29] This aspect was discussed at length in the literature between the early 1970s and 1990. The discussion was about what is actually measured as electrode potentials are measured. Now a general consensus seems to have been achieved. While readers are referred to the original literature,[3,5,15,17,29–31] the main conclusions are summarized here.

The measurement of $(\phi^M - \phi^S)$ requires that the two terminals of the measuring instruments be connected to M and to S, respectively. While the former is a metal–metal contact, the latter implies immersion of the metal of the terminal (e.g., Cu) in solution. Thus a new interface (a new electrode) is created. Instead of $(\phi^M - \phi^S)$, the sum of three $\Delta\phi$ is thus measured[29]:

$$(\phi^{Cu} - \phi^M) + (\phi^M - \phi^S) + (\phi^S - \phi'^{Cu}) \tag{9}$$

where ϕ'^{Cu} differs from ϕ^{Cu} for the electrical state of the metal. Since Cu and M are in electronic equilibrium $(\tilde{\mu}_e^{Cu} = \tilde{\mu}_e^M)$:

$$(\phi^{Cu} - \phi^M) = (\mu_e^{Cu} - \mu_e^M)/F \tag{10}$$

From Eqs. (9) and (10):

$$\Delta E = E^M - E^{Cu} = [(\phi^M - \phi^S) - \mu_e^M/F] - [(\phi^{Cu} - \phi^S) - \mu_e^{Cu}/F] \tag{11}$$

Equation (11) shows that instead of $(\phi^M - \phi^S)$, or a relative value of $(\phi^M - \phi^S)$, a difference in electronic energy (expressed in volts) is actually measured. This is perfectly reasonable since electrons move in an external circuit because their total energy (and not only the electrical part) is different in the two electrodes.

A more general approach has been recently provided by Trasatti.[32,33] Let us consider the cell illustrated in Fig. 1(a), whose potential difference is ΔE:

$$\text{Cu} \mid \text{M} \mid \text{S} \mid \text{R} \mid \text{Cu}' \tag{12a}$$

If M and R are in the same solvent S containing only an inert, surface-inactive supporting electrolyte, ΔE equals the difference in the potentials of zero charge between the two metals:

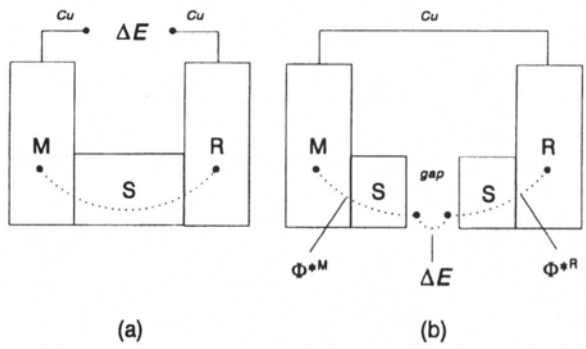

Figure 1. Sketch of an electrochemical cell whose equilibrium (open circuit) potential difference is ΔE. (a) Conventional configuration and (b) short-circuited configuration with an air gap. M and R are the electrodes, S is the solvent (electrolyte solution). Cu indicates the cables connecting the two electrodes to a measuring instrument (or to each other). Φ^* is the work to transfer an electron from M (or R) to the exterior of the phase through S.

$$\Delta E = E^{M}_{\sigma=0} - E^{R}_{\sigma=0} \tag{13}$$

Cu is the metal constituting the cables connecting the terminals of the cell to the measuring instrument. The work to bring an electron from M to R is equal to $e\Delta E$ along the external circuit and includes the contributions of the two electrodes [Eq. (13)] which, however, cannot be measured separately if only cell (a) is used.

Actually, since the terminals are of the same metal, we have

$$\Delta E = (\tilde{\mu}_e^{Cu} - \tilde{\mu}_e^{Cu'})/F = \psi^{Cu'} - \psi^{Cu} \tag{14}$$

i.e., the measured potential difference equals the Volta potential difference between the two terminals. Therefore

$$\Delta E = (\psi^{Cu'} - \psi^{M}) + (\psi^{M} - \psi^{S}) + (\psi^{S} - \psi^{R}) + (\psi^{R} - \psi^{Cu}) \tag{15}$$

Let us consider now the same cell but in a different configuration, shown in Fig. 1(b):

$$S \mid M \mid Cu \mid R \mid S \tag{12b}$$

If the two Cu cables are short circuited while the cell is broken into two parts by splitting the liquid phase, it can easily be proved that the same ΔE as for cell (12a) is measured as a contact potential difference (cpd) between the two solutions. In fact

$$\Delta E = (\psi^S - \psi^R) + (\psi^R - \psi^{Cu}) + (\psi^{Cu} - \psi^M) + (\psi^M - \psi^S) \qquad (16)$$

Since $\Delta\psi$ depends only on the nature of the phases in contact and not on their actual electrical state, ΔE in Eq. (16) must equal ΔE in Eq. (15). However, in the cell of Fig. l(b) it is readily seen that the work to bring an electron from M to R is zero, so that

$$e\Delta E = \Phi^{*M} - \Phi^{*R} \qquad (17)$$

where Φ^* is the work to extract an electron from the metal across the solvent. Therefore Φ^* measures the energy of the electrons in the metal constituting the electrode.[34]

Equation (17) is similar to Eq. (13); in both cases the outcome is that ΔE measures a difference in electronic energy. However, Eq. (17) is more complete since it consists of measurable quantities while Eq. (13) is incomplete for a constant term, which turns out to be dropped. This is a consequence of the approach used to separate ΔE into the various components.

(ii) Components of the Electrode Potential

Equation (17) expresses the cell potential difference in a general way, irrespective of the nature of the electrodes. Therefore, it is in particular valid also for nonpolarizable electrodes. However, since Φ^* can be better envisaged in terms of interfacial structure, only polarizable electrodes at their potential of zero charge will be discussed here. It was shown earlier that the structural details are not different for nonpolarizable electrodes, provided no specifically adsorbed species are present.

As a metal comes in contact with a liquid polar phase (a solvent), the situation can be depicted as in Fig. 2. The electron work function will be modified by $\Delta\Phi$ so that

$$\Phi^* = \Phi + \Delta\Phi \qquad (18)$$

where Φ is the electron work function in UHV (metal/vacuum) conditions. $\Delta\Phi$ is a contact potential difference between M and S:

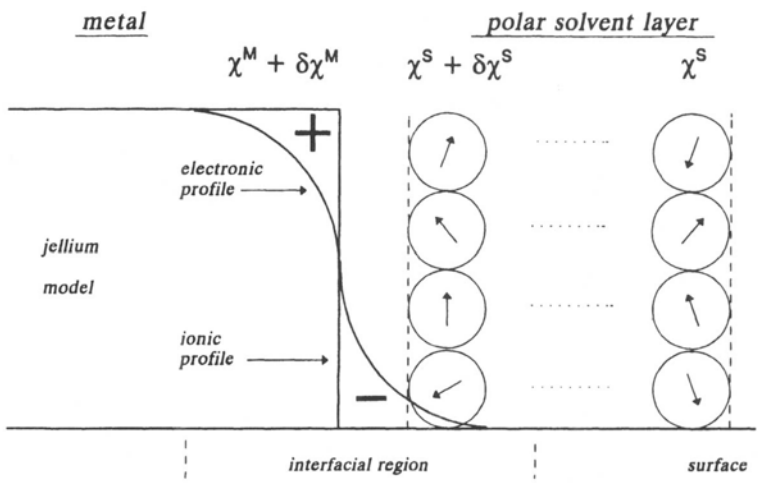

Figure 2. Sketch of an uncharged metal surface (simulated by the jellium model) covered by a macroscopic solvent layer, showing the components of the electric potential drop. $\chi^M + \delta\chi^M$ is the surface potential of the metal modified by the solvent layer; $\chi^S + \delta\chi^S$ is the surface potential of the solvent modified by the contact with the metal; χ^S is the unmodified surface potential of the solvent layer at the external surface.

$$\Phi^* = \Phi + e(\psi^M - \psi^S) \tag{19}$$

thus $\Delta\Phi$ is a measurable quantity.

According to Fig. 2, as M comes in contact with S,[3,4] the electron distribution at the metal surface (giving the surface potential χ^M) will be perturbed ($\delta\chi^M$). The same is the case for the surface orientation of solvent molecules ($\chi^S + \delta\chi^S$). In addition, a potential drop has to be taken into account at the free surface of the liquid layer toward the air (χ^S). On the whole, the variation of the electron work function (if no charge separation takes place as assumed at the pzc of a polarizable electrode) will measure the extent of perturbation at the surfaces of the two phases, i.e.,

$$\Delta\Phi = e(\psi^M - \psi^S) = e(\delta\chi^M + \delta\chi^S) \tag{20}$$

where $\delta\chi^M$ and $\delta\chi^S$ depend on the nature of S and M, respectively. In addition, they are in principle, especially $\delta\chi^S$, sensitive to the presence of free charges. Thus, for a metal at a different potential from $E_{\sigma=0}$, $\Delta\Phi$ includes one more term:

$$\Delta\Phi_\sigma = e(\psi^M - \psi^S)_\sigma = e(\delta\chi^M + \delta\chi^S)_\sigma + g(\text{ion}) \qquad (21)$$

where the subscript σ is used to denote a charged interface. $g(\text{ion}) = 0$ as $\sigma = 0$. Clearly, contact potential differences for charged electrodes do not possess any straightforward structural character in view of the non-separability of the two terms on the r.h.s. of Eq. (21).

(iii) Potentials in the UHV Scale

From Eqs. (13) and (17) it is readily evident that

$$eE^M_{\sigma=0} \text{ vs. UHV} = \Phi^{*M} \qquad (22)$$

Equation (22) shows that since electrode potentials measure electronic energies, their zero level is the same as that for electronic energy. Equation (22) expresses the possibility of a comparison between electrochemical and UHV quantities. Since the definition of Φ is[6] "the *minimum* work to extract an electron from the Fermi level of a metal in a vacuum," the definition of electrode potential in the UHV scale is "the minimum work to extract an electron from the Fermi level of a metal covered by a (macroscopic) layer of solvent."

While there are no problems in the definition of the configuration leading to Φ^*, difficulties are encountered in the procedure to reproduce the electrochemical situation. In fact, Eq. (17) has meaning only if the M/S interface has exactly the same structure during the measurement of E (relative to a reference electrode–electrochemical configuration) as well as during the measurement of Φ^*.

For correlating relative $E_{\sigma=0}$ values with values in the UHV scale (Φ^* values), two quantities must be known: Φ and $\Delta\Phi$. Contact potential measurements at metal/solution interfaces can be measured.[4] In that case the interfacial structure is exactly that in the electrochemical situation (bulk liquid phase, room temperature). However, Φ to convert E into Φ^* must be independently known. It may happen that the metal surface state is not exactly the same during the measurements of Φ and $\Delta\Phi$.

On the other hand, surface physicists often measure Φ^* which represents the work function of metals as modified by adsorption of polar (water) molecules.[35–39] What they are measuring (although they may not realize it) is precisely the potential of zero charge of the given metal in the UHV scale. The value of Φ is exactly known in that case, but the relevance of the value of $\Delta\Phi$ is in doubt.[32,33] In fact, only a few layers of a solvent

on a metal surface may not reproduce the actual electrochemical situation in which the liquid phase possesses the properties of a bulk phase. Moreover, Φ^* measurements are customarily carried out at very low temperatures (150–200 K) at which the interfacial structure may differ from the actual one at an electrode. Finally, UHV conditions of measurement ensure neutrality of the interface, not of the metal surface, as required by the electrochemical situation. In a case of partial charge transfer, the UHV configuration may include an additional term, or one differing in some way from that at the actual electrode interface.

A third experimental configuration was proposed by Kolb and Hansen[40]: emersed electrodes. If an electrode is emersed from a solution while the control of the potential is maintained, the solvent layer dragged off with the metal (Fig. 3) would reproduce UHV conditions, but with potential control and at room temperature, as in the actual electrode situation. This appears to be the most convenient configuration for measuring Φ^*. However, there are doubts that the solvent layer retains the properties of a bulk phase. It has in fact been demonstrated[41] that a contact potential difference exists between an electrode in the emersed state and the same electrode regularly immersed in solution.

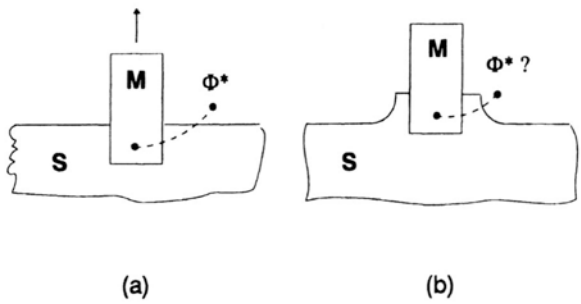

Figure 3. Sketch of an emersed electrode. M is the metal, S is the solvent (electrolyte solution). (a) Φ^* is the work to extract an electron from M through S. (b) The emersed electrode drags a liquid layer with it, through which the measurement of Φ^* is apparently the same as in (a). The question mark is meant to cast doubts on that.

(iv) $E^\circ(H^+/H_2)$ *versus UHV*

Electrode potentials are customarily tabulated on the standard hydrogen electrode (SHE) scale (although the SHE is never actually used experimentally because it is inconvenient in many respects). Therefore, conversion of potentials into the UHV scale requires the determination of $E^\circ(H^+/H_2)$ vs. UHV. According to the concepts developed above, such a potential would measure the energy of electrons in the Pt wire of the hydrogen electrode, modified by the contact with the solution.

Table 1 shows that two ranges of experimental values are available for the SHE in the UHV scale: one, determined with higher accuracy,[5] is 4.44 V (4.44 eV is the energy of electrons in the metal of the electrode), and the other is close to 4.8 V. It is intriguing that the first value has been obtained with an Hg jet electrode in two different laboratories[42,43] about 30 years apart with a reproducibility of better than 3 mV. In practice, $\Delta\Phi$ has been measured between Hg and a suitable solution. All of the uncertainty comes[5] from the value of the work function of Hg taken from the literature as **4.50 ± 0.02 eV.** The uncertainty concerns[44] in particular whether the Hg surface in the stream is really bare, or if it is contaminated by the atmosphere (water vapor and oxygen).

Experiments carried out by Hansen *et al.*[45,46] have demonstrated that there should be no effect of the atmosphere on the state of the Hg surface, which is thus to be regarded as clean. However, it is remarked that no

Table 1
Experimental Values of the Potential of the Standard Hydrogen Electrode in the UHV Scale

$E^\circ(H^+/H_2)$ vs. UHV/V	References
4.44 ± 0.02	42
4.73 ± 0.05	44
4.7	40
4.44 ± 0.02	43
4.85	47
4.456 ± 0.025	45
(4.7)[a]	49
(4.9)[a]	48

[a]Estimated indirectly.

recent Φ value has been reported for Hg, which is presumably related to problems of metal evaporation under UHV conditions.

A value close to 4.8 V has been obtained in four different laboratories using quite different approaches (solid metal/solution $\Delta\psi$,[44] emersed electrodes,[40,47] work function changes[48]), and is apparently supported by indirect estimates of electronic energy levels. The consistency of results around 4.8 V suggests that the value of 4.44 V is probably due to the value of Φ not reflecting the actual state of an Hg jet or pool. According to some authors,[44] the actual value of Φ for Hg in the stream should be 4.8 V in that the metal surface would be oxidized.

It seems hard to support the above hypothesis on the basis of work function measurements for Hg in the presence of residual gases. Adsorption of water indeed reduces the work function and this is also the case with inert gases. There remains the possibility of surface oxidation by residual oxygen, but the values of $\Delta\psi$ measured with the Hg stream have been shown[42,43] to be stable even in the presence of O_2 impurities provided the gas flows rapidly, as was the case during the experiments. The same conclusion has been reached recently by measuring the work function of Hg in ambient gas.[46]

On the other hand, potential measurements at the free surface of purified water have shown[50] that the value for a flowing surface differs by about 0.3 V from that for a quiescent surface, as a result of adsorption of surface-active residual impurities in the solution (probably also coming from the gas phase). Since emersed electrodes drag off the surface layer of the solution as they come out of the liquid phase, the liquid layer attached to emersed solid surfaces might also be contaminated.

It is intriguing that upon emersion the value of $\Delta\Phi$ changes up to about 0.3 V compared with the immersed state.[41] This has been attributed[42,51] to the different structure of the liquid interfacial layer in the two conditions. In particular, the air/solvent interface is missing at an emersed electrode because of the thinness of the solvent layer, across which the molecular orientation is probably dominated by the interaction with the metal surface.

The situation believed to exist at an emersed electrode is sketched in Fig. 4. It is seen that while $\Delta\Phi$ in the immersed state is given by Eq. (20) rewritten as

$$\Delta\Phi = e[\delta\chi^{M} + g^{S}(\text{dip}) + \chi^{S}] \qquad (23)$$

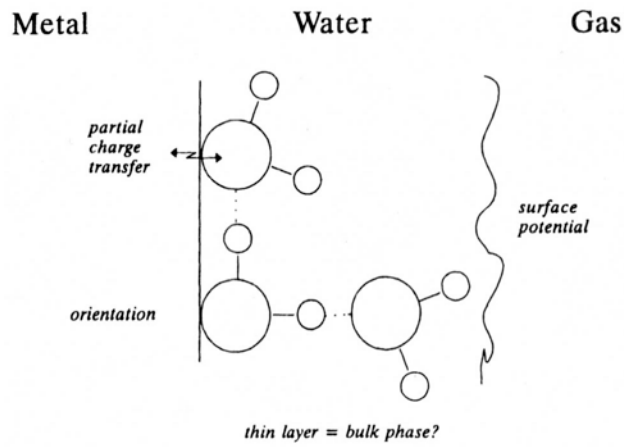

Figure 4. Sketch to illustrate the situation believed to exist at a metal surface upon adsorption of water from the gas phase (or at the surface of an emersed electrode). In particular, the layer thickness is so small that the orientation of solvent molecules at the external surface is strongly affected by the orientation at the internal surface.

where $g^{S}(\mathrm{dip})$ is the surface potential contribution due to oriented solvent dipoles at the metal surface, $\Delta\Phi$ in the emersed state can be tentatively written as

$$\Delta\Phi = e[\delta\chi^{M} + g^{S}(\mathrm{dip}) + g'^{S}(\mathrm{dip})] \qquad (24)$$

where χ^{S} is the dipole contribution at the unperturbed solvent surface toward air; its value is estimated[7] to be positive around 0.1 V. $g'^{S}(\mathrm{dip})$ is the dipole contribution beyond the normal surface layer. In view of the thickness of the solvent layer, the orientation in these layers is probably the same as that in the surface layer adjacent to the metal, which is believed to make a negative contribution.[22] Therefore, assuming $\delta\chi^{M}$ and $g^{S}(\mathrm{dip})$ do not change in the two cases, the difference in work function between immersed and emersed states amounts to $[\chi^{S} - g'^{S}(\mathrm{dip})]$. The experiments carried out by Samec *et al.*[41] provide unquestionable proof that emersed electrodes are not the most appropriate tool for determining potentials in a UHV scale.

There remains the estimated value of $E^{\circ}(H^{+}/H_2)$ vs. UHV based on binding energies for image potential-induced surface states,[49] which is,

however, difficult to assess both quantitatively and qualitatively. For the above reasons, for the time being the value of 4.44 V is preferred here and will be used in what follows. This value, however, does not convince most surface physicists, as mentioned earlier. The debate will not be completely terminated as long as a new determination of work function for Hg is carried out under conditions believed to be the most appropriate for such a system. A further contribution to the discussion will be provided in the following section on the basis of indirect evidence.

(v) Mercury: A Reference Surface

Although liquid Hg would never be used as a reference (model) surface in surface physics because its liquid state and high vapor pressure do not allow appropriate UHV conditions, this metal turns out to be a reference surface in electrochemistry for precisely the same reasons: reproducibility of the surface state, easy cleaning of its surface, and the possibility of measuring the surface tension (surface thermodynamic conditions). In particular, the establishment of a UHV scale for potentials is at present based on data obtained for Hg.

The contact potential difference between Hg and water (actually a dilute aqueous solution of a surface-inactive electrolyte) has been measured[42,43] to be –0.25 V. The negative sign means that the work function of Hg decreases upon contact with water. Since **4.50(±0.02) eV** is the currently accepted[5] value for Φ of Hg, the value of Φ^* for the uncharged metal (at the potential of zero charge) is 4.25 eV.

There are no direct, reliable measurements of Φ^* based upon adsorption of water from the gas phase. Therefore, 4.25 eV applies to a macroscopic water layer as in the electrochemical configuration. The decrease in Φ upon water adsorption is a general occurrence with metals. The value of $\Delta\Phi$ observed with Hg is the lowest among those available in the literature.[35,36] With reference to Eq. (20), this means that the perturbations of the surfaces of the two phases are small for the Hg/water contact. In other words, the interaction between Hg and water is weak (hydrophobic).

The decrease in Φ implies a negative value of $\delta\chi^M$ or $\delta\chi^S$, or both. No attempt will be made here to separate the two contributions: this has been done elsewhere.[6,7,25,52] We keep here to the measured value. What we can say is that the modifications occurring in the surface regions of the two phases are such as to decrease Φ and that even larger modifications are observed with other metals, always in the negative direction. Since χ^S

for water is estimated to be around 0.1 V, a negative $\delta\chi^S$ implies a reorientation leading to a less positive value. A negative value of $\delta\chi^M$ (the electronic theory of metals tells us[3] that the spillover of electrons produces positive χ^M, even for solid surfaces) implies that the electron tail contracts as the metal comes in contact with the solvent.

The potential-of-zero charge of Hg in water is known with high precision, i.e.,[53] **−0.192(±0.001)V** vs. saturated calomel electrode (SHE). It can be converted to the UHV scale if Φ^* for the SHE is known. Actually, the value of 4.44 V vs. UHV for SHE has been derived[5] from

$$E^\circ(H^+/H_2) \text{ vs. UHV} = E_{\sigma=0}(\text{Hg}) \text{ vs. UHV} - E_{\sigma=0}(\text{Hg}) \text{ vs. SHE} \quad (25)$$

Conversely, let us examine the situation from a different point of view. Let us suppose that the UHV value for SHE is about 4.8 V. In this case the UHV value for $E_{\sigma=0}$ of Hg would work out to be 4.61 V. This would measure Φ^*, the work function of Hg in contact with water. If Φ for clean Hg is indeed 4.50 V as measured, the outcome is that the work function of Hg would increase by 0.11 eV upon contact with water. This result is highly improbable on the basis of common observations.

On the other hand, the objection of some surface physicists is that the Φ of Hg under the conditions of experiments carried out with a stream would be different from 4.50 eV because of surface contamination. If this is the case, the actual work function would be higher. However, contamination normally leads to a decrease in work function, especially if the contaminating species is water[35,36] or an inert gas.[54] An increase in work function would be possible if oxygen were chemisorbed, which has been ruled out experimentally. If an oxide layer is formed, a decrease in Φ is also expected.

On the other hand, if the Φ of Hg in the stream is modified by contamination in the cpd measurement, this should not be the case during the measurement of the potential-of-zero charge. If the value of 4.8 eV is accepted for the SHE in the UHV scale, the value of 4.61 eV for Φ^* of Hg at the pzc would imply that for Φ to decrease upon water adsorption, the Φ of clean Hg should be substantially higher than 4.61 eV. No experimental evidence exists for this for the time being.

In conclusion, acceptance of 4.8 V as the potential of the SHE in the UHV scale leads to apparently contrasting arguments: on one hand, the experiments with the streaming electrode leading to 4.44 V are vitiated by surface contamination of Hg, whose actual Φ would be about 4.8 V during the experiments. On the other hand, a decrease in Φ upon contact with

water in the measurement of $E_{\sigma=0}$ for Hg vs. SHE would require that Φ be substantially higher than 4.61 V. Thus the two arguments would converge to claim almost the same value of Φ for the clean as well as the contaminated surface of Hg.

The discrepancy would be resolved if about 4.8 eV were the actual work function of *clean* Hg. In this case, however, it would be difficult to understand why 4.50 eV has been consistently measured: it is hard to imagine what kind of contamination is responsible for such a highly reproducible situation. On the other hand, if 4.80 eV were the value of Φ for clean Hg, then most of the other metals would show a decrease in work function upon water adsorption less negative than Hg, which is at variance with the expected chemistry of metal surfaces (see later discussion).

3. Relation of the Potential of Zero Charge to Other Quantities

(i) Electrode Potential versus Work Function

Equation (17) shows the relationship between electrode potentials and electronic energy. The electrode potential is measured by the electron work function of the metal, modified by the contact with the solution (solvent). This establishes a straightforward link, not only conceptually but also experimentally, between electrochemical and UHV situations.[6,32] In many cases, electrochemical interfaces are "synthesized" in UHV conditions[55–58] by adding the various components separately, with the aim possibly of disentangling the different contributions. While the situation can be qualitatively reproduced, it has been shown above that there may be quantitative differences that are due to the actual structural details.

In principle, a measurement of Φ upon water adsorption gives the value of the electrode potential in the UHV scale. *In practice,* the interfacial structure in the UHV configuration may differ from that at an electrode interface. Thus, instead of deriving the components of the electrode potential from UHV experiments to discuss the electrochemical situation, it is possible to proceed the other way round, i.e., to examine the actual UHV situation starting from electrochemical data. The problem is that only relative quantities are measured in electrochemistry, so that a comparison with UHV data requires that independent data for at least one metal be available. Hg is usually chosen as the reference (model) metal for the reasons described earlier.

For an electrochemical cell consisting of a metal at the potential of zero charge in a solution of surface-inactive electrolyte and a reference electrode (let us assume that any liquid junction potential can be neglected), the electrode potential is given by (cf. Eq. (20)]

$$E_{\sigma=0} \text{ vs. Ref.} = \Phi^{M} + \delta\chi^{M} + \delta\chi^{S} + \text{const} \tag{26}$$

The two perturbation terms are specific to the given interface and are experimentally inseparable. They measure the contact potential difference at the M/S contact. However, since no cpd is measured in this case $\delta\chi^{M} + \delta\chi^{S}$ are grouped into a single quantity denoted by X, called the *interfacial term*[34]:

$$E_{\sigma=0} \text{ vs. Ref.} = \Phi + X + \text{const} \tag{27}$$

The constant term includes the contributions from the reference electrode.

In purely electrochemical experiments the constant term is unknown. Therefore, from a measure of $E_{\sigma=0}$, no information can be derived about the interfacial structure. However, if two metals are compared,

$$\Delta E_{\sigma=0} = \Delta\Phi + \Delta X \tag{28}$$

Equation (28) shows that the constant term is eliminated. Nevertheless, $\Delta\Phi$ must be known independently in order to derive information about ΔX. There is no way to avoid this; it is a consequence of the nature of the electrode potential [see Section I.2(ii)].

$E_{\sigma=0}$ is measured in electrochemistry and is usually known with an accuracy to ± 0.01 V or better.[8] On the other hand Φ is measured with surface physics techniques that have an accuracy of 0.05 eV, rarely better and often worse (because of imperfect surfaces).[59] Thus, Eq. (28) does not ensure an appropriate accuracy for ΔX, so that the uncertainty may outweigh the value itself. The best way to proceed is to plot $E_{\sigma=0}$ vs. Φ for a number of metals and to derive information about ΔX from eventually recognizable graphical correlations using statistical analysis.

Figure 5 shows a sketch of the plot of $E_{\sigma=0}$ vs. Φ according to Eq. (28). If a metal is taken as a reference surface, a straight line of unit slope through its point would gather all metals with $\Delta X = 0$, i.e., those whose sum of perturbation terms is exactly the same. For these metals the difference in pzc is governed only by the difference in Φ.

In Fig. 5 two more points are shown for exemplification. Metal M_1 is on the left of M (i.e., has a more negative $E_{\sigma=0}$), while M_2 is on the right

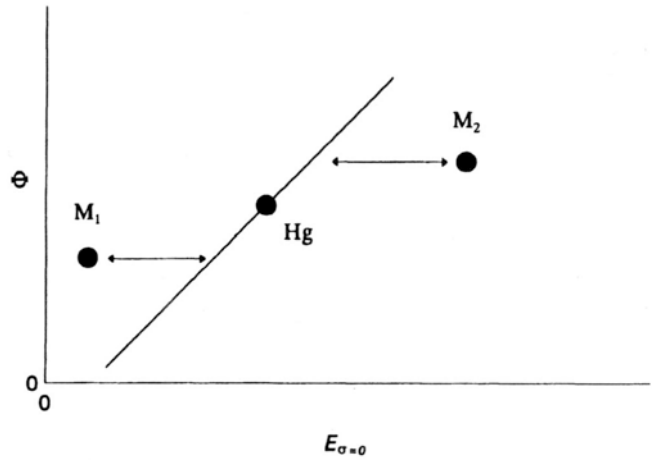

Figure 5. Sketch of a work function–potential of zero charge plot. The line through the point of Hg has unit slope. The horizontal distance of M_1 and M_2 from the line measures ΔX in Eq. (28).

(i.e., has a more positive $E_{\sigma=0}$ than expected from the straight line). For these metals, the horizontal distance of the point from the straight line precisely measures $\Delta X = X_1^M - X^M$, i.e., the interfacial term measured relative to that of metal M. Thus, for metal M_1 X_1^M is more negative than X^M, while the case is opposite for M_2. In UHV terms, X measures $\Delta\Phi$ upon water adsorption; therefore, $\Delta X = \Delta\Phi_1^M - \Delta\Phi^M$. Knowing $\Delta\Phi$ for metal M, $\Delta\Phi$ can be known for any other metal and compared with values measured directly in UHV. This will be done in the last part of this chapter after experimental data on $E_{\sigma=0}$ are collected.

The main problem in the analysis of $E_{\sigma=0}$ vs. Φ plots is that the two quantities are usually measured independently on different samples. It may happen that the surface structure differs somewhat so that Φ for the sample on which $E_{\sigma=0}$ is measured is different from that of the sample used in UHV experiments. This is especially the case with polycrystalline surfaces, whose structural reproducibility is occasional, but it is also the case with well-defined crystal faces if reconstruction phenomena are possible.[60] The problem persists also in the absence of reconstruction since the concentration and/or distribution of surface defects may be different.[33,61]

The preparation of metal surfaces as a rule differs in UHV and in electrochemistry. In the former case, "dry" procedures are used[62] (sputtering, annealing, etc.), while "wet" treatments prevail with electrodes[63] (electropolishing, chemical polishing, voltammetry, etc.). In some cases a particular kind of flame annealing is used for electrodes, which are then immediately dipped into the solution. However, the surface structure may change upon contact with the liquid or upon polarization, so that it is necessary to check the surface structure before and after the experiments.[64]

The most appropriate experimental procedure is to treat the metal in UHV, controlling the state of the surface with spectroscopic techniques (low-energy electron diffraction, LEED; atomic emission spectroscopy, AES), followed by rapid and protected transfer into the electrochemical cell. This assemblage is definitely appropriate for comparing UHV and electrochemical experiments. However, the effect of the contact with the solution must always be checked, possibly with a backward transfer. These aspects are discussed in further detail for specific metals later on.

(ii) Crystal-Face Specificity

It is well known that the Φ of a metal depends on the surface crystallographic orientation.[6,65,66] In particular, it is well established that Φ increases with the surface atomic density as a consequence of an increase in the surface potential χ^{M}. More specifically, for metals crystallizing in the face-centered cubic (fcc) system, Φ increases in the sequence **(110) < (100) < (111);** for those crystallizing in the body-centered cubic (bcc) system, in the sequence **(111) < (100) < (110);** and for the hexagonal close-packed (hcp) system, **(1120) < (1010) < (0001).**

It is clear from Eq. (27) that owing to the crystal face specificity of Φ, $E_{\sigma=0}$ is expected to vary with the crystallographic orientation as well. Moreover, since the interfacial term X results from interfacial molecular interactions, it must be face-specific also. For a well-defined metal surface, Eq. (27) becomes

$$E_{\sigma=0}\,(hkl) = \Phi\,(hkl) + X(hkl) + \text{const} \qquad (29)$$

where (*hkl*) are general Miller indices of crystal faces. Polycrystalline surfaces are sometimes used with solid electrodes, although their use is progressively becoming obsolete. The metal surface can be regarded as consisting of patches of single-crystal faces. Equation (29) applies to each of the patches, but as a consequence of the surface heterogeneity and the

equipotentiality of the metal surface, the condition of zero charge cannot be fulfilled everywhere. At most, it is fulfilled as an average condition over the entire metal surface.[67,68]

The applicability of Eq. (27) to polycrystalline surfaces depends on whether the various quantities are averaged in the same way over the whole surface. This turns out to depend on the particular property and the experimental method used to measure it.

Thermodynamically, an average work function can be defined for a polycrystalline surface[3,6]:

$$\langle \Phi \rangle = \sum_i \Phi_i \theta_i \tag{30}$$

where Φ_i is the work function of patch (face) i and θ_i is the fraction of surface occupied by face i on the actual sample. The "average" value of Φ can be obtained only by the method of contact potential difference, which is a thermodynamic experimental approach. Other techniques possess more local character and may probe some specific spots.[69]

The potential of zero charge is very often obtained by observing the condition of maximum diffusiveness of the ionic atmosphere around the electrode surface, for instance from the minimum of the experimental capacitance.[1,8,9] While it has long been recognized[70] that the heterogeneity of a surface reduces the sharpness of the results, it has been shown quantitatively[67,68] that because of the asymmetric behavior of double-layer properties around the potential of zero charge, ionic atmosphere diffusiveness effects for the different patches on an electrode surface turn out not to be averaged as simply as in the case of the electrode work function. This makes $E_{\sigma=0}$ for polycrystalline surfaces a questionable quantity that should be handled with caution.

The degree of heterogeneity of a metal surface is determined by the looseness of its surface atoms. This is qualitatively measured by the melting point and more specifically by the lattice cohesion and the atomic mass, which govern the tendency of atoms to autodiffuse.[71] More quantitatively, the variation of Φ from face to face may give a straightforward idea of the degree of heterogeneity of a polycrystalline surface of a given metal.

The heterogeneity of a metal surface is responsible for the curvature of the Parsons–Zobel (PZ) plot ($1/C$ vs. $1/C_d$, where C is the experimental capacitance and C_d the diffuse layer capacitance calculated on the basis of

the Gouy–Chapman theory).[72] Such a plot emerges from the Gouy–Chapman–Stern–Grahame (GCSG) model of the electrical double layer and has often been used to determine the "true" surface area of solid electrodes.[63,73,74] A recent model calculation by Foresti *et al.*[75] has examined the problem of the linearity of these plots.

The potential-of-zero charge is an intensive quantity and does not depend on the extent of the surface area. However, it depends on the heterogeneity of the metal surface if the method to determine it is affected by such a feature. It was mentioned earlier that the measurement of Φ by the cpd method is expected to respond to the average surface structure. Similarly, the immersion method,[8,9] which consists of measuring the charge flow as a clean metal is dipped in solution, should provide an average value of $E_{\sigma=0}$ that is different from that obtained with the minimum capacitance method. In principle, the immersion method should provide $E_{\sigma=0}$ directly with truly clean, inert metal surfaces in the absence of impurities in solution, as well as in the absence of strong chemical interactions with the solvent.

(iii) Effect of Temperature

With reference to Eq. (26), an effect of temperature is expected since both Φ^{M} and the perturbation terms depend on temperature. In particular, the effect can be written as a temperature coefficient:

$$\partial E_{\sigma=0}/\partial T = \partial\Phi/\partial T + \partial(\delta\chi^{M})/\partial T + \partial(\delta\chi^{S})/\partial T + \text{const}' \qquad (31)$$

where the const′ includes the temperature coefficient of the reference electrode. Alternatively, the reference electrode can be kept at constant temperature, but this implies neglecting any thermodiffusion potential at liquid junctions.

All contributions on the r.h.s. of Eq. (31) are in principle different from zero. In terms of the interfacial term X, Eq. (31) becomes

$$\partial E_{\sigma=0}/\partial T = \partial\Phi/\partial T + \partial X/\partial T + \text{const}' \qquad (32)$$

The temperature coefficient of the potential of zero charge has often been suggested to indicate the orientation of solvent molecules at the metal/solution interface. However, this view is based only on the response of a simple two-state model for the interfacial solvent, and on neglecting any contribution from the electronic entropy.[76,77] This is in fact not the case. The temperature coefficient of Φ in many instances is negative and of the

same order of magnitude as the temperature coefficient of $E_{\sigma=0}$.[34] It is thus in principle difficult to assign the sign of a $\partial E_{\sigma=0}/\partial T$ to the first or the second term on the r.h.s. of Eq. (32).[26]

Equation (32) suffers from the same shortcomings as Eq. (27). In particular, $\partial\Phi/\partial T$ must be known independently for the same metal sample as the one used as an electrode. Moreover, in view of the crystal-face specificity of $E_{\sigma=0}$, its temperature coefficient is also expected to depend on the crystallographic orientation. Being a differential quantity, $\partial E_{\sigma=0}/\partial T$ is an even more delicate experimental quantity than $E_{\sigma=0}$ itself.

For Hg, the temperature coefficient of $E_{\sigma=0}$ was determined by Randies and Whiteley[78] and found to be equal to $0.57\ \text{mV K}^{-1}$. On the basis of a simple up-and-down molecular model for water,[79] this positive value has been taken to indicate a preferential orientation, with the negative end of the molecular dipole (oxygen) toward the metal surface. While this may well be the case, the above discussion shows that the analysis of the experimental value is far more complex.

While no other value exists for Hg (which testifies to the delicacy of the experimental approach), Farrell and McTigue[80] have measured the temperature coefficient of the cpd between Hg and water. This quantity is $\partial X/\partial T$, from which a value of $-0.4\ \text{meV K}^{-1}$ has been estimated for $\partial\Phi/\partial T$ for Hg. It is thus evident that relating $\partial E_{\sigma=0}/\partial T$ to the interfacial structure is much more difficult than for $E_{\sigma=0}$, which suggests that one should always proceed cautiously in trying to decode experimental quantities in molecular terms.

In principle, the situation can be simplified to some extent by comparing temperature coefficients for the same metal in different solvents,[81] and for different faces of the same metal in the same solvents.[32,34] In these cases, correlations are possible which allow some rationalization of the experimental picture. Specific discussions will be provided later on.

(iv) Effect of Ionic and Nonionic Adsorbates

The potential of zero charge depends on the composition of the solution if adsorption takes place. If partial or total charge transfer occurs, the situation becomes more complex than in a perfect condenser,[82] as discussed in Section I.1(iii).

As ionic adsorption takes place, normally the potential of zero charge varies linearly with the amount adsorbed.[83] Such a variation is used[84,85] as a means of extrapolating to zero concentration of the adsorbing sub-

stance to find out the actual potential of zero *free* charge. Under similar circumstances, the specifically adsorbed charge is balanced at $\sigma = 0$ by a diffuse layer of oppositely charged ions.[32] At the same time, the ionic adsorbate can modify the solvent orientation around itself (thus modifying $\delta\chi^S$), as well as the electron distribution at the surface of the metal, at least at the metal site where it is adsorbed (thus modifying $\delta\chi^M$). It is evident that the variation of $E_{\sigma=0}$ includes all effects, among which the one related to the ionic layer as a rule prevails.

In the case of ionic adsorbates, the variation in $E_{\sigma=0}$ is normally unable to provide a clue to the molecular structure of the solvent since free charge contributions outweigh dipolar effects. In this case UHV experiments are able to give a much better resolved molecular picture of the situation. The interface is synthesized by adsorbing ions first and solvent molecules afterward. The variation of work function thus provides evidence for the effect of the two components separately and it is possible to see the different orientation of water molecules around an adsorbed ion.[58,86,87] Examples are provided in Fig. 6.

While from a structural point of view metal/solution and metal/vacuum interfaces are qualitatively comparable even if quantitatively dissimilar, in the presence of ionic adsorbates the comparability is more difficult and is possible only if specific conditions are met.[33] This is sketched in Fig. 7. A UHV metal surface with ions adsorbed on it is electrically neutral because of a counter-charge on the metal phase. These conditions cannot be compared with the condition of $\sigma = 0$ in an electrochemical cell, but with the conditions in which the adsorbed charge is balanced by an equal and opposite charge on the metal surface, i.e., the condition of zero diffuse-layer charge. This is a further complication in comparing electrochemical and UHV conditions and has been pointed out in the case of Br^- adsorption on Ag single-crystal faces.[88]

In the case of adsorption of neutral polar molecules, the effect on $E_{\sigma=0}$ is more tractable in molecular terms.[7,89] Adsorption is believed to occur[79] by displacement of solvent molecules close to the metal surface which are replaced by adsorbate molecules.[90] At $\theta = 0$ (no adsorbate), $E_{\sigma=0}$ is more conveniently written from Eq. (26) as

$$E_{\sigma=0} = \Phi + \delta\chi^M + g^S(\text{dip}) + \text{const} \tag{33}$$

where

$$g^S(\text{dip}) = \chi^S + \delta\chi^S \tag{34}$$

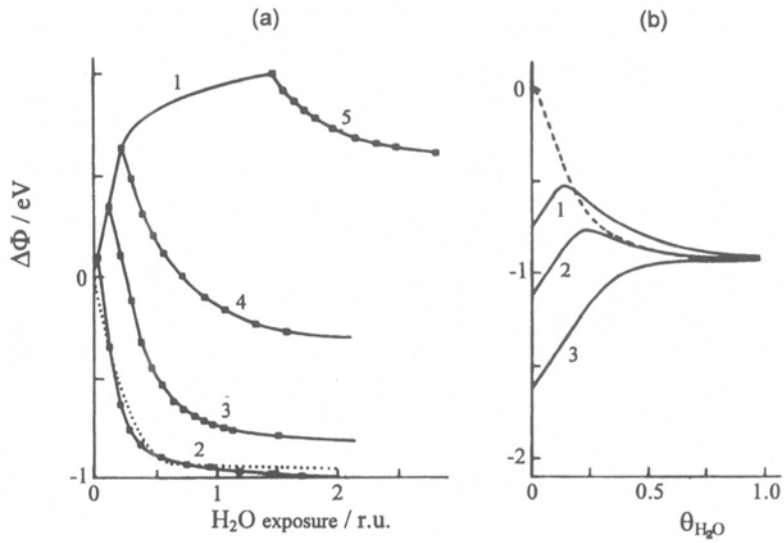

Figure 6. Effect of coadsorption of water with other species on Cu(110). (a) Coadsorption with various doses of bromine (to simulate anion adsorption). (.....) Water only; (1) bromine only; (2) to (5) water on increasing amounts of bromine. (b) Coadsorption with various doses of Cs (to simulate cation adsorption). (------) Water only ($\theta_{Cs} = 0$); (1) to (3) water on different coverages of Cs. θ_{Cs}: (1) 0.03, (2) 0.05, and (3) 0.07. Adapted from Refs. 58 and 87. [Figure 6(a) from D.E. Grider, K. Bange, and J.K. Sass, *J. Electrochem. Soc.* **30**, 247, Fig. 2, 1983. Reproduced by permission of the Electrochemical Society, Inc. Figure 6(b) reprinted from J.K. Sass, J. Schott, and D. Lackey, *J. Electroanal. Chem.* **283** 441, Fig. 2, 1990, © 1990 with permission from Elsevier Science.]

is the solvent dipole contribution at the interface and the term χ^S has been included in the constant term. When the surface is saturated with adsorbate ($\theta = 1$), the pzc can be written as

$$E'_{\sigma=0} = \Phi + \delta\chi'^{M} + g^{B}(\text{dip}) + \text{const} \tag{35}$$

where $g^{B}(\text{dip})$ is the surface contribution from the adsorbate molecules replacing the solvent. Comparison of Eq. (35) with Eq. (34) gives

$$E'_{\sigma=0} - E_{\sigma=0} = \Delta E_{\sigma=0} = (\delta\chi'^{M} - \delta\chi^{M}) + g^{B}(\text{dip}) - g^{S}(\text{dip}) \tag{36}$$

Equation (36) shows that information on $g^{S}(\text{dip})$ can be obtained only if $\delta\chi' = \delta\chi$ and $g^{B}(\text{dip}) = 0$ or is precisely known. Both cases are difficult to meet.

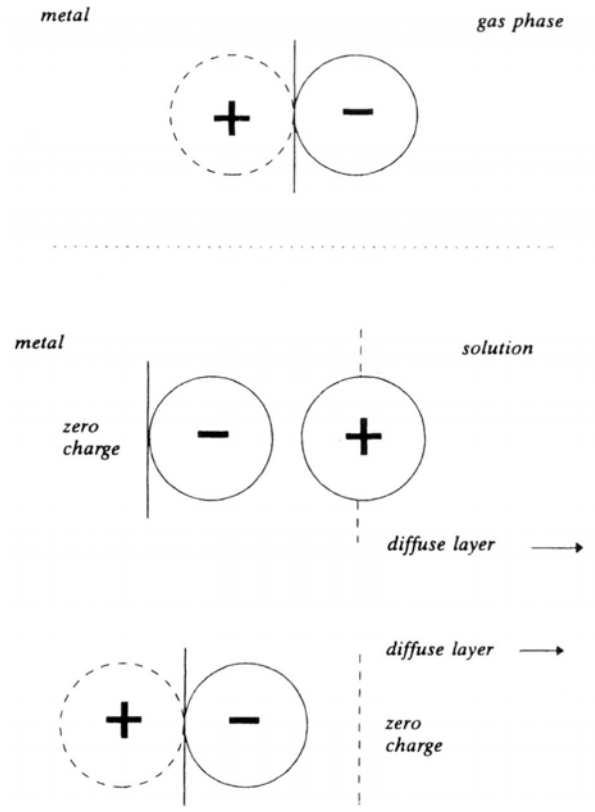

Figure 7. Adsorption of an electronegative species from the gas phase onto a metal surface generates a dipolar layer due to electron transfer from the metal to the species. Adsorption of anions onto an electrode simulates the situation when the positive charge on the metal compensates for the adsorbed negative charge (zero diffuse-layer charge), and not when the charge on the metal is zero.

While Eq. (36) is valid for $\theta \approx 1$, a qualitatively similar equation is obtained at any value of θ. Since the condition $\theta = 1$ is difficult to reach experimentally, the value of $\Delta E_{\sigma=0}$ (adsorption potential shift) is often estimated by means of extrapolation to $\theta = 1$. This procedure is very delicate and the result is often misleading. The variation of $E_{\sigma=0}$ with θ may be linear or nonlinear, depending on lateral interactions between

molecules (assuming for simplicity that no chemical interaction with the metal surface takes place). If the replacement of a solvent molecule at the electrode surface does not involve any disturbance of the neighboring particles (this might be defined as a "regular" behavior), the potential shift is a linear function of θ. If lateral interactions are involved (including those with the metal surface), other terms that are not explicit in Eq. (36) become operative.[91,92]

An aspect that is difficult to treat is the nature of the boundary between the adsorbate layer and the bulk of the solution. Solvent molecules are now in contact with an organic layer and the kind of interaction is expected to differ substantially from that with a bare metal surface. The layers of solvent molecules in the immediate proximity of the adsorbate might exhibit some preferential orientation, which is not explicitly accounted for in Eq. (36), and this adds some additional ambiguity to the physical interpretation of the results.

A comparison of the adsorption of a given molecule at the air/solution and at the metal/solution interface is a convenient way of obtaining some information on the role of the metal surface.[93,94] At the air/solution interface the potential shift is simply

$$\Delta\chi' = g^{B}(\mathrm{dip})_{air} - \chi^{S} \tag{37}$$

From Eqs. (36) and (37),

$$\Delta E_{\sigma=0} - \Delta\chi' = \Delta\delta\chi^{M} + \delta\chi^{S} + g^{B}(\mathrm{dip}) - g^{B}(\mathrm{dip})_{air} \tag{38}$$

Equation (38) still includes the electronic term. On the other hand, $g^{B}(\mathrm{dip})_{air}$ may differ from $g^{B}(\mathrm{dip})$ at the metal surface as a consequence of different interactions with the environment. Therefore the interpretation of adsorption potential shifts is always subject to a number of assumptions that cannot be easily checked.

Figure 8 shows an example of the most common behavior of $\Delta E_{\sigma=0}$ as a function of adsorbate coverage. Linear behavior, if ever observed, is seen at the air/solution interface.[93] At metal/solution interfaces, if chemical interactions with the metal can be ruled out, electrostatic interactions cannot be avoided, and these are responsible for the downward curvature.[91] Upward curvatures are often observed at air/solution interfaces as a consequence of lateral interactions.[95]

Models have been proposed to reproduce the curves in Fig. 8. Behavior at metal electrodes was discussed by Frumkin and Damaskin in this

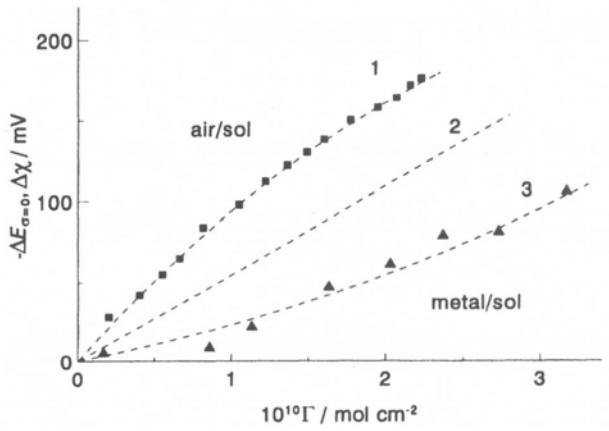

Figure 8. Typical adsorption potential shifts as a function of adsorbate surface concentration. (1) At the free surface of a solution (real behavior), (2) ideal behavior, and (3) at a metal (Hg)/solution interface. Experimental points for adsorption of 1,4-butanediol from Ref. 328.

series[96] in terms of two capacitors in parallel. The curves are reproduced by means of macroscopic experimental quantities such as capacitance at $\theta = 0$ and $\theta = 1$. The same authors have also discussed linear behavior in terms of two capacitors in series. In both cases molecular details are not very evident.

A "macroscopic" model for "regular" air/solution interfaces has been proposed by Koczorowski *et al.*[97] The model is based on the Helmholtz formula for dipole layers using macroscopic quantities such as dielectric constants and dipole moments. The model quantitatively reproduces $\Delta\chi'$ values [Eq. (37)], but it needs improvement to account for lateral interaction effects.

More recently, the curvature at air/solution interfaces has been accounted for by Nikitas and Pappa-Louisi[98] in terms of a specific molecular model that predicts a linear dependence of $(1/\Delta\chi')$ on $(1/\theta)$. The same model also reproduces the behavior at metal/solution interfaces, specifically Hg electrodes, for which most of the experimental data exist. Nikitas' treatment provides a method for an unambiguous extrapolation of the adsorption potential shift to $\theta = 1$. However, the interpretation of the results is subject to the difficulties outlined above. Nikitas' approach does provide

some physical interpretation of the experimental parameters, e.g., the slope and the intercept of the straight lines.

II. EXPERIMENTAL ASPECTS

The electrical double-layer structure at various metals has been discussed in many papers.[1–34,99–129] A large number of techniques have been developed for the experimental determination of the potential of zero charge.[1,9,10,12,128–219] These methods can be roughly classified as follows: (1) interfacial and surface tension methods (contact angle, capillary rise, tension vibration measurement); (2) impedance (capacitance) measurement methods; (3) immersion, open-circuit (streaming electrode), and potentiostatic scrape methods; (4) methods based on ionic, organic, and gas adsorption; (5) repulsion of diffuse double layers; (6) friction methods (oscillating Herbert pendulum, static friction); (7) ultrasonic methods (ultrasonic potential, dispersion of the electrode); and (8) optical and spectroscopic methods (photoemission, light intensity minimum, striascopic, Koester laser interferometry, Fourier transform infrared (FTIR) and subtractively normalized interfacial Fourier transform infrared spectroscopy (SNIFTIRS), and other methods).

The following are among the more suitable methods: electrocapillary, streaming electrode, capacitance, immersion, scrape, static friction and tension vibration. For liquid metals (Hg, Ga) and liquid alloys [In(Ga), Tl(Ga)], good agreement ($|\Delta E_{\sigma=0}| \leq 0.01$ V) has been achieved[1,3,4,7,10,25,26,120,125] between the $E_{\sigma=0}$ values obtained by the streaming electrode, electrocapillary maximum, and impedance methods. For solid polycrystalline electrodes, the agreement between the $\Delta E_{\sigma=0}$ values determined for a given metal by various methods is rather poor.[7,8,10,15,24,25,32] The greatest success has been achieved only with capacitance measurements at ideally polarizable single-crystal face/electrolyte solution interfaces.[15,24–34,61,63,64,67,74,107,149–156] A description of the methods for determining $E_{\sigma=0}$ was given by Perkins and Andersen in a previous chapter in this series,[9] and by Frumkin *et al.*[8,10]

(i) Interfacial and Surface Tension Methods

In the case of liquid metals and alloys [Hg, Ga, In(Ga), Tl(Ga)], $E_{\sigma=0}$ can be derived directly from the maximum of the corresponding electrocapillary curve (γ, E-curve).[7,8,10,15,16,18,25,99–109,120,125] As shown by several authors,[1–8,10,131–137] the thermodynamic laws that give the relation between the interfacial tension γ, the electrode potential E, and the Gibbs adsorption (Γ_i) and activity (a_i) of ions and molecules in the solution are applicable to the electrode/electrolyte solution interface. At constant pressure (p) and temperature (T), the fundamental electrocapillary equation for a liquid electrode/electrolyte interface can be written in the form

$$d\gamma = -qdE - \sum_i \Gamma_i d\mu_i = -\sigma dE - RT \sum_i \Gamma_i d\ln a_i \qquad (39)$$

where γ is the interfacial tension, q is the charge density, R is the gas constant, μ_i is the chemical potential, and a_i is the activity of component i. In the general case, the quantity q in Eq. (39) is the Gibbs adsorption of potential-determining ions, expressed in electric units. In the case of ideally polarizable electrodes (i.e., electrodes having a large energy barrier for charge transfer), q coincides with the surface charge density σ. Thus, according to Eq. (6), the charge of an electrode/solution interface is zero at the maximum of the electrocapillary curve.

It should be noted that there are no difficulties in the conception of the pzc for an ideally polarizable interface. Difficulties appear as one has to deal with a nonpolarizable (or as in the usual case, with a partly polarizable) electrode, because as charge flows into an electrode and its potential undergoes a change, some of the charge is retained on the electrode surface while some is transferred to the other side of the interface, namely, some electrode reaction occurs. This aspect was discussed by Lorenz[110] and later by Vetter and Schultze[111] in the development of the concept of partial charge transfer in adsorption at interfaces. The analysis by Frumkin *et al.*[8,11] in 1970 led to the conclusion that it is possible to thermodynamically treat not only polarizable but also nonpolarizable electrodes. A detailed thermodynamic analysis of polarizable and nonpolarizable interfaces has been given by Parsons[1] (see Section I).

While the method based on the surface tension measurement has been established since the pioneering work of Gouy,[128,130] conceptual and experimental problems arise with solid electrodes, whose surfaces cannot

be considered in structural and energetic equilibrium. Substantial work has been done in this area during the past 20 years. The electrocapillary equation for a solid electrode under elastic strain at constant T and p can be written as[1,136–138]

$$d\gamma = -\left[\sigma + (\gamma - Y)\left(\frac{\partial \varepsilon_e}{\partial E}\right)_{T,P,\mu_i}\right] dE - \sum_i \left[\Gamma_i + (\gamma - Y)\left(\frac{\partial \varepsilon_e}{\partial \mu_i}\right)_{T,P,E}\right] d\mu_i \tag{40}$$

where γ (specific surface work) is the reversible work spent in forming a unit new area of the surface by cleavage; Y (elastic surface stress) is the reversible work required to form a new unit area of surface by stretching; ε_e is the elastic surface strain [for liquid electrodes $\gamma = Y$; the strain terms disappear and the above equation reduces to Eq. (39)]. For solid electrodes the usual derivatives give

$$-\left(\frac{\partial \gamma}{\partial E}\right)_{T,P,\mu_i} = \sigma + (\gamma - Y)\left(\frac{\partial \varepsilon_e}{\partial E}\right)_{T,P,\mu_i} \tag{41}$$

$$-\left(\frac{\partial \gamma}{\partial \mu_i}\right)_{T,P,\mu_j \neq \mu_i} = \Gamma_i + (\gamma - Y)\left(\frac{\partial \varepsilon_e}{\partial \mu_i}\right)_{T,P,E_i} \tag{42}$$

If the surface strain changes under an electric field (electrostriction) or by adsorption of surface-active species, the left-hand side of Eqs. (41) and (42) is not equal to σ and Γ_i, respectively. Some authors[136,137] have reported unrealistically high values of $(\gamma - Y)$,[1] while Murphy and Wainwright[138] have provided evidence that the surface stress term is negligible. However, to a first approximation, the electrostriction term can be regarded as a second-order effect; thus, the second term in Eq. (41) can be neglected. Also, as shown by Parsons,[1] to a first approximation, the dependence of ε_e on the chemical potential of component i can be neglected, and in this case the second term in Eq. (42) disappears. Therefore, γ can be taken as the appropriate quantity, and the specific surface work-electrode potential (γ, E) curve can be used to obtain information about the electrical double-layer structure $(E_{\sigma=0})$ of solid electrode/electrolyte interfaces.

(a) Surface tension methods

The $E_{\sigma=0}$ for Hg, as well as for other liquid metals has been obtained using the Lippman electrometer[12] (γ, E curve method) modified by Gouy,[128] Frumkin,[131] Koening,[132] and others. The principles of the technique and its problems have been extensively described in previous reviews[1,10,16] and will not be dealt with further here.

Another method for measuring γ that is based on the study of the geometrical form of a sessile drop of a liquid metal has been discussed by Butler[157] and Smoulders and Duyvis.[158] Vos *et al.*[165] have used a spectroscopic laser imaging procedure to obtain the absolute surface tension of an Hg sessile drop electrode. This approach has been further developed by Melik-Gaikazyan *et al.*,[159] Kuãera,[160] and Barradas *et al.*[161] A detailed discussion of these methods has been given by Frumkin,[10] Levich,[162] and Conway *et al.*[163,164]

A novel method for the determination of the pzc of Hg or liquid amalgams has been described by Conway and Colledan.[163] The method is based on the effect of potential on the surface tension of the liquid metal, which gives rise to changes in the curvature of an Hg (liquid electrode) drop. These are transduced to a varying light-intensity signal through reflection of a collimated thin laser beam that is incident on the top of the drop. The values of $E_{\sigma=0}$ for aqueous solutions of various electrolytes have been found to be in good agreement with those obtained from impedance and surface tension data.[10,112]

The measurement of $E_{\sigma=0}$ in nonaqueous solvents encounters the problem of the unknown contribution of the liquid junction potential of the reference electrode/solution contact. Comparison of $E_{\sigma=0}$ in different solvents on a common potential scale is a problem for which an unambiguous solution has not yet been found. However, in practice, $E_{\sigma=0}$ values are often recalculated in the bis-bipihenylchromium (BBCr) (I/0) scale, which is assumed to be solvent independent.[108,109] Half-wave potentials of BBCr, measured in a given solvent vs. an aqueous calomel electrode in 0.1 M NaCl, are given in Table 2.[108,109] A comparison of various data[10,107,127,163] shows that the accord between $E_{\sigma=0}$ values obtained by different methods is good. On this basis, Conway and Colledan[163] have noted that their new method is applicable in various nonaqueous solvents with various concentrations of electrolyte.

There have been many attempts to apply the surface tension (γ, E curve) method to solid electrodes, and various experimental approaches

Table 2
Physical Properties of Solvents and Half-Wave Potential $E_{1/2}$ of Bis-biphenylchromium (BBCr), in 0.1 M $NaClO_4$ Solution

Solvent[a]	Dielectric constant (ε_s)	Dipole moment (μ_s/D)[b]	Polarizability ($10^3 \times \alpha_s$/nm^3)	$E_{1/2}$/V vs. SHE
DMSO	46.7	3.96	10.5	−0.60
DMF	36.7	3.86	7.8	−0.51
PC	64.4	4.98	9.0	−0.67
AN	36.0	3.92	4.40	−0.59
AC	20.7	2.88	6.33	−0.36
MeOH	32.7	1.7	3.3	−0.56
H_2O	78.3	1.85	1.5	−0.65
NMF	182.4	3.73	5.91	−0.43
EtOH	25.3	1.44 (trans)	5.41	—
1-propanol	20.8	1.55 (trans)	6.74	—
2-propanol	20.2	1.58 (trans)	7.61	—
1-butanol	17.8	1.66	8.88	—
2-methyl-1-propanol	17.3	1.64	8.92	—
2-butanol	17.9	—	—	—

[a]DMSO, dimethylsulfoxide; DMF, dimethyl formamide; PC, propylene carbonate, AN, acetonitrile; AC, acetone; NMF, N-methylformamide.

[b]1 D = 3.35×10^{-30} C m.

have been proposed.[10,100,138,168–171] However, the interfacial tension method has turned out to be applicable without reservation only to liquid electrodes. As shown by Gokhstein,[168] who has been able to relate the vibrations induced by an oscillating potential of an L-shaped electrode to charge, the solidification of an electrode has a considerable influence on the dependence of γ on E. The *estance* (a term introduced by Gokhstein) $\partial\gamma/\partial\sigma$ can have several *null points,* whereas for a liquid electrode such a derivative passes through zero only once, i.e., at $E_{\sigma=0}$. The shift of the estance zero from $E_{\sigma=0}$ has been related to the dependence of the work function on the elastic deformation.[168] Values of $E_{\sigma=0}$ only slightly different from those obtained by impedance have been obtained.[168]

Fredlein and Bockris[100,101,170] used a laser optical system to measure the bending caused by potential changes in a thin glass strip metallized on one side; they found that their $\Delta\gamma$, E dependence ($\Delta\gamma = \gamma_0 - \gamma$) gave $E_{\sigma=0}$ values with an accuracy of ±0.1. V compared with other (impedance)

methods. Murphy and Wainwright[138] have measured γ for solid metals by determining the change of weight upon immersion, which according to the authors is related to the force of the metal/solution interface tension. These measurements have provided evidence that the surface stress term is negligible.[138,171]

A new technique based on electrocapillary phenomena at partially immersed solid metal electrodes has been developed by Jin-Hua *et al.*[146,147] The method involves the detection of the rise of a solution meniscus by a bulk acoustic wave sensor.[146,147,172] The method was used to measure the $E_{\sigma=0}$ of pc-Ag[146] and pc-Au.[147] Good agreement with other methods was found. This method has been shown to be applicable to concentrated and dilute as well as nonaqueous solutions, and the effect of the pseudo-capacities existing in the capacitance method do not need to be considered. This method appears to make it possible to determine the $E_{\sigma=0}$ values of any metallic or nonmetallic conductor and semiconductor that is not corroded in the tested solutions.[146,147]

The problem of surface tension of solid electrodes has recently been carefully studied by Heusler and Lang.[173–176] These authors have shown that the anisotropic specific surface energies of solids change in different ways after a change in state, depending on the possibility of mass transport between the equilibrium surfaces. If mass transport is impossible, the solid is deformed by a nonhydrostatic stress field and the chemical potentials of the components become anisotropic.[173] In order to establish full equilibrium with constant chemical potentials throughout the whole system, mass transport is necessary. Since it is slow for solids, there will be irreversible contributions to the specific surface energy. Changes in specific surface energy were measured[175] as a function of E and electrolyte composition by the Koesters laser interferometry method and compared with changes in mass and charge. In all cases investigated, the electrocapillary curves for pc-Au in aqueous solution of various electrolytes [Na_2SO_4, NaCl, $Pb(ClO_4)_2$, $ZnSO_4$] changed slowly with time, thus confirming that surface relaxation and modification occurred. The method has also been applied to adsorption of neutral substances.[176]

(ii) Impedance (Capitance) Measurement Methods

For (ideally) polarizable metals with a sufficiently broad double-layer region, such as Hg, Ag, Au, Bi, Sn, Pb, Cd, Tl, and others, $E_{\sigma=0}$ can be obtained from measurements of the double-layer capacitance in dilute

solutions, where it is detected by a pronounced minimum in the capacitance-potential (C,E) curve.[1,4–8,10] In contrast to the electrocapillary curves, which can be obtained only by a limited number of methods, the capacitance of the electrical double layer can be measured by a great variety of techniques.[10,11,16,100,105,114–116,177] In the case of ideally polarized or "blocked" interfaces, direct measurement of σ, as for example in chronocoulometric experiments, is possible. The related differential capacitance, C, defined as

$$C = (\partial\sigma/\partial E)_{T,P,\mu_i} = (\partial^2\gamma/\partial E^2)_{T,P,\mu_i} \tag{43}$$

can be measured directly with an impedance bridge or a phase-sensitive detector as in a frequency response analyzer. At a high electrolyte concentration, linear sweep voltammetry can provide similar information since the current density is given by

$$j = d\sigma/dt = (d\sigma/dE)(dE/dt) \tag{44}$$

where dE/dt is the sweep rate v. If C is constant with v,

$$j = Cv \quad \text{and} \quad C = j/v \tag{45}$$

There are several other possibilities for obtaining a measure of C, as discussed in detail in many papers.[10,16,100,101,105,114–116]

The model more generally accepted for metal/electrolyte interfaces envisages the electrical double layer as split into two parts: the inner layer and the diffuse layer, which can be represented by two capacitances in series.[1,3–7,10,15,32] Thus, the total differential capacitance C is equal to

$$C^{-1} = C_i^{-1} + C_d^{-1} \tag{46}$$

where C_i is the inner (Helmholtz) layer capacitance,[99,112] independent of the surface-inactive electrolyte concentration and C_d is the diffuse (Gouy) layer capacitance,[128,129] expressed according to the Gouy–Chapman theory[8,10,99–101,128,129] for a z,z-type electrolyte by

$$C_d = \frac{d\sigma}{d\phi_d} = \frac{|z|F}{2RT}\sqrt{4A^2c + \sigma^2} \tag{47}$$

ϕ_d is the potential drop in the diffuse layer equal to

$$\phi_d = \frac{2RT}{|z|F} \operatorname{arcsh}\left(\frac{\sigma}{2A\sqrt{c}}\right) \tag{48}$$

where $A = \sqrt{2\varepsilon_0\varepsilon_d RT}$; ε_d is the dielectric constant of the diffuse layer, usually taken to be equal to the macroscopic dielectric permittivity of the solvent. Thus, according to Eq. (46), C_d, E curves have a minimum at $E_{\sigma=0}$ ($\sigma = 0$) since at this potential the value of C_d decreases linearly with $\sqrt{c}$. According to the Gouy–Chapman–Stern–Grahame model,[1,10–16,99,128,129] in a surface-inactive electrolyte solution the value of the inner layer capacitance C_i does not depend on c, and to a first approximation the potential of the differential capacitance minimum in the C,E curve would correspond to the condition $\sigma = 0$, i.e., to an $E_{\sigma=0}$ value. $E_{\sigma=0}$ in the presence of adsorption can be obtained by linear extrapolation of E_{min} as a function of the electrolyte concentration.[177a] As shown in some work,[125,178] a small dependence of E_{min} on $c_{el} \geq 0.01$ M must exist irrespective of the occurrence of specific adsorption, and its value depends on the value of C_i, $\partial C_i/\partial\sigma$, as well as on σ at which the maximum in C_i, σ curves occurs. Depending on the above parameters, there exists a critical electrolyte concentration (c_{cr}) above which the diffuse-layer minimum in the experimental C,E curve disappears. It is thus possible to estimate $\Delta E_{cr} = E_{min} - E_{\sigma=0}$[125,178] at $c = c_{cr}$ ($E_{\sigma=0}$ is the "true" zero charge potential). The value of ΔE_{cr} was found to be equal to 96, 100, 110, 35, and 45 mV for Hg, Bi(111), Sb(111), In, and Ag(111) electrodes, respectively. However, ΔE_{cr} decreases rapidly with the dilution of the electrolyte solution[125,178,179] and for a 0.05 M NaF aqueous solution, ΔE was found to be 30, 33, 36, and 27 mV for Hg, Bi(111), Sb(111) and Ag(111), respectively. For 0.01 M NaF, the calculated value of ΔE_{cr} is only a few millivolts. Thus, only an appreciable dependence of E_{min} on c at $c_{el} \leq 0.01$ M can be taken as an indication of weak specific adsorption of the anion around $E_{\sigma=0}$ at an ideally polarizable electrode. The value of $|\sigma_{cr}|$ for Hg, Bi(111), Sb(111), In, and Ag(111) electrodes is on the order of 2 to 2.5 μC cm^{-2}, and the value of c_{cr} was found to be equal to 0.075, 0.08, 0.09, 0.03, and 0.12 M[125,178,179] for these electrodes. It should be noted that the values of ΔE_{cr} and c_{cr} are influenced by the nature of the metal through the so-called "hydrophilicity" of the electrode material (C_i, σ curves), i.e., by the metal–water interaction strength.

The concentration dependence of the diffuse-layer minimum potential in dilute solution was determined by Levich *et al.*[177,180,181] using an

amplitude demodulation method. The values of $E_{\sigma=0}$ thus obtained were in good agreement with surface tension and impedance data.[1,10,99,100]

(iii) Immersion, Open-Circuit, and Potentiostatic Scrape Methods

The differential capacitance method cannot be used for reactive metals, such as transition metals in aqueous solutions, on which the formation of a surface oxide occurs over a wide potential region. An *immersion* method was thus developed by Jakuszewski *et al.*[182,183] With this technique the current transient during the first contact of a freshly prepared electrode surface with the electrolyte is measured for various immersion potentials. The electrode surface must be absolutely clean and discharged prior to immersion.[182–184] A modification of this method has been described by Sokolowski *et al.*[185] The values of $E_{\sigma=0}$ obtained by this method have been found to be in reasonable agreement with those obtained by other methods, although for reactive metals this may not be a sufficient condition for reliability.

The immersion method at a modern experimental level has been applied by Hamm *et al.*[140] to determine $E_{\sigma=0}$ for $Pt(111)/H_2O$ and $Au(111)/H_2O$ interfaces. Clean and well-ordered Au(111) and Pt(111) electrodes were prepared in a UHV chamber by several cycles of sputtering and annealing until no impurities could be detected by AES and the surface yielded sharp LEED spots. After such a preparation, the $(22 \times \sqrt{3})$ reconstruction of Au(111) was found. The Au(111) and Pt(111) electrodes were then transferred to the electrochemical cell by a closed system and immersed in $0.1\ M\ HClO_4$ aqueous solution at various *Es*. The current transients during the potential-controlled immersion experiments were recorded by a digital storage oscilloscope. The value of $E_{\sigma=0}$ was derived from σ, E plots where σ is the charge flowing during the contact with the electrolyte under $E = \text{const}$. The Au(111) electrode was used as a test system and the value of $E_{\sigma=0}$ was found to be in good agreement with that obtained by the impedance method.[140,187,188]

The well-known streaming electrode method, used with liquid electrodes (including Ga and its liquid alloys), belongs to the group of methods where a new electrode surface is formed underneath the solution surface at open circuit. In the case of liquid electrodes, the surface renewal is accomplished by injecting into the solution a fine stream of microscopic metal droplets. The streaming electrode method was first used by Pachen[166] and developed by Grahame *et al.*,[53] Randles and Whiteley,[78] as

well as by Jenkins and Newcombe.[167] The method is very useful in the case of nonaqueous electrolyte solutions, where electrode contamination with organic impurities is possible. In the case of liquid metals, the agreement between $E_{\sigma=0}$ values obtained from the electrocapillary maximum, the streaming electrode, and the impedance methods is very good ($\Delta E_{\sigma=0} \leq 0.01$ V).[10,100]

The open-circuit scrape method was developed by Andersen *et al.*[9,141,189,190] to obtain $E_{\sigma=0}$ values of some solid metals. The principle of this method is the same as that for the streaming liquid electrode method: a transitory fresh metal surface is produced over the entire electrode and the open-circuit potential is measured before subsequent reactions can appreciably change the electrode surface. It is possible to obtain $E_{\sigma=0}$ because the high activation energy for a transfer of charge across the double layer enables one to measure the preexisting potential. Simple inorganic ions are under equilibrium conditions during the entire process.

Variants of this method have been implemented by Noninski and Lazarova[191] and Zelinskii and Bek[192] Various specific aspects have been discussed by Lazarova.[193,194] Theoretical treatments have been provided by Safonov *et al.*[195]

When the electrode/solution system contains substances that are oxidized or reduced faster than the surface can be renewed, the potentials observed during the surface renewal are shifted.

(iv) Adsorption Methods

According to the theory of organic compound adsorption at electrodes, the maximum adsorption of neutral aliphatic compounds at Hg-like metals (physical adsorption) takes place in the region of $E_{\sigma=0}$; thus methods based on back integration and the salting-out effect have been worked out.[8,10,154] More recently Clavilier *et al.*,[196] using CO adsorption at fixed potentials on Pt single crystals to measure the related charge transient, have provided definite $E_{Q=0}$ values for Pt(110) and Pt(111) in 0.1 M $HClO_4$ (with the assumption that the CO dipole contributes negligibly to the double-layer potential). However, the measurement of a charge transient point by point along the potential axis is difficult, and since a transient charge from the whole surface is measured, it is not yet clear whether this method can be used to distinguish between the local potential of zero total charge of terraces and steps. Attard and Ahmadi [197] have used a method based on the adsorption and electroreduction of N_2O to estimate

the $E_{Q=0}$ values of single-crystal Pt-metal electrodes. A direct correlation has been found between $E_{Q=0}$ and the maximum rate of N_2O reduction.

Long ago Balashova and Kazarinov[142] suggested an approach based on the determination of the adsorption of anions and cations as a function of potential using a radiotracer technique. Equal surface concentrations of cationic and anionic charges indicate a zero free surface charge ($z_-\Gamma_-F = z_+\Gamma_+F$). An advantage of this method is that it can be applied to any materials (metals, nonmetals, semiconductors, ets.); a disadvantage is that it is restricted to ions with radioactive isotopes emitting α or β radiation. Actually, γ emitters are difficult to use because the range of γ rays is such that the background overwhelms the emission from the electrode. This method gives the concentration of nuclei in the double layer, but it does not distinguish between free and total charge; only dilute surface-inactive electrolyte solutions can be studied.

(v) Friction Methods

The interaction between two double layers was first considered by Voropaeva *et al.*[145] These concepts were used to measure the friction between two solids in solution. Friction is proportional to the downward thrust of the upper body upon the lower. However, if their contact is mediated by the electrical double layer associated with each interface, an electric repulsion term diminishes the downward thrust and therefore the net friction. The latter will thus depend on the charge in the diffuse layer. Since this effect is minimum at $E_{\sigma=0}$, friction will be maximum, and the potential at which this occurs marks the minimum charge on the electrode.

Bockris and Parry-Jones[198] were the first to carry out experiments with a pendulum to measure the friction between a wetted substrate and the pivot upon which the pendulum swung. It should be noted that Rebinder and Wenstrom[199] used such a device for an objective similar to that of Bockris and Parry-Jones, but they claimed that the characteristics of the pendulum oscillations reflected the hardness of the solid surface. The plastic breakdown determining this would be a function of ν and this is a potential-dependent value.[100,101] More extensive determinations were made later by Bockris and Argade[200]; the theoretical treatment was given by Bockris and Sen.[201] In the absence of adjustable parameters in the theory, a good agreement between theory and experimental data was assumed.[201] The studies by Bockris and Parry-Jones indicated that the

maximum in the friction potential relation corresponds to $E_{\sigma=0}$. The method should be applicable to any conducting material.[100,101]

(vi) Optical and Spectroscopic Methods

Barker *et al.*[202] have developed a photoemission method to obtain $E_{\sigma=0}$ at metal/electrolyte interfaces. Later, the method was applied by Brodsky *et al.*[203–205] to Pb, Bi, Hg, Cd, and In; good agreement ($\Delta E_{\sigma=0}$ = 0.02 V) with impedance data[10] was found.

In situ Fourier transform infrared and *in situ* infrared reflection spectroscopies have been used to study the electrical double layer structure and adsorption of various species at low-index single-crystal faces of Au, Pt, and other electrodes.[206–210] It has been shown that if the ions in the solution have vibrational bands, it is possible to relate their excess density to the experimentally observed surface.

According to experimental data,[208,209] the SNIFTIR technique can be used to probe the electrical properties of the electrical double layer even in more concentrated solutions where cyclic voltammetry (cv), impedance, chronocoulometry, and other techniques are not applicable. Iwasita and Xia[210] have used FTIR reflection-adsorption spectra to identify the potential at which the orientation of water molecules changes from hydrogen down to oxygen down.

Another spectroscopic technique, high-resolution electron energy loss spectroscopy (HREELS), has been used by Wagner and Moylan[211] in combination with cyclic voltammetry to estimate $E_{\sigma=0}$ of a Pt(111) electrode from the reaction of H_3O^+ formation.

Recently, Koesters laser interferometry has been used to detect the minute deformations of the electrode that are due to changes in specific surface energy.[173,174,212] The experimental details are given in the original papers. It has been found that the specific surface energy of the pc-$Au/K_2SO_4 + H_2O$ interface shows a maximum at $E = 0.00$ V (SCE) and this potential is independent of electrolyte concentration and solution pH. In the presence of KC1, $E_{\sigma=0}$ shifts to more negative values as the electrolyte concentration increases, which indicates specific adsorption of Cl^- on gold.[24] For both electrolytes, the specific surface energy was observed to continue to change with time after the mass became constant as a consequence of surface stress relaxation. It has been shown that faradaic currents do not affect surface energy or mass.[173,174,212]

The piezoelectric method should be noted as another technique for measuring the pzc. Introduced by Clavilier and Huong,[213] and used by Bard *et al.*,[214,215] the piezoelectric method has been used more recently by Seo *et al.*[216] and Dickinson *et al.*[217]

2. Estimation of the Surface Area of Solid Electrodes

The estimation of the working surface area of solid electrodes is a difficult matter owing to irregularities at a submicroscopic level.[10,15,20,24,32,63,64,67,68,73,74,218–224] Depending on the irregularity-to-probe size ratio, either the entire surface or only a fraction of it is accessible to a particular measurement. Only when the size of the molecule or ion used as a probe particle is smaller than the smallest surface irregularity can the entire surface be evaluated.[10,15,32,73,74,218]

Various *in situ* and *ex situ* methods have been used to determine the real surface area of solid electrodes. Each method[10,15,32,67,73,74,218] is applicable to a limited number of electrochemical systems so that a universal method of surface area measurement is not available at present. On the other hand, a number of methods used in electrochemistry are not well founded from a physical point of view, and some of them are definitely questionable. *In situ* and *ex situ* methods used in electrochemistry have been recently reviewed by Trasatti and Petrii.[73] A number of methods are listed in Table 3.

The *in situ* methods more commonly used to obtain the surface roughness $R = S_{real}/S_{geom}$ (where S_{real} and S_{geom} are the working surface and the geometric area, respectively) of electrodes are[10,24,63,73,74,218] (1) differential capacitance measurements in the region of ideal polarizability,[10,15,20,24,32,63,64,67,68,73,219-224] including the Parsons–Zobel plot,72 Valette-Hamelin approach,[67] and other similar methods [24,63,74,218,225]; (2) mass transfer under diffusion control with an assumption of homogeneous current distribution[73,226]; (3) adsorption of radioactive organic compounds or of H, O, or metal monolayers[73,142,227-231]; (4) voltammetry[232,233]; and (5) microscopy [optical, electron, scanning tunneling microscopy (STM), and atomic force microscopy (AFM)][234-236]; as well as a number of *ex situ* methods.[237-246]

Microscopy is one of the most direct physical methods for determining surface roughness. The resolution can go from macroscopic to atomic size, depending on the technique. Thus the order of magnitude of the range of observation is the millimeter for optical microscopy, the micrometer for

Table 3
Methods for the Determination of the Real Surface Area of Rough and Porous Electrodes

Method	References
In situ	
Measurements of double-layer capacitance	10, 24, 63, 70, 74, 218–225
Drop weight (or volume)	
Capacitance ratio	
Measurements based on the Gouy–Chapman–Stern theory to determine the diffuse double-layer capacitance	10, 24, 72, 74
Parsons–Zobel plot	
Measurements of the extent of monolayer adsorption of an indicator species	226–231
Hydrogen adsorption from solution	
Oxygen adsorption from solution	
Underpotential deposition of metals	
Adsorption of probe molecules from solution	
Voltammetry	232, 233
Open-circuit potential relaxation	237
Negative adsorption	238
Ion-exchange capacity	239
Mass transfer	73, 226
Scanning tunneling microscopy (STM)	234–236
Atomic force microscopy (AFM)	
Ex situ	
Gravimetric methods	241, 242
Volumetric methods	241, 242
Adsorption of probe molecules from the gas phase	240
Weighing of a saturated vapor adsorbed on a solid	241, 242
Hysteresis of adsorption isotherms	243–245
Thermodesorption	243, 244
Porosimetry	242
Liquid permeability and displacement	242
Gas permeability and displacement	242
Wetting heat (Harkins–Jura method)	243, 244
Surface potential of pure metal thin films	245
Metal dissolution rate	245
SEM, STM, AFM, profilometer, and stereoscan method	246
Diffuse light scattering	241
X-ray diffractometry	241
Nuclear magnetic resonance spin-lattice relaxation	241
Radioisotopes	242, 243

Source: Trasatti and Petrii.[73]

scanning electron microscopy (SEM), and the nanometer for atomic force microscopy and for scanning tunneling microscopy. Advances in AFM and STM are making their use *in situ* possible.[218,234–236] A lateral resolution of 1 nm and vertical resolutions better than 0.1 nm can be achieved.[234–236] However, it is useful to stress again that the value of R depends on the method used.[10,15,24,32,63,64,73,74,218–234] Further scrutiny of the various methods is thus welcome.

(i) Applicability of the Gouy–Chapman–Stern–Grahame Model to Solid Electrodes

The dependence of the C,E curves for a solid metal on the method of electrode surface preparation was reported long ago.[10,20,67,70,219–225] In addition to the influence of impurities and faradaic processes, variation in the surface roughness was pointed out as a possible reason for the effect.[10,67,70,74,219] For the determination of R it was first proposed to compare the values of C of the solid metal (M) with that of Hg, i.e., $R = C^{M}/C^{Hg}$.[10,74,219–221] The data at $E_{\sigma=0}$ for the most dilute solution (usually 0.001 M) were typically used for such a comparison to eliminate the influence of possible differences in the inner-layer capacities. However, C_i of different solid metals, as well as of liquid Ga, In(Ga), and Tl(Ga) alloys have shown such a large variation that this approach can hardly be considered as appropriate. It should be noted that the error in C, which for solid electrodes is much higher than for liquid electrodes, increases with the decrease of c_{el}; further, as shown later (Section II.2 (iv)), the effects of surface crystallographic inhomogeneity also prove especially appreciable.[24,67,74]

Frumkin was the first to give a qualitative consideration of the electrochemical properties of pc electrodes.[10,20,70] He noted that the charge σ_j at individual faces j may be different at a fixed value of the potential E and this may change the form of the capacitance curve near the diffuse-layer capacitance minimum. Important results were obtained in a pioneering paper by Valette and Hamelin.[67] They compared experimental capacitance curves for a pc-Ag electrode and its three basic faces. They found that the capacitance of a pc-Ag electrode can be obtained by the superposition of the corresponding C_j, E curves for individual faces exposed at the pc surface, i.e.

$$C_{pc}(E) = \sum_j \theta_j C_j(E) \qquad (49a)$$

A weighted sum of C,E curves for the faces was found to be similar to the C,E curve for a pc electrode. According to Valette and Hamelin,[67] all main Ag faces [(111), (100), and (110)] are exposed on the surface, their fractions θ_j on the surface being 0.31, 0.23, and 0.46, respectively. These authors demonstrated that the diffuse-layer capacitance minimum potential E^{pc}_{min} of a pc-Ag electrode was only slightly less negative (30 mV) than the pzc of the Ag(110) face, i.e., for the face with the more negative value of $E_{\sigma=0}$. The diffuse-layer capacitance minimum for pc-Ag was wider and less deep than for the Ag faces.

The influence of the crystallographic inhomogeneity of polycrystalline and monocrystalline electrodes (with various surface defects) has been discussed for various metals in many papers.[24,67,74,75,149–156,247–267] Bagotskaya *et al.*[262] showed that integration of the partial C,E curves from $E_{\sigma=0}$ of each face to E^{pc}_{min} on the polycrystalline electrode with account taken of the fraction of plane gives $\sigma^{pc}_{Ag} = -0.04$ C m^{-2} at E^{pc}_{min} where $\sigma^{pc}_{Ag} = \Sigma_j \theta_j \sigma_j$. At E_{min} the Ag(110) plane has a positive charge ($\sigma = 0.01$ to 0.02 C m^{-2}) and other planes a negative charge ($\sigma_{Ag(001)} = -0.02$ to -0.04 C m^{-2}; $\sigma_{Ag(111)} = -0.03$ to -0.06 C m^{-2}); at the surface of pc-Ag there are no surface regions with $\sigma = 0$. The same conclusions hold for pc-Au ($\sigma^{pc}_{Au} = -0.03$ C m^{-2}), pc-Bi ($\sigma^{pc}_{Bi} = -0.005$ C m^{-2}) and for other pc electrodes.[262–267]

Mathematical simulation of C_{pc}, E curves shows that the shape of the diffuse-layer capacitance minimum depends on the difference of $E_{\sigma=0}$ in individual faces and their fractions, as well as on the shape of partial C_j, E curves (Fig. 9).

The results of experimental capacitance studies at two plane model pc-Bi electrodes were in agreement with these conclusions.[264–266] Thus it has been shown that the potential of the diffuse-layer capacitance minimum for a pc electrode does not correspond to the zero charge potential of the whole surface, i.e., $\Sigma_j \theta_j \sigma_j \neq 0$ at E_{min}.

(ii) Parsons–Zobel Plot

Substantial contributions to the interpretation of the experimental data for solid electrodes have been made by Leilas *et al.*[223,224] and by Valette and Hamelin.[67] Both approaches are based on the same model: the

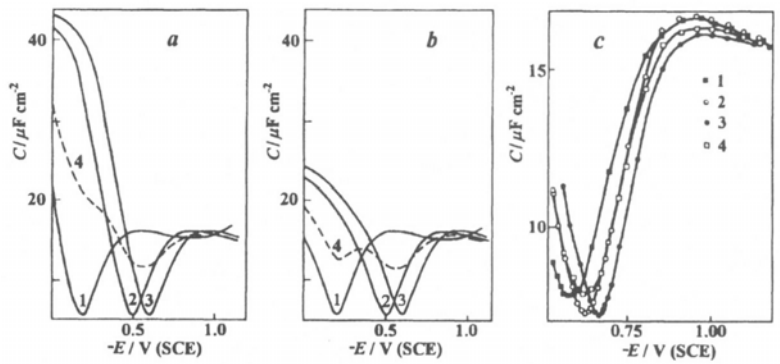

Figure 9. Theoretical *C,E* curves (1, 2, 3) for single-crystal faces and (4) for a model polycrystalline surface calculated by the superposition of the *C,E* curves at E = const [Eq. (49)] with $\theta_1 = \theta_2 = \theta_3 = 1/3:1$. (a) Faces with strong hydrophilicity and (b, c) faces with weak hydrophilicity. (a, b) $\Delta E_{\sigma=0}(\max) = 0.4$ V and (c) $\Delta E_{\sigma=0}(\max) = 0.09$ V.

value of $E_{\sigma=0}$ and of the inner-layer capacitance per unit of "true" surface area C_i are assumed to be constant over the whole surface.[67,223,224] Thus, the GCSG model is considered as applicable to the capacitance characteristics related to the unit of "true" surface area, which differ by a factor R^{-1} from those per unit "apparent" surface area

$$C_{\text{real}}(E) = R^{-1}C_{\text{geom}}(E) \quad \text{and} \quad \sigma_{\text{real}}(E) = R^{-1}\sigma_{\text{geom}}(E) \tag{50}$$

$$[C_i(\sigma_{\text{real}})]^{-1} = [C_{\text{real}}(\sigma_{\text{real}})]^{-1} - [C_d(\sigma_{\text{real}})]^{-1} \tag{51}$$

where $C_d(\sigma)$ is the diffuse-layer capacitance obtained according to the Gouy–Chapman theory.[1,10,128,129]

The idea in these papers[67,223,224] was to identify the potential of the capacitance minimum in dilute electrolyte solutions with the actual value of $E_{\sigma=0}$ (i.e., $\sigma_{\text{geom}}(E_{\min}) = 0$ for the whole surface) and to obtain the value of R as the inverse slope of the Parsons–Zobel plot at $E_{\min}$.[72] Extrapolation of C^{-1}_{geom} vs. C_d^{-1} to $C^{-1}_{\text{geom}} = 0$ provides the inner-layer capacitance in the $RC^{-1}_{i,\text{geom}}$, and not $C^{-1}_{i,\text{real}}$ as assumed in several papers.[67,68,223,224] In the absence of ion-specific adsorption and for ideally smooth surfaces, these plots are expected to be linear with unit slope. However, data for Hg and single-crystal face electrodes have shown that the test is somewhat more complicated.[63,74,219,247–249] More specifically,[247,248] PZ plots for Hg/

surface-inactive electrolyte solution interfaces at $\sigma = 0$ as well at $\sigma < 0$, albeit usually linear, exhibit reciprocal slopes that are somewhat greater than unity. The main reason for this has been shown[152,247–249] to be experimental errors in measuring C, as well as the hyperbolic form of C in the GCSG model. The GCSG model predicts that $C_d = f(c_{el})$ while C_i, which is not directly measurable, can be derived from Eq. (46) provided ions are not specifically adsorbed.

The error in C_i is the total differential of Eq. (52):

$$dy = dC_i = \frac{1}{x^2} \cdot \frac{1}{C^2} dC \tag{52}$$

where dC, for a given value of σ, includes the experimental error in the determination of C and the error from the integration of the differential capacitance-potential curves. When $x\,(x = C^{-1} - C_D^{-1})$ is small, dC_i is large and tends to infinity; when x is large, dC_i is small and tends to dC.[247,248] For a given positive x (at $E_{\sigma=0}$ for instance), the smaller C_d, the more an error in C affects C_i. As shown,[154,247–249,254] the same error for Bi, Cd, and Ag at fixed c_{el} causes the error in C_i to increase in the same order of metals since the value of C_i increases. The same experimental error entails a larger uncertainty in C_i for the lowest c_{el} and σ. At $|\sigma| >> 0$, the uncertainty in C does not bear on C_i since x is large. Error analyses show that at $\Delta C = \pm 0.2$ μF cm^{-2} $\Delta C_i = \pm 5$ μF cm^{-2} if $c_{NaF} = 0.001$ M, $C_i = 26$ μF cm^{-2} and $\sigma = 0$. At $|\sigma| \geq 3$ μC cm^{-2} and $\Delta C = \pm 0.2$ μF cm^{-2}, $\Delta C_i = \pm 0.15$ μF cm^{-2}, which is a high accuracy for C.[249]

In the case of liquid Hg, the uncertainty in the measurement may be induced by possible errors connected with (1) experimental measurement of C, (2) preparation of solutions of the exact c_{el}, (3) incomplete dissociation of electrolytes, (4) slight specific adsorption of anions, and (5) deviations from the Gouy–Chapman theory.[247,248] In the case of solid electrodes, in addition to the above-mentioned reasons, sources of inaccuracy are the possible erratic preparation of the electrodes with the same geometric surface area and the same crystallographic orientation.[10,247–260] Studies with wedge-shaped, two-faced Bi electrodes show that with increasing $\Delta E_{\sigma=0}$ of different faces exposed at a model pc electrode surface, the deviation of the Parsons–Zobel plot from linearity increases and the value of f_{PZ} also increases.[152,153,264–266] A comparison of the data for F^-, BF_4^-, and ClO_4^- solutions shows that f_{PZ} increases in the order $F^- < BF_4^- < ClO_4^-$ with increasing weak specific adsorption.[254]

The use of Parsons–Zobel plots to determine the roughness factor $R = f_{PZ}$ has been questioned recently.[75,250] It has been remarked that the experimental value of f_{PZ} depends on the surface charge density and sometimes on the electrolyte concentration c_{el}. The real R cannot depend on σ and on c_{el}. However, experimental PZ plots for single-crystal face electrodes in the region of $E_{\sigma=0}$ $(-3 < \sigma < 3\ \mu C\ cm^{-2})$ often show slopes increasing with $|\sigma|$, i.e., the apparent R decreases as $|\sigma|$ rises.[24,63,67,74,251–254] These findings indicate that f_{PZ} is not a real measure of the actual R. The only possibility of testing the validity of the GC theory consists[75,250] in finding experimental conditions for which the potential drop in the diffuse layer $|\phi_d| < 70$ mV. Thus, the practically unit slope of the C^{-1}, C_d^{-1} plots for Hg, Bi, Cd, Sb, Ag, and Au,[24,63,73,74,247–262] and for other systems with correlation coefficients better than 0.996 provides convincing evidence both for the validity of the GC theory and for the lack of experimentally detectable deviations of the roughness factor from unity. Slopes of C^{-1}, C_d^{-1} plots much lower than unity very near $E_{\sigma=0}$ $(-0.5 \leq \sigma < 1\ \mu C\ cm^{-2})$ can be interpreted[75,250] as deviations from the simple GC theory caused by the roughness of the electrode surface.

(iii) Surface Roughness and Shape of Inner-Layer Capacitance Curves

In 1973 Valette and Hamelin[67] proposed another method to determine the roughness factor R of solid polycrystalline surfaces and to test the GCSG theory on the basis of Eqs. (50) and (51). For each c_{el}, a set of C_i, σ curves was calculated* for various R values and the optimum value of R was selected on the basis of the assumption that near E_{min} the C_i, σ curve must be smooth. The experimental values of R were found to increase as c_{el} decreased (1.40 to 1.80). This was explained by the fact that R is a complex quantity, being $R = f_R f_{CR}$, where f_{CR} is a factor of crystallographic inhomogeneity of the polycrystalline electrode surface. f_{CR} is higher the larger the difference between $E_{\sigma=0}$ of individual planes (homogeneous regions exposed at a pc surface) and the more dilute the solution, and f_{CR} decreases as $|\sigma|$ increases, f_R was assumed to be the actual surface roughness factor independent of c_{el} and σ. Using the experimental C,E

*In Ref. 67 the shape of $C_{i,geom}, \sigma_{real}$ curves was analyzed using the following equation: $[C_{i,geom}(\sigma_{real})]^{-1} = [C_{geom}(\sigma_{real})]^{-1} - R^{-1}C_d^{-1}(\sigma_{real})$

curves for Ag single-crystal faces, the C,E curve for a pc-Ag electrode was calculated by the superposition of C,E curves at E = const,

$$C_{pc}^{real}(E) = R \sum_j \theta_j C_j(E) \tag{49b}$$

where $C_j(E)$ refers to the unit area of the true surface and C_{pc}^{real} refers to the unit area of the apparent surface of the electrode.

For pc-Au/electrolyte interfaces, Clavilier and Nguyen Van Huong[256] also concluded that the crystallographic inhomogeneity factor depends on c_{el}. Later, the influence of the crystallographic inhomogeneity of pc and monocrystalline electrodes (with various surface defects) was discussed in many papers.[75,152,154,156,247–259] It has been shown that the potential of the diffuse-layer capacitance minimum for a polycrystalline electrode does not correspond to $E_{\sigma=0}$ of the whole surface, i.e., $\Sigma_i \theta_i \sigma_i \neq 0$ at E_{min}.

(iv) Electrical Double-Layer Models for Polycrystalline Electrodes

Current theories describe pc solid electrode surfaces as a combination of different monocrystalline faces.[10,67,68,223,224,260–267] [cf. Eq. (49b)]. As discussed above, the coefficient R expresses the geometric roughness of the surface area to which the measured differential capacitance is referred. For solid electrodes, R also reflects the energetic inhomogeneity of the surface caused by crystallographically different grains (single-crystal faces), grain boundaries, and other crystallographic defects exposed at the surface of solid polycrystalline electrodes, as well as at the surface of *real* (as opposed to *ideal*) single-crystal faces.[67,74,247–267]

Electrical double-layer models for pc electrodes can be roughly classified into two groups.[67,68,74,153,154,261–267] Models in the first group consider a pc electrode surface as consisting of relatively large monocrystalline regions with a linear parameter $y^* \gg 10$ nm (y^* is the characteristic length), corresponding to macropolycrystallinity (MPC).[74,263] Within these areas both the inner and the diffuse layers are envisaged as independent. Accordingly,

$$C_{pc}^{real} = R \sum_j x_j C_{ij} C_{dj} / (C_{ij} + C_{dj}) \tag{53}$$

where C_{ij} and C_{dj} are the inner-layer and diffuse-layer capacitances of face j, respectively. This is the model of independent diffuse layers (IDL) [Fig. 10(a)].

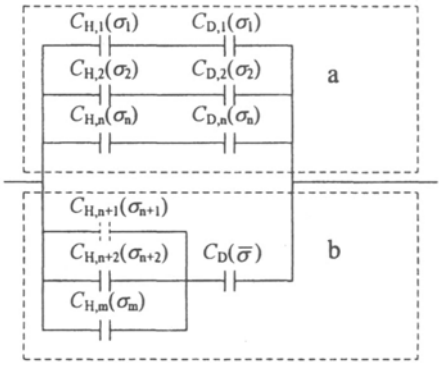

Figure 10. Theoretical model for the electrical double layer at an electrode with a polycrystalline surface. (a) Model of independent diffuse layers [Eq. (53)], and (b) model of common diffuse layer [Eq. (54)].

In the second group of models, the pc surface consists only of very small crystallites with a linear parameter y^*, whose sizes are comparable with the electrical double-layer parameters, i.e., with the effective Debye screening length in the bulk of the diffuse layer near the face j.[262,263] In the case of such electrodes, inner layers at different monocrystalline areas are considered to be independent, but the diffuse layer is common for the entire surface of a pc electrode and depends on the average charge density $\bar{\sigma}_{pc} = R\,\Sigma_j \theta_j \sigma_j$ [Fig. 10(b)]. The capacitance C_{pc}^{real} is obtained by the equation

$$C_{pc}^{real} = \frac{C_d(\bar{\sigma}) R\,\Sigma_j \theta_j C_{ij}}{C_d(\bar{\sigma}) + R\,\Sigma_j \theta_j C_{ij}} \tag{54}$$

This model is known as the model of the common diffuse layer (CDL).[262]

Both models can describe only some limiting cases[263] and the expression for the total capacitance of a pc electrode (equivalent circuit) depends on the relationship among three lengths: (1) the characteristic size of the individual faces at the pc electrode surface, y^*; (2) the effective screening length in the bulk of the diffuse layer near face j $[L_{D_j}(\sigma_j)]$ where L_D is the Debye screening length, and (3) εL_{i_j}, where ε is the bulk dielectric constant of the solvent and the length L_{i_j} is determined by the capacitance of the inner layer of face j.

According to a theoretical analysis,[262,267] the CDL model is valid for pc electrodes with very small grains ($y^* < 5$ to 10 nm) with a moderate difference of $E_{\sigma=0}$ for the different faces ($\Delta E_{\sigma=0} \approx 0.1$ to 0.15 V) and for dilute electrolyte solutions ($c \leq 0.01$ M) near the point of total zero charge. For the other cases, the IDL model should be valid.

According to electron diffraction studies,[153,219] a solid drop Bi electrode with a remelted surface ($BiDE^R$) consists of comparatively large homogeneous surface regions with $y^* > 10$ nm and Miller indexes of (001), (111), and (101). Between large homogeneous areas there are aggregates that consist of very small crystallites whose $y^* < L_D(\sigma)$. The electrical double-layer at such patches of $BiDE^R$ is described by the CDL model and the total capacitance of $BiDE^R$ at E = const can be expressed by the relation[265]

$$C_{pc}^{app} = R \sum_{j=1}^{n} \frac{\theta_j C_{ij} C_{dj}}{C_{ij} + C_{dj}} + \theta_{m+1} \left[\frac{C_d(\bar{\sigma}) R \sum_{j=n+1}^{m} \theta_j C_{ij}}{C_{dj}(\bar{\sigma}) + R \sum_{j=n+1}^{m} \theta_j C_{ij}} \right] \qquad (55)$$

with $\theta_{m+1} + \Sigma_{j=1}^{n} \theta_j = 1$, $\Sigma_{j=n+1}^{m} \theta_j = 1$, $m > n$. The results of computer simulations[264–266] of many experimental C_{pc}^{exp}, E curves for various $BiDE^R$ show that the standard deviation $\Delta(\Delta C)$ is smaller if Eq. (55) is used instead of (53) or (54), and thus 10–30% of the whole surface of $BiDE^R$ is covered with small crystallites ($y^* < 10$ nm). Studies of the wedge-shaped, two-faced model pc electrode show that the fraction of small crystallites at the surface is not more than 5–10%. It should be noted that the value of $\bar{\sigma}$ at E_{min} for a pc electrode is never zero and E_{min} depends on the shape of the C,E curves of individual planes, as well as on θ_j, but E_{min} mainly corresponds to $E_{\sigma=0}$ for the face with the most negative pzc.[63,68,74,152–154,260–267]

(v) Electrical Double-Layer and Fractal Structure of Surfaces

Electrochemical impedance spectroscopy (EIS) in a sufficiently broad frequency range is a method well suited for the determination of equilibrium and kinetic parameters (faradaic or nonfaradaic) at a given applied potential.[268,269] EIS has been used to study polycrystalline Au, Cd, Ag, Bi, Sb, and other electrodes.[152,249,270–273]

The main difficulty in the analysis of impedance spectra of solid electrodes is the "frequency dispersion" of the impedance values, referred to the constant phase or fractal behavior[268,269,274] and modeled in the equivalent circuit by the constant phase element (CPE). The frequency dependence is usually attributed to the geometric nonuniformity and the roughness of pc surfaces having a fractal nature with self-similarity or self-affinity of the structure, resulting in an unusual fractal dimension of the interface according to the definition of Mandelbrot.[275] Such a structural nonuniformity may result in a nonuniform distribution of σ at the electrode surface owing to the different $E_{\sigma=0}$ of the different grains existing at the electrode surface. The fractal carpet model[275] is representative of this approach.

The impedance of a fractal electrode is

$$Z = R_S + Z_0(j\omega)^{-\alpha} \tag{56}$$

where Z_0 is a preexponential factor (analogous to the inverse of the capacitance of the electrical double-layer ($1/C$)), $\omega = 2\pi\nu$ is the angular frequency, $j = \sqrt{-1}$, and α is a dimensionless parameter with a value usually between 0.5 and 1. The CPE angle φ is related to α by

$$\varphi = \frac{\pi}{2}(1 - \alpha) \tag{57}$$

The value $\alpha = 1$ corresponds to ideal capacitive behavior. The fractal dimension D introduced by Mandelbrot[275] is a formal quantity that attains a value between 2 and 3 for a fractal structure and reduces to 2 when the surface is flat. D is related to α by

$$\alpha = 1/(D - 1) \tag{58}$$

The CPE model has been used[152,154,270–274] and it has been found that for electrochemically polished surfaces, the surface roughness is very small compared with mechanically polished surfaces.

(vi) Surface Roughness and Debye Length-Dependent Roughness Factor

A new approach to the double-layer capacitance of rough electrodes has been given by Daikhin *et al.*[276–278] The concept of a Debye length-dependent roughness factor [i.e., a roughness function $\tilde{R}(L_D)$ that deter-

mines the deviation of capacitance from Gouy–Chapman model for a flat interface] has been introduced. It has been shown[276–278] that in the low charge limit, a limiting value of capacitance at short Debye lengths L_D should follow the equation

$$C_{GC} = \varepsilon\varepsilon_0 S_{geom}/L_D \tag{59}$$

but with S_{geom} replaced by $S_{real} = RS_{geom}$, i.e.,

$$C_{GC} = \varepsilon\varepsilon_0 S_{real}/L_D \tag{60}$$

In the limit of large Debye lengths (low electrolyte concentrations) the roughness would not bear on capacitance, which would thus obey Eq. (59).

In other words, two limiting cases may be considered: (1) L_D is shorter than the smallest characteristic correlation length of roughness l_{min} $[\tilde{R}(\infty)] = R > 1$ and (2) $L_D > l_{max}$ (i.e., L_D is greater than the maximal correlation length l_{max}, $R = 1$). It should be noted that the two limiting conditions can be realized experimentally by changing, for instance, c_{el} or σ. The concept of characteristic correlation length is not valid for fractal surfaces.[276–278]

The slope of Parsons–Zobel plots is predicted to be lower than 1 at higher c_{el} (small L_D values) monotonically approaching unity in the region of small c_{el}.[276–278] simple extrapolation to the high concentration limit $(1/C_d \to 0)$ will considerably reduce the apparent value of C_i^{-1}. Thus the treatment of capacitance data for rough surfaces should be reconsidered: (1) The value of the roughness factor cannot be derived from the reciprocal slope of the Parsons–Zobel plot in the range of small c_{el}. (2) The intercept obtained by extrapolation of the plot from the range of small c_{el} into the high c_{el} limit does not give $1/RC_i^{\sigma=0}$. In order to get this value, one should treat the whole $1/C(1/C_d)$ curve by nonlinear regression.[277,278]

Considerable curvature of Parsons–Zobel plots has been found in the region of small c_{el}; thus this plot is not convenient for the characterization of surface roughness. More convenient would be the plot of $\tilde{R}(L_D) \approx [(1/C - 1/C_i)]^{-1}$ $(1/C_{GC})$ vs. L_d, where the value of C_i is evaluated from the measurements at high concentration $(c \approx 0.1\ M)$ according to the Valette–Hamelin method.[67] $\tilde{R}(L_D)$ is a roughness function ranging from 1 for $1/L_D = 0$ to >1 for $1/L_D = \infty$. At $c > 0.1$ M there is another source of deviation from the GC theory that is due to the structure of the solvent [discussed in Section II.2(vii)] which could partially compensate for the deviations caused by surface roughness.[276–278] As noted,[278] if the accuracy is high, limiting cases can be studied, enabling one to obtain

important roughness parameters. A nonlinear regression fit of the whole curve would give the lateral correlation lengths of roughness. It should be noted that the predicted effects could be screened by the crystallographic inhomogeneity of a rough surface, which is not taken into account.[276–278] Contrary to the theoretical model,[276–278] deviations of experimental Parsons–Zobel plots toward lower values of C^{-1} have been systematically observed if c_{el} decreases.[24,28,63,67,75,152–254,250–267,271–273] This effect is mainly caused by the crystallographic nonuniformity of the real solid electrode surface (single-crystal faces with various surface defects).

(vii) Electrical Double-Layer Structure in Concentrated Electrolyte Solutions

The division of the interface into an inner layer and a diffuse layer has been a matter of discussion in view of the molecular dimensions of the inner layer.[122–126,279–285] However, the contribution of a constant capacitance is an experimental fact. Furthermore, molecular theories for electrolytes near a charged hard wall[282] as well as phenomenological nonlocal electrostatic theories[283] predict such a component without artificial introduction of any "inner layers." This turns out to be an effect of the short-range structure of the solvent.[279–285]

Carnie and Chan[279] and Blum and Henderson[280] have calculated the capacitance for an idealized model of an electrified interface using the mean spherical approximation (MSA). The interface is considered to consist of a solution of charged hard spheres in a solvent of hard spheres with embedded point dipoles, while the electrode is considered to be a uniformly charged hard wall whose dielectric constant is equal to that of the electrolyte (so that image forces need not be considered).

The full MSA expression for the capacitance is complex. However, at low c_{el} it is composed of concentration-independent and concentration-dependent terms.[281] The concentration-independent term is not associated with any specific region of the interface, but quantitative agreement between experimental and theoretical values of capacitance at low c_{el} is achieved only if the contribution of the metal phase is included.

Schmickler and Henderson[282] have studied several solvents and metals, using the jellium model for the metal and the MSA for the solution. Deviations of the Parsons–Zobel plot from linearity in the experimental results[72,286–288] at the highest concentration have been attributed to the onset of ion-specific adsorption. However, data at other electrode charges

show a similar behavior, whereas specific adsorption of anions should increase with increasing electrode charge. The effect of specific adsorption, as illustrated for **Hg/HCl + H_2O**,[72] is clearly different.

The extent of the agreement of the theoretical calculations with the experiments is somewhat unexpected since MSA is an approximate theory and the underlying model is rough. In particular, water is not a system of dipolar hard spheres.[281] However, the good agreement is an indication of the utility of recent advances in the application of statistical mechanics to the study of the electric dipole layer at metal electrodes.

The nonlocal diffuse-layer theory near $E_{\sigma=0}$ has been developed[283] with a somewhat complicated function of L_D and of solvent structural parameters. At low concentrations, $f(L_D)$ approaches unity, reaching the Gouy–Chapman C_d at $c \to 0$. At moderate concentrations, deviations from this law are described by the "effective" spatial correlation range Λ of the orientational polarization fluctuations of the solvent.

Thus, deviations from linearity of Parsons–Zobel plots are comparable with expectations from nonlocal electrostatic theory, although the analysis is restricted to only a single point on these plots.[283] The physical meaning of this interpretation is similar to a recently reported interpretation in terms of the MSA of a dipole–ion mixture near a weakly charged hard wall.[279–281,284] This approximation provides a microscopic calculation of the spheres to which both the constant capacitance term and the deviation from the Parsons–Zobel plots were scaled. The correlation length Λ for such a model is proportional to the radius of the spheres. It may be simulated by a modification of the Gouy theory for a Debye plasma in a semi-infinite continuum with a dielectric constant that varies with the distance from the boundary. Furthermore, it is independent of specific solvent models, relying only on the assumption of an exponential decay of the polarization correlations with a characteristic spatial length Λ.[283,284]

The local solvent structural information inherent in deviations from Parsons–Zobel plots suggests that this effect deserves further experimental investigation.[126,283,284] The reported accuracy of recent capacitance data (5%) for dilute solutions,[285] however, must be improved before unambiguous conclusions about deviations can be drawn.

(viii) Parsons–Zobel Plot in the Case of Nonideal Solutions

Data from many experiments[64,71,72,74,287–289] indicate that the differential capacitance of an ideally polarizable electrode at $E_{\sigma=0}$ in nonideal

solutions can be described by a straight line dependence in the C^{-1}, C_d^{-1} coordinates, whose slope is very close to unity. This experimental fact has been explained on the basis of a theoretical analysis of the diffuse-layer theory carried out by Grafov and Damaskin,[290] in which the theory of the diffuse layer near $E_{\sigma=0}$ is built up in a general form without using the concept of ideal solution. The differential capacitance for ideal solutions differs from the capacitance C_d of the diffuse layer in nonideal electrolyte solutions. However, according to the authors, C_d at $E_{\sigma=0}$ in nonideal electrolyte solutions is closely related to the capacitance calculated on the basis of the Gouy–Chapman theory if the correction term indicating activity coefficients is small. For example, the concentration derivative of the mean activity coefficient ranges up to 0.10 only in concentrated NaOH solutions; thus, to a first approximation, in a wide concentration region ($c \leq 0.1$ M) one can expect that $C_d^{id}/C_d \approx 1$. The above considerations can serve as a plausible explanation for the experimental behavior of the differential capacitance of ideally polarizable electrodes at $E_{\sigma=0}$ in nonideal electrolyte solutions.[290]

In concentrated NaOH solutions, however, the deviations of the experimental data from the Parsons–Zobel plot are quite noticeable.[72] These deviations can be used[290] to find the derivative of the chemical potential of a single ion with respect to both the concentration of the given ion and the concentration of the ion of opposite sign. However, in concentrated electrolyte solutions, the deviations of the Parsons–Zobel plot can be caused by other effects,[126,279–284] e.g., interferences between the solvent structure and the Debye length. Thus various effects may compensate each other for distances of molecular dimensions, and the Parsons–Zobel plot can appear more straight than it could be for an ideally flat interface.

3. Experimental Data

(i) *Mercury*

(a) Hg in aqueous solutions

Mercury in aqueous solutions is undoubtedly the most investigated electrode interface and has been discussed in many reviews.[1–10,84,99–109, 120, 121] There is little to add to what is already known.

A variety of methods have been used to measure $E_{\sigma=0}$ in the absence of specific adsorption (essentially, NaF and Na_2SO_4 solutions at $c \to 0$).

A typical set of experimental data[290a,290b] is shown in Fig. 11. All measurements converge to the value measured by Grahame.[286] At present, the $E_{\sigma=0}$ of Hg in water can be confidently indicated[5] as -0.433 ± 0.001 V (SCE), i.e., -0.192 ± 0.001 V (SHE). The residual uncertainty is related to the unknown liquid junction potential at the boundary with the SCE, which is customarily used as a reference electrode. The temperature coefficient of $E_{\sigma=0}$ of the Hg/H_2O interface has been measured and its significance discussed.[7,106,108,291]

(b) Hg in nonaqueous solutions

The effect of the solvent on $E_{\sigma=0}$ has been discussed in the literature.[1,10,31,108,109,112–127,286–288,291–324] Experimental data are summarized in Table 4, where the potential in the BBCr scale is also indicated.[108,109] The temperature coefficient of $E_{\sigma=0}$ is also available for a number of solvents.[108] It is mostly positive as for aqueous solutions, but for alcohols such as methanol and ethanol, it is negative.

The entropy of formation of the Hg/solution interface has been determined for a number of solvents.[81,108,291–294,304] It is positive for all

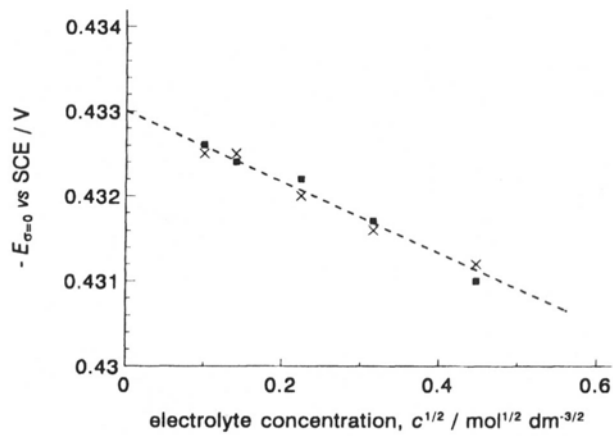

Figure 11. Extrapolation of $E_{\sigma=0}$ of Hg, as determined by means of a streaming electrode, to zero electrolyte concentration. (■) Na_2SO_4 solutions,[290a] and (×) NaF solutions.[290b]

Table 4
Potentials of Zero Charge of Hg in Various Solvents

Solvent[a]	Electrolyte	$E_{\sigma=0}$/V vs. aq. SHE	$E_{\sigma=0} \pm 0.010$/V vs. BBCr[b]	References
H_2O	NaF	-0.192 ± 0.001	0.458 ± 0.001	5
	NaF	-0.193 ± 0.005	0.457 ± 0.005	10, 94
	NaF, Na_2SO_4	-0.192 ± 0.001	0.458 ± 0.001	290a, 290b
AC	0.01 M KPF_6	0.10	0.46	330
	0.1 M $NaClO_4$	0.05	0.41	108
AN	$LiClO_4$	−0.03	0.56	109, 312
DMSO	$LiClO_4$	−0.08	0.52	108, 109, 294
DMF	$LiClO_4$	0.00	0.51	109, 310
	0.1 M $NaClO_4$	0.03	0.54	108
NMF	0.1 M $NaClO_4$	−0.05	0.38	108
PC	$NaClO_4$	−0.08	0.59	109, 312
	0.1 M $NaClO_4$	−0.09	0.58	108
MeOH	KF	−0.05	0.51	109, 305
	0.1 M $NaClO_4$	−0.06	0.50	108
EtOH	$LiClO_4$	−0.05	—	127, 293, 319
PrOH	$LiClO_4$	−0.07	—	320
Ethanediol	$LiClO_4$, KF	-0.089 ± 0.005	—	323
1,2-Propanediol	$LiClO_4$, KF	-0.084 ± 0.005	—	323
1,2-Butanediol	$LiClO_4$, KF	-0.094 ± 0.005	—	323
2,3-Butanediol	$LiClO_4$, KF	-0.089 ± 0.005	—	323
1,3-Propanediol	$LiClO_4$, KF	-0.154 ± 0.005	—	323
1,3-Butanediol	$LiClO_4$, KF	-0.154 ± 0.005	—	323
1,4-Butanediol	$LiClO_4$, KF	-0.129 ± 0.005	—	323

[a]Ac, acetone; An, acetonitrile; DMSO, dimethyl sulfoxide; DMF, dimethylformamide; NMF, *N*-methylformamide; PC, propylene carbonate.

[b]In order to avoid unknown liquid junction potentials between organic solvents and aqueous reference electrodes, pzc data have been recalculated to the bis-biphenylchromium (BBCr) (I/0) scale, which is assumed to be solvent independent.[37,108,109]

solvents investigated and smaller than in the bulk of the solution. This implies that Hg possesses a "structure-making" ability for these solvents. The preferential orientation of solvent molecules at the free liquid surface as well as at the Hg/solvent interface has been discussed.[1,10,15,32,81,295]

The structure of Hg/alcohol interfaces has been investigated in several papers.[108,127,293,295,305,314,317–319] The Hg/MeOH interface has been stud-

ied by Borkowska and Fawcett[127,293] in the presence of KF and $LiClO_4$. These authors have measured $E_{\sigma=0}$ (–0.326 V vs. SCE in H_2O) and the effect of temperature. The observed T dependence of capacitance is considerably lower than for the Hg/H_2O interface.

The experimental data have been interpreted in terms of a three-state model[309] for the solvent at the interface. The three states correspond to solvent dipoles oriented up, down, and flat. The model has been found to reproduce the experiments at negative charges and around $E_{\sigma=0}$, but not at strongly positive charges. This is because more orientations should be considered and in addition solvent molecules do not behave as hard spheres.

Fawcett *et al.*[317–319] have studied the Hg/EtOH interface in the presence of various anions (BF_4^-, ClO_4^-, Cl^-, Br^-, I^-). The surface activity of the anions has been found to increase in the above order. The double-layer data for Hg/EtOH have been found to be similar to those for MeOH,[127,293] with some difference attributable to the bigger size of EtOH molecules. The double-layer thickness has been found to differ from that expected from the real cross section of the solvent molecules.[325]

The higher capacitance at $\sigma = 0$ for EtOH than for MeOH has been explained by a higher association of EtOH compared with MeOH.[127,293,317] This concept has been criticized by Guidelli[326] on the basis of Nikitas' analysis[327] on the role of images. The effect of temperature was also studied at the Hg/ethanol interface.[311–319] The results are very similar to those for the Hg/MeOH interface.[37,293]

The electrical double layer in $1\text{-}PrOH + NaClO_4$ has been studied by Protskaya *et al.*[320] and the value of $E_{\sigma=0}$ from the potential of the electrocapillary maximum was equal to –0.31 V (SCE in H_2O).

Japaridze *et al.*[321–323] have studied the interface between Hg and a number of vicinal and nonvicinal diols such as 1,2-, 1,3-, 2,3- and 1,4-butanediol (BD), ethanediol (ED), and 1,3-propanediol. KF and $LiClO_4$ were used as surface-inactive electrolytes. The potential of zero charge was measured by the capacitance method against an SCE in water without correction for the liquid junction potential at the $solvent/H_2O$ contact (such a potential drop is estimated to be in the range of 20 to 30 mV). The potential of the capacitance minimum was found to be independent of the electrolyte concentration while capacitance decreased with dilution. Therefore, E_{min} was taken to measure $E_{\sigma=0}$. These values are reported in Table 4.

The experimental data with the diols are such that the solvents can be split into two groups: (1) those for which $E_{\sigma=0}$ is constant (–0.33 V vs. SCE in H_2O) (ED, 1,2-BD, and 2,3-BD) and the simple GCSG model is not followed because of the occurrence of specific adsorption, and (2) those for which $E_{\sigma=0}$ is somewhat more negative by 40 to 60 mV and whose interfacial behavior confirms the simple GCSG model of an electrode interface. Similar splitting has also been observed in the adsorption of these diols at the free surface of water.[328]

It has been pointed out[321–324] that the two groups of solvents differ by some definite structural features. In particular, ED, 1,2-BD, and 1,3-BD possess vicinal OH groups that can form *intra*molecular hydrogen bonds. For these solvents, the ability of the organic molecule to interact with neighboring molecules is reduced. This results in the possibility of a different orientation at the interface because of different interactions of the OH groups with the Hg surface.[323] The different molecular structure leads to different dipolar cooperative effects. As a result, the dependence of C on the bulk permittivity follows two different linear dependencies.

The Hg/*N*-methylformamide (NMF) interface has been studied by the capacitance method as a function of temperature.[108,294,303] The potential of Hg was measured with respect to the reference electrode Ag/0.05 M $AgClO_4$ + 0.05 M $NaClO_4$ in water. The specific adsorption of ClO_4^- was found to be negligible at $\sigma < 6\ \mu C\ cm^{-2}$. The experimental capacitance data have been discussed in terms of the four-state model,[121,291,294] which assumes the presence of both monomers and clusters in the surface layer of the solvent. The model has been found to describe the experimental picture qualitatively but not quantitatively. This is related to the fact that NMF is a strongly associated solvent.[108,109,294,303]

The Hg/NMF interface has been studied more recently also by Amokrane and Badiali[122] on the basis of their new theoretical approach to capacitances.

The Hg/dimethyl formamide (DMF) interface has been studied by capacitance measurements[10,120,294,301,310] in the presence of various tetraalkylammonium and alkali metal perchlorates in the range of temperatures –15 to 40°C. The specific adsorption of $(C_2H_5)_4NClO_4$ was found to be negligible.[108,109] The properties of the inner layer were analyzed on the basis of a three-state model. The temperature coefficient of the inner-layer potential drop has been found to be negative at $E_{\sigma=0}$, with a minimum at –5.5 $\mu C\ cm^{-2}$. Thus the entropy of formation of the interface has a maximum at this charge. These data cannot be described

by a three-state model which proves inappropriate for that specific case despite the fact that DMF is an unassociated aprotic solvent.

Impedance and electrocapillary measurements of the Hg/propylene carbonate (PC) interface have been carried out in a range of temperatures by Payne[312] and Cuong Nguyen *et al.*[302] In 0.1 M KPF_6 solution, the interfacial tension of Hg was found to exhibit a maximum at $E = -0.216$ V vs. a calomel electrode in 0.5 M $(C_2H_5)_4NClO_4$. The difference in $E_{\sigma=0}$ between the two techniques was less than 1 mV. $E_{\sigma=0}$ was observed to move toward more negative values as the temperature was increased.

The behavior of the Hg/pc interface is very similar to the Hg/DMF interface.[294,301,310] It can be qualitatively described by a multistate model.[291] However, although the model can reproduce the electric field and temperature dependencies of the inner-layer properties, the shortcomings of the approach should not be overlooked.[311]

The Hg/dimethyl sulfoxide (DMSO) interface has been studied by electrocapillary and capacitance measurements in a range of temperatures.[291,304] $E_{\sigma=0}$ was measured using the streaming electrode method. All potentials were recorded in a nonisothermal cell against a 0.1 M NaCl calomel electrode (CE) in water at 25°C. The potential difference of the cell CE/0.1 M $NaClO_4$ (aq.)/0.1 M $NaClO_4$ (DMSO)/CE was –0.096 V. This value was used to recalculate the data.[312]

The entropy of formation of the interface was calculated from the temperature coefficient of the interfacial tension.[304] The entropy of formation has been found to increase with the nature of the electrolyte in the same sequence as the single cation entropy in DMSO.[108,109,329] The entropy of formation showed a maximum at negative charges. The difference in ΔS between the maximum and the value at $E_{\sigma=0}$ can be taken as a measure of the specific ordering of the solvent at the electrode/solution interface. Data [108,109,304,314] have shown that $\Delta(\Delta S)$ decreases in the sequence $NMF > DMSO > DMF > H_2O > PC > MeOH$.

A negative temperature coefficient of the inner-layer potential drop was observed, –0.8 mV K^{-1}. Estimates of dipole potential drops due to solvent molecules[22,23,29,30] gave much larger values for DMSO than for H_2O, which can be explained by a strong preferential orientation of DMSO at the Hg surface.[26,81,304]

Capacitance and interfacial tension measurements were used to study the interface between Hg and mixtures of acetone + nitromethane.[330] The potential was measured against an SCE in H_2O and corrected for the liquid junction potential by measuring the half-wave potential of the ferrocene–

ferrocinium redox couple. In 0.01 M KPF_6, the pzc in pure acetone (AC) is 140 mV vs. SCE, while in pure nitromethane it is –385 mV. With the correction of the potential scale, the pzc in pure acetone becomes –220 mV.

Studies of pzc in mixed solvents were also carried out by Blaszczyk *et al.*[331] using the dipping method. They worked in mixtures of formamide and NMF and estimated the shift of the standard potential of the hydrogen electrode, of the surface dipole potential at Hg, and of the liquid junction potential.

The vibrating interface method was used by Meynczyk and coworkers[332] to measure the pzc of Hg in various nonaqueous solvents, such as methanol, acetone, glycerol, formamide, *N*,*N*-dimethylformamide, propylene carbonate, and 1,4-dioxane–water mixtures. KPF_6 and $NaClO_4$ were mostly used as supporting electrolytes.

(ii) Gallium, Indium(Ga), and Tallium(Ga)

The double-layer structure of Ga and its liquid alloys was discussed by Trasatti in a chapter in this series in 1980[7] and by Bagotskaya in 1986.[120] Other discussions can be found in books of the NATO series.[25,26]

(a) Ga, In(Ga), and Tl(Ga) in Aqueous Solutions

The electrical double-layer structure at the liquid Ga/H_2O interface has been studied by Frumkin and Bagotskaya *et al* [10,103,120,333–335] Pezzatini *et al.*[336–338] Butler and Meehan,[339] Horanyi and Takas,[340] and Doubova *et al.*[341] Studies of the double-layer structure at the liquid gallium electrode in aqueous surface-inactive electrolyte solutions have formed the basis for the concept of specific interaction of the electrode metal atoms with the negative (oxygen) end of water molecules.[10,103,120] Later it was found that the specific interaction of the solvent with the electrode depends on the lyophilic properties of the solvent.[10,120,334] The electrical double-layer structures of Ga/H_2O, $In(Ga)/H_2O$, and $Tl(Ga)/H_2O$ interfaces have been reported by Bagotskaya[120,342,343] and Frumkin[10] and in this work we give only a very short review of these data. Indium and thallium are surface-active compounds in these liquid alloys, so their electrochemical properties are close to those of the pure metals indium[344,345] and thallium[220,224,346,347] if their atomic percentages in the alloys are 16.4 and 0.02%, respectively.

The values of $E_{\sigma=0}$ for Ga, In(Ga), and Tl(Ga) electrodes have been obtained using the unpolarized streaming electrode method as well as the impedance method, and are summarized in Table 5. In the case of the Ga/H_2O interface, the potential of the diffuse layer minimum in *C,E* curves depends on the concentration of ClO_4^-, Cl^-, and SO_4^{2-} anions, and for these systems the values of $E_{\sigma=0}$ have been obtained by extrapolation of the E_{min}, $c_{el}^{1/2}$ dependence to $c_{el}^{1/2} \rightarrow 0$.[10,120] The values of $E_{\sigma=0}$ obtained from the dependence of the maximum of the electrocapillary curve on $c_{ClO_4^-}$ are in good agreement with the $E_{\sigma=0}$ values obtained from *C,E* measurements. It is interesting that the E_{min} value for the $Ga/H_2O + LiClO_4$ interface becomes more positive if $c_{ClO_4^-}$ increases ($\Delta E_{\sigma=0} \approx 0.09$ V if c_{NaClO_4} rises from 0.01 to 1.0 M), which is in contradiction to the behavior expected for the specific adsorption of Cl^- and other surface-active anions at the Ga/H_2O interface.[10,120,343] This effect was explained by the specific structure of the Ga/H_2O interface or by the negative adsorption of ClO_4^- anions at the Ga/H_2O interface. For the other systems [In(Ga) and Tl(Ga)], E_{min} was practically independent of $c_{ClO_4^-}$.

Guidelli and co-workers[336–338] measured the potential of zero charge by chronocoulometry. They found that the pzc was independent of the electrolyte concentration in both $NaClO_4$ and Na_2SO_4. However, $E_{\sigma=0}$ in the presence of sulfates was ca. 40 mV more negative. These authors have explained this apparent discrepancy in terms of the perturbation of the solvent structure at the interface by the ions at the electrode surface, which are, however, nonspecifically adsorbed.

Butler and Meehan[339] have measured $E_{\sigma=0}$ for the Ga/0.1 M $HClO_4$ interface. Horanyi and Takas[340] measured the pzc of liquid Ga in a variety of electrolyte solutions using a modified version of the streaming electrode that takes into account the possibility of faradaic current contributions with nonideally polarizable electrodes such as Ga near the pzc. These authors[339,340] have found pzc values in close agreement with those measured by Guidelli and co-workers.

The differential capacity, as well as the inner-layer capacity at $\sigma << 0$, $C_i^{\sigma<<0}$, were independent of the metal, except Tl(Ga), for which $C_i^{\sigma<<0}$ was somewhat higher than for Ga or In(Ga).[10,120,343] According to the experimental data,[341] the differential capacity of the dropping Ga electrode at strongly negative charges is somewhat higher (20%) than that of the Hg dropping electrode. These results are in good agreement with recent coulometric experiments.[336] Thus there is some contradiction between experimental results (*C,E* curves) obtained by different groups. As the

Table 5
Potentials of Zero Charge of Liquid Ga, In(Ga), and Tl(Ga) in Various Solvents

Electrode	Solution	$E_{\sigma=0} \pm 0.010$/V vs. aq. SHE	$E_{\sigma=0} \pm 0.010$/V vs. BBCr	References
Ga	H_2O + 0.05 M Na_2SO_4	−0.69	−0.04	10, 120, 342
	H_2O + $NaClO_4$ + $HClO_4$	−0.65 ± 0.05	0.00	336–338
	H_2O + 0.1 M $HClO_4$	−0.64	0.01	339
	H_2O + 0.1 M $HClO_4$	−0.65	0.00	340
In(Ga)	H_2O + 0.05 M Na_2SO_4	−0.68	−0.03	10, 109, 120
In	H_2O + 0.003 M NaF	−0.65	0.00	345
Tl(Ga)	H_2O + 0.05 M Na_2SO_4	−0.69	−0.04	10, 120
Tl	H_2O + 0.03 M NaF	−0.71	−0.06	10, 347
Ga	MeOH[a] + $LiClO_4$	~−0.62	−0.06	360
In(Ga)		~−0.59	−0.03	360
Tl(Ga)		~−0.58	−0.02	360
Ga	EtOH[a] + $LiClO_4$	~−0.60	—	361
In(Ga)		~−0.58	—	361
Tl(Ga)		~−0.57	—	361
Ga	AN + 0.1 M $LiClO_4$	−0.32[b]	0.27	120, 343, 355
In(Ga)		−0.45[b]	0.14	120, 343, 355
Tl(Ga)		−0.58[b]	0.01	120, 343, 355
Ga	DMSO + $LiClO_4$	−0.79[c]	−0.19	120, 343, 356, 357
In(Ga)		−0.71[c]	−0.11	120, 343, 356, 357
Tl(Ga)		−0.67[c]	−0.07	120, 343, 356, 357
Ga	DMF + $NaClO_4$	−0.64[d]	−0.13	109, 358
In(Ga)		−0.60[d]	−0.09	109, 358
Tl(Ga)		−0.61[d]	−0.10	358
Ga	NMF + $NaClO_4$	−0.64[e]	−0.21	359
In(Ga)		−0.61[e]	−0.18	359
Tl(Ga)		−0.60[e]	−0.17	359

[a] The values of $E_{\sigma=0}$ have been derived from figures in published papers[360,361]; therefore the error in $E_{\sigma=0}$ is on the order of ±10 to 15 mV.

[b] Recalculated from $\Delta E_{\sigma=0}$ with respect to Hg with $E_{\sigma=0}$(HgIAN) = −0.03 V (SHE).[120]

[c] Recalculated from $\Delta E_{\sigma=0}$ with respect to Hg with $E_{\sigma=0}$(HgIDMSO) = −0.08 V (SHE).[120]

[d] Recalculated from $\Delta E_{\sigma=0}$ with respect to Hg with $E_{\sigma=0}$(HgIDMF) = 0.03 V (SHE).[358]

[e] Recalculated from $\Delta E_{\sigma=0}$ with respect to Hg with $E_{\sigma=0}$(HgINMF) = −0.05 V (SHE).[359]

negative charge decreases, C and C_i start to increase owing to the specific adsorption of the solvent, and the value of C_i becomes clearly dependent on the chemical nature of the electrode material. For this reason, at $\sigma \approx 0$ the σ,E curves are nonlinear, and the deviation from linearity increases in the sequence Hg ≤ Tl(Ga) < In(Ga) < Ga. Thus the specific adsorption energy of H_2O molecules increases in the same order of metals.

The capacity of the metal phase (C_M) and the potential drop in the thin metal surface layer have been discussed by Amokrane and Badiali,[122,348] as well as by Damaskin *et al.*[349–353] The value of C_M^{-1} was found to increase in the order Ga < In(Ga) < Tl(Ga) ≤ Hg if it was assumed that the capacity of a solvent monolayer C_S = const. The negative value of the surface charge density σ, at which the C_S^{-1},σ curve has a maximum, decreases in the order Ga > In(Ga) > Hg, i.e., as the hydrophilicity of the electrode decreases.

(b) Ga, In(Ga), and Tl(Ga) in nonaqeous solutions

The electrical double layer at the Tl(Ga), In(Ga), and Ga/AN + $LiClO_4$ interface has been investigated by the impedance method.[10,103,120,343,344,354,355] It was found that C at $\sigma < -0.04$ C m^{-2} depends very slightly on E and on the metal studied, and increases in the order Ga < Tl(Ga) ≤ In(Ga) < Hg. The values of $E_{\sigma=0}$ have been obtained using the unpolarized streaming electrode, as well as the C,E curve method (Table 5). The value of $E_{\sigma=0}$ was independent of c_{LiClO_4}. At $\sigma > -0.04$ C m^{-2}, the capacity starts to increase as σ rises; and at $\sigma = 0$, the value of C as well as C_i increases in the order Hg < Tl(Ga) < In(Ga) < Ga. Compared with H_2O, the dependence of C on E (C_i on σ) is remarkably less pronounced, and the σ,E curves are linear in a very wide region of σ (–0.10 C m^{-2} < σ < –0.02 C m^{-2}). At $\sigma > -0.02$ C m^{-2}, the σ,E curves are only slightly nonlinear and this nonlinearity increases in the order Hg < Tl(Ga) < In(Ga) < Ga. Accordingly, the specific interaction of AN molecules with the surface is thought to increase in the above sequence of electrodes.

The electrical double layer at Ga, In(Ga), and Tl(Ga)/DMSO + $LiClO_4$ interfaces has been investigated by the impedance and streaming electrode methods.[355,356] The value of E_{min} was independent of $c_{ClO_4^-}$. The applicability of the GCSG model has been verified.[357] In contrast to acetonitrile (AN) + $LiClO_4$ and H_2O + $LiClO_4$ solutions, σ,E plots for DMSO + $LiClO_4$ solution are linear only at very negative σ (σ < –0.12 C

m^{-2}). As the negative charge density decreases, C starts to increase owing to the specific adsorption of the solvent, and the value of C_i at $\sigma = 0$ increases in the order Hg < Tl(Ga) < In(Ga) < Ga.[120,355,356] The maximum of the C_i,σ curves for Ga/DMSO and In(Ga)/DMSO interfaces is located at small negative charge densities [for In(Ga) at $\sigma \approx -0.03$ C m^{-2}, and for Ga at $\sigma \approx -0.05$ C m^{-2}]. The specific interaction energy of solvent molecules with the metal surface increases in the order of solvents AN < H_2O < DMSO, and for all solvents in the sequence of electrodes Hg ≤ Tl(Ga) < In(Ga) < Ga.

The electrical double-layer structure at Ga/DMF, In(Ga)/DMF, and Tl(Ga)/DMF interfaces upon the addition of various amounts of $NaClO_4$ as a surface-inactive electrolyte has been investigated by differential capacitance, as well as by the streaming electrode method.[358] The capacitance of all the systems was found to be independent of the ac frequency, ν. The potential of the diffuse layer minimum was independent of c_{NaClO_4} and ν.

For Ga, In(Ga), and Tl(Ga) electrodes, the potential measured by the streaming electrode was ~30 mV less negative than the value of $E_{\sigma=0}$ from C,E curves. For Hg there was no such difference.[301,358] The reason for the dependence of E_{min} on the method used was not discussed. At high negative charge densities, C is apparently independent of the electrode studied, being mainly determined by the size of the solvent (0.068 F m^{-2}). As the negative value of σ decreases, C begins to increase and becomes dependent on the nature of the electrode. At $E_{\sigma=0}$, the value of C increases in the order Hg ≤ Tl(Ga) < In(Ga) < Ga. According to the data in Table 5, the specific adsorption energy of solvent (DMF) molecules increases in the sequence Hg < Tl(Ga) < In(Ga) < Ga.

Parsons–Zobel plots have been constructed for all the systems at $\sigma \simeq 0$ in the range $0.02 < c < 0.2$ M. These plots were linear, with the value of the slope very close to unity. The values of C_i obtained by extrapolation of the C^{-1}, C_d^{-1} plots to $C_d^{-1} = 0$ were in good agreement with those calculated from the C,E curves for the 0.1 M $NaClO_4$ + DMF system according to the GCSG model.[358] The value of C_i increases in the sequence of electrodes Hg < Tl(Ga) < In(Ga) < Ga as the hydrophilicity of the electrode surface rises.

Ga, In(Ga), Tl(Ga), and Hg in *N*-methylformamide + $NaClO_4$ solutions have been studied by the impedance method.[359] The capacitance of the electrical double-layer for all electrodes in the frequency range 200 Hz < ν < 5000 Hz was independent of ν. The values of $E_{\sigma=0}$ were usually

determined by the streaming electrode, as well as from the dependence of C on E for dilute surface-inactive electrolyte solutions. In the case of Ga, the value of E_{min} is constant, but for In(Ga), Tl(Ga), and Hg electrodes, E_{min} depends on c_{el}, shifting to less negative values as the solution is diluted. Thus slight specific adsorption of ClO_4^- at In(Ga) and Tl(Ga) seems possible.

The applicability of the GCSG model has been tested by the Parsons–Zobel approach; the Parsons–Zobel plots were linear for all systems, with the value of f_{PZ} very close to unity. The values of $C_i^{\sigma=0}$ obtained by extrapolation of the $1/C(1/C_d)$ curves to $1/C_d = 0$ were in good agreement with the values of $C_i^{\sigma=0}$ calculated by Grahame's method. The C_i,σ curves for Ga, In(Ga), Tl(Ga), and Hg apparently merge at $\sigma, << 0$, but at $E_{\sigma=0}$ the value of C_i increases in the sequence Hg < Tl(Ga) < In(Ga) < Ga as the lyophilicity of the electrode rises.

Theoretical C,E and C, σ curves have been compared with experimental capacitance curves.[359] In a wide range of potentials, the coincidence was good and it was concluded that the GCSG model is acceptable for Ga, In(Ga), Tl(Ga), and Hg electrodes in NMF + $NaClO_4$ solution.

The electrical double layer at Hg, Tl(Ga), In(Ga), and Ga/aliphatic alcohol (MeOH, EtOH) interfaces has been studied by impedance and streaming electrode methods.[360,361] In both solvents the value of E_{min} was independent of c_{el} ($0.01 < c_{LiClO_4} < 0.25$ M) and ν. The Parsons–Zobel plots were linear, with f_{PZ} very close to unity. The differential capacity at $\sigma << 0$ was apparently independent of the metal nature, but at $\sigma = 0, C_i$ rises in the order Tl(Ga) < In(Ga) < Ga. Thus, as for other solvents,[120,343] the interaction energy of MeOH and EtOH molecules with the surface increases in the given order of metals. The distance of closest approach of solvent molecules and other fundamental characteristics of Ga, In(Ga), Tl(Ga)/MeOH interfaces have been obtained by Emets *et al.*[362]

(iii) Silver

(a) Pc-Ag in aqueous solutions

The electrical double layer at a pc-Ag/aqueous solution interface has been discussed by Leikis *et al.*, Valette and Hamelin, and Beck *et al.* in many papers.[24,63,67,146,223,272,363–368] Detailed reviews have been given by Hamelin[63] and Vorotyntsev[74]; in this work only a few comments will be added. First, the diffuse-layer minimum in the C,E curve was obtained[363]

at E = –0.94 to –0.96 V (SCE) and thereafter this value was reported in many works.[24,63,74,223,272,363–367] Recently a value of -0.985 ± 0.005 V (SCE) in 0.05 M $NaClO_4$ solution was reported by Doubova *et al.*[368] A small effect of specific adsorption is probably present (Table 6).

Leikis *et al.*[223] used the Parsons–Zobel method to obtain the roughness factor f_{PZ} for pc/Ag electrodes. It was found that $f_{PZ} \geq 1.2$, which was explained by the geometric inhomogeneity of the pc-Ag electrode surface. A more detailed analysis is given in Section II.2. Thus it should be noted that in the case of pc electrodes with appreciable differences of $E_{\sigma=0}$ values for the various planes ($\Delta E_{\sigma=0} > 100$ mV), it is impossible to obtain the "true" roughness coefficient, the actual $E_{\sigma=0}$, and the inner-layer capacity.

The electrical double-layer structure and fractal geometry of a pc-Ag electrode have been tested by Sevastyanov *et al.*[272] They found that the geometrical roughness of electrochemically polished pc-Ag electrodes is not very high ($f_{PZ} \sim 1.5$ to 1.25), but the dependence of C_i, σ curves on c_{el}, as well as on f_{PZ}, is remarkable (C_i = 30 to 80 $\mu F\ cm^{-2}$ if f_{PZ} = 1.5 to 1.0).

A novel method for measuring the change in interfacial tension at a solid electrode/aqueous solution interface and for determining $E_{\sigma=0}$ has been developed by Jin-Hua *et al.*[146,147] A bulk acoustic wave (BAW) sensor was used to determine the change in electrode mass and oscillating medium that resulted from the change in interfacial tension at a pc-Ag/solution interface. A plot of the frequency change with the electrode potential E for a pc-Ag electrode in Na_2SO_4 solutions exhibits a maximum at $E_{\sigma=0}$, which was independent of $c_{Na_2SO_4}$. $E_{\sigma=0}$ = –0.919 ± 0.015 V (SCE) was in reasonable agreement with the value of –0.944 ± 0.015 V (SCE) obtained by the capacitance method.[369] The values of $E_{\sigma=0}$, obtained by the BAW sensor as well as by impedance,[24,224,366] are more negative than those obtained by the open-circuit method[189] [$E_{\sigma=0}$ = –0.900 V (SCE)] and by the friction method[370] [$E_{\sigma=0}$ = –0.890 V (SCE)]. The value of $E_{\sigma=0}$ for $HClO_4 + H_2O$ solution increases from –0.927 to –0.904 V (SCE) as c_{HClO_4} increases from 1×10^{-3} to 5×10^{-3} M, and for NaF + H_2O it decreases from –0.906 ± 0.008 to –0.917 ± 0.008 V (SCE) as c_{NaF} increases from 1×10^{-3} to 1×10^{-1} M.[146] Thus the effect of the anions on $E_{\sigma=0}$ varies in the order $F^- \geq SO_4^{2-} \geq ClO_4^-$.

(b) Pc-Ag in nonaqueous solutions

Surface-enhanced Raman scattering (SERS) and differential capacitance methods have been used to study the interfacial solvent structure and

Table 6
Electrical Double-Layer Parameters of Ag in Aqueous Solutions

Electrode	Surface preparation method	Electrolyte	$E_{\sigma=0}$/V vs. SHE	$(dE_{min}/dc)/$ (mV dm^3 mol^{-1})	f_{PZ}	Atomic density/cm^{-2}	Method	References
pc-Ag	Electrochem. polish.	NaF	–0.70 to –0.72	—	1.2	—	Impedance	223
	Electrochem. polish.	NaF	–0.70 to –0.72	—	1.9	—	Impedance	67
	Electrochem. polish.	NaF (pH = 4)	–0.71 ± 0.01	—	2.72	—	Impedance	366
	Electrochem. polish.	$NaClO_4$	–0.744 ± 0.005	—	—	—	Impedance	368
	Electrochem. polish.	$LiClO_4$	–0.69 ± 0.01	—	—	—	Impedance	375
	Electrochem. polish.	Na_2SO_4	–0.678 ± 0.015	—	—	—	BAW[a]	146, 147
	Electrochem. polish.	Na_2SO_4	–0.703 ± 0.015	—	—	—	Impedance	369
			–0.66 ± 0.02	—	—	—	Open circuit scrape	189
			–0.65 ± 0.01	—	—	—	Friction	9, 190
Ag(111)	Electrolytic growth	NaF	–0.45 ± 0.01	—	1.02	1.380×10^{15}	Impedance	377
	Electrochem. polish.	NaF	–0.454 ± 0.010	—	1.07 ± 0.10	—	Impedance	67, 150, 384, 385
	Electrochem. polish.	NaF	–0.454 ± 0.010	—	—	—	Impedance	63
	Chem. polish.	NaF	–0.450 ± 0.016	140	—	—	Impedance	32
	Electrolytic growth	KF, NaF	–0.460 ± 0.002	—	—	—	Impedance	151

(*continued*)

Table 6
Continued

Electrode	Surface preparation method	Electrolyte	$E_{\sigma=0}$/V vs. SHE	(dE_{min}/dc)/(mV dm^3 mol^{-1})	f_{PZ}	Atomic density/cm^{-2}	Method	References
Ag(100)	Electrolytic growth	KF	−0.609 ± 0.002	—	1.02	1.195×10^{15}	Impedance	151
	Electrochem. polish.	NaF	−0.621 ± 0.005	—	1.15	—	Impedance	67, 384, 385, 388
	Chem. polish.	NaF	−0.616 ± 0.015	85.7	—	—	Impedance	32
Ag(110)	Electrochem. polish.	$NaBF_4$, $LiClO_4$	−0.734 ± 0.005	—	1.10–1.20	0.844×10^{15}	Impedance	24, 388
	Electrochem. polish.	NaF	−0.734 ± 0.005	~75.0	—	—	Impedance	395
	Chem. polish.	NaF	−0.735 ± 0.007	38.1	—	—	Impedance	32
Ag(311)	Electrochem. polish.	NaF	−0.664 ± 0.005	~50.0	—	0.724×10^{15}	Impedance	395
	Chem. polish.	NaF	−0.663 ± 0.008	74.0	—	—	Impedance	32
Ag(331)	Electrochem. polish.	NaF	−0.670 ± 0.010	—	—	—	Impedance	395
Ag(210)	Electrochem. polish.	NaF	−0.750 ± 0.010	—	—	0.536×10^{15}	Impedance	393

[a]BAW, bulk acoustic wave sensor.

to obtain the $E_{\sigma=0}$ values for pc-Ag/nonaqueous solution interfaces ($C_nH_{2n+1}OH$, n = 1 to 5)[371,372] and several butanol isomers (1–butanol, 2–butanol and 2–methyl–1–propanol) (Table 7).[373,374] Differential capacitance data have been treated using the Hurwitz–Parsons analysis to extract the coverage of specifically adsorbed Br^- as a function of electrode potential. The pzc values have been estimated from the data. Based on a quantitative comparison of spectral data at Ag and Au electrodes as a function of the rational potential, it is concluded that the solvent structure at Au electrodes resembles that previously proposed for Ag electrodes. The potential-dependent orientations of these solvents appear to be driven by interactions of the O nonbonding electrons and the alkyl chain with the electrode, and hydrogen bonding of the hydroxy group with specifically adsorbed Br^-. At potentials positive to the pzc at both metals, 1-butanol and 2-butanol hydrogen bond with specifically adsorbed Br^- with their alkyl moieties relatively close to the electrode surface. As more negative potentials are applied, Br^- is repelled from the surface, and the alkyl groups move away from the electrode surface as much as possible. Only minor changes in orientation are observed as a function of potential for 2-methyl-1 -propanol at these electrodes owing to the symmetry of its alkyl structure.[374]

The electrical double layer at an Ag electrode chemically polished in $H_2O + NaCN$[24] was studied using impedance and cyclic voltammetry.[375]

Table 7
Potentials of Zero Charge of pc-Ag in Nonaqueous Solutions

Solvent	Electrolyte	$E_{\sigma=0}$/V vs. aq. SHE	$E_{\sigma=0}$/V vs. BBCr	f_{PZ}	References
MeOH	0.4 M LiBr + 0.1 M $LiClO_4$	~–0.66[a]	~–0.10	—	371
EtOH	0.4 M LiBr + 0.1 M $LiClO_4$	~–0.76[a]	—	—	372
EtOH	$LiClO_4$	–0.54 ± 0.02	—	1.27	375
PrOH	0.4 M LiBr + 0.1 M $LiClO_4$	~–0.76[a]	—	—	372
1-butanol	0.4 M LiBr + 0.1 M $LiClO_4$	~–0.72[a]	—	—	373, 374
2-butanol	0.4 M LiBr + 0.1 M $LiClO_4$	~–1.08[a]	—	—	373, 374
2-methyl-1-propanol	0.4 M LiBr + 0.1 M $LiClO_4$	~–1.23[a]	—	—	373, 374

[a]By the Hurwitz–Parsons method.

The potential of the diffuse layer minimum (E_{min}) was independent of the ac frequency ν. The relative capacitance for the pc-Ag/EtOH + $LiClO_4$ interface was $f_\nu = C_{\nu=110\ Hz}/C_{\nu=1100\ Hz} = 1.27$, which indicates that the surface of chemically polished pc-Ag is to some extent crystallographically inhomogeneous. A noticeable dependence of E_{min} on c_{LiClO_4} has been found, indicating a weak specific adsorption of ClO_4^-, as for aqueous solutions of $LiClO_4$.[67,364,365] $E_{\sigma=0}$ at $c_{LiClO_4}=0$ was established by linear extrapolation of the $E_{min}(1/c_{LiClO_4})$ dependence to $1/c_{LiClO_4}=0$ (Table 7) and was found to be ≈ 150 mV more positive than $E_{\sigma=0}$ for pc-Ag in $H_2O + LiClO_4$.[375] Unfortunately, a direct comparison of absolute values of $E_{\sigma=0}$ for H_2O and EtOH is impossible because BBCr potentials in EtOH are not known. However, the small variation of $E_{\sigma=0}$ from EtOH to H_2O shows that the difference in lyophilicity of Bi, Hg, and Ag electrodes from H_2O to EtOH is not remarkable.[375]

(c) Ag single-crystal faces in aqueous solutions

Ag crystallizes in the same fcc system as Au, and its melting point is 1235 K. The electrical double-layer structure at Ag single-crystal faces has been studied extensively.[6,10,15,22,24,32,61,63,75,85,149–151,177a,188,250–252,376–441] Various procedures for preparation of the electrode surface have been used. Vitanov, Popov, and Sevastyanov *et al.*[61,151,376–382,394] have used electrodes electrolytically grown in a Teflon capillary, which they call "quasi-perfect" Ag(100) and Ag(111) planes, and the impedance-bridge method for recording the *C,E* curves. Valette and Hamelin [67,150,251,383–390] have used electrolytically polished Ag single crystals, and Trasatti *et al.* [15,32,85,149,177a,396–398,441] have used chemically polished (in $CrO_3 + H_2O$ solution) Ag crystal faces. In some experiments cyclic voltammetry was used to clean the Ag electrode surface,[258,400] but it was shown[402–404] that surface relaxation is probable after oxidation-reduction cycles. Lecoeur *et al.*[258] have shown that the Ag(111) and Ag(100) planes are stable if the potential is cycled in a well-defined potential region. Hamelin *et al.*[397] have shown that surface roughness increases if surface oxide reduction and hydrogen evolution take place. A method of thermal annealing (normally used with Au electrodes) was also used to prepare Ag single-crystal face electrodes,[392] but the experimental conditions of operation with Ag are much more critical than those with Au, mainly because of the higher affinity of Ag for oxygen.[6,405,406]

The influence of the crystallographic structure of Ag on the electric double-layer parameters has been discussed in many review papers[32,34,63,74,406,412]; for this reason, in this chapter only a concise survey of the experimental data is given. The more probable values of $E_{\sigma=0}$ for Ag single-crystal planes have been summarized in Table 6. The occurrence of weak specific adsorption of F^-, PF_6^-, and other anions (ClO_4^-, BF_4^-, SO_4^{2-}), has been the subject of many discussions.[5,6,10,15,31,32,34,149,150,177a,376–397]

Based on the shift of the diffuse layer minimum potential, Valette[150,251] has found that the adsorption of F^- anions is weak, increasing in the order of electrolyticaliy polished planes Ag(111) < Ag(100) < Ag(110). For the more dilute aqueous solutions ($c_{el} \leq 0.005$ M NaF or KF), the value of E_{min} was independent of the electrolyte.[150,251,388–390] In aqueous KPF_6 and KBF_4 solutions, E_{min} for Ag single-crystal planes was independent of c_{el} in the range 0.1 to 0.005 M and the Parsons–Zobel plots at $\sigma = 0$ were linear, with the values f_{PZ} very close to unity.[251,387–390] In 0.1 M NaF and $LiClO_4$ for Ag(111) and Ag(100), the E_{min} values were shifted ~20 mV and ~30 mV toward more negative E, respectively, and the Parsons-Zobel plots ($\sigma = 0$) were linear (within the interval of c_{NaF} from 0.005 to 0.04 M), with somewhat higher values of f_{PZ}. Specific adsorption of anions increases in the order $PF_6^- \leq BF_4^- \leq F^- < ClO_4^-$ for Ag(100) and Ag(111) (the same order as for Hg) and in the order $BF_4^- \leq PF_6^- < ClO_4^- < F^-$ for Ag(110).[150,251,387,388]

In the case of ClO_4^-, the activity of Ag electrodes increases in the sequence Ag(110) < Ag(100) < Ag(111), but for F^- in the reverse order. This was explained by the decrease in hydrophilicity in the order Ag(111) < Ag(100) < Ag(110) because the adsorption of the large structure-breaking ClO_4^- anion from H_2O at Ag surfaces is mainly caused by the squeezing-out effect. According to some authors,[24,74] the weak specific adsorption of F^- at Ag electrodes is mainly due to the metal-F^- interaction and this interaction seems to be energetically more favorable at stepped surfaces, i.e., at an Ag(110) surface.[24,74] Using polished (with CrO_3)Ag single-crystal electrodes, it was found that the weak specific adsorption of F^- increases in the order (110) ≤ (311)<(100)<(111),[15,32,149,177a] i.e., as the reticular density of planes increases. Probably the reverse order of planes can be explained by a less pronounced hydrophilicity of Ag(111) than Ag(110).

Vitanov and Popov *et al.*[151,377] have found on "quasi-perfect" surfaces that $E_{min} \neq f(c_{el})$ and have suggested that weak specific adsorption of ions

takes place at surface defects only.[151,381] The Parsons–Zobel plots were linear, with $f_{PZ} \approx 1.02$ for Ag(111) and Ag(100) (NaF, KF). Weak specific adsorption of anions increases in the order $F^- < SO_4^{2-} < ClO_4^-$; as noted,[381] the SO_4^{2-} anion adsorption takes place at steps only. It was demonstrated that with an increase of step density L at the electrode surface, the value of E_{min} shifts toward more negative E ($\Delta E = -100$ mV if L rises ~10×), and SO_4^{2-} adsorption increases also. At $L \rightarrow 0$, the value of $E_{min} \rightarrow -0.75$ V(SCE)for Ag(111). The shift of the $E_{\sigma=0}$ value ~50 mV toward more negative E for SO_4^{2-} compared with the value of $E_{\sigma=0}$ for F^- was explained by the nonsymmetric type of electrolyte and by a weak specific adsorption of SO_4^{2-} anions at Ag(111). The specific adsorption of ClO_4^- was more noticeable at Ag(100) than at Ag(111) [$\Delta E_{\sigma=0}$ is equal to –20 mV for Ag(111) and –40 mV for Ag(100)]. The Parsons–Zobel plot for Ag(111) was linear, with $f_{PZ} = 1.35$. For Ag(100), this dependence was nonlinear and this was explained by a higher specific adsorption of ClO_4^- at Ag(100) compared with Ag(111), as well as with F^- anions. The value of the Essin-Markov coefficient for ClO_4^- was equal to –20 mV for Ag(111) and –40 mV for Ag(100). A more pronounced shift of E_{min} toward more negative E for SO_4^{2-} than for ClO_4^- was observed with an increase in L at Ag surfaces. This effect was more pronounced for Ag(111) than for Ag(100). The more pronounced influence of L on SO_4^{2-} adsorption was explained by the higher negative charge density of SO_4^{2-} anions compared with ClO_4^-.[151,381]

Although the inverse slope of the Parsons–Zobel plot is often given the meaning of a roughness factor, it can be much higher than the actual roughness even if flat, perfect surfaces are used, provided small asperities of a critical size are present. This has been definitely proved by Guidelli *et al.*[75,250] in the case of Ag(111) surfaces by comparing experimental data with data simulated by means of an appropriate model for surface asperities.

The contradictions in the data presented[149–151,251,377–399] might be explained by different surface structures of electrodes, i.e., by various concentrations of surface defects that are claimed to be minimal on electrolytically grown Ag(111) and Ag(100), and somewhat higher on electrolytically and chemically polished electrodes.[15,32,177a,394] STM measurements were carried out on chemically polished macroelectrodes (real) and electrochemically grown (in 6 M $AgNO_3$ + 0.1 M HNO_3) microelectrodes in air, as well as under potential-controlled electrochemical conditions. The real macroelectrodes show a much higher surface

corrugation than the quasi-perfect microelectrodes, which have large atomically flat terraces separated by monoatomic steps.[235,416–422] At the surface of Ag electrodes prepared by thermal, chemical, or electrochemical pretreatment methods and by vapor deposition, a high density of crystal imperfections exists, especially the emergence of edge and screw dislocations, which lead to the appearance of mono- and multiatomic steps and a relatively high surface corrugation.[235,416–420] Much better-defined single-crystal silver and cadmium surfaces can be prepared by electrolytic growth,[423–425] and Ag(100), Ag(111), and Cd(1000) were found to be free of screw dislocations and atomically smooth. However, according to a recent work,[421] the surface structure of real Ag single-crystal faces was observed with STM to be very smooth and atomically perfect. For thermally grown and thereafter chemically polished Ag surfaces, the correct LEED pattern has been obtained.[422] However as noted[10,63,74,262] and experimentally shown,[264–266] the large difference of $E_{\sigma=0}$ values existing for the various faces should cause a marked dependence of E_{min} on the surface geometry and the crystallographic heterogeneity of the electrodes. However, the data in Table 6 demonstrate a surprisingly good agreement among the $E_{\sigma=0}$ values obtained by different groups.

$E_{\sigma=0}$ is found to depend on the crystallographic orientation of Ag faces, increasing with the atomic density of the faces. The dependence of $E_{\sigma=0}$ on the density of broken bonds on the surface of fee metals has been discussed by De Levie[426] and Trasatti and Doubova.[32] They found that $E_{\sigma=0}$ becomes less negative as the density of broken bonds increases.[32,426] These aspects are discussed in more detail in Section HI.

On the hydrophilicity scale of sp- and sd-metals, silver has been proposed either as a hydrophilic metal[15,32,64,391,405,411] comparable to Ga (from the magnitude of C_i values) or as a hydrophobic metal comparable to Hg (from the symmetry of the C_i,σ curve, high ionic adsorbility, and the heat of oxide formation).[150,388] The C_i,σ curves have been calculated,[150,387,388] and $C_i^{\sigma=0}$ increases in the sequence of planes Ag(111) < Ag(100) < Ag(110) as the reticular density of the planes decreases. This order of planes is in good agreement with the conclusions of Leiva and Schmickler,[428,429] who represented the metal as a jellium (with and without pseudo-potentials) and the electrolyte solution as an ensemble of hard sphere ions and dipoles.[430–435] According to this work,[428,429] the most compact plane should have the smallest, and the most open face the largest interfacial capacitance. This rule was found to be the electrochemical analog of the rule that the most compact plane has the highest electronic

work function.[3,5–7,15,32,406–410] The capacitance of the metal phase C_M of the Ag(111) face, and the capacitance of the solvent monolayer C_S have been studied by Amokrane *et al.*[122,414,415]

Good agreement between C_i and the dipole moment of the solvent (H_2O) molecules (i.e., by the hydrophilicity of metals) established by Trasatti [25,31] was found and the reasons for this phenomenon were explained.[428] The Valette and Hamelin data[150,251,387–391] are in agreement with the data from quantum-chemical calculations of water adsorption at metal clusters,[436–439] where for fcc metals it was found that the electrode-H_2O interaction increases as the interfacial density of atoms decreases.

The adsorption of aliphatic alcohols, which adsorb on metals with the hydrocarbon tail facing the electrode surface, shows different patterns on real Ag crystal faces[440,441] with respect to quasi-perfect single-crystal face electrodes.[442–444] This specific point will be discussed in detail in Section III.

According to Vitanov *et al.*,[61,151] C_i varies in the order Ag(100) < Ag(111), i.e., in the reverse order with respect to that of Valette and Hamelin.[24,63,67,150,383–390] The order of electrolytically grown planes clashes with the results of quantum-chemical calculations,[436,439] as well as with the results of the jellium/hard sphere model for the metal/electrolyte interface.[428,429,435] A comparison of C_i values for quasi-perfect Ag planes with the data of real Ag planes shows that for quasi-perfect Ag planes, the values of $C_i^{\sigma=0}$ are remarkably higher than those for real Ag planes. A definite difference between real and quasi-perfect Ag electrodes may be the higher number of defects expected for a real Ag crystal.[15, 32, 125, 401, 407–410, 416–422] Since the defects seem to be the sites of stronger adsorption, one would expect that quasi-perfect surfaces would have a smaller surface activity toward H_2O molecules and so lower $C_i^{\sigma=0}$ values. The influence of the surface defects on H_2O adsorption at Ag from a gas phase has been demonstrated by Klaua and Madey.[445]

The temperature dependence of the electrical double-layer parameters has been determined for real[393,398] as well as quasi-perfect Ag planes.[382,394] For quasi-perfect Ag electrodes, the value of $\partial E_{\sigma=0}/\partial T$ has been found to be higher for Ag(100) than for Ag(111), and so it was concluded that Ag(111) is more hydrophilic than Ag(100). For real surfaces,[382,385,386] $\partial E_{\sigma=0}/\partial T$ increases in the order (110) < (100) < (111). The same order of planes has been observed for Au.[446–448] $\partial E_{\sigma=0}/\partial T$ linearly increases as ΔX (interfacial parameter) decreases, i.e., as the hydrophilicity of Ag and Au electrodes decreases.[15,32,393,397,398,446–448]

Ag single-crystal face/electrolyte interfaces have been studied[449] by electroreflectance spectroscopy. The shift in transition energy E_{dip} with E is a direct measure of the potential gradient in the electrical double layer. It reflects the potential difference between the metal surface and the location of the maximum density of the surface state. In the region of $E_{\sigma=0}$, there is a marked change in the slope of the $E_{dip}(E)$ curve. For $\sigma < 0$, the slope is typically between 0.2 and 0.3 eV V^{-1}, while for $\sigma > 0$, the slope is between 0.9 and 1.2 eV V^{-1} for Ag and Au if there are specifically adsorbed anions in solution.[449,450] These results are in agreement with those obtained from surface plasmon excitation[451,452] and second harmonic generation (SHG)[453] experiments, in which the optical response varies with E much more at $\sigma > 0$ than at $\sigma < 0$. These effects show that at $\sigma > 0$ the perturbation of the metal's electronic properties is due to a closely packed layer of anions.

The electronic structure of Ag single-crystal face/H_2O + NaF interfaces has been studied by Chao *et al.*[454–456] by ellipsometry and differential capacitance. They found that the optical spectra at $E_{\sigma=0}$ vary strongly with the crystallographic orientation of the electrode surface, i.e., the bulk properties are different because of the anisotropy of n_0/m^* (the ratio of the free electron density to its effective mass). The adsorption tail height increases as the atomic roughness of the Ag surface increases in the order (111) < (100), which is the order of decrease in the corresponding $E_{\sigma=0}$ values.[15,32,63] The large variation of Δ with σ at $\sigma > 0$, which strongly depends on the crystal orientation, has been explained in terms of a strong anddifferent Ag/H_2O interaction. According to experimental data,[434–456] the Δ,σ dependence rises in the order Ag(100) < Ag(111), which can be explained by a more pronounced hydrophilicity of Ag(111) than Ag(100), or by a higher adsorption activity of F^- at Ag(111) than at Ag(100). A very small interaction of Ag with H_2O is possible.[454]

(iv) Gold

(a) Pc-Au in aqueous solutions

The electrical double layer at a pc-Au/H_2O interface has been studied mainly by Clavilier and Nguyen Van Huong,[213,256,457–464] Hamelin,[465–467] Beck *et al.*,[468–470] and others.[471,472] Detailed reviews have been given by Frumkin,[10] Hamelin,[63] and Vorotyntsev.[74] Only a few comments will be added here.

Table 8
Potentials of Zero Charge of pc-Au in Various Solvents

Solvent	$E_{\sigma=0}$/V vs. aq. SHE	$E_{\sigma=0}$/V vs. BBCr	References
H_2O + (NaF, $KClO_4$, $HClO_4$)	0.20	0.85	213, 462
NaF	0.16	0.81	465
DMSO + $LiClO_4$	0.39	0.99	473
	0.24	0.84	477
AN + KPF_6	0.90	1.49	392
PC + $NaClO_4$	0.44	1.11	473, 481
DMF + $LiClO_4$	0.51	1.02	310
MeOH + 0.4 M LiBr + 0.1 M $LiClO_4$	0.25[a]	0.81	482
1-butanol	−0.07[a]	—	374
2-butanol	0.17[a]	—	374
2-methyl-1-propanol	0.22[a]	—	374

[a]By the Hurwitz–Parsons method.

A diffuse-layer minimum was found at E = –0.04 V (SCE) for **pc-Au/H_2O (NaF, $KClO_4$, $HClO_4$)** (Table 8).[213,462] Its potential was independent of solution pH and c_{NaF}, but showed a slight negative shift with increasing c_{KClO_4} and c_{HClO_4}. The Parsons-Zobel plots at E_{min} gave an average slope $f_{PZ} \approx 2.0$ for NaF, but for $LiClO_4$ the linear region of these plots was very narrow. At $\sigma << 0$, only a small dependence of C_i on c_{el} was found, but at $\sigma \geq 0$, this dependence was remarkable. This was explained in terms of electrode surface contamination or weak specific adsorption of ClO_4^- ions.[256] It was concluded that the GCSG theory, taking into account the roughness factor, is applicable to pc-Au electrodes.[213,256,457–464] This conclusion has been questioned by Bagotskaya *et al.*[262] since the experimental results conform to the predictions of the independent electrode model [see Section II.2(iv)]. According to Hamelin,[467] the pc-Au spheres used by Clavilier[462] can be considered as nearly well-defined surfaces, but all the possible crystallographic orientations exist on such a surface.

The **pc-Au/H_2O** + NaF (0.01 to 0.5 M) interface has been studied by Zelinsky *et al.*[468] $E_{min} = -0.08 \pm 0.01$ V (SCE) with a small negative shift at higher c_{el} and f_{PZ} = 1.56 was found. Theoretical C,E curves were calculated. Since the agreement with the experimental curves was good,

it was concluded that the GCSG theory can be used to describe pc-Au/H_2O interfaces without any correction for the crystallographic inhomogeneity of the metal surface.

Zelinsky and Tolochko[471] have carried out an X-ray analysis of the electrode surface structure by using synchrotron radiation. A fraction of an amorphous state has been found on the surface of mechanically renewed electrodes. In addition, crystalline faces of low indices are present on the pc-Au surface with a characteristic size of about 5 to 6 nm and fractions of surface area are different from those for annealed samples. However, the conclusion has been that the effect of the crystallographic inhomogeneity of the electrode surface does not dominate the electrical double-layer capacity. This conclusion is questionable because a size of 5 to 6 nm is large enough to induce effects of surface crystallographic inhomogeneity [see Section II.2(iv)].

The E_{min} obtained for pc-Au does not correspond to $\bar{\sigma}_{PC} = \Sigma_i \theta_i \sigma_i = 0$, and C_i at E_{min} does not correspond to $C_i^{\sigma=0}$.[10,67,262,263]

(b) Au in nonaqueous solutions

The electrical double-layer structure at a pc-Au/DMSO + $LiClO_4$ surface has been studied by Jarzabek and Borkowska.[473] The value of E_{min} (Table 8) was independent of c_{el} and ν. The capacitance of the pc-Au/DMSO interface is far lower than that of the Hg/DMSO interface, except at $\sigma << 0$, where it is almost the same for Au, Hg, Bi, In(Ga), TI(Ga), and Pt.[334,473–476] $f_{PZ} = 1.2$, as well as C_i at $\sigma = 0$ and at $\sigma << 0$ have been obtained.[473]

The electrical double-layer structure at Au(111), Au(110), Au(100), and Au(210) faces and at a pc-Au electrode has been studied in 5×10^{-3} and 1×10^{-2} M $LiClO_4$ solutions in DMSO by cyclic voltammetry and impedance methods.[477] The electrodes were cleaned by heating in a flame; they were cooled and transferred to the cell under pure Ar.[63,186,392] The hanging electrolyte method was used.[478] For all faces as well as for pc-Au, E_{min} shifted positively with time t, but this was independent of the negative limit of E.[477] The evolution of the capacitance C_{min} at E_{min} differs from one face to another: for (100) and (210), C_{min} increases with time; for (111) it generally decreases for 3 and 4 min and then increases. As a consequence of this phenomenon, the reproducibility of the C,E curves was difficult to estimate. After about 1 hr, pseudo-stable C,E curves were established. In general, the negative sweeps of the C,E curves are almost identical to the

positive sweeps. Only for Au(l00) was a slight hysteresis with E found, which disappeared when the potential cycling was limited to $E \geq -0.9$ V (SCE in H_2O); this is typical behavior for the Au(l00) orientation in aqueous solutions.[63]

The value of E_{min} in the pseudo-stable state has been found to increase in the sequence (111) ≤ (100)<pc-Au ≤ (110) < (210), and this sequence is reversed with respect to Au single-crystal faces in aqueous solutions. It has been concluded that the Au–DMSO interactions vary much more with the atomic structure of the gold surface than the Au–H_2O interactions and that the Au–DMSO interactions are stronger than for H_2O.[477] Following Trasatti's relation,[7] the values of $\Delta(\delta\chi_M - \delta\chi_S)$ have been obtained for different planes of Au. It has been found that the difference $(\delta\chi_M - \delta\chi_S)$ for Au(110) and Au(111) planes is greater than 0.5 V.[477] It should be noted that the same order of Au(111) and Au(210) has been found in a 2.5×10^{-3} M KPF_6 + AN solution.[63,392,477]

The electrical double-layer at a pc-Au/AN interface has been studied by impedance. pc-Au, flame treated and cooled in Ar, was transferred to the cell in an Ar atmosphere.[186,392] The C,E curve showed a minimum at 0.42 ± 0.03 V vs. $Ag/AgNO_3$ (0.01 M) in AN containing KPF_6 to avoid liquid junction potentials. The corrected value of $E_{\sigma=0} = 0.65$ V (SCE in H_2O) or $E_{\sigma=0} = 1.49$ (BBCr) has been compared with the $E_{\sigma=0}$ values for Hg, Pb, Ga, Bi, and In(Ga) in a surface-inactive ($LiClO_4$) electrolyte. In contrast to the Au/DMSO interface, the value of E_{min} for the Au/AN interface was somewhat higher than that for In(Ga), Ga, Bi, and Hg.[120,479,480] The σ,E curve is linear in the range of E studied,[392] and as for Hg, T1(Ga), In(Ga), Ga, Pb, and Bi,[7,25,120,480] the interaction of AN with pc-Au appears to be small.

The pc-Au/propylene carbonate (PC) + $NaClO_4$ interface has been studied by Nguyen Van Huong.[481] A flame-annealed ($O_2 + H_2$) pc-Au sphere was used. Before each experiment the pc-Au electrode was cleaned in an $NaClO_4$ aqueous solution by a few potential cycles involving oxidation-reduction of the surface until the i,E and C,E curves exhibited stable character. The C,E curves were recorded in the interval $15 \leq \nu \leq 150$ Hz, where the capacity dispersion does not exceed 10%. According to the experimental results, E_{min} depends slightly on c_{NaClO_4}, and at $\sigma << 0$ it decreases with the dilution of the solution. The Parsons–Zobel plot at E_{min} showed an inverse slope, $f_{PZ} = 2.22$. The values of $C_i^{\sigma=0}$ and $C_i^{\sigma<<0}$, calculated according to the GCSG model, are noticeably lower than those for pc-Au/H_2O[481] or for Hg/PC.[312] In contrast to pc-Au/H_2O, the depend-

ence of C_i on σ was rather weak for pc-Au/PC; and this was explained by a less pronounced reorientation of the adsorbed propylene carbonate molecules compared with the adsorbed H_2O dipoles.

Data for the pc-Au/DMF + $LiClO_4$ interface have been collected by Borkowska and Jarzabek.[109] The value of $E_{\sigma=0}$ was found to be 0.27 V (SCE in H_2O) and the roughness factor f = 1.3 (Table 8). Unlike Hg, Bi, In(Ga), and Tl(Ga) electrodes and similarly to the Ga/DMF interface, the inner-layer capacity for pc-Au in DMF depends weakly on σ, and thus the effect of solvent dipole reorientation at pc-Au is less pronounced than at In(Ga), Bi, and other interfaces.

The pc-Au/MeOH interface has been studied by Brzostowska-Smolska and Mine.[482] The $E_{\sigma=0}$ was found at 0.013 V (SCE in H_2O) and this value was independent of c_{el}.

Surface-enhanced Raman scattering and differential capacitance have been used to study the interfacial solvent structure in LiBr solutions of three isomers of butanol—1-butanol, 2-butanol, and 2-methyl-l-propanol—at pc-Au electrodes.[374] The potential-dependent spectral behavior in the regions containing the ν(C-C), ν(C-O), and ν(C-H) modes of these isomers at pc-Au electrodes has been compared with that observed at pc-Ag electrodes[371,373] as a function of rational potential. The differential capacitance measurements were made at smooth pc-Au, while SERS measurements were made at electrochemically roughened pc-Au. The differential capacitance data were treated using the Hurwitz–Parsons method[483,484] to obtain the surface coverage of specifically adsorbed Br^- as a function of E. The values of $E_{\sigma=0}$ were estimated from these data by extrapolation of the Γ_{max},E_{min} dependence to $\Gamma_{max} = 0$. The $E_{\sigma=0}$ values were consistent with those obtained from a qualitative evaluation of the impedance data,[374] and fall approximately between the Br^- adsorption and the solvent reorientation peaks, as expected. The value of the limiting surface coverage of Br^- at pc-Au increases in the order of solvents: 2-butanol < 2-methyl-l-propanol < 1-butanol; and in the order of electrodes: pc-Au < pc-Ag.[374]

(c) Au single crystal faces in aqueous solutions

Au crystallizes in the same system (fcc) as Ag; accordingly, the (111), (110), (311), and (210) faces should exhibit an extreme behavior.[24,63,391.485,486] Its electronic structure is $5d^{10}6s^1$, with the 5d band complete. The Au melting point is 1336 K.

Since the early 1960s single-crystal gold electrodes have been the object of extensive studies.[15,24–26,32,63,74,188,247,257,391,412,485–552] Since the early results (1960–1980) have been summarized and discussed,[15,24,32,63,74,188,412,485–488,534] only a few more recent works will be discussed in this review. Experimental data obtained by cyclic voltammetry, electrochemical impedance, scanning tunneling microscopy, atomic force microscopy, surface X-ray scattering (SXRS), and other techniques show that the electrical double layer and interfacial properties depend strongly on the crystallographic structure of the electrode surface, and the surface charge density, as well as the chemical composition of the solvent and the electrolyte. It has been found that the value of $E_{\sigma=0}$ increases in the order (110) < (100) < (111), i.e., as the reticular density of planes rises.[15,24,32,63,74] As demonstrated by Hamelin,[502] De Levie,[426] and Trasatti,[6,7,32] a good correlation exists between $E_{\sigma=0}$ and the number of broken bonds per atom on an fcc metal surface, as well as between $E_{\sigma=0}$ and the crystallographic orientation of the faces (see Section III for more details).

In the 1970s it was observed that for Au(100) in 0.1 M KI and Na_2SO_4 solutions, the form of the C,E curve depends on the negative limit of E explored.[32,63,553,554] Later, it was observed that this phenomenon exists for all Au faces,[63,247,495,506] except (210).[467,491,513,514] It has been suggested by comparison with UHV observations[526–531] that the origin of this phenomenon is an alteration of the ideal atomic structure of the Au face. It should be noted that most of the results before 1980 were obtained with gold faces isolated by a noncontaminating resin and cycled before use at 20 or 50 mV s^{-1} in dilute Na_2SO_4 or H_2SO_4 solutions until a stable, reproducible CV was obtained.[24,63,74] From 1980 onward, most of the results were obtained after a flame annealing treatment was applied in a way similar to that originally used for ordered Pt electrodes.[186] The surface cleanliness achieved by this method allowed investigations to be made in a meaningful way during the first or initial scans of the CV.

Over the past 10 years it has been demonstrated by a variety of *in situ* and *ex situ* techniques[187,188,485,487,488,534] that flame-annealed Au faces are reconstructed in the same way as the surfaces of samples prepared in UHV,[526–534] and that the reconstructed surfaces are stable even in contact with an aqueous solution if certain precautions are taken with respect to the potential applied and the electrolyte composition.[485,487,488] A comprehensive review of reconstruction phenomena at single-crystal faces of various metals has been given by Kolb[534] and Gao *et al.*[511,513]

In many works[471,505,512,516–518] the Au(100)/electrolyte interface has been studied using STM and impedance simultaneously. In a slightly adsorbing electrolyte ($HClO_4$), the bulk termination structure has been found to prevail at $E \sim E_{\sigma=0}$, whereas at $\sigma < 0$ the formation of a reconstructed structure featuring an approximate (5×27) unit cell, 14-atom close-packed strings and other structural mutations have been observed.[467,505,510,516] This reconstruction is similar to the so-called "hex" reconstruction, which occurs spontaneously on clean Au(100) in UHV.[527–531] In a $HClO_4 + H_2O$ solution, charge-induced changes are slow[257,504,508,510] and when σ is positive, the surface atoms slowly go back to the symmetry of the underlying lattice.

For Au(111) in nearly nonadsorbing solutions ($0.1\ M\ HClO_4$) at E = –0.3 V (SCE), a reconstruction similar to that existing in UHV has been detected by STM, while at $\sigma > 0$ the (1×1) structure has been observed.[188,467,538] At $\sigma > 0$, strings and clusters of atoms disappearing with time have been found on the deconstructed surface. Therefore the more positive $E_{\sigma=0}$ value is probably related to the reconstructed surface (Table 9).[188,487,488]

The surface reconstruction of Au(110) is more rapid than that of Au(111) and Au(100).[257,467,504–514,516–518] Au(533) and Au(311), localized in the [(110)-(100)] zone, and Au(221) and (331), localized in the [(111)-(110)] zone, exhibit stable terrace step structural arrangements largely free from disordering and facetting.[485] Au(210) and (410), localized in the [(100)-(110)] zone, display only a short-range structural order related to the especially "open" nature of these faces.

The fractality plot [i.e., $n(E)$ plot] showed[273] for Au(210) $1 < n < 0.95$ in the whole E range, but the deviation from ideal ($n = 1$) is rather small. The deviation depends on E, and this indicates that other factors, not necessarily related directly to the surface uniformity or topography, may influence the fractal behavior of solid electrodes.[274] As noted by Hamelin,[273] other factors can be the inelastic relaxation of charge-induced surface stresses or a relaxation of molecules and ions in the electrical double-layer. The deviation of the $Au(210)/H_2O$ interface from the ideal is largest at small positive surface charges. The relaxation has been explained in terms of reorientation of H_2O molecules at the potential of the inner-layer maximum. Tentative conclusions do not rule out some contribution from the mechanical relaxation of the metal surface, whose mechanical (damping) properties also depend on σ and c_{el}, as verified for metal–gas[556] and electrochemical systems.[557]

Table 9
Potentials of Zero Charge of Au Single-Crystal Faces in Aqueous Solutions

Electrode	Solution	$E_{\sigma=0} \pm 0.01$/V vs. SHE	Method	References
Au(111)	0.05 to 0.2 M NaF	0.56	Impedance	24, 63
Au(100)	0.05 to 0.2 M NaF	0.33	Impedance	516
	0.05 to 0.2 M NaF	0.30	Impedance	24, 63
Au(110)	0.05 to 0.2 M NaF	0.19	Impedance	24, 63
Au(210)	0.05 to 0.2 M NaF	0.11	Impedance	24, 63
Au(311)	0.05 to 0.2 M NaF	0.25	Impedance	24, 63
Au(111) (22 × √3)	0.1 M H_2SO_4	0.56	Impedance	188,488,538
	0.1 M $HClO_4$	0.55	Immersion	140
	0.01 M $HClO_4$	0.58	Impedance	140
Au(111) (1 × 1)	0.1 M H_2SO_4	0.47	Impedance	538
Au(100) "hex"	0.1 M H_2SO_4	0.54	Impedance	188, 488, 538
Au(100) (1 × 1)	0.1 M H_2SO_4	0.32	Impedance	188, 488, 538
(755)	NaF, $LiClO_4$	0.40	Impedance	561
(11.9.9)		0.47	Impedance	561
(433)		0.43	Impedance	561
Au(111)	0.01 M $HClO_4$	0.47	Voltammetry	525
Au(100)	0.01 M $HClO_4$	0.29	Voltammetry	525
Au(110)	0.01 M $HClO_4$	0.19	Voltammetry	525

According to the data obtained with SXRS in salt solutions,[519,520] at $\sigma < 0$ the surface of Au(111) forms a $(\sqrt{3} \times 22)$ structure as in a vacuum. At $\sigma > 0$ the reconstruction disappears and the (1 × 1) structure is observed. On the reconstructed Au(111) surface there are 4.4% more atoms than on the (1 × 1) structure and on the reconstructed Au(100) there are 24% more atoms than on the (1 × 1) structure.[506,519] This phase transition shifts in the negative direction with the adsorbability of the anion. The adsorption-induced surface reconstruction of Au(111) electrodes has been studied *in situ* by second harmonic generation by Pettinger *et al.*[521]

According to LEED, X-ray diffraction, electron microscopy, and STM studies, Au(110) is reconstructed in UHV and (1 × 2) and (1 × 3) symmetries are observed.[519,520,527–531] In contact with 0.1 M $KClO_4$ at $\sigma <$

0, stacked sets of parallel ribbon segments have been observed using STM along the [1$\bar{1}$0] direction.[467,504] Shifting the potential in the positive direction results in the disappearance of the reconstructed surface within a few seconds and formation of the (1 × 1) structure. These potential-induced structural changes are reversible and rapid; the reconstructed surface forms 2 s after the potential is moved from $\sigma > 0$ to E = –0.3 V (SCE).

According to Kolb *et al.*[538,540] the reconstruction of an Au(111) surface involves a 4% compression along one of the three [110] directions, which yields a (1 × 23) superstructure pattern in LEED[538] and imposes a twofold symmetry on top of the threefold one.[540] The STM images of a reconstructed Au(111) surface show pairwise arranged corrugation lines[541] with a periodicity of approximately 6.4 nm and a corrugation height of about 0.02 nm. A reconstructed Au(111) electrode has an $E_{\sigma=0}$ that is about 90 mV more positive than that of the unreconstructed Au(111) (Table 9).[488]

A freshly prepared flame-annealed Au(100) surface has been found to be reconstructed[188,487,534,538] and the surface atoms exhibit a hexagonal close-packed structure to yield the (hex)-structure. One-directional long-range corrugation of 1.45 nm periodicity and 0.05 nm height has been found on the Au(100) surface.[188,488] When the reconstruction is lifted due to specific adsorption of SO_4^{2-} anions at more positive E, the surface changes to a (1 × 1) structure.[538]

The influence of the cooling procedure after flame annealing has been studied.[541] The crystal was allowed to cool in air for several minutes. Thereafter the electrode was immersed in the electrochemical cell (0.1 M H_2SO_4) under potential control at about –0.2 V (SCE). The Au(100) surface was clean, well-ordered, and completely reconstructed.[538,541] In a second experiment, after flame annealing, the Au(100) electrode was allowed to cool in air for about 4 s before being quenched in ultrapure H_2O. The electrode was transferred into the electrolyte (0.1 M H_2SO_4) at E = –0.2 V (SCE) in a droplet of H_2O. The reconstruction rows covered about 70–80% of the total surface, but on some parts of the surface the reconstruction had been lifted upon contact with the electrolyte, and on some places monoatomic Au islands were found.[538] After a potential cycle up to 0.25 V (SCE), the reconstruction was lifted by specific adsorption of SO_4^{2-}. The unreconstructed surface is covered with small monoatomic gold islands, which are formed out of the more densely packed (hex) structure. These islands are roughly 1–2 nm in diameter, but they grow

with time owing to surface diffusion (two-dimensional Ostwald ripening).[538,541,542]

Finally, after flame annealing, the gold crystal was immediately quenched in ultrapure water in order to eventually reduce the danger of surface contamination in air, and immersed into the 0.1M H_2SO_4 solution at $E = -0.2$ V (SCE). According to STM studies,[538,540,541] this treatment yields a highly disordered surface that seems to be in a rather unreconstructed state. The subsequent application of a positive scan to eventually lift existing areas with a (hex) structure did not produce extra gold islands, supporting the view that a rapid quenching does not yield reconstructed surface areas of any significant extent.

The phenomenon of surface diffusion has been studied[538]: the rate of electrochemical annealing increases with E and is higher for strongly adsorbing anions. A few oxidation-reduction cycles change the surface topography by creating monoatomic deep holes that are more or less uniformly distributed over the terraces. These holes increase considerably in size at each successive oxidation-reduction cycle; they merge and form channels, while the number of newly created monoatomic deep holes remains small. The growth of the holes did not reflect any preferential crystallographic orientation. However, the merging and formation of channels suggest a preferential removal of the substrate material between neighboring holes during the oxidation-reduction cycle.[538]

Kolb and Franke have demonstrated how surface reconstruction phenomena can be studied *in situ* with the help of potential-induced surface states using electroreflectance (ER) spectroscopy.[449,488,543,544] The optical properties of reconstructed and unreconstructed Au(100) have been found to be remarkably different. In recent model calculations it was shown that the accumulation of negative charges at a metal surface favors surface reconstruction because the increased sp-electron density at the surface gives rise to an increased compressive stress between surface atoms, forcing them into a densely packed structure.[532]

A modified immersion method has been used by Hamm *et al.*[140] to obtain $E_{\sigma=0}$ of an Au(111) electrode. Clean and well-ordered Au(111) electrodes were prepared in a UHV chamber, transferred to an electrochemical cell by a closed-transfer system, and immersed in 0.1 M $HClO_4$ solution at various £. $E_{\sigma=0}$ was derived from the charge flowing during the contact with the electrolyte under potential control. For the reconstructed Au(111)-$(22 \times \sqrt{3})$/0.1 M $HClO_4$ interface, $E_{\sigma=0} = 0.31 \pm 0.04$V (SCE) (Table 9). Using the impedance method, $E_{\sigma=0} = 0.34$ V (SCE) for recon-

structed Au(111)/0.01 M $HClO_4$ has been obtained.[538] The 30-mV shift of $E_{\sigma=0}$ has been explained by weak specific adsorption of anion.[140]

The behavior of Au faces in pH > 7 solutions has been studied.[24,63,391,545–546] Surface oxide formation is a two-step process: a peak at a less positive E has been explained by OH^- specific adsorption[24,63,188,391,485,547]; that at a more positive E in terms of irreversible oxide formation by examining the negative moving i, E profile at various Es.[501,548]

The specific adsorption of OH^- ions depends on the electrode surface structure increasing in the order Au(111) < Au(100) < Au(311).[391] The similarity of the results obtained in alkaline solutions and those observed in acid and neutral media have led the authors of many papers to conclude that surface reconstruction occurs at $\sigma < 0$ and is removed at $\sigma > 0$.

The temperature behavior of low[446,491,503,558] as well as high Miller index crystal faces of Au[447,448] has been examined in 0.01 M perchloric acid solutions. For all gold surfaces studied, C_{min} was found to decrease and $E_{\sigma=0}$ moved to less negative values with increasing T.[446–448,491,503,558] $E_{\sigma=0}$, T plots were found to be linear: values of $dE_{\sigma=0}/dT$ are presented in Table 10. The values of $E_{\sigma=0}$ were in good agreement with those obtained by Lecoeur *et al.*[559] for the same faces. For the faces of the same zone, the values of $E_{\sigma=0}$ are less positive the higher the step density on the surface.[24,63,446–448,503,558]

The faces situated in the [01$\bar{1}$] zone—(511), (311), (533), (755)—exhibit the lowest values of $dE_{\sigma=0}/dT$, while the faces situated in the other two zones ([001] and [1$\bar{1}$0]) have approximately similar values of $dE_{\sigma=0}/dT$, though slightly higher for the [1$\bar{1}$0] zone.[446–448,558] The values of the temperature coefficient obtained for the three singular faces are the highest, which confirms earlier observations that the introduction of steps lowers the values of both $E_{\sigma=0}$ and $dE_{\sigma=0}/dT$. $dE_{\sigma=0}/dT$ increases for the following step-terrace combinations: (111)-(100) < (100)-(110) < (111)-(111); i.e., the decrease in $dE_{\sigma=0}/dT$ is higher because the step orientation is different from the terrace orientation. This effect has been explained by Lecoeur *et al.*[559] with a model in which the adsorption of the solvent dipoles on steps occurs with the oxygen atom away from the metal, thus leading to a positive contribution of the solvent dipole to the potential and to a simultaneous reduction in the metallic dipole moment. This effect has been considered to be larger for quaternary sites of Au(100) than for ternary sites of Au(111).

Table 10
$E_{\sigma=0}$ at 298 K and $dE_{\sigma=0}/dT$ for Au Single-Crystal Faces in 0.01 M $HClO_4$ Aqueous Solutions

Miller index of the face	Lang notation	$E_{\sigma=0}$ ± 0.01/V vs. SHE	$dE_{\sigma=0}/dT$/mV K^{-1}
(111)	—	0.52	2.3
(332)	6(111)-(111)	0.22	0.5
(331)	3(111)-(111) 2(110)-(111)	0.22	0.6
(771)	7/3(111)-(111)	0.18	0.7
(100)	—	0.29	1.0
(511)	3(100)-(111)	0.22	0.2
(311)	2(100)-(111) 2(111)-(100)	0.24	0.05
(533)	4(111)-(100)	0.31	0.2
(110)	2(111)-(111)	0.20	0.9
(320)	3(110)-(100)	0.13	0.4
(210)	2(100)-(110) 2(110)-(100)	0.12	0.5
(410)	4(100)-(110)	0.20	0.6

Source: Silva, Sottomayer, and Martins, *J. Chem. Soc. Faraday Trans.* **92**, 3695, Table 1. Reproduced with permission of The Royal Society of Chemistry.

Owing to the smoothing effect suggested by Smoluchowski,[560] a separate account of the effects of steps and terraces is not possible for the faces studied, since the terrace width is not larger than six Au atoms.[561] However, the randomizing effect of an increased dT is certainly smaller for more strongly adsorbed dipoles on steps than for dipoles adsorbed on terraces. According to the results,[64,561,562] the (110), (311), and (111) faces are reconstructed in a vacuum while the (1 × 1) structure is present in solution near $E_{\sigma=0}$. The $(\sqrt{3} \times 22)$ surface reconstruction of the Au(111) face under UHV has been described previously using LEED[140] and STM.[188,471,538,545] It has been shown[562] that the Au vicinal planes of the n(111) × (100) type, situated on the $[01\bar{1}]$ zone between the (111) and (755) ⇔ 6(111) × (100) faces, have an identical atomic structure in solution and in UHV [faceted or (1 × 1) structure]. Crystal faces, such as (11,9,9) ⇔ 10(111) × (100) or (433) ⇔ 7(111) × (100) for example, show an electrochemical behavior similar to that of a surface consisting of (755)

and (111) faces. The (111) and (755) orientations have their own $E_{\sigma=0}$, and so each vicinal face has a pseudo-pzc $E_{p,\sigma=0}^{Au(hkl)}$. Unlike a true $E_{\sigma=0}$, the value of $E_{p\sigma=0}$ cannot be determined directly using the *C*,*E*-curve method since the C_{min} observed in dilute solution does not correspond to the pseudo-pzc of the vicinal face studied. A method for the determination of $E_{p,\sigma=0}^{Au(hkl)}$ has been developed.

A plausible explanation for the apparent contradiction of views[24,63,188,467,487,488,519,520,552] has been offered by Kornyshev and Vilfan.[563] On the basis of model calculations for noble metal (110), (111), and (100) faces, an interplay has been demonstrated between a direct effect of the electric field and field-induced ionic adsorption. A phase diagram in the charge-temperature plane has been obtained theoretically[563] which shows that deconstruction from the (1 × 2) phase to the (1 × 1) phase as σ changes to more positive values proceeds via three transitions. Starting at negative potentials and going toward positive *E*, the surface first constructs to a disordered phase by an order-disorder Ising transition and thereafter undergoes a roughening transition of the Kosterlitz-Thouless universality class. Finally, at more positive charge, deroughening of the electrode surface takes place by another transition to the 1 × 1 phase. The range of σ within which the intermediate surface state exists is $1\ \mu C\ cm^{-2}$. The interaction of the surface with fluctuating H_2O molecules may affect the phase transitions. The double-humped structure of the *C*,*E* curve for Au(110) has been related to the difference in the pattern of molecular reorientations on the two different surface configurations: the hump at more positive *E* is composed of two peaks, one of which is due to the deroughening of the Au(110) surface to the (1 × 1) phase structure. The missing spike at the ordering transition to the (1 × 1) structure has been explained by the existence of water feedback but it might be only an extra smeared maximum with a width one-fourth of the separation between the humps.[563]

(v) Copper

(a) Pc-Cu in aqueous solutions

Pc-Cu samples as well as single-crystal planes have been studied[564–587] in contact with various aqueous electrolyte solutions. The data are somewhat controversial, since the main experimental difficulty with Cu is its great tendency to surface oxidation. The potential of the minimum in *C*,*E*

curves depends on the electrolyte as well as on the method of surface preparation[564–566,568] and lies at small negative E (Table 11), i.e., outside the region of ideal polarizability of Cu electrodes. This minimum probably corresponds to Cu covered with surface oxides.

Using the open-circuit potentiostatic scrape method, remarkably negative values of $E_{\sigma=0}$ have been obtained for fresh pc-Cu electrodes.[141,570,580] According to these data, the value of $E_{\sigma=0}$ for pc-Cu is independent of the nature of nonadsorbed electrolytes (NaF, Na_2SO_4), while it becomes more negative in the sequence $NaClO_4$ < NaF < Na_2SO_4 < NaCl < NaOH < KI. Adsorption of SO_4^{2-} has been confirmed by radiotracer and SERS studies.[581,582] $E_{\sigma=0}$ is independent of the nature of the cation.[141,580] Using an immersion method, Turowska and Sokolowski[583] have found $E_{\sigma=0} = -0.06$ V (vs. Ag/AgCl in 0.01 M LiCl) in 0.01 M sulfate solution. Although the pzc has been found to be independent of pH between 2 and 8.5, and the authors rule out surface oxidation, the value falls suspiciously close to the high range of pzc values.

Electroreflectance data for pc-Cu[579] confirm that the capacity minimum at $E = -0.2$ to -0.3 V (SCE) is due to the oxidation of the electrode surface. According to impedance data,[564,565] as for pc-Ag and pc-Au,[63,67,74] the roughness factor for a pc-Cu electrode is approximately 2, which has been explained by the high surface inhomogeneity of the electrode surface.

Using impedance data of TBN^+ adsorption and back-integration,[259,588] a more reliable value of $E_{\sigma=0}$ was found for a pc-Cu electrode[574,576] (Table 11). Therefore, differences between the various $E_{\sigma=0}$ values are caused by the different chemical states and surface structures of pc-Cu electrodes prepared by different methods (electrochemical or chemical polishing, mechanical cutting). Naumov *et al.*[585] have observed these differences in the pzc of electroplated Cu films prepared in different ways.

(b) Cu single-crystal faces in aqueous solutions

Cu crystallizes in the fcc and its melting point is 1356 K. The experimental data for single-crystal Cu/H_2O interfaces are also controversial.[567–570,572–578] The first studies with Cu(111), Cu(100), and Cu(110) in surface-inactive electrolyte solutions (NaF, Na_2SO_4) show a capacitance minimum at E less negative than the positive limit of ideal polarizability of Cu electrodes (Table 11). E_{min} depends on the method of surface

Table 11
Double-Layer Parameters of Cu in Aqueous Solutions

Electrode	System	E_{min}/V vs. SHE	$E_{\sigma=0}$/V vs. SHE	f_{PZ}	Atomic density/cm^{-2}	Method	References
pc-Cu	0.001–0.1 M NaF	0.09	0.09	—		Impedance	571
	0.1 M NaF	—	0.50	—		oc Scrape	9, 141
	0.050 M Na_2SO_4 + TBN^+	—	−0.64 ± 0.05	—		Impedance	576
Cu(111)	0.007–0.05 M NaF	−0.01	−0.01	2.0	1.772×10^{15}	Impedance	572
	0.050 M Na_2SO_4 + TBN^+	—	−0.33 ± 0.02[a]			Impedance	576
	0.001–0.04 M $KClO_4$	−0.20 ± 0.01	−0.20 ± 0.01	1.0		Impedance	578
Cu(100)	0.007–0.05 M NaF	−0.04	−0.04	2.0	1.535×10^{15}	Impedance	572
	0.050 M Na_2SO_4 + TBN^+	—	−0.46 ± 0.05[a]			Impedance	576
	0.001–0.04 M $KClO_4$	−0.54 ± 0.01	−0.54 ± 0.01	1.0		Impedance	578
Cu(110)	0.007–0.1 M NaF	−0.07	−0.071	2.0	1.084×10^{15}	Impedance	572
	0.05 M Na_2SO_4 + TBN^+	—	−0.63 ± 0.05[a]			Impedance	576
	0.005 M $NaClO_4$	−0.69 ± 0.01	−0.69 ± 0.01			Impedance	587

[a]By back-integration.

preparation (electrochemical polishing, selective chemical polishing).[564,571–578] E_{min} decreases as the reticular density of the plane increases. Thus the difference between $E_{\sigma=0}$ for various planes is approximately 200 mV and the value of E_{min} for pc-Cu is somewhat less negative than E_{min} for the plane with the less negative value of $E_{\sigma=0}$.[571]

The applicability of the GCSG theory to Cu single-crystal face electrodes has been tested[572] by the Parsons-Zobel method. At E_{min}, f_{PZ} is equal to 2 and this large value has been explained by the joint effect of a large surface roughness and the energetic inhomogeneity of the faces. However, it is thought that the large value of f_{PZ} can be explained by the surface oxidation of Cu electrodes. The same tendency has been found for electropolished single-crystal faces of Bi, slightly oxidized at moderate anodic potentials in neutral surface-inactive electrolyte solutions, for which the value of the reciprocal slope of the PZ plot increases as the oxidation of Bi takes place.[588a]

More reliable values of $E_{\sigma=0}$ for Cu single-crystal faces have been obtained by Lecoeur and Bellier[578] with electropolished Cu(111) and Cu(100) in $NaClO_4 + H_2O$ solutions (Table 11). E_{min} has been found to be independent of c_{NaClO_4} and ν, i.e., ClO_4^- anions are surface inactive at Cu single-crystal faces. The Parsons-Zobel plots are linear, with values of f_{PZ} very close to unity. Foresti *et al.*[587] have been able to study the Cu(110)/aqueous solution interface by impedance as well as chronocoulometry. These authors have found $E_{\sigma=0} = -0.93 \pm 0.01$ V (SCE). Also, the validity of the GCSG model has been verified.

As for Zn single-crystal electrodes, reliable values of $E_{\sigma=0}$ have been obtained indirectly from the dependence of the adsorption-desorption peak potential E^{max} of TBN^+ on the crystallographic orientation.[574,576] It has been found that E^{max} shifts toward more negative potentials in the sequence Cu(111) < Cu(100) < Cu(110), and this order is related to the increase of $E_{\sigma=0}$ for the corresponding face. Thus the value of $E_{\sigma=0}$ decreases as the atomic density of the face decreases, which is in good agreement with the general behavior observed with fcc metals (Au, Ag)[15,24,63] (see Section III for more details). Romanowski[589] has attempted theoretical calculations of the capacitance and work function of Cu faces.

Reconstruction of the Cu(111) close-packed surface at room temperature upon oxygen adsorption has been reported by Niehus.[590] This result is in good agreement with data on cyclic voltammetry and second-harmonic generation[591]; it has been concluded that oxygen-containing spe-

cies are present on the Cu(111) surface, which implies that the Cu(111)/ $H_2O + NaClO_4$ (pH~7) interface is not ideally polarizable in the electrical double-layer region.

In situ atomic force microscopy has been used to study the interfacial properties of the low-index faces of Cu single crystals in aqueous H_2SO_4 and $HClO_4$ solutions.[592,593] Cu(111) has been found to exhibit the correct hexagonal structure in $H_2O + HClO_4$ solution (pH = 1 to 3), while an oxo-overlayer has not been found. Cu(100) at E = -0.63 V (SCE) in 0.1 M $HClO_4$ solution shows a square configuration with an atomic spacing of 0.26 ± 0.02 nm, which is the correct structure and spacing for the Cu(100) orientation. Upon sweeping to more positive E [(-0.08 V (SCE)], a square lattice was also evident, but it was rotated 45° with respect to the underlying substrate with an interatomic separation of 0.36 ± 0.02 nm; i.e., this structure was consistent with a c2 × 2 overlayer.[592]

In situ resolution of the crystalline order has been achieved by Villegas *et al.*[594] on Cu(100) electrodes purposely disordered by oxidation or ion bombardment. Ordering was achieved by chemical and electrochemical etching and confirmed by LEED, SEM, and STM.

The Cu(110) surface in dilute (0.003 M, pH=2.5) $HClO_4$ at E= –0.13 V (SCE) (160 mV more negative than the rest potential) exhibits a correct unreconstructed structure.[393] Sweeping the potential back to the rest potential created additional features whose most probable source is an oxide (or hydroxide) adlayer. The behavior of these adlayers qualitatively obeys the Pourbaix diagram.[592–594] Results[593] obtained in the pH-potential region of the Pourbaix diagram,[595] where the bulk Cu_2O oxide formation is thermodynamically unfavorable, indicate that these adlayers are related to the initial stage of oxide formation on Cu(100) and Cu(110).

The strength of the Cu–O bond will be lower on the Cu(111) face than on the Cu(100) and Cu(110).[593] Indeed, the Cu–O stretching frequency in UHV is lowest on the (111) face and only a disordered oxygen structure is observed.[596] These results suggest that a specific Pourbaix pH–E phase diagram is needed to describe the behavior of each low-index face of Cu.

The electrical double layer at Cu(111) electrodes in aqueous electrolytes (NaF and Na_2SO_4) at various pH values has been studied by CV and ac impedance methods by Hartinger and Doblhofer.[597] The electrode pretreatment consisted of electrochemical polishing (3 min in $H_3PO_4 + H_2SO_4$ solution) followed by annealing in a nitrogen atmosphere (3 hr at 600 °C). These authors found that in the whole region of E, the prerequisite

of "ideal polarizability" of the Cu(111) electrode in aqueous electrolytes is not satisfied owing to the occurrence of H_2O electrosorption, and no information on $E_{\sigma=0}$ of the Cu(111)/H_2O + NaF interface can be deduced from these features.

From radiotracer studies it has been known that the adsorption of ClO_4^-, HSO_4^-, and Cl^- at Cu starts at very negative E.[143,598] It has also been shown that the surface coverage with ions depends on the solution's pH and on E. This suggests that both specifically adsorbed anions as well as OH^-_{ads} are present on the surface of a Cu(111) electrode and the mixed-phase oxides are plausible at pH < 7, whereas Cu_2O is predicted to be unstable in the potential and pH region studied by Hartinger and Doblhofer. It is concluded that the electrosorption reaction is likely to involve coadsorbed anions along with hydroxyl groups.[597]

(vi) Lead

(a) Pc-Pb in aqueous and nonaqueous solutions

The impedance characteristics of pc-Pb have been obtained in aqueous[220,221,599–607] and nonaqueous (glacial acetic acid, MeOH, EtOH, dimethyl formamide)[10,74,608–612] surface-inactive electrolyte solutions. The first attempt to obtain the potential of zero charge of pc-Pb with a mechanically polished and remelted surface was made by Borissova *et al.*[220,221] in 1948 and 1950. Pc-Pb anodically polished in H_2O + NaF ($0.001 < c_{NaF} < 0.1$ M) was studied by Rybalka and Leikis.[599] The value of $E_{min} = -0.810 \pm 0.02$ V (SCE) was found to be independent of c_{NaF}; the GCSG theory was examined with the assumption of an R (roughness factor) value close to unity. The C_i, σ curve for 0.1 M NaF solutions was calculated ($C_i^{\sigma=0} = 0.325$ F m^{-2} and $C_i^{\sigma<<0} = 0.205$ F m^{-2}).

Later, polished and unpolished pc-Pb electrodes were studied[600] and the Parsons–Zobel plots at $c \geq 0.005$ M NaF were found to be linear, with the value of $f_{PZ} = 1.15$ for the polished electrode. At $c \leq 0.005$ M NaF, nonlinear Parsons–Zobel plots, which are characteristic of solid pc electrodes, were observed. The C_i, σ curves, calculated for polished pc-Pb taking into account the roughness of the surface ($C_i^{\sigma=0} = 0.26$ F m^{-2}, $C_i^{\sigma<<0} = 0.18$ F m^{-2}), were compared with those obtained on the basis of the GCSG theory for liquid Hg. C, E curves were obtained for NaF + H_2O solutions with the addition of various amounts of thiourea (TU). The

Parsons–Zobel plot was linear, with f_{PZ} equal to unity for pure NaF solution and somewhat lower for a solution with the addition of thiourea.

The effect of temperature has been studied in the range $5 < T < 85$ °C. Anomalously low values of C_i have been obtained ($C_i^{\sigma=0} = 0.23$ F m^{-2} and $C_i^{\sigma<<0} = 0.163$ F m^{-2}). A noticeable concentration dependence of the differential capacitance at $\sigma << 0$ has been observed. Also, $\partial C_i^{\sigma=0}/\partial T = -4.8 \times 10^{-4}$ F m^{-2} K^{-1} at $\sigma = 0$; and $\partial C_i^{\sigma<<0}/\partial T = 1.9 \times 10^{-4}$ F m^{-2} K^{-1} at $\sigma << 0$. The intersection point of C_i, σ curves for various temperatures is less negative than the value of σ_{min} at which the C_i, σ curves have a minimum.[600] The same feature is evident for pc-Cd electrodes.

The data available up to 1971 have been collected by Carr *et al.*,[602] who have also reported a pzc value of -0.59 ± 0.02 V (SCE) for a melted, cut, mechanically polished, and finally electrochemically and chemically etched electrode.

Chemically polished pc-Pb electrodes have been studied by impedance.[195,603] The E_{min} was independent of c_{NaF}, as well as of $c_{Na_2SO_4}$. The Parsons–Zobel plot for NaF solutions was linear (Table 12). The value of $C_i^{\sigma=0}$, determined by the extrapolation of the C^{-1}, C_d^{-1} curve to $C_d^{-1} = 0$ and corrected by the value of f_{PZ}, has been obtained ($C_i^{\sigma=0} = 0.32$ F m^{-2}). Adsorption studies of $(C_4H_9)_4NI$ at a polished pc-Pb show splitting of the adsorption-desorption peaks, which can be explained by the energetic inhomogeneity of the surface. The difference between $E_{\sigma=0}$ values of various Pb faces has been estimated to be on the order of 50–60 mV.[604]

A solid drop Pb electrode with additionally remelted surface ($PbDE^R$) has been studied in $H_2O + KF$ and $H_2O + LiClO_4$.[605] The E_{min} was independent of c_{el}. The Parsons–Zobel plot at $\sigma = 0$ was linear (NaF), with $f_{PZ} = 1.06$ (Table 12). $C_i^{\sigma=0} = 0.32$ F m^{-2} without correction and $C_i^{\sigma=0} = 0.29$ F m^{-2} with correction for roughness have been found. The cathodic minimum in the C_i, σ curve lay at $\sigma = -0.14 \pm 0.02$ C m^{-2}, and the corrected $C_i^{\sigma<<0}$ was $0.18^5 \pm 0.005$ F m^{-2}.

Amplitude demodulation has been used to determine $E_{\sigma=0}$ for pc-Pb. In 0.01 M $NaF + H_2O$, $E_{\sigma=0} = -0.83 \pm 0.01$ V (SCE in H_2O).[606] The dependence of $E_{\sigma=0}$ on c_{NaF} as well as on c_{KF} has been found to be negligible.

Recently, a constant-phase element has been found[607] to be present at pc-Pb/$KF + H_2O$ interfaces by impedance measurements. The Pb electrode was cathodically reduced before use. The assumption has been made that the CPE is due to the inhomogeneity of the metal surface. Frequency-

Table 12
Electrical Double-Layer Parameters of Pb in Various Solvents

Electrode	Solvent	Electrolyte	$E_{\sigma=0}$/V vs. aq. SHE	$E_{\sigma=0}$/V vs. BBCr	f_{PZ}	Method	References
pc-Pb	H_2O	0.01 M NaF	-0.60 ± 0.02	0.05 ± 0.02	1.10	Impedance	195, 603
		0.005 M Na_2SO_4	-0.60 ± 0.02[a]	0.05 ± 0.02	—	Impedance	195, 603
pc-Pb		0.01 M NaF	-0.56 ± 0.02	0.09 ± 0.02	1.0	Impedance	599
pc-PbDE		KF, $LiClO_4$	-0.60 ± 0.01	0.05 ± 0.01	1.06	Impedance	605
pc-Pb		KF	-0.59 ± 0.01	0.06 ± 0.01	—	AD[b]	606
		KNO_3	-0.59 ± 0.02	0.06 ± 0.02	—	Impedance	602
	MeOH	KF	-0.43 ± 0.02	0.13 ± 0.02	1.16	Impedance	195, 608
	CH_3COOH	CH_3COOH	-0.58 ± 0.02	—	1.15	Impedance	610, 611
	FM[c]	$NaClO_4$	-0.61 ± 0.02	—		Immersion	612
Pb(111)	H_2O	0.01 M NaF	-0.62 ± 0.01	0.03 ± 0.01	1.05	Impedance	195, 603
		0.005 M Na_2SO_4	-0.62 ± 0.01[a]	0.03 ± 0.01	—	Impedance	195, 603
Pb(100)		0.01 M NaF	-0.59 ± 0.01	0.06 ± 0.01	1.10	Impedance	195, 603
		0.005 M Na_2SO_4	-0.59 ± 0.01[a]	0.06 ± 0.01	—	Impedance	195, 603
Pb(110)		0.01 M NaF	-0.58 ± 0.01	0.07 ± 0.01	1.10	Impedance	195, 603
		0.005 M Na_2SO_4	-0.58 ± 0.01[a]	0.07 ± 0.01	—	Impedance	195, 603
Pb(112)		0.01 M NaF	-0.58 ± 0.01	0.07 ± 0.01	1.15	Impedance	195, 603
		0.005 M Na_2SO_4	-0.58 ± 0.01[a]	0.07 ± 0.01	—	Impedance	195, 603

[a]Corrected by the asymmetry of the electrolyte (0.03 V).
[b]Amplitude demodulation.
[c]FM, formamide.

independent capacitances have been recalculated. It has been found that incomplete reduction of the Pb surface lowers the double-layer capacitance and increases the surface inhomogeneity. Compact-layer capacitances have been found quantitatively, which is in agreement with those for Hg at negative charges.

Chemically polished pc-Pb has been studied by impedance in MeOH + KF.[608,609] The value of C was stable with time and E_{min} was independent of c_{KF}. Capacitance dispersion with c_{KF} was appreciable at $\sigma << 0$ and was probably caused by weak specific adsorption of ions. The Parsons–Zobel plot at $\sigma = 0$ was linear, with $f_{PZ} = 1.16$. The higher value of f_{PZ} for **pc-Pb/CH_3OH + KF**,[608,609] similar to **Bi**[74,219] is presumably related to weak specific adsorption of F^- at these metals from methanolic solutions. The inner-layer capacitance for the pc-Pb/**CH_3OH + KF** interface has been derived from the GCSG model.[608,609] Despite the weak specific adsorption of anions, a very good agreement has been observed between experimental and theoretically calculated C,E curves at $c_{KF} = 0.01$ M and 0.001M. Small discrepancies have been explained either by experimental errors or by effects of the crystallographic inhomogeneity of the pc-Pb surface. According to Vorotyntsev,[74] however, good agreement of the data[608,609] is mainly due to some computational errors.

The pc-Pb/glacial **CH_3COOH ($0.25 < c_{CH_3COONa} < 2.0$ M)** interface has been studied by impedance.[610,611] The capacitance dispersion with ν is moderate **(3 to 5% at $210 \leq \nu \leq 2000$ Hz)** in the region $-1.6 < E < -0.6$ V (SCE in **H_2O**). A very well-defined diffuse layer minimum is observed at $E_{min} = -0.82 \pm 0.02$ V (SCE), independent of ν and c_{CH_3COONa}. The Parsons–Zobel plot and C_i, σ curve have not been derived.

Other interfaces studied have been pc-Pb/EtOH and pc-Pb/formamide.[62] A clear minimum is visible in the C, E curve for pc-Pb/formamide + **$NaClO_4$** at -0.85 ± 0.03 V (SCE in **H_2O**). However, the many experimental problems faced[15] suggest that these data should be accepted with reservations for the time being.[612]

(b) Pb single-crystal faces in aqueous solutions

Pb crystallizes in the fcc system and its melting point is 601 K. Pb(111), Pb(100), Pb(110), and Pb(112) faces have been studied.[195,603] The capacitance dispersion was not greater than 10% at $210 < \nu < 1010$ Hz. The potential of the minimum in C,E curves was independent of c_{NaF},

as well as of $c_{Na_2SO_4}$. The dependence of $E_{\sigma=0}$ on the atomic density of the faces is weak ($\Delta E_{\sigma=0} = 40$ mV), and the value of $E_{\sigma=0}$, becomes less negative as the atomic density decreases. This behavior is in contradiction to that observed for other fcc metals (Au, Ag, Cu).[10,15,24,63,74] The inner-layer capacitance at $\sigma = 0$ increases in the sequence Pb(100) ≤ Pb(110) ≤ Pb(112) ≤ pc-Pb ≤ Pb(111), which has been explained by the hydrophilicity increasing in the same order.[195]

(vii) Tin

Results for tin have been reported in a few papers[613–621]; the applicability of the GCSG theory has been tested only by Bartenev *et al.*[615] and Khmelevaya and Damaskin.[621] Since F^- anions have been found to be slightly surface active,[615] Na_2SO_4 has been used as a surface-inactive electrolyte. The values of E_{min}, found to be independent of $c_{Na_2SO_4}$, and $E_{\sigma=0}$, corrected by the asymmetry of the electrolyte (a 30-mV shift toward less negative *E),* are presented in Table 13. The specific adsorption of Cl^-, Br^-, and I^- anions has been found to increase in the sequence given. The Parsons-Zobel plot at $\sigma = 0$ has been constructed[615] ($f_{PZ} = 1.1$ and $C_i^{\sigma=0} = 0.39$ F m^{-2}). However, in the case of a 2:1 electrolyte, it is incorrect[74,125] to use the values of C_d at E_{min} to build up the Parsons–Zobel plots and to obtain $C_i^{\sigma=0}$, as done by Bartenev *et al.*[615] The corrected Parsons–Zobel

Table 13
Electrical Double-Layer Parameters of Sn in Aqueous Solutions

Electrode	Electrolyte	$E_{\sigma=0}$/V vs. SHE	f_{PZ} ±0.02	References
pc-Sn	Na_2SO_4	−0.43	1.1	615
	$NaClO_4$ + ($HClO_4$)	−0.43 ± 0.02	—	613
	K_2SO_4	−0.37 ± 0.02[a]	1.27	616
	$KClO_4$	−0.39 ± 0.02	0.99	616
	Na_2SO_4	−0.39 ± 0.01[a]	—	617
	Na_2SO_4	−0.39 ± 0.01[a]	1.1	621
Sn(001)	Na_2SO_4	−0.37 ± 0.01[a]	1.1	621
Sn(T10)	Na_2SO_4	−0.37 ± 0.01[a]	1.1	621
Sn(110)	Na_2SO_4	−0.38 ± 0.01[a]	1.1	621

[a]Corrected by the asymmetry of the electrolyte (0.03 V).

plot[74] turns out to be nonlinear, which is in accordance with data for pc-electrodes in dilute aqueous solutions.[10,63,67,74]

The electrical double layer has been studied at the interface of acidified (pH = 3) $KClO_4$ and K_2SO_4 solutions in contact with an Sn solid drop electrode with an additionally remelted surface ($SnDE^R$).[616] The E_{min} is independent of c_{el} as well as of the electrolyte. Weak specific adsorption of ClO_4^- at $SnDE^R$ is probable around $\sigma = 0$. This view is supported by the high value of f_{PZ} for $SnDE^R/H_2O + KClO_4$ ($f_{PZ} = 1.27$). A value of $f_{PZ} = 0.99$ for $SnDE^R/H_2O + K_2SO_4$ indicates that the surface of $SnDE^R$ is geometrically smooth and free from components of pseudo-capacitance.[616]

Khmelevaya and Damaskin[621] have studied the electrical double-layer structure at electrochemically polished pc-Sn. $E_{\sigma=0} = -0.63$ V (SCE) (corrected by the asymmetrical type of electrolyte); the applicability of the GCSG theory has been tested; and the values of f_{PZ} and $C_i^{\sigma=0}$ have been reported.

Adsorption of $(C_4H_9)_4N^+$ cations on pc-Sn electrodes shows splitting of the adsorption-desorption capacitance peak into a doublet with the potential difference $\Delta E^{max} \sim 50$ to 60 mV. This supports the suggestion that the differences between $E_{\sigma=0}$ values for different Sn planes may be of the same order.[621] These data point to a surface of electropolished pc-Sn that is geometrically and energetically inhomogeneous.

The electrical double-layer structure of electrochemically polished monocrystalline Sn has been studied by impedance measurements.[621] Sn crystallizes in the tetragonal system and the surface atomic density increases in the sequence Sn(110) < Sn(100) < Sn(111). The melting point of Sn is 505 K. The capacitance dispersion was not greater than 10% in the range $210 < \nu < 1010$ Hz. Linear Parsons-Zobel plots with f_{PZ} independent of the crystallographic orientation have been obtained, $C_i^{\sigma=0}$ values independent of the crystallographic structure of the electrode surface have been found,[621] $E_{\sigma=0}$ increases only slightly with the atomic density of faces, which is in good agreement with the adsorption data of $(C_4H_9)_4NI$ at pc-Sn.[621] This is in accord with the general trend observed with Au, Ag, Cu, Bi, Sb, Zn, and Cd electrodes.[6,7,32,63,67,74] According to impedance data,[621] the specific adsorption of anions increases in the sequence $SO_4^{2-} < F^- < Cl^- < Br^- < I^-$.

(viii) Zinc

(a) Pc-Zn in aqueous solutions

The electrical double layer at **pc-Zn/H_2O** interfaces has been studied in many works,[154,190,613–629] but the situation is somewhat ambiguous and complex. The polycrystalline Zn electrode was found to be ideally polarizable for sufficiently wide negative polarizations.[622–627] With pc-**Zn/H_2O,** the value of $E_{\sigma=0}$ was found at –1.15 V (SCE)[615,628] (Table 14). The values of E_{min} are in reasonable agreement with the data of Caswell *et al.*[623,624] Practically the same value of $E_{\sigma=0}$ was obtained by the scrape method in **$NaClO_4$ + H_2O** solution (pH = 7.0).[190] Later it was shown[154,259,625,628] that the determination of $E_{\sigma=0}$ by direct observation of E_{min} on *C,E* curves in dilute surface-inactive electrolyte solutions is not possible in the case of Zn because Zn belongs to the group of metals for which $E_{\sigma=0}$ is close to the reversible standard potential in aqueous solution.

Therefore some indirect methods have been worked out to determine the value of $E_{\sigma=0}$.[154,259] In particular (1) salting out of organic compounds from a surface-inactive electrolyte solution, (2) E^{max} for 1-pentanol or other organic compounds with a high attractive interaction constant *a,* and (3) dependence of the capacitance minimum on thiourea concentration. It should be noted that indirect estimates based on TU adsorption give $E_{\sigma=0}$ for pc-Zn in acidified solution **(Na_2SO_4 + H_2SO_4),**[154,259] which is in good agreement with earlier results.[623,627] Thus, this seems to be the more probable value of $E_{\sigma=0}$ for a pc-Zn electrode. However, the value of E_{min} for pc-Zn depends remarkably on the pretreatment of the electrode surface. Adsorption studies of organic compounds with high *a* at pc-Zn have indicated that the difference between $E_{\sigma=0}$ for various crystallographic regions (different grains) is appreciable **($\Delta E \approx 100$ mV),** but the fraction of different grains on the pc-Zn surface depends on the surface preparation method.[154,259,628,629]

(b) Zn single-crystal faces in aqueous solutions

Zinc crystallizes in the hexagonal close-packed system; its electronic structure is $4s^2$ and the melting point is 693 K. Since the zinc dissolution takes place at potentials very close to $E_{\sigma=0}$, the differential capacitance curves in the region of $E_{\sigma=0}$ in pure surface-inactive electrolyte solutions (KC1, pH = 3.7) can be determined directly for the **Zn(11$\bar{2}$0)** face only

Table 14
Potentials of Zero Charge of Zn in Aqueous Solutions

Electrode	Electrolyte	E_{min}/V vs. SHE	$E_{\sigma=0}$/V vs. SHE	Atomic density/cm^{-2}	Method	References
pc-Zn	$NaClO_4$ (pH = 7)	—	–0.92		oc Scrape	190
	$NaClO_4$ (pH = 3.48)	–0.90	–0.90		Impedance	623
	0.1 M KCl + TU[a]	–0.91	–0.91		Impedance	254
	0.1 M KCl	–0.93 to –0.91	–0.93 to –0.91		Impedance	628
Zn(0001)	$NaClO_4$ (pH = 3.48)	–0.90	–0.90 ± 0.01	1.630×10^{15}	Impedance	623
Zn(0001)	0.3 M NaF + camphor[b]	—	–0.77 ± 0.02		Impedance	154, 259
Zn(0001)	0.1 M KCl + TU[a]	—	–0.78 ± 0.02		Impedance	154, 259
Zn(0001)	0.1 M KCl + $C_5H_{11}OH$[c]	—	–0.76 ± 0.02		Impedance	154, 259
Zn(10$\bar{1}$0)	0.2 M NaF + camphor[b]	—	–0.85 ± 0.02	1.315×10^{15}	Impedance	154, 259
Zn(10$\bar{1}$0)	0.1 M KCl + TU[a]	—	–0.84 ± 0.02		Impedance	154, 259
Zn(11$\bar{2}$0)	0.2 M NaF + camphor[b]	—	–0.87 ± 0.02	0.876×10^{15}	Impedance	154, 259
Zn(11$\bar{2}$0)	0.1 M KCl + TU[a]	—	–0.87 ± 0.02		Impedance	154, 259
Zn(11$\bar{2}$0)	3×10^{-3} M KCl	–0.85 ± 0.01	–0.85 ± 0.01		Impedance	154, 259

[a]Dependence of capacitance minimum on c_{TU}. TU, thiourea.
[b]Potential of adsorption-desorption peak for n-$C_5H_{11}OH$ (0.1 M).
[c]Salting out.

(Table 14).[154,259] For this face $E_{\sigma=0}$ was somewhat more negative than the rest potential of Zn [$E = -1.09$ V (SCE)]. A weak dependence of $E_{\sigma=0}$ on c_{KCl} was observed, which can be explained by weak specific adsorption of Cl^-.

More reliable values of $E_{\sigma=0}$ for other faces, i.e., basal Zn(0001) and prismatic Zn(10$\bar{1}$0), have been obtained from the dependence of E^{max} on c_{el} (salting-out method), as well as by the dependence of E_{min} in the C,E curves on c_{KCl} in solutions in the presence of thiourea at $c_{TU} = 3 \times 10^{-3}$ M. The values of $E_{\sigma=0}$ obtained by the salting-out method [–1.11 V (SCE) for Zn(11$\bar{2}$1)] and by the dependence of E_{min} on c_{KCl} at $c_{TU} = const$, are in good agreement with the values of $E_{\sigma=0}$ obtained from the C, E curves for pure KCl solutions. The maximum difference between the $E_{\sigma=0}$ values for the various faces of Zn is about 90 to 100 mV[254,259] and this is in good agreement with earlier estimates.[622,623]

The σ,E curves, obtained by integration of C,E curves for surface-inactive electrolyte solutions, were linear and parallel for various Zn faces for $\sigma < -0.03$ C m^{-2}.[259] The shift of σ, E curves along the E-axis was explained by the variation in the electron work function Φ from Zn(0001) to Zn(11$\bar{2}$0). For $\sigma > -0.03$ C m^{-2}, the curves were nonlinear, which was related to an increase in C_i in the order (0001) < (10$\bar{1}$0) < (11$\bar{2}$0). The same order was obtained by computer interpolation of the calculated C_i, σ curves at $\sigma = 0$.[28]

Studies in surface-inactive electrolyte solutions with various organic compounds (cyclohexanol, 1-pentanol, 2-butanol, camphor, tetra-buthyl ammonium ion, TBN^+) show that the adsorption-desorption peak shifts to more negative potentials in the order (0001) < (10$\bar{1}$0) < (11$\bar{2}$0); this was explained by the increasing negative value of $E_{\sigma=0}$ in the same direction.[259,629–635]

C, E curves have been obtained for Zn(0001) and Zn(10$\bar{1}$0) at various c_{KCl} with different additions of TU.[630,634–636] The data for Zn(0001) at $c_{TU} = const$ have been used to obtain C^{-1}, C_d^{-1} plots. Nonlinear plots have resulted, with the value of the reciprocal slope remarkably dependent on c_{TU}. At $c_{TU} = 0.1$ M, the reciprocal slope of the PZ plot is 1.1, increasing with decreasing c_{TU}. Such an effect has been related to the weak specific adsorption of OH^- on Zn. This explanation has been critically discussed by Vorotyntsev,[74] who has assumed that the effect[635,636] is connected with the variation in the compact layer composition of the $Zn/H_2O + TU$ interface as c_{TU} varies.

The R of electropolished Zn single-crystal face electrodes has been obtained from the shape of the adsorption-desorption peak of cyclohexanol at various Zn and Hg surfaces.[154] The roughness factor of Zn electrodes has been found to increase in the order **Zn(0001) < Zn(10$\bar{1}$0) < Zn(11$\bar{2}$0)** with values in the range 1.1 to 1.25.

(ix) Cadmium

(a) Pc-Cd in aqueous solutions

The electrical double layer of pc-Cd electrodes has been studied in many works,[10,220,221,271,637,662] but the picture is still somewhat unclear. The first attempt to determine the electrical double layer parameters at solid Cd, Pb, and Tl electrodes by the impedance method was made by Borisova *et al.*[220,221] A diffuse-layer minimum was found in the C, E curves, but the capacitance dispersion was appreciable and the value of C at E_{min} for Cd was higher than that calculated using the C, E curve for Hg.[10,220,221] It was noted[10] that one of the reasons for this was the roughness of the pc-Cd surface. Therefore, Cd, Pb, and Tl electrodes were remelted in an inert atmosphere to give solidified drop electrodes. The capacitance dispersion was somewhat lower, but the difference between calculated and experimental capacitance was still substantial.[221]

According to experimental results,[10,220–224,637–643] only F^- appears to be surface inactive at **pc-Cd/H_2O** interfaces, with E_{min} independent of c_{NaF} and v. Specific adsorption of anions increases in the order $F^- \leq SO_4^- < ClO_4^- < OH^- < NO_3^- \leq NO_2^- < Cl^- < Br^- < I^-$. The Parsons–Zobel plot was linear and at $E_{\sigma=0}$ gave the value $f_{PZ} = 1.30$.[637] In some papers[222,638] the f_{PZ} obtained for pc-Cd/NaF+H_2O ranged from 1.10 to 1.15 The same value was obtained for 0.005 to **0.1 M KF + H_2O** solutions.[271]

C_i, σ curves have been reported in some papers,[10,74,120,271,357,644] but the spread of C_i values at $\sigma = 0$ was remarkable ($\Delta C_i = \pm 15\ \mu F\ cm^{-2}$). A realistic value of $C_i^{\sigma=0}$ probably ranges from 30 to 40 $\mu F\ cm^{-2}$ and at $\sigma << 0$, C_{min} ranges from 18.0 to 18.5 $\mu F\ cm^{-2}$ and $f_{PZ} = 1.1$. It has been suggested that hydrophilicity rises in the sequence **Hg ≤ Bi < Cd <** Ag(100).[6,7,10,15,74,120] It must be noted that for pc-electrodes with an energetically nonhomogeneous surface structure, the marked dependence of C_i on the surface pretreatment is caused by the appearance of various planes at the electrode surface. C_i, σ curves for pc-Cd have been simulated[74,120,354] according to the Parsons[1] and Damaskin[663] models.

The pzc of a pc-Cd renewed by cutting was determined in dilute fluoride and sulfate solutions by capacitance measurements.[645,646] The C, E curves exhibited distinct minima whose depth increased with increasing dilution of the solution (Table 15). This value is ca. 30 mV more negative than that for polished electrodes and reflects the more disturbed surface structure of a renewed electrode. Adsorption of aliphatic alcohols and acids has also been studied on these electrodes.[645,646]

The dependence of the electrical double-layer parameters of pc-Cd on temperature (0 to 85 °C) has been studied[647,648] in $H_2O + KF$ solutions. The E_{min} depends slightly on T, the temperature coefficient $\partial E_{min}/\partial T$ being $0.15\ mV\ K^{-1}$. C_i at $\sigma_{min} < -0.09\ C\ m^{-2}$ has been found to decrease as the temperature increases. C_i rises if σ decreases and at $\sigma = 0$ the inner-layer temperature coefficient $\partial C_i/\partial T$ is equal to $0.058\ \mu F\ cm^{-2}\ K^{-1}$. It has been pointed out that the intersection point of C_i, σ curves at various temperatures lies at a less negative σ than the charge σ_{min}, at which the C_i, σ curves have the minimum value. The same is the case with pc-Pb electrodes,[649] but for Hg/H_2O the opposite is observed.[305]

The effective fractal dimension D and the fractional exponent α for chemically polished pc-Cd electrodes have been obtained from impedance data[271,651] according to the method described in the literature.[268,269,274,275,658] The capacitance dispersion for chemically polished pc-Cd electrodes ranges from 8 to 10%. For surface-inactive electrolyte solutions, as well as for weakly surface-active electrolyte solutions (0.01 MKCl) at $-1.30 < E < -1.6$ V(SCE), the values of α and D are independent of σ and electrolyte nature ($\alpha = 0.94$ and D = 2.06). α decreases and D increases as the polarization of the negative electrode decreases; at low positive charge densities, α for 0.01 M KCl is lower and D higher than for 0.01 M KF solution at $\sigma \geq 0$. This has been explained by the weak specific adsorption of anions, as well as by the incipient oxidation of the Cd electrode surface at $\sigma > 0$. Thus, other factors that are not directly related to surface nonuniformity or topography can influence the fractal behavior of solid electrodes, as recently established for other pc-solid electrodes.[274] According to these data,[651] the deviation of polished pc-Cd from ideal behavior ($\alpha = 1$; $D = 2$) is not large, which can be explained by the rather low micrononuniformity of polished pc-Cd electrodes.

Using amplitude demodulation,[180,181] the $E_{\sigma=0}$ for pc-Cd/aqueous NaF and Na_2SO_4 solutions has been found to be very close to that measured by impedance.[10,74,637–644] A slight variation of $E_{\sigma=0}$ with c_{el} has

Table 15
Electrical Double-Layer Parameters of Cd in Various Solvents

Electrode	Surface preparation	Solution	$E_{\sigma=0}$/V vs. SHE	$R(\nu = 210\text{H})$	$(\partial E_{min}/\partial \log c)$/ mV	α^a	D^b	Atomic density/cm^{-2}	References
pc-Cd		H_2O/KF	–0.72	—	—			—	647, 648
		H_2O/KF, $LiClO_4$	–0.73 ± 0.02			0.94	2.06		271
		H_2O/NaF	–0.72 to –0.73	1.30					255, 643
		H_2O/KF	–0.73	1.10 to 1.15					10
		H_2O/NaF	–0.76 ± 0.01	2.0					645
		H_2O/NaF	–0.70 ± 0.01[c]	3.0					654
		H_2O/NaF, Na_2SO_4	–0.74 ± 0.01[d]						180, 181
		DMF/$LiClO_4$	–0.60 ± 0.01[c]						654, 655
		i-PrOH/Na_2SO_4	–0.75 ± 0.01						656, 657
Cd(0001)	Electr. grown	H_2O/NaF	–0.75 ± 0.01	1.09	—	—	—	1.308×10^{15}	156
Cd(0001)	Electr. grown	$H_2O/LiClO_4$	–0.78 ± 0.01	—	—	—	—		660
Cd(0001)	Electr. polish.	H_2O/NaF	–0.73 ± 0.01	1.06	20	0.98	2.01		249

(continued)

Table 15
Continued

Electrode	Surface preparation	Solution	$E_{\sigma=0}$/V vs. SHE	$R(\nu = 210H)$	$(\partial E_{min}/\partial \log c)$/ mV	α^a	D^b	Atomic density/cm^{-2}	References
Cd(0001)	Cleaved	H_2O/NaF	-0.75 ± 0.01	1.11	30	0.94	2.07		249
Cd(0001)	Chem. treated	H_2O/NaF	-0.760 ± 0.015	1.15	40	0.91	2.10		249
Cd(10$\bar{1}$0)	Electr. polish.	H_2O/NaF	-0.77 ± 0.01	1.12	20	0.97	2.03	1.038×10^{15}	249
Cd(10$\bar{1}$0)	Chem. treated	H_2O/NaF	-0.750 ± 0.015	1.28	30	0.92	2.09		249
Cd(11$\bar{2}$0)	Electr. polish	H_2O/NaF, $LiClO_4$	-0.75 ± 0.01	1.1	—	—	—	0.692×10^{15}	255
Cd(11$\bar{2}$0)	Electr. polish.	H_2O/NaF	-0.78 ± 0.01	1.22	20	0.98	2.02		249
Cd(11$\bar{2}$0)	Cleaved	H_2O/NaF	-0.78 ± 0.01	2.0 to 2.1	—	—	—		255
Cd(11$\bar{2}$0)	Chem. treated	H_2O/NaF	-0.760 ± 0.015	1.26	40	0.92	2.09		249
Cd(10$\bar{1}$1)		H_2O/NaF	-0.760 ± 0.015	1.24	20	0.94	2.07	0.544×10^{15}	249
Cd(11$\bar{2}$1)		H_2O/NaF	-0.750 ± 0.015	1.25	20	0.95	2.06	0.442×10^{15}	249

[a]Fractional exponent, dimensionless parameter.
[b]Fractal dimension, dimensionless parameter.
[c]Scrape method.
[d]Amplitude modulation.

been explained by the concentration dependence of the inner-layer properties and by the influence of the asymmetry of Na_2SO_4.[180,181]

(b) Pc-Cd in nonaqueous solutions

Attempts to determine electrical double-layer parameters in nonaqueous surface-inactive electrolyte solutions have been made in different laboratories.[610,654–657] Impedance data for pc-Cd/1.0 M CH_3COONa solution in glacial acetic acid show that the capacitance dispersion is dramatic ($C_{210}/C_{2000} \leq 20\%$); moreover, in contrast to H_2O, a diffuse-layer minimum is not observed. However, a comparison of C, E curves for pc-Pb and pc-Cd in glacial acetic acid suggests that $E_{\sigma=0}$ for pc-Cd is probably 250 to 300 mV more negative than for pc-Pb[610] (Tables 12 and 15).

The pc-Cd/DMF interface has been studied by the scrape method.[9] $E_{\sigma=0}$ in 1.5 M $LiClO_4$ + DMF solution is -0.842 V (SCE in H_2O).[654,655] The value of $E_{\sigma=0}$ for pc-Cd/0.01 M $NaF + H_2O$ obtained by the scrape method is -0.940 V (SCE in H_2O) with a roughness factor $f \approx 3.0$.[655]

A chemically polished pc-Cd/1-PrOH + Na_2SO_4 interface has been studied by impedance; a diffuse-layer capacitance minimum has been observed, with E_{min} slightly dependent on v.[657,638] The dispersion is somewhat higher (6 to 8%) than for the pc-Cd/H_2O interface. The σ, E curves in 1-PrOH have been obtained by back-integration assuming that at $\sigma << 0$ the difference between σ, E curves for Hg and pc-Cd is the same as the difference in electron work function in UHV ($\Delta\Phi = 0.36$ V). The value of pzc obtained by back-integration is practically the same as the E_{min} observed in C,E curves (Table 15). The value of $\Delta E_{ads}^{Hg\text{-}Cd} = \Delta E_{\sigma=0}^{Hg\text{-}pc\text{-}Cd} - \Delta E_{\sigma<<0}^{Hg\text{-}pc\text{-}Cd}$ has been found to be equal to 0.32 ± 0.03 V, which is somewhat higher than for H_2O. This has been explained by the stronger interaction of Cd with 1-PrOH than for Hg.[320,656,658] The applicability of the GCSG theory has been tested by the Grahame method, i.e., by calculating the C, E curve for a 0.01 M solution and taking the C, E curve for a 0.1 M $NaClO_4$ solution as a reference.

(c) Cd single-crystal faces in aqueous solutions

Cadmium crystallizes in the hcp system. Its electronic structure is $5s^24p^2$ and the melting point is 594 K. The first attempt to determine $E_{\sigma=0}$ of (0001) and (1010) Cd faces by C, E curves was made by Abdullin

et al.[659] in 1.0 M Na_2SO_4 and 0.1 M Na_2SO_4 + ethylenediamine solutions (at pH = 3.9 to 4.2). The negative region for the basal (0001) face was shifted in the positive direction compared with that for the prismatic (1010) face with $\Delta E_{\sigma=0} \approx 100$ mV. The E_{min} was estimated to be at very negative potentials [$E_{min} = -1.5$ V (SCE) for Cd(0001)].

Korotkov *et al.*[255] have established that in surface-inactive electrolyte solutions (NaF, $LiClO_4$), the $E_{\sigma=0}$ of Cd (11$\bar{2}$0) is slightly shifted to more negative potentials compared with the pzc of polished pc-Cd. On a scraped surface of Cd(11$\bar{2}$0), $E_{\sigma=0}$ is more negative than on a polished one, and this difference can be related to the greater inhomogeneity of the scraped surface. The Parsons–Zobel plot for scraped Cd(11$\bar{2}$0) is linear, with f_{PZ} = 2.0 to 2.1. The value of f_{PZ} for a chemically polished Cd(11$\bar{2}$0) electrode is 1.1. The GCSG theory has been found to be applicable to chemically polished Cd(11$\bar{2}$0). Impedance studies in aqueous Na_2SO_4 solution with the addition of $(C_2H_5)_4N^+$, $(C_3H_7)_4N^+$, and $(C_4H_9)_4N^+$ have shown that surfaces of polished pc-Cd and Cd(11$\bar{2}$0), as well as the scraped surfaces, are energetically nonuniform since they give rise to splitting of the adsorption-desorption peaks. The difference in E^{max} is ~60 to 70 mV, and this should be considered as the probable difference of $E_{\sigma=0}$ values for Cd faces.

Vitanov and Popov *et al.*[156,660-662] have studied Cd(0001) electrolytically grown in a Teflon capillary in an aqueous surface-inactive electrolyte solution. The E_{min} is independent of c_{el} and ν. The capacity dispersion is less than 5%, and the electrode resistance dispersion is less than 3%. The adsorption of halides increases in the order $Cl^- < Br^- < I^-$.[661] A comparison with other electrodes shows an increase in adsorption in the sequence Cd(0001) < pc-Cd < Ag(100) < Ag(111). A linear Parsons–Zobel plot with $f_{PZ} = 1.09$ has been found at $\sigma = 0$. A slight dependence has been found for the C_i, σ curves on c_{el} (~5%) in the entire region of σ. Theoretical C, E curves have been calculated according to the GCSG model.

The temperature dependence of the electrical double-layer parameters has been studied for Cd(0001).[662] The positive value of $\partial E_{\sigma=0}/\partial T$ (0.33 ± 0.03 mV K^{-1}) is taken to indicate that the H_2O dipoles are oriented with their negative end toward the metal surface.[121,663] The value of $\partial E_{\sigma=0}/\partial T$ increases in the order Ag(111) < Ag(100) < Cd(0001), which is explained in terms of enhanced disorientation of physically adsorbed H_2O dipoles in the same order.[662]

$C_i^{\sigma=0}$ increases if T increases, and this result is in accord with the data for electrolytically grown Ag(111) and Ag(100).[662] For electrochemically

polished Ag single-crystal faces, $\partial C_H^{\sigma=0}/\partial\sigma \approx 0$ and for Hg this value is negative.[15,108,298] The entropy of electrical double-layer formation ΔS^* calculated from the experimental data shows a maximum at $\sigma = -0.05$ C m^{-2}.[662] This value is very close to that obtained for chemically polished Ag(111) and Ag(100).[32] The hydrophilicity of the electrodes is suggested to increase in the order Cd(001) < Ag(100) < Ag(111).[662]

Electrochemically polished and chemically treated Cd(0001), Cd(10$\bar{1}$0), Cd(11$\bar{2}$0), Cd(10$\bar{1}$1), and Cd(11$\bar{2}$1) electrodes have been studied by impedance and cyclic voltammetry by Lust *et al.*[152,153,249,664,665] A slight variation of capacitance (3 to 6%) has been observed with ν. In the case of chemically treated electrodes, a somewhat higher (5 to 10%) dependence of C on ν has been explained by the geometric roughness of the electrode surface.

The $C(E)$ curves for electrochemically polished Cd faces show a slight dependence of E_{min} on c_{el} at $c_{NaF} \geq 0.003$ M. This suggests a slight specific adsorption of F^- at the pzc. The Essin-Markov coefficient is $\partial E_{min}/\partial \log c < 0.58$ mV, which to a first approximation rules out any discreteness of specifically adsorbed F^- anions around $\sigma \approx 0$. Therefore the values of $E_{\sigma=0}$ given in Table 15 have been obtained by extrapolation of E_{min} vs. $(\sqrt{c})$ to $\sqrt{c} = 0$. The values of $E_{\sigma=0}$ for the electrochemically polished Cd(11$\bar{2}$0) electrode in NaF solutions[152,153] are in good agreement with those obtained by Korotkov *et al.*[255] For $c_{NaF} \geq 0.005$ M, the values of E_{min} for electrochemically polished Cd(0001) are in good agreement with E_{min} obtained for Cd(0001) electrochemically grown in a Teflon capillary.[156,660,661] The difference between $E_{\sigma=0}$ for the electrochemically polished (10$\bar{1}$0), (11$\bar{2}$0), (11$\bar{2}$1), and (10$\bar{1}$1) faces does not exceed 30 mV, but $E_{\sigma=0}^{(0001)}$ is to some extent higher than the $E_{\sigma=0}$ of other faces.[152,153,249] The same trend is observed with Zn single-crystal electrodes,[24,154,259] where $\Delta E_{\sigma=0}$ for the (10$\bar{1}$0) and (11$\bar{2}$0) faces does not exceed 30 mV, but the value of $E_{\sigma=0}$ for Zn(0001) is about 90 mV more positive than the $E_{\sigma=0}$ for the other planes. This has been explained on the basis of a specific surface state of cadmium and zinc atoms in the most densely packed basal plane (0001).[152,153,249]

The value of $E_{\sigma=0}$ for pc-Cd[10,637,643] as well as for pc-Zn lies between the $E_{\sigma=0}$ values of these two groups of planes. $E_{\sigma=0}$ for a cut Cd(0001)^c electrode is in good agreement with that for electrochemically polished Cd(0001). For chemically treated Cd electrodes, a remarkable dependence of E_{min} on c_{NaF} has been observed.[249] These results are confirmed by data for other electrodes with a polycrystalline surface structure,[10,74] and can

be explained in terms of specific adsorption of F^- on surface defects.[74] However, the Essin-Markov coefficient is < 0.58 mV, and accordingly any discreteness of the electrical double layer may be ruled out around $\sigma \approx 0$. The values obtained by extrapolation of E_{min} vs. $(\sqrt{c})$ to $\sqrt{c} = 0$ are in agreement with the values for pc-Cd,[10,221,643] and can be explained by the inhomogeneous surface structure of chemically treated electrodes.

Experimental investigations in aqueous solutions of "structure-breaking" ions (ClO_4^-, BF_4^-) show some new features with respect to NaF: (1) a moderate shift of E_{min} to more negative potentials with increasing c_{el}, (2) higher values of capacitance at E_{min}, (3) higher values of f_{PZ} for $LiClO_4$ than for NaF solutions, and (4) higher values of $C_i^{\sigma=0}$. On the basis of these features it can be concluded that the surface activity of ClO_4^- is higher than that of F^-.[249]

D and fractional exponent α (Table 15) show that the surface of electrochemically polished Cd electrodes is flat and free from components of pseudo-capacitance. The somewhat higher values of D for electrochemically polished high-index planes and for chemically treated electrodes indicate that the surface of these electrodes is to some extent geometrically and energetically inhomogeneous. However, the surface of chemically treated Cd electrodes, in comparison with the surface of mechanically polished or mechanically cut electrodes, is relatively flat.[153,249]

The inner-layer capacitance of Cd faces increases as the atomic density decreases. It has been suggested that hydrophilicity increases in the order $Cd(0001) < Cd(10\bar{1}0) < Cd(11\bar{2}0)$. The same order has been proposed on the basis of data on organic compound adsorption.[153]

(x) Bismuth

The electrochemical properties of bismuth solid drop electrodes have been studied extensively[219,254,666–697] and several reviews[74,153,219,254,670–672] have been published.

(a) Pc-Bi in aqueous solutions

The pc-Bi/aqueous solution interface has been studied mainly by Palm *et al.*[666–669] $E_{\sigma=0}$ and other fundamental characteristics were obtained. The electrical double-layer structure at a bismuth solid drop electrode with remelted surface $(BiDE^R/H_2O)$ was investigated by Salve

and Palm[670] (Table 16). F^- and SO_4^{2-} as well as Li^+ and Na^+ were found to be surface inactive, while ClO_4^-, K^+, Pb^+, and Cs^+ showed weak specific adsorption. The dispersion of C with ν in the region $60 < \nu < 20{,}000$ Hz was 5 to 6%.[666–612] The Parsons–Zobel plots were linear for $-0.03 < \sigma < 0.02$ C m^{-2} with $f_{PZ} \approx 1.01$ to 1.03. These data have been interpreted in terms of a high geometric uniformity of $BiDE^R$.[670]

C_i, σ curves for the $BiDE^R/H_2O$ interface have been simulated by the Parsons[308] and Damaskin-Frumkin[663,673] models.[672] Unlike the data for Hg and Cd, in the case of $BiDE^R$, the agreement of the experimental results with theoretical calculations is not good for $\sigma \geq -0.03$ C m^{-2}. Better agreement has been observed after correction of the inner-layer model for the component of the potential drop in the metallic layer (i.e., for the capacitance of the metallic phase). In spite of the high geometrical uniformity, the surface of $BiDE^R$ is energetically (crystallographically) inhomogeneous, as indicated by the splitting into three or four independent maxima of the adsorption-desorption peaks for various organic compounds.[153,219,254,671] Electronographic studies show that at the $BiDE^R$ surface, monocrystalline regions with a linear parameter $l > 10$ nm exist. A more detailed discussion is given in Section II.2 (iv).

Table 16
Potentials of Zero Charge of pc-Bi in Various Solvents

Solvent	$E_{\sigma=0} \pm 0.01$/V vs. aq. SHE	$E_{\sigma=0} \pm 0.01$/V vs. BBCr	References
H_2O	−0.38	0.27	666, 667, 670, 675
MeOH	−0.25	0.31	677, 678
EtOH	−0.11	—	683
1-PrOH	−0.21	—	691
2-PrOH	−0.18	—	692
1-BuOH	−0.23	—	696
2-Me-1-PrOH	−0.24	—	696
2-BuOH	−0.20	—	696
EG[a]	−0.28	—	697
AN	−0.21	0.38	480, 681
DMF	−0.14	0.37	679, 680
DMSO	−0.24	0.36	475

[a]EG, ethylene glycol.

Thermally evaporated thin bismuth films (thickness 20 to 150 nm) have been studied in aqueous solution of various electrolytes (NaF, Na_2SO_4, $LiClO_4$) by the resistometric method.[674] An important feature of the resistometric response of Bi is the intersection of the ΔG, E curves (ΔG = surface conductance change) at E = –0.6 V (SCE), which is somewhat more positive than $E_{\sigma=0}$ for pc-Bi [-0.625 ± 0.01 V (SCE)].[666–672] This has been explained by the fact that ΔG is mainly determined by the electrode free charge σ and the surface scattering effect of the carriers is small. The values of C for thicker films[674] are in the range 15 to 20 $\mu F\ cm^{-2}$, which are in agreement with C values measured by impedance.[666–672]

Mishuk *et al.*[675,676] have applied the modified amplitude demodulation method to electrochemically polished pc-Bi in aqueous NaF solution. The curves of the real component of the nonlinear impedance Z'' as a function of the electrode potential, unlike pc-Cd and pc-Pb, intersect for various c_{NaF} at E = –0.62 V (SCE),[674] i.e., at $E_{\sigma=0}$ for pc-Bi, as obtained by impedance.[666–672] The different behavior of pc-Bi from pc-Cd and pc-Pb at $\sigma > 0$ has been explained by the semimetallic nature of pc-Bi electrodes. A comparison of inner-layer nonlinear parameter values for Hg, Cd, and Bi electrodes at $\sigma < 0$ shows that the electrical double-layer structure at negative charges is independent of the metal.[675,676]

Small amounts of molecular oxygen can influence the value of $E_{\sigma=0}$.[675] With the rise of the O_2 concentration in the electrolyte solution, the form of the Z'', E curve changes and the value of $E_{\sigma=0}$ shifts toward less negative values. However, the effect is weak; after saturation of the solution with molecular hydrogen and holding the pc-Bi electrode for 30 min at E = –1.35 V (SCE), the original shape of the Z'', E curves and the original value of $E_{\sigma=0}$ is restored. This indicates that oxidation and reduction of a pc-Bi electrode surface are reversible processes.

(b) Pc-Bi in nonaqueous solutions

The electrical double layer at $BiDE^R$ has been studied in various nonaqueous solutions: MeOH,[677,678] DMF,[679,680] AN,[480,681,682] DMSO,[475] EtOH,[683–690] 1-prOH,[691] 2-prOH,[692] isomers of BuOH,[693–696] and ethylene glycol (EG).[697]

The $BiDE^R$/MeOH interface has been studied in the presence of various electrolytes (Na^+, K^+, Rb^+, Cs^+, NH_4^+, and F^-, ClO_4^-). The Parsons–Zobel plots show a remarkable curvature at $c_{el} < 0.05$ M KF (Table 16). At $c < 0.01$ M, a more remarkable deviation from linearity has

been observed.[677,678] These deviations for more dilute KF solutions have been explained by weak specific adsorption of K^+ ions at $\sigma << 0$ and F^- anions at $\sigma \geq -0.03$ C m^{-2}, as well as by ionic association in the bulk of the solution and an abnormal dielectric constant value within the Gouy-Chapman layer. Critical discussions of the data for the $BiDE^R$/MeOH system have been given.[74,153,254] A more detailed analysis of this system shows that a more probable reason for this effect is the crystallographic inhomogeneity of the $BiDE^R$ electrode. C_i, σ curves have been derived and for $c_{KF} \leq 0.01$ M, a noticeable deviation of the C_i, σ curve from that for concentrated KF has been observed. This deviation can be explained by experimental errors in obtaining the values of C, c_{el}, and S_{geom} as well as by the crystallographic and energetic inhomogeneity of the $BiDE^R$ electrode surface.[152,153,677,678]

The $BiDE^R$/DMF + $NaClO_4$ interface has been investigated for $0.002 \leq c_{NaClO_4} \leq 0.5$ M by impedance.[679,680] The capacitance dispersion with *v is* not greater than 2-3%. A very deep diffuse-layer minimum was observed, and E_{min} is independent of c_{NaClO_4} as well as of v. Thus ClO_4^- and Na^+ are surface inactive at this interface. Parsons–Zobel plots in the range $-0.03 \leq \sigma \leq 0.03$ C m^{-2} are linear, with f_{PZ} very close to unity. Higher values of f_{PZ} at $\sigma \approx 0.02$ C m^{-2} have been explained by weak specific adsorption of ClO_4^-. C_i obtained according to the GCSG method is independent of $c_{ClO_4^-}$. Thus the deviation of the $BiDE^R$/DMF + $NaClO_4$ interface from the GCSG model is substantially smaller than in AN or MeOH.[480,677–682.]

The influence of the content of H_2O in DMF (from o to 90%) has been studied in a 0.01 M KF solution.[679,680] If the addition of H_2O is ≤ 20%, the value of $E_{min} \approx$ const. A pronounced dependence of E_{min} on the amount of H_2O (>25%) is observed; and for 90% H_2O + 10% DMF, $E_{min} \approx E_{\sigma=0}$ for H_2O + KF solution.

The $BiDE^R$/AN interface has been studied by impedance in $LiClO_4$ as well as in solutions containing Cl^-, Br^-, I^-, and SCN^-.[480,681] In $LiClO_4$ solution, the capacitance dispersion in the region $90 \leq \nu < 1100$ Hz is no greater than 2–5%. The diffuse-layer minimum potential E_{min} is independent of $c_{ClO_4^-}$ for $c_{ClO_4^-} < 0.005$ M. For more concentrated solutions, a moderate shift of E_{min} to the negative side has been observed, which is explained by the weak specific adsorption of ClO_4^-. C_i, σ curves have been calculated for various c_{el} according to the GCSG theory. At $c_{el} > 0.02$ M, a small dependence of C_i on c_{el} has been observed. A high value of f_{PZ}= 1.30 has been obtained. According to data for Bi single-crystal face

electrodes in AN,[152,154,682] a probable reason for the deviation of $BiDE^R/AN + LiClO_4$ from the GCSG model is the crystallographic inhomogeneity of a polycrystalline Bi surface.

The $BiDE^R/DMSO + LiClO_4$ interface has been studied by impedance and a very well-developed diffuse layer minimum has been observed, with E_{min} independent of c_{LiClO_4}.[475] The capacitance dispersion was no greater than 2 to 3% in the region $-1.5 \leq E < -0.3$ V (SCE in H_2O). Linear Parsons–Zobel plots with f_{PZ} very close to unity were obtained, C_i was independent of c_{LiClO_4}.

The $BiDE^R$/EtOH interface has been studied in various electrolyte solutions [$LiClO_4$, LiF, KF. $(C_4H_9)_4NClO_4$, LiC1, LiI, LiSCN] using impedance.[683,690] The capacitance dispersion in the range $60 < \nu < 5000$ Hz was negligible (3 to 4%). E_{min} was independent of c_{LiClO_4} and v. The same value of E_{min} has been obtained using very dilute KF + EtOH solutions. The Parsons–Zobel plots for $-0.03 < \sigma < 0.02$ C m^{-2} were linear, with f_{PZ} very close to unity (1.01). C_i, σ curves at various electrolyte concentrations have been calculated using the GCSG model. At $-0.11 < \sigma < 0.03$ C m^{-2}, the dependence of C_i on c_{el} is insignificant; thus specific adsorption of ClO_4^- appears to be very weak. At $\sigma > 0.04$ C m^{-2}, the dependence of C_i on c_{LiClO_4} is remarkable. The charge of specifically adsorbed anions, σ_i, was obtained by the Grahame-Soderberg method,[698,699] as well as by the Damaskin method.[672,676,700–702] In the explored region of σ, $|\sigma_i| < |\sigma|$, i.e., specific adsorption of ClO_4^- anions at the $BiDE^R/EtOH$ interface is weak.

The temperature dependence of the inner-layer properties has been studied by Väärtnõu *et al.*[688–690] over a wide interval, –0.15°C < T < 50°C. The inner-layer integral capacitance K_i, σ curves have been simulated using the Parsons[308] and Damaskin[672,673] models. The experimental K_i, T dependence has a minimum at T = 20°C. The influence of the potential drop in the metal phase has been taken into account.

The electrical double layer at $BiDE^R/PrOH$ and $BiDE^R$/2-PrOH interfaces with the addition of various electrolytes ($LiClO_4$, Lil, LiSCN, KSCN) has been studied using impedance.[691–693] The E_{min} was independent of c_{el} and ν. A weak dependence of C on ν has been found at $c_{LiClO_4} < 0.01$ M and at $\sigma > -0.03$ C m^{-2}, and the equilibrium differential capacitance $C_{\omega=0}$ has been obtained by linear extrapolation of C vs. $\omega^{1/2}$ to $\omega^{1/2} = 0$. Parsons–Zobel plots at $\sigma = 0$ are linear, with $f_{PZ} = 1.01 \pm 0.01$. The values of σ_1^- have been obtained according to Grahame and Soder-

berg,[698,699] and at all σ and $c_{LiClO_4}|\sigma_i^-| < |\sigma|$, i.e., the specific adsorption of anions is weak.

The electrical double layer at $BiDE^R$ in 1-butanol, 2-methyl-1-propanol, and 2-butanol + $LiClO_4$ solution has been studied by impedance.[693–696] The values of c_{LiClO_4} have been recalculated taking into account the incomplete dissociation of $LiClO_4$ and the effect of ionic association in butanolic solutions. The values of C have been extrapolated to $\omega = 0$ using the C, $\omega^{1/2}$ dependence. The capacitance dispersion was small at $\sigma << 0$, but at $\sigma \geq -0.03$ C m^{-2}, it increased somewhat ($\Delta C = 5\%$ at $\sigma = 0$). E_{min} was independent of c_{LiClO_4} for all butanol isomers. The Parsons–Zobel plots were linear, with f_{PZ} close to unity. The C_i, σ curves at $\sigma << 0$ were independent of the butanol isomer, but $C_i^{\sigma=0}$ increases in the sequence 2-methyl-l-propanol < 1-BuOH < 2-BuOH. The inner layer integral capacity $K_i(\sigma)$ plots have been calculated, K_i at σ_{min} increases in the sequence 2-BuOH < 2-PrOH < 1-BuOH < 1-PrOH < EtOH < MeOH. But at $\sigma = 0$, K_i for 2-PrOH and 2-BuOH is remarkably higher than for MeOH, EtOH, and 1-PrOH. For solvents with a linear hydrocarbon chain, σ_{min} is independent of the length of the hydrocarbon chain, while for solvents with a nonlinear hydrocarbon chain, σ_{min} is appreciably more negative. This has been explained in terms of decreasing specific interaction between solvent molecules and metal atoms in the order 1-PrOH < 2-PrOH < 2-BuOH, as well as by a more pronounced association of 2-PrOH and 2-BuOH in the inner layer compared with EtOH, 1-PrOH, and 1-BuOH. Thus the increase of the negative value of $E_{\sigma=0}$ in the sequence of solvents **2-PrOH < 1-PrOH < EtOH < MeOH < H_2O** can be explained by an increasing specific interaction of solvent molecules with surface Bi atoms.[696]

The $BiDE^R$/ethylene glycol interface has been studied in KF, $LiClO_4$, $LiNO_3$, LiCl, NaBr, NaI, and CsCl solutions using impedance. The dispersion of C with ν in $LiClO_4$, $LiNO_3$, and KF solutions is no greater than 2–3% if $110 < \nu < 1100$ Hz. The adsorption of ions increases in the sequence of cations $Li^+ < Na^+ < K^+ < Cs^+$, and in the sequence of anions $F^- < ClO_4^- < NO_3^- < Cl^- < Br^- < I^-$.[697] E_{min} was independent of c_{KF} and ν. The linear character of the σ, E curves is taken to indicate that the potential drop in the adsorbed solvent layer and thus the orientation of EG molecules is independent of σ for Bi as well as Hg electrodes.[323,697,703] The distance between the σ, E curves for Hg and Bi at $\sigma << 0$ is equal to the difference in the zero-charge potential for the same metals in EG: $\Delta_{Bi}^{Hg}E_{\sigma<<0} = 0.18$ V. Only at $\sigma \geq 0$ is the curvature of the σ, E curve

somewhat higher for Hg/EG than for Bi/EG. This has been explained by stronger specific adsorption of ClO_4^- at the Hg/EG interface[703] than at the $BiDE^R$/EG interface.[697]

(c) Bi single-crystal faces in aqueous solutions

The Bi external electronic configuration is (s^2p^3); it crystallizes in a rombohedral system, with two Bi atoms linked to each lattice point of the unit cell. The melting point is 544 K.

Electrochemically polished Bi single-crystal faces were first used for electrical double-layer studies by Frumkin, Palm, and co-workers[704] in 1974 using impedance. The E_{min} (Table 17) was observed to be shifted 30 mV toward more negative potentials compared with $BiDE^R$ and electrochemically polished polycrystalline Bi (pc-Bi).[666–670] The $E_{\sigma=0}$ for Bi(111) in Na_2SO_4 solution was 30 mV more negative than in NaF (KF) solutions owing to the nonsymmetrical type of electrolyte.[704] Parsons–Zobel plots in KF solution were linear, with f_{PZ} very close to unity for BiDE and pc-Bi, whereas a higher value $f_{PZ} = 1.25$ was obtained[704] for Bi(111).

Later, Bi(01$\bar{1}$), Bi(2$\bar{1}$ $\bar{1}$), Bi(001), and Bi(101) faces were studied.[28,152,253,254,705] The accuracy of the experimental results has been established by statistical analysis. A very slight variation in capacitance (3-6%) with v (from 60 to 21,000 Hz) was observed for electrochemically polished single-crystal Bi. Therefore, to a first approximation, the measured admittance was identified with the differential capacitance *C*.

In the case of the (001), (01$\bar{1}$), (101), and (2$\bar{1}$ $\bar{1}$) Bi faces, the dependence of $E_{\sigma=0}$ on the atomic density of the face is small (ΔE =20 mV) (the s^2p^3 electron configuration is the same), but a definite trend of $E_{\sigma=0}$ to become more negative with increasing atomic density can be detected.[28,253,254] However, the difference between $E_{\sigma=0}$ for the above faces and the Bi(111) face is noticeably higher (55–75 mV) and this can be explained by the different surface states of the Bi faces. According to Pearson,[706] the surface atoms of the (001), (101), (01$\bar{1}$), and (2$\bar{1}$ $\bar{1}$) Bi faces have unsaturated covalent bonds (s^2p^3-valence state) whereas the surface atoms of the Bi(111) face are chemically saturated, being able to form bonds with the aid of hybridized sp^3d^2 orbitals. Moreover, the electronic properties of Bi strongly depend on the crystallographic orientation, and it may be assumed[707,708] that in the case of Bi(111), the value of the dielectric permittivity of the Bi phase $\varepsilon_M = \varepsilon_{33} = \varepsilon_{\parallel} \approx 78$, while for

Table 17
Electrical Double-Layer Parameters of Bi Single-Crystal Faces in Various Solvents

Solvent	Electrode	$E_{\sigma=0}$/V vs. aq. SHE	$E_{\sigma=0}$/V vs. BBCr	$(\partial E_{min}/\partial \log c)$/ mV	f_{PZ}	D	Atomic density/cm^{-2}	References
H_2O	Bi(111)	−0.434 ± 0.005	0.22	5	1.04	2.03	5.6×10^{14}	28, 152
	Bi(10$\bar{1}$)	−0.34 ± 0.01	0.31	15	1.07	2.05	4.5×10^{14}	28, 152
	Bi(001)	−0.35 ± 0.01	0.30	20	1.06	2.05	5.3×10^{14}	28, 152
	Bi(01$\bar{1}$)	−0.35 ± 0.01	0.30	15	1.05	2.04	6.4×10^{14}	28, 152
	Bi(2$\bar{1}$1)	−0.33 ± 0.015	0.32	20	1.14	2.06	7.4×10^{14}	28, 152
AN	Bi(111)	−0.25 ± 0.01	0.34	5	1.06	2.04		28, 682
	Bi(10$\bar{1}$)	−0.18 ± 0.01	0.41	15	1.01	2.04		28, 682
	Bi(001)	−0.17 ± 0.01	0.42	10	0.98	2.03		28, 682
	Bi(01$\bar{1}$)	−0.18 ± 0.01	0.41	15	1.08	2.06		28, 682
	Bi(2$\bar{1}$1)	−0.17 ± 0.015	0.42	20	1.03	2.05		28, 682
MeOH	Bi(111)	−0.28 ± 0.01	0.28	10	1.05	—		152, 153
	Bi(001)	−0.21 ± 0.01	0.35	20	1.07	—		152, 153
	Bi(01$\bar{1}$)	−0.23 ± 0.01	0.33	30	1.10	—		152, 153
EtOH	Bi(111)	−0.21 ± 0.01	—	10	1.03	2.04		152, 712
	Bi(001)	−0.18 ± 0.01	—	20	1.08	2.07		152, 712
	Bi(01$\bar{1}$)	−0.20 ± 0.01	—	20	1.07	—		152, 153
	Bi(2$\bar{1}$1)	−0.22 ± 0.01	—	25	1.12	—		152, 153
i-PrOH	Bi(111)	−0.21 ± 0.01	—	10	1.02	—		152, 715
	Bi(001)	−0.170 ± 0.015	—	25	1.07	—		152, 715
	Bi(01$\bar{1}$)	−0.220 ± 0.015	—	30	1.03	—		152, 715

Bi(01$\bar{1}$) and Bi(2$\bar{1}$ $\bar{1}$), $\varepsilon_M = \varepsilon_{\parallel} = \varepsilon_{22} = \varepsilon_{\perp} \approx 100$. Taking the Thomas–Fermi reciprocal length roughly independent of the crystallographic orientation, $(k_{TF})^{-1} = 0.38$ nm, the thickness l_M and the potential drop in the metal phase can be calculated.[28,152,153,254] According to these calculations, l_M and the potential drop in the surface layer of Bi(111) are somewhat higher than for Bi(2$\bar{1}$ $\bar{1}$) and Bi(01$\bar{1}$). Thus the work function is lower for Bi(111) than that for Bi(01$\bar{1}$) and Bi(2$\bar{1}$ $\bar{1}$), and therefore $E_{\sigma=0}$ must have a more negative value for Bi(111) than for other Bi planes.[28,253,254]

Parsons–Zobel plots are linear [except for Bi(2$\bar{1}$ $\bar{1}$)] for $0.003 < c_{NaF} < 0.1$ M with $f_{PZ} = 1.01$ to 1.10 at $\sigma = 0$.[28,152,153,254] The Parsons–Zobel plot for Bi(2$\bar{1}$ $\bar{1}$) is linear only for $0.007 \leq c_{el} \leq 0.1$ M. The nonlinear character of the Parsons–Zobel plot for Bi(2$\bar{1}$ $\bar{1}$) at $c_{el} < 0.007$ M has been explained by the nonsingular surface structure of this plane (Section II.2).[152,153]

Fractal dimension D and fractional exponent α, presented in Table 17, show that the surface of electrochemically polished Bi electrodes is flat and free from components of pseudo-capacitance. A comparison of the data for LiF, NaF, and KF solutions with those for $LiClO_4$ and $NaBF_4$ solutions shows that a very weak specific adsorption of BF_4^- and ClO_4^- anions occurs at the Bi/H_2O interface as $\sigma \geq 0$. At the potential of the shallow capacity minimum ($\sigma << 0$), only a very slight rise in the capacity has been observed in the sequence $LiF \leq LiClO_4 \leq NaF < NaBF_4 < KF$. The E_{min} for $NaBF_4$ and $LiClO_4$ aqueous solutions is shifted approximately 15 to 30 mV and 30 to 50 mV, respectively, to more negative values compared with NaF aqueous solution. The Parsons–Zobel factor f_{PZ} and the height of the capacitance "hump" in the C_i, σ curve at $0.03 < \sigma < 0.05$ C m^{-2} increase in the sequence $NaF \leq KF < NaBF_4 < LiClO_4$, which can be explained by stronger adsorption of ClO_4^- than of F^-.[152,153]

C_i, σ curves have been derived according to the GCSG theory and the Valette–Hamelin approach.[67] C_i rises as the atomic density of the face decreases, except for Bi(111).[28] This is in good agreement with the theoretical calculations by Leiva and Schmickler,[429] which predicted the lowest interfacial capacitance for the most densely packed planes. The capacitance of the metal phase C_M has been calculated according to the Amokrane–Badiali model, and the thickness $l_M = 1/4\pi C_M$ as a function of σ decreases in the order Bi(111) > Bi(101) > Bi(2$\bar{1}$ $\bar{1}$) > Bi(01$\bar{1}$) > Bi(001), which is in agreement with other data.[28,152,153,707,708]

The influence of the surface pretreatment of Bi single-crystal faces has been studied, and a noticeable dependence of $E_{\sigma=0}$ on the surface structure has been established.[152,133]

The effect of the addition of various surface-active organic compounds (cyclohexanol, camphor) to an aqueous solution of Na_2SO_4 in contact with Bi single-crystal faces has been studied by Raud *et al.*[709–711] using ellipsometry. SO_4^{2-} was not specifically adsorbed, but at $E > -0.5$ V (SCE), slight oxidation of the Bi faces was possible.

(d) Bi single-crystalfaces in nonaqueous solutions

The admittance of Bi single-crystal faces in alcohol + $LiClO_4$ (methanol, ethanol, and 2-propanol) has been measured between 80 and 410 Hz.[28,152,153,712-717] Only a slight variation of C with ν (3—5%) has been found. Equilibrium C values have been obtained by extrapolation of the linear C, $\omega^{1/2}$ dependence to $\omega^{1/2} \rightarrow 0$. The E_{min} was independent of $c_{ClO_4^-}$ in $1 \times 10^{-3} < c_{ClO_4^-} < 7 \times 10^{-3}$ M, but at $c_{el} > 7 \times 10^{-3}$ M, a shift of E_{min} toward more negative values has been explained by weak specific adsorption of ClO_4^-. Parsons-Zobel plots are linear for $3 \times 10^{-3} < c_{ClO_4^-} <$ 0.5 M, with f_{PZ} slightly depending on the crystallographic orientation (Table 17). As for H_2O, f_{PZ} rises in the sequence Bi(111) < Bi(01$\bar{1}$) < Bi(001) < Bi(2$\bar{1}\bar{1}$). For MeOH, EtOH, and 2-PrOH solutions, the values of $C_i^{\sigma=0}$ and $C_i^{\sigma<<0}$ increase in the order Bi(111) < Bi(01$\bar{1}$) < Bi(001). The value of $C_i^{\sigma<<0}$ depends weakly on the crystallographic orientation of the face. The weak dependence of C_i on c_{el} has been explained by the small geometric roughness of the electrochemically polished surface.[28,152,153,712–717]

The electrical double layer at Bi(001), (101), (01$\bar{1}$), (2$\bar{1}\bar{1}$), and (111) in acetonitrile solutions of $LiClO_4$ has been studied by impedance.[682] $HClO_4$ was added to the solutions to the level of 2.5×10^{-4} M to raise the stability of the electrodes at $E > E_{\sigma=0}$. The effect of ν on C was about 6–10% (60 to 610 Hz), For dilute $LiClO_4$ solutions ($c_{LiClO_4} < 0.03$ M), E_{min} was independent of c_{LiClO_4} and v.

As for H_2O, the difference in $E_{\sigma=0}$ between the (001), (101) (01$\bar{1}$), and (2$\bar{1}\bar{1}$) faces is no greater than 10–20 mV (Table 17), while the difference between the (111) face and the other faces is 80–90 mV.[28,152,153,.682] The Parsons–Zobel plots for $-0.02 < \sigma < 0.01$ C m^{-2} were linear, with f_{PZ} very close to unity, somewhat decreasing as $|\sigma|$ rose. The somewhat higher values of f_{PZ} at $\sigma = 0$ are caused by the crystallographic (energetic) inhomogeneity of the Bi surface. With the exception of the (111) and (101) faces, the rule that predicts lower capacitances[479] for the closer packed planes was observed.[28,682] C_M and l_M have been calcu-

lated[28,152,153] according to the Amokrane–Badiali[414] model. In all solvents studied, the thin metal surface-layer thickness increases in the order **Bi(001) ≤ Bi(101) ≤ Bi(01$\bar{1}$) ≤ Bi(2$\bar{1}\bar{1}$) < Bi(111),** but the difference in l_M for Bi(001) and Bi(111) is only slightly higher than the error in obtaining l_M itself. The value of l_m^{max} increases in the order AN < H_2O < MeOH < EtOH, which has been explained by a slight deviation of practical systems from the Amokrane–Badiali model.

(xi) Antimony

(a) $SbDE^R$ in aqueous and nonaqueous solutions

The electrical double layer at solid drop Sb electrodes **($SbDE^R$)** in various aqueous and nonaqueous solutions has been studied by impedance measurements[718–724] (Table 18). The capacitance dispersion in the range of ideal polarizability is no greater than 4 to 5% with 200 < ν < 5000 Hz. A diffuse layer minimum in *C,E* curves has been observed, with E_{min} independent of c_{el} (NaF, KF) and ν, respectively.[717–724] The value of E_{min} for an Na_2SO_4 solution is shifted ~20 to 30 mV and for $KClO_4$ ~10 mV toward more negative values of *E*. The surface activity of the various anions increases in the order $F^- < SO_4^{2-} \leq NO_3^- < ClO_4^- < Cl^- < CH_3COO^- < Br^- < I^-$,[718–724] i.e., in the same order as for $BiDE^R$.[666–669] Linear Parsons–Zobel plots have been obtained with $f_{PZ} = 0.90$ to 0.95 for $SbDE^R/H_2O + KNO_3$,[720] but for $SbDE^R/KF$ or $NaF + H_2O$, $f_{PZ} = 1.10$ to 1.14,[721] which has been explained by the geometric roughness of the $SbDE^R$. The lower values of $C_i^{\sigma=0}$ and $C_i^{\sigma<<0}$ (corrected by the roughness factor $f_{PZ} = 1.10$) have been explained in terms of lower hydrophilicity, as well as the more pronounced influence of C_M for Sb than for Hg, Bi, Cd, and Zn.[721,724]

Adsorption of aliphatic alcohols and tetra-alkylammonium cations from $Na_2SO_4 + H_2O$ solutions on Sb electrodes has been investigated.[721,724] Splitting of the adsorption-desorption peak into two independent maxima has been found[725,726] for cyclohexanol adsorption at an electrochemically polished pc-Sb electrode; accordingly, the difference between the $E_{\sigma=0}$ of individual faces has been estimated to be on the order of 80 to 100 mV.

Pullerits *et al.*[723] studied specific adsorption of I^- from an aqueous solution at constant ionic strength.

Table 18
Electrical Double-Layer Parameters of Sb in Various Solvents

Solution	Electrode	$E_{\sigma=0}$/V vs. aq. SHE	$E_{\sigma=0}$/V vs. BBCr	$(\partial E_{min}/\partial \log c)$/mV	f_{PZ}	D	References
$H_2O + KNO_3$	$SbDE^R$	-0.18 ± 0.01	0.47 ± 0.01	—	0.90–0.95	—	720
H_2O + KF; NaF	$SbDE^R$	-0.17 ± 0.01	0.48 ± 0.01	—	1.10–1.14	—	721
H_2O + NaF	pc-Sb	-0.16 ± 0.02	0.49 ± 0.02	—	1.03	2.05	725, 726
$MeOH + HClO_4$	$SbDE^R$	-0.02 ± 0.025	0.54 ± 0.025	—	1.08		724
H_2O + KF	Sb(111)	-0.22 ± 0.01	0.43 ± 0.01	10	1.06	2.04	28, 152, 725, 726
	Sb(001)	-0.13 ± 0.01	0.52 ± 0.01	20	1.04	2.04	28, 152, 725, 726
	Sb(01$\bar{1}$)	-0.15 ± 0.01	0.50 ± 0.01	30	1.18	2.08	28, 152, 725, 726
	Sb(2$\bar{1}\bar{1}$)	-0.10 ± 0.015	0.55 ± 0.015	50	1.25	2.10	28, 152, 725, 726
$EtOH + LiClO_4$	Sb(111)	-0.02 ± 0.01	—	15	1.01	—	28, 152, 714
	Sb(001)	0.05 ± 0.01	—	20	1.04	—	28, 152, 714

In $MeOH + HClO_4$, E_{min} was independent of c_{HClO_4} as well as of v; thus it has been taken as $E_{\sigma=0}$ of Sb in MeOH (Table 18). The values of $C_i^{\sigma=0}$ derived from the experimental data[724] are somewhat lower than for the Bi/methanol interface.

(b) Sb single-crystal faces in aqueous and nonaqueous solutions

Sb possesses the same external electronic configuration (s^2p^3) and crystallizes in the same rombohedral system as Bi. Its melting point is 904 K.

Single-crystal Sb electrodes were prepared with the same method as that developed for Bi electrodes.[28,152,153,725,726] The (111) face is the most perfect, and the (001) plane is the additional plane of cleavage of Sb; therefore the (111) and (001) orientations can also be defined by cleaving the massive crystal at the temperature of liquid nitrogen. The final surface was prepared by electrochemical polishing in saturated aqueous solution of KI with 0.5% HC1. Impedance measurements have shown that the $E_{\sigma=0}$ of the (111) and (001) faces is roughly equal to –0.46 V and –0.37 V (SCE), respectively, i.e., $E_{\sigma=0}$ is about 30 to 50 mV more positive than the potential at which the oxidation of the Sb single-crystal faces starts. Therefore, cyclic voltammograms and impedance measurements were made in weakly acidified (with HC1, pH = 4 to 5) NaF solutions. As for Bi single-crystal faces in H_2O, Sb(111) exhibits an appreciably more negative value of $E_{\sigma=0}$ compared with the other planes (Table 18). The difference in $\Delta E_{\sigma=0}$ for Sb(001), $Sb(01\bar{1})$, and $Sb(2\bar{1}\bar{1})$ is no more than 0.05 V, and $E_{\sigma=0}$ decreases as the atomic density of the surface increases. The $E_{\sigma=0}$ for the $SbDE^R$ electrode has an intermediate value.[28,152,153] According to the independent diffuse-layer electrode model,[67,260–263] this result indicates that the faces, which have more positive values of $E_{\sigma=0}$ than Sb(111), predominate at the $SbDE^R$ surface.

The Parsons-Zobel plots are linear in the range of concentrations $0.002 < c_{el} \leq 0.1$ M, with f_{PZ} somewhat higher than unity. Just as for Bi single-crystal faces, f_{PZ} decreases slightly with increasing v and $|\sigma|$. This indicates that an f_{PZ} somewhat higher than unity at $\sigma = 0$ is mainly caused by the crystallographic inhomogeneity of the electrode surface. The fractal dimension D for Sb single-crystal faces is somewhat higher than for Bi, which can be explained by the higher energetic and crystallographic anisotropy of the Sb electrode surface or by a more pronounced anion adsorption at $\sigma \approx 0$.[28,725,726]

The C_i values for Sb faces[28,725,726] are noticeably lower than those for Bi. Just as for Bi, the closest-packed faces show the lowest values of C_i [except Bi(111) and Sb(111)].[28,152,153] This result is in good agreement with the theory[428,429] based on the jellium model for the metal and the simple hard sphere model for the electrolyte solution. The adsorption of organic compounds at Sb and Bi single-crystal face electrodes[28,152,726] shows that the surface activity of Bi(111) and Sb(111) is lower than for the other planes. Thus the anomalous position of Sb(111) as well as Bi(111) is probably caused by a more pronounced influence of the capacitance of the metal phase compared with other Sb and Bi faces.[28]

The electrical double-layer structure in the region of ideal polarizability of Sb(111)/EtOH and Sb(001)/EtOH interfaces has been investigated by impedance and cyclic voltammetry.[28,714] The value of E_{min} is independent of $c_{ClO_4^-}$, with an accuracy of ± 10 mV in the range $5 \times 10^{-4} < c_{ClO_4^-} < 5 \times 10$–3 M. AS for H_2O,[152,725,726] $\Delta E_{\sigma=0}$ in EtOH for Sb(001) and Sb(111) is higher than for Bi(111) and Bi(001). The Parsons-Zobel plots in EtOH are linear with f_{PZ} somewhat lower than for aqueous solutions, which can be attributed to the weaker dependence of the values of $E_{\sigma=0}$ on the crystallographic orientations in EtOH than in H_2O. The C_i, σ curves calculated according to the Valette-Hamelin approach[67] are monotonic since the fitting coefficient is equal to 1.03 for Sb(111) and 1.06 for Sb(001) at $c_{LiClO_4} = 0.1$ M. $C_i^{\sigma=0}$ for Sb single-crystal faces in EtOH are lower than for Bi, which has been explained by the lower lyophilicity of Sb, as well as the higher thickness of the thin metal layer.[28,152,153]

(xii) Iron

(a) Pc-Fe in aqueous and nonaqueous solutions

Fe electrodes with electrochemically polished (cathodically pretreated for 1 hr) and renewed surfaces have been investigated in $H_2O + KF$ and $H_2O + Na_2SO_4$ by Rybalka *et al.*[727,728] by impedance. A diffuse-layer minimum was observed at E = –0.94 V (SCE) in a dilute solution of Na_2SO_4 (Table 19). In dilute KC1 solutions E_{min} was shifted 40 to 60 mV toward more negative potentials. The adsorbability of organic compounds (1-pentanol, 1-hexanol, cyclohexanol, diphenylamine) at the Fe electrode was very small, which has been explained in terms of the higher hydrophilicity of Fe compared with Hg and Hg-like metals.

Table 19
Electrical-Double Layer Parameters of Fe in Various Solvents

Solvent[a]	Electrode	System	$E_{\sigma=0}$/V vs. aq. SHE	$E_{\sigma=0}$/V vs. BBCr	f_{PZ}	Atomic density/ cm^{-2}	References
H_2O	pc-Fe	KF (0.01 M) (pH = 3.5)	−0.70 ± 0.02	−0.05	—	—	727, 728
		Na_2SO_4 (pH = 2.5)	−0.70	−0.05	—	—	730
		$NaClO_4$ (pH = 7)	−0.64	0.01	—	—	190
	Fe(111)	$NaClO_4$ (pH = 2.5)	−0.69 ± 0.01	−0.04	1.43	0.707×10^{15}	739
	Fe(100)	$NaClO_4$ (pH = 2.5)	−0.72 ± 0.01	−0.07	1.33	1.222×10^{15}	739
TMU	pc-Fe	$LiClO_4$	−0.56	—	5.0	—	729
DMF	pc-Fe	$LiClO_4$	−0.41	0.10	—	—	729
DMAA	pc-Fe	$LiClO_4$	−0.31	—	—	—	729
MPF	pc-Fe	$LiClO_4$	−0.61	—	—	—	729
HMPA	pc-Fe	$LiClO_4$	−0.56	—	4.8	—	729

[a]TMU, tetramethylurea; DMAA, *N,N*,-dimethylacetamide; MPF, *N*-methyl-*N*-2-pyridylformamide; HMPA, hexamethylphosphoramide.

$(1/\omega C)$, E curves of pc-Fe electrodes with a renewed surface have been recorded 1 min after the electrode was cut by a ruby knife.[728] In KF solution $E_{\sigma=0}$ was in good agreement with $E_{\sigma=0}$ for electrochemically polished Fe electrodes.[727] As in the case of Hg and other "Hg-like" electrodes,[10] $E_{\sigma=0}$ for Fein $Na_2SO_4 + H_2O$ solution is 30 mV more negative than in KF (NaF, LiF) solution, owing to the asymmetry of the electrolyte.

A diffuse-layer minimum in C,E curves has not been found with electrodes kept 3 min at $E = -0.74$ V, i.e., at a potential close to the rest potential of Fe.[728] Complete cathodic reduction at $E << -0.74$ V (SCE) is not achieved since a diffuse-layer minimum is not found for cathodically reduced electrodes. This effect has been explained by the oxidation of Fe. According to impedance data, strong specific adsorption of Cl^- anions at renewed Fe electrodes occurs since a very large shift of $E_{\sigma=0}$ takes place going from KF to KC1 solutions.

According to Safonov *et al.*,[729] the $E_{\sigma=0}$ for pc-Fe obtained in aqueous solutions[727,728] corresponds to an active iron surface, free from any oxides. A dependence of the pzc on pH has been observed and discussed by Lazarova.[730] A collection of experimental data up to 1994 is given in a paper by Turowska and Sokolowski.[731]

The electrical double layer at the renewed $Fe/LiClO_4$ interface has been studied in nonaqueous aprotic solvents by Safonov *et al.* using impedance.[729,732–736] Renewed Fe electrodes are ideally polarizable in a limited region of potentials in the following aprotic $LiClO_4$ solutions: 1,1,3,3-tetramethylurea (TMU); *N*,*N*-dimethylformamide; *N*,*N*-dimethylacetamide (DMAA); *N*-methyl-*N*-2-pyridylformamide (MPF), and hexamethylphosphoramide (HMPA). The rest potential of a renewed Fe electrode in an $LiClO_4 + TMU$ system is equal to –0.35 V (SCE in H_2O), independent of c_{LiClO_4}. AN and DMSO were unstable in contact with a renewed Fe surface.[733] The E_{min} in C,E curves depends on time; for $Fe/TMU + LiClO_4$, $E_{min} = -0.8$ V (SCE in H_2O) just after surface renewal and –0.35 V (SCE in H_2O) after 15 min. One minute after the Fe electrode is cut, the decrease in the components of impedance $(1/C_\omega$ and $R)$ at $E =$ const is no greater than 5 to 7% in the region $-1.4 \text{ V} < E < 0$ V, and the dispersion of C with ν (70 to 1000 Hz) is no greater than 10%.[729,732–734] The values obtained[729] for $E_{\sigma=0}$ are summarized in Table 19. The Parsons-Zobel plot at E_{min} is linear, with f_{PZ} equal to 5.0 in TMU and 4.8 in HMPA.[729] The surface structure of renewed electrodes consists mainly of patches of close-packed faces with a linear parameter of 5–6 nm. The relaxation of the surface back to the equilibrium state is very slow ($\tau \sim$

10–15 min.). X-ray diffraction data show that in some places the surface of renewed Fe, Pt, and Ag electrodes is amorphous and the thickness of such a "Beilby" layer is on the order of 5 to 10 nm. Thus, reconstruction of the surface is probable during the experiments with a decrease in surface roughness with time.[729]

In the region of E_{min}, a very good correspondence has been found between experimental and calculated C,E curves and this has been taken to indicate that the electrical double-layer structure conforms to the GCSG theory. Comparison of the C_i,E curves for Hg/TMU and Fe/TMU shows that the dependence of C_i on E *is* less pronounced for an Fe electrode than for Hg/TMU, and the values of C_i for Fe are remarkably lower than for Hg.[729] The same is the case for Fe/DMF, DMAA, MPF, and HMPA interfaces.[732–736]

On the basis of σ,E curves obtained by integration of C,E curves, it has been estimated that the contribution of the solvent to the interfacial potential drop is substantially higher for Fe than for Hg in TMU. Accordingly, strong chemisorption of solvent molecules, weakly depending on E, is probable at an Fe/TMU interface.[729,732–736] Cl^- has been found to be specifically adsorbed. However, at $\sigma \geq +2.0\ \mu C\ cm^{-2}$, the values of C (in 0.02 KCl) are lower than those in 0.02 M $LiClO_4$. The same effect has been reported for Ni, Cu,[567,737,738] and Pt, and has been explained by a partial charge transfer from Cl^- to the metal.[729] If $c_{Cl^-} > 0.02$ M, at $\sigma > 0$, anodic dissolution of Fe occurs. The activity of anions at the Fe/TMU interface increases in the sequence $ClO_4^- < Cl^- < Br^- < I^-$. The values of C at E = const are independent of the chemical nature of the cations.[729]

(b) Fe single-crystal faces in aqueous solutions

Fe crystallizes in the bcc system and its melting point is 1808 K. The atomic density of the faces increases in the order Fe(111) < Fe(100) < Fe(110) (Table 19).

Fe(100) and (111) single-crystal faces in sulfate or perchlorate solutions (pH = 2.5) have been studied by impedance.[739] The electrodes were grown at 750 to 780°C from $FeBr_2$ in pure H_2 atmosphere and reduced for 1 hr at E = –0.95 V (SCE) in the working solution. A diffuse-layer capacitance minimum was observed, with E_{min} independent of c_{el} (Na_2SO_4, KCl, $NaClO_4$). Thus, SO_4^{2-} and ClO_4^- are surface inactive on Fe single-crystal faces. The Parsons-Zobel plots for Fe(100) and Fe(111) were linear, with f_{PZ} somewhat higher than unity. This has been explained

by problems related to obtaining the exact working area of the Fe single crystal. The inner-layer capacitance decreases from Fe(111) to Fe(100) as the atomic density of the face increases.

(xiii) Nickel

(a) Pc-Ni in aqueous solutions

The $E_{\sigma=0}$ of pc-Ni is located in the negative potential range and depends strongly on the solution's pH.[730,740,741] According to impedance data,[740] E_{min} in aqueous H_2SO_4 depends on pH: E_{min} (V, SCE) = –0.461, –0.493, –0.528, and –0.572 for pH = 0.94; 1.4, 2.14, and 2.97, respectively. Using the method of galvanostatic pulses, minima have been found at E = –0.38 V and –0.68 V for pH 3.5 and 5.8, respectively.[741] Using the closed-circuit scrape method, E_{min} = –0.48 V at pH = 3 and –0.61 V at pH = 5.6.[730] Using the hardness method, Tyurin *et al.*[742] have reported two pzc values ($E^1_{\sigma=0}$ and $E^2_{\sigma=0}$) for pc-Ni as a function of potential. pH effects have also been observed [at pH<4, $E^1_{\sigma=0}$ = –0.44 V; $E^2_{\sigma=0}$ = –0.64 V(SCE)]. Thus, widely scattered E_{min} values have been reported by different authors[730,740–742] at similar solution pHs (Table 20).

(b) Ni single-crystal faces in aqueous solutions

Ni crystallizes in the fee system: the atomic density of the faces increases in the order (110) < (100) < (111). Its melting point is 1726 K.

Ni single-crystal faces in $H_2O + HClO_4$ or H_2SO_4 solutions have been investigated by Arold and Tamm using impedance.[743] Ni (100), (110), and (111) single-crystal faces were prepared by the method described by

Table 20
Electrical Double-Layer Parameters of Ni in Aqueous Solutions

Electrode	Solution	E_{min}/V vs. SHE	f_{PZ}	Atomic density/cm^{-2}	Refererices
pc-Ni	H_2SO_4 (pH = 2.97)	–0.33	—	—	740
	H_2SO_4 (pH = 3.5)	–0.11	2.2	—	741
	H_2SO_4 (pH = 3.0)	–0.24	—	—	730
Ni(100)	$HClO_4$ (0.003 M)	–0.39 ± 0.02	1.0	1.614×10^{15}	743
Ni(110)	$HClO_4$ (0.003 M)	–0.53 ± 0.02	1.0	1.141×10^{15}	743

Batrakov and Naumova.[739] A diffuse-layer minimum has been observed, with E_{min} independent of v and c_{el} (Table 20). In the case of Ni(111) and pc-Ni, the capacity also decreases with dilution, but no deep minimum was observed in the *C,E* curves.[743]

The Parsons-Zobel plot at E_{min} was linear, giving an $f_{PZ} \approx 1$. Very low C_i values have been obtained. This result is surprising in light of Ni and Fe hydrophilicity: by analogy with sp-metals (Ga, Zn), one would expect relatively high C_i values. The difference between sp- and sd-metals has been explained by a different strength of the interaction between the metal surface and solvent molecules.[743] The E_{min} for Ni(100) is slightly dependent on $c_{H_2SO_4}$, and unlike $HClO_4$ solutions, a maximum at C_i, σ curves has been found at $\sigma > 0$. These observations probably indicate that weak specific adsorption of SO_4^{2-} or HSO_4^- occurs. This has been suggested[743] as a plausible reason for the marked dependence of E_{min} on a solution's pH[730,740–742]

Water adsorption and dissociation on Ni(111) and $Ni_8(6 + 2)$ clusters have been studied by ab initio quantum-chemical calculations.[744–746]

(xiv) Aluminum

First attempts to study the electrical double layer at Al electrodes in aqueous and nonaqueous solutions were made in 1962–1965,[182,747,748] but the results were not successful.[190] The electrical double-layer structure at a renewed Al/nonaqueous solution of surface-inactive electrolytes such as $(CH_3)_4NBF_4$, $(CH_3)_4NClO_4$, $(CH_3)_4NPF_6$, and $(C_4H_9)_4NBF_4$, has been investigated by impedance.[749–751] γ-butyrolactone (γ-BL), DMSO, and DMF have been used as solvents. In a wide region of E [$-2.5 < E < -1.0$ V (SCE in H_2O)], C is independent of time, and renewed Al electrodes can be considered ideally polarizable. C increases in the sequence γ-BL $\leq$ DMSO < DMF.

In dilute solutions, a minimum in the *C,E* curves has been observed, with E_{min} independent of c_{el}. The Parsons-Zobel plots for various solvents are linear, with the values of f_{PZ} in the range 1.12 (DMSO) to 2.0 (γ-BL)[749,751] (Table 21).

C,E curves were integrated to obtain σ,E curves. As in the case of Fe/DMSO, Fe/DMF. Pt/DMF, Pt/AN, Pd/DMSO, and Pd/AN,[108,109,729] the $d\sigma/dE$ for Al/DMF and Al/γ-BL system is half that for Hg or Bi.[10,749–751] The value of $d\sigma/dE$ for an Al/DMSO system is comparable with Hg/DMSO. A comparison of the *C,E* curves for Al electrodes with the corresponding

Table 21
Electrical Double-Layer Parameters of Al in Nonaqueous Solutions

Electrode	Solvent	$E_{\sigma=0}$/V vs. aq. SHE	$E_{\sigma=0}$/V vs. BBCr	$f_{PZ} \pm 0.02$	References
Al	γ-BL[a]	−1.36	—	2.0	750, 751
	DMSO	−1.51	−0.91	1.12	750, 751
	DMF	−1.84	−1.33	1.92	750, 751

[a]γ-BL, γ-butyrolactone.

curves for Hg, Bi, Ga, and In(Ga) shows that C increases in the order Hg < Bi < Ga < Al and for Al electrodes in the order **γ-BL** < DMSO < DMF.[749–751]

(xv) Platinum-Group Metals

(a) Pc-Pt-group metals in aqueous solutions

Pt and Pt-group metals (poly- and single crystals) have long been among the most intensively studied systems in electrochemistry[6,8,10,11,14,25,140,186,188,206,412,752–796.] nevertheless reliable $E_{\sigma=0}$ values have been determined only recently.

The first attempt to obtain the pzc of Pt-group metals in H_2O by impedance was made in 1956.[622,758] The E_{min} was found to depend on solution pH. These results and other experimental problems have been critically discussed by Frumkin *et al.*[8,10,11,759] A dependence of E_{min} on solution pH for a pc-Pt electrode (heated a few minutes in a hydrogen atmosphere at 673 K and thereafter for 4–5 hr in pure Ar at 723 K) was reported by Bockris *et al.*,[370,760] who provided a quantitative relation E_{min} = 0.56–2.3 (*RT/F*) pH (SHE). As noted by Frumkin,[10] a pH-dependent E_{min}[370,760] probably corresponds to a pc-Pt surface covered by chemisorbed OH radicals. The capacitance at anodically polarized pc-Pt electrodes was measured by Schuldiner *et al.*[761,762] using very short current pulses. In H_2SO_4 solution, a minimum in the *C,E* curve was observed at $E_{min} = 0.23$ V versus the reversible hydrogen electrode (RHE). The effect of heat treatment on the $E_{\sigma=0}$ of platinized Pt has been investigated by Petrii and Ushmaev.[763] $E_{\sigma=0}$ has been found to shift to the negative side with increasing temperature of the heat treatment.

Frumkin *et al.*'s analysis[8,11,14] in 1970 led to the conclusion that in the case of nonpolarizable electrodes, since the Pt-group metals are in the regions of H or O adsorption, two values of zero-charge potential can be defined: $E_{\sigma=0}$ and $E_{Q=0}$ (see Section I). The pzc of H-adsorbing metals depends on a solution's pH, and the values are given in Table 22. A "classical" adsorption method has been used to determine pzc, and the surface excess of protons has been obtained by titration: at $E_{Q=0}$, $\Gamma_{H^+} = 0$. The values of $E_{\sigma=0}$ obtained by the scrape method [$E_{\sigma=0}$ = -0.22 V at pH = 7.0; $E_{\sigma=0}$ = -0.54 V (SCE) at pH = 11.0][190] are in reasonable agreement with the data of Frumkin *et al.*[8,10,11] On the basis of the pronounced influence of anions on hydrogen adsorption on pc-Pt,[8,10,11,14] it has been inferred that $E_{\sigma=0}$ must lie in that potential region. However, such a small positive $E_{\sigma=0}$ value is in contradiction to the high work function of pc-Pt ($\Phi \geq 5.7$ eV).[782,783] Recently it has been established that specific adsorption of various anions (SO_4^{2-}) also occurs on negatively charged surfaces.[140,186,188] It is thus an inadequate approximation to relate the value of $E_{\sigma=0}$ to the potential where anion adsorption commences. The influence of foreign metal adatoms on $E_{\sigma=0}$ of Pt and Rh has been investigated by Podlovchenko and co-workers.[764-765]

It should be stressed that in the case of pc-Pt electrodes the crystallographic structure of the surface probably exerts a very pronounced influence, so that the experimental pzc and pztc values do not correspond to the condition $\bar{\sigma}_{PC} = 0$.

Results for other metals of the Pt-group are due to Frumkin and co-workers[8,10,11,14] (Table 22). However, an electrode with the surface renewed in closed circuit has been used by Lazarova[767] to study $E_{\sigma=0}$ of Rh as a function of pH. In 0.005 M Na_2SO_4, $E_{\sigma=0}$ = –0.09 ± 0.02 V (SCE), while in 0.5 M Na_2SO_4, pH2.5, $E_{\sigma=0}$ = –0.22 V is reported. $E_{\sigma=0}$ has been found to depend linearly on pH with a slope of ca. 55 mV. This has been explained by the adsorption properties of Rh toward H and O, which shift $E_{\sigma=0}$ to more negative values. Anions have been observed to specifically adsorb on Rh more strongly than on Pt in the sequence $SO_4^{2-} < Cl^- < Br^- < I^-$.[767]

(b) Pt-group metal single-crystalfaces in aqueous solutions

The surface electrochemistry of Pt single-crystal electrodes has been exhaustively studied using cyclic voltammetry.[100,186,188,197,209,412,753–756,771,–773,779–788,794–796] This technique has been proved to be highly

Table 22
Potentials of Zero Charge of Polycrystalline Pt-Group Metals in Aqueous Solutions

Metal	Electrolyte	$E_{\sigma=0}$/V vs. SHE	$E_{\sigma=0}$/V vs. SHE	Method	References
Pt	0.3 M HF + 0.12 M KF (pH = 2.4)	0.185	0.235	Titration	8, 10, 11, 14
	0.5 M Na_2SO_4 + 0.005 M H_2SO_4 (pH = 2 + 4)	0.16	0.20	Titration	8, 10, 11, 14
	0.5 M Na_2SO_4 + 0.001 M NaOH (pH = 12)	—	–0.25	Titration	8, 10, 11, 14
	0.1 M KCl + 0.01 M HCl (pH = 2.0)	—	–0.14	Titration	8, 10, 11, 14
	1 M KCl + 0.01 M HCl	0.05	0.14	Titration	8, 10, 11, 14
	1 M KBr + 0.01 M HBr	–0.03	0.06	Titration	8, 10, 11, 14
	1 M KBr + 0.01 M KOH	–0.39	–0.33	Titration	8, 10, 11, 14
	0.05 M Na_2SO_4 + 0.005 M H_2SO_4 + 0.005 M $ZnSO_4$	0.27	0.29	Titration	8, 10, 11, 14
	$NaClO_4$ (pH = 1.0)	–0.24	—	Scrape	190
	$NaClO_4$ (pH = 7.0)	0.02	—	Scrape	190
	$NaClO_4$ (pH = 11.0)	–0.30	—	Scrape	190
Pd	0.05 M Na_2SO_4 + 0.001 M H_2SO_4 (pH = 3)	0.10	0.26	Titration	8, 10, 11, 14
	$NaClO_4$ (pH = 7.0)	0.00	—	Scrape	190

(*continued*)

Table 22
Continued

Metal	Electrolyte	$E_{\sigma=0}$/V vs. SHE	$E_{\sigma=0}$/V vs. SHE	Method	References
Rh	0.3 M HF + 0.12 M KF (pH = 2.4)	–0.005	0.085	Titration	8, 10, 11, 14
	0.5 M Na_2SO_4 + 0.005 M H_2SO_4	–0.04	0.03	Titration	8, 10, 11, 14
	0.005 M Na_2SO_4 (pH = 2.0)	0.15	—	Scrape	767
	0.5 M Na_2SO_4 + H_2SO_4 (pH = 2.5)	0.02	—	Scrape	767
	0.1 M KCl + 0.01 M HCl (pH = 2.0)	–0.13	0.02	Titration	8, 10, 11, 14
	$NaClO_4$ (pH = 1.0)	0.17	—	Scrape	190
	$NaClO_4$ (pH = 7.0)	–0.02	—	Scrape	190
Ir	0.3 M HF + 0.12 M KF (pH = 2.4)	–0.01	—	Titration	8, 10, 11, 14
	0.5 M Na_2SO_4 + 0.005 M H_2SO_4 (pH = 2.4)	–0.06	0.10	Titration	8, 10, 11, 14
	0.1 M KCl + 0.01 M HCl (pH = 2.0)	–0.13	0.06	Titration	8, 10, 11, 14
	$NaClO_4$ (pH = 1.0)	0.21	—	Scrape	190
	$NaClO_4$ (pH = 7.0)	0.52	—	Scrape	190

sensitive both to the crystallographic structure and to the surface chemical composition of Pt. Its use for *in situ* surface characterization has been widely developed in the past few years and a detailed description has been achieved for stepped surfaces at an atomic level.[754–756] Phenomena such as step reconstruction[755] and step coalescence[756] have been investigated by voltammetry. Most adsorption studies have been carried out at Pt(l 11), which is a relatively simple surface without reconstruction over a wide range of interfacial conditions (E, chemical composition); nevertheless, its electrochemical behavior is not yet fully understood.[186,754–756,785,794–796]

A detailed study of the voltammograms of Pt(l 11) prepared by the flame annealing method shows anomalous peaks associated with the specific adsorption of anions rather than with hydrogen adsorption.[754–756] In the case of $HClO_4$ and HF solutions, such features have been attributed to the adsorption of OH^-, but in H_2SO_4 solution they are explained by SO_4^{2-} or bisulfate adsorption.[757] Double-layer charging has been observed only in a very narrow potential region [$0.1 < E < 0.35$ V (SCE) in 0.05 M H_2SO_4] which depends on the chemical nature of the anion. Recent LEED and electrochemical STM studies have brought some insight into the relationship between the microscopic surface structure and the electrochemical properties of Pt electrodes.[768,769]

In several recent *in situ* infrared (IR) studies, potential-dependent ion adsorption has been discussed in terms of spectral parameters, such as band splitting, band intensity, and band center shifts.[206,207,210,770–772] Some data for anion adsorption suggest an influence of H_2O on their adsorption. Vibrational spectra of H_2O adsorbed at the gas/solid interface have been obtained for different metals. EELS data at Pt(l 11) indicate the predominance of intermolecular H-bonding, giving rise to icelike structures matching the pattern of the metal substrate.[774] More recently, isolated water molecules adsorbed on Pt(l 11) have been observed at low coverages ($\theta <$ 0.13).[775] Wagner and Moylan[211] have estimated for Pt(111) in HF aqueous solutions the value of 0.22 V (RHE) for $E_{\sigma=0}$ by comparing voltammetric curves and high-resolution electron energy loss spectroscopic data for water + H^+ coadsorption from the gas phase. However, the number of other methods useful for liquid/solid interfaces is limited and among these, X-ray scattering should be mentioned,[776,777]

Some $E_{\sigma=0}$ measurements with Pt single-crystal faces have been published recently.[140,210,773] Iwasita and Xia[210] prepared platinum single crystals according to the method of Clavilier *et al.*[186,773] After flame annealing and cooling in an H_2 + Ar mixture, the electrode was protected

with a droplet of H_2O and transferred into the cell. Cyclic voltammograms were recorded to locate the double-layer region $0.35 < E < 0.6$ V(RHE). FTIR reflection adsorption spectra for Pt(111) in $H_2O + HClO_4$ (0.1 M)[210] have shown bands corresponding to O–H stretching and H–O–H in-face deformation of adsorbed H_2O molecules. At 0.35 V (RHE), water orientation changes from hydrogen down to oxygen down and this has been taken to indicate that the zero-charge potential of Pt(111) is close to this value. In the potential region corresponding to the anomalous peaks of Pt(111), the bending frequency decreases consistently with a strengthening of the H_2O–Pt interaction. Surface water clusters (trimers, tetramers) prevail on the surface at 0.35 V (RHE), adsorbed molecules being tilted with respect to the surface. At higher potentials, the molecular plane becomes oriented perpendicularly and lateral H-bonds are broken. Above 0.50 V (RHE), the H_2O–metal interaction has been observed to increase, with eventual dissociation of H_2O at the surface.[210]

Hamm *et al.*[140] treated a Pt(111) surface in a UHV chamber by sputtering and annealing until the surface was clean and well ordered.[779,780] Transfer of the electrode to the electrochemical cell was carried out in an Ar atmosphere in a closed system. The voltammogram in 0.1 M $HClO_4$ was identical to that for flame-annealed Pt electrodes in a conventional electrochemical cell.[140,186,753,780,781] The current peaks in the potential range -0.16 to 0.13 V (SCE) were attributed to hydrogen adsorption with a total charge density $140 \pm 20\ \mu C\ cm^{-2}$, and in the range $0.28 < E < 0.58$ V (SCE) to OH^- adsorption (H_2O decomposition) (total charge density $106 \pm 12\ \mu C\ cm^{-2}$). A very narrow potential region, $0.13 < E < 0.28$ V (SCE), is left to bare double-layer charging with a capacitance $C = 110 \pm 13\ \mu F\ cm^{-2}$. Only in this region is a Pt(111) surface free from surface adlayers. The immersion method was used, the integration of the current transients in 0.1 M $HClO_4$ solution at various constant immersion potentials giving the immersion charge density Q,E curve. The Q,E plot has been found to go through zero at 0.56 V (SCE), which to a first approximation has been identified with the potential-of-zero total charge $E_{Q=0}$.[140] Changes in the sign of Q at E=0.56 V have been attributed to the decomposition of adsorbed H_2O molecules and the chemisorption of OH^-. The agreement between the charge density curves from the integration of cyclic voltammograms with the assumption of $E_{Q=0} = 0.56$ V (SCE), and those from immersion experiments is good. Immersion of Pt(111) at E = 0.23 V (SCE) gave a negative value of Q; therefore the pzc was inferred to be more positive than 0.56 V (i.e., more positive than $E_{Q=0}$). The

negative sign of Q may be caused by strong specific adsorption of H_2O molecules and ClO_4^-. Assuming that the double-layer capacitance is independent of E, $E_{\sigma=0}$ was derived by *linear* extrapolation of the Q,E curve from the double-layer charging region to $Q = 0$, as 1.08 V (SCE). Assuming a small dependence of C on E, a somewhat less positive $E_{\sigma=0}$ has been estimated as ~0.88 V (SCE).

Clavilier *et al.*[196,794–796] have studied CO adsorption on electrochemically faceted Pt(111) and Pt(110) electrodes and from the charge transients, with the provision that the CO dipole has a negligible contribution to the electrical double-layer potential; these authors have provided a "definite" determination of $E_{Q=0}$. However, electrochemically faceted Pt(111) electrodes have a polycrystalline surface structure, and thus the value of $E_{Q=0}$ for such electrodes lies between $E_{Q=0}^{(111)}$ for terraces and $E_{Q=0}^{(110)}$ for steps.[197,786,787]

A novel nondestructive method for the determination of total charges and hence of $E_{Q=0}$, that is based on the CO displacement experiments has been worked out.[795,796] This method has been applied to Pt(111) and Pt(1 10) electrodes in contact with solutions at different pHs. For both Pt faces, the potential-of-zero total charge lies in a potential region similar to that for pc-Pt.[8,10,11] It was found that the pztc depends on pH in different ways for Pt(1 11) and Pt(1 10), which demonstrates that not only is the pztc structure sensitive, but also that it varies with pH.[795] The value of pztc for Pt(1 11) is more positive than that for Pt(1 10), and $\partial E_{Q=0}/\partial pH$ is higher for Pt(111) than for Pt(110).

A detailed study of N_2O reduction on a variety of single-crystal Pt-group metal electrodes has been reported by Attard *et al.*[197,786,787] Single crystals were polished to a mirror finish, flame annealed several hours, and quenched in dilute HF. Cyclic voltammograms were recorded in 0.1 M $HClO_4$. By comparison with previous experimental data[196,783] it has been noted that N_2O reduction current maxima occurred exactly at Clavilier's $E_{Q=0}$. Thus, it has been suggested that there is a direct correspondence between $E_{Q=0}$ and the potential of N_2O reduction at a maximum rate.[197,786,787] The importance of a local value of $E_{Q=0}$ has been emphasized, especially with respect to reconstructing metal surfaces such as Pt(100) and Pt(110), which can be prepared in a variety of crystallographic states. The sensitivity of N_2O reduction to local pztc, $E_{Q=0}^{local}$, has been suggested to derive from blocking N_2O adsorption by ionic species, whose surface concentration is a function of the local surface charge. $E_{Q=0}^{local}$ values estimated by Attard *et al.*[46] are reported in Table 23.

Table 23
Potentials of Zero Charge of Pt-Group Metal Single-Crystal Faces in Aqueous Solutions

Electrode	Electrolyte	Adsorbed anion	$E^{local}_{Q=0}$/V vs. SHE	$E_{\sigma=0}$/V vs. SHE	Adsorption state (terrace)	Atomic density/cm^{-2}	References
Pt(111)	0.1 M $HClO_4$	—	0.34		(111)	1.503×10^{15}	197
	0.1 M $HClO_4$		0.29				210
	0.1 M $HClO_4$		0.27				795
	0.1 M $HClO_4$		0.78	1.1			140
	0.1 M $HClO_4$		0.22	0.07			785
	0.5 M H_2SO_4		0.28				796
	0.5 M H_2SO_4	HSO_4^-	0.30		(111)		197
	$HClO_4$ + $NaClO_4$ (pH = 1.0)		0.26		(111)		795
	NaH_2PO_4 + Na_2HPO_4 (pH = 2.3)		0.19				795
Pt(110)	0.1 M $HClO_4$	—	0.16		(110)-(1 × 2)[a]	0.920×10^{15}	197
			0.22		(110)-1D[b]		197
			0.35–0.40		(110)-2D[c]		197
		Cl^-	0.10		(110)-(1 × 2)[a]		197
	0.1 M $HClO_4$		0.17		(110)-(1 × 1)		795
	NaH_2PO_4 + Na_2HPO_4 (pH = 1.8)		0.06		(110)-(1 × 1)		795
	0.1 M H_2SO_4	HSO_4^-	0.07		(110)-(1 × 2)[a]		197
			0.21		(110)-1D[b]		197
	0.5 M H_2SO_4	HSO_4^-	0.12		(110)-(1 × 1)		795

Pt(100)	0.1 M $HClO_4$	—	0.25	(100)-1D	1.302×10^{15}	197
		—	0.37	(100)-2D[c]		197
	0.1 M H_2SO_4	HSO_4^-	0.21	(100)-1D[b]		197
		—	0.33	(100)-2D[c]		197
Rh(111)	0.1 M $HClO_4$	—	0.16–0.17	(111)	1.599×10^{15}	197
		Cl^-	*0.05*	*(111)*		*197*
	0.1 M H_2SO_4	HSO_4^-	0.04–0.09	(111)		197
Ir(111)	0.1 M $HClO_4$	—	0.13	(111)	1.574×10^{15}	197
		Cl^-	0.03	(111)		197
	0.1 M H_2SO_4	HSO_4^-	0.01	(111)		197
Pd/Pt	0.1 M $HClO_4$	—	0.27	(111)		197
		Cl^-	0.19	(111)		197
Rh	0.1 M H_2SO_4	HSO_4^-	0.05–0.09	pc		197
	0.1 M $HClO_4$	—	0.12	pc		197
		Cl^-	0.07	pc		197
Pd	0.1 M $HClO_4$	—	0.20	pc (no adsorbed H)		197
			0.30	pc (adsorbed H)		

[a]Potentials in Ref. 197 are given vs. Pd(H). They have been converted to SHE by subtracting (57 × pH – 60) mV.[197]
[b]Reconstructed missing-row surface.
[c]One-dimensionally ordered surface.
[d]Two-dimensional long-range ordered surface.

According to Table 23, the values of $E_{Q=0}$ for single-crystal face electrodes are in reasonable agreement with those for pc-Pt metal electrodes, although on (111) surfaces possessing good long-range order, the value of $E_{Q=0}^{local}$ tends to lie at more negative E than $E_{Q=0}$. As a function of the metal, the sequence is $E_{Q=0}^{Pt,local} > E_{Q=0}^{Pd,local} > E_{Q=0}^{Rh,local} > E_{Q=0}^{Ir,local}$. However, in contradiction to the trend expected on the basis of the atomic density of Pt surfaces and experimental results for other FCC metals[6–8,24,74] (i.e., $E_{Q=0}^{(111)} > E_{Q=0}^{(100)} > E_{Q=0}^{(110)}$), the observed experimental order for Pt is $E_{Q=0}^{(100)(2D)} \approx E_{Q=0}^{(110)(2D)} > E_{Q=0}^{(111)(2D)}$. It should be noted (see Section I) that $E_{Q=0}$, by its nature, cannot be related to the work function as definitely as $E_{\sigma=0}$. Therefore expectations based on the behavior of $E_{\sigma=0}$ are inadequate for $E_{Q=0}$.

$E_{Q=0}^{local}$ shifts toward negative values as anions are adsorbed. Thus the anomalous position of $E_{Q=0}^{(111)(2D)}$ can be explained by higher anion adsorption (probably ClO_4^-) at Pt(111) in accordance with the general behavior of fcc metals. For the same reason, the value of $E_{Q=0}$ for terraces has been found to be more positive than that for steps. As mentioned, the value of $E_{Q=0}$ reported by Clavilier *et al.*[196] for an electrochemically faceted Pt(111) surface lies between $E_{Q=0}^{(111)terrace}$ and $E_{Q=0}^{(111)step}$. It should be stressed that for pc electrodes a single value of $E_{Q=0}$ is ambiguous, and it is better to refer to such a potential as "pseudo-potential of total zero charge" since both positively and negatively charged regions may coexist on the surface ($\bar{\sigma} = 0$) (see Section II.2).

(c) Pt-group metals in nonaqueous solutions

Pt and Pd with a renewed surface obtained by cutting with a ruby knife under the working solution have been studied by Petrii and Khomchenko[797] in AN. The roughness factor of platinum, obtained from the hydrogen desorption peak in an aqueous solution,[798] was about 3.9–4.0, and for Pd 3.3-3.4 (Table 24). The frequency dependence of capacitance did not exceed 10-12% in 0.01 M $LiClO_4$ and 15% in 0.001 M $LiClO_4$. A minimum appears in the C,E curves in dilute solutions of $LiClO_4$ in AN, and its potential [-0.48 ± 0.02 V (Ag/0.1 M $AgNO_3$ in AN)] does not shift with the electrolyte concentration. The Parsons-Zobel approach has been used to study the nature of the minimum.[797] The PZ plot has been found to be linear, which has been attributed to the diffuseness of the electrical double layer. The slope of the plot is close to 1, which has been taken as supporting the correctness of the choice of the roughness factor and of the

Table 24
Potentials of Zero Charge of Pt-Group Metals in Nonaqueous Solutions

Metal	Solvent	Electrolyte	$E_{\sigma=0} \pm 0.03$ V vs. aq. SHE	$E_{\sigma=0} \pm 0.01$ V vs. FerriFerro[a]	$E_{\sigma=0} \pm 0.02$ V vs. BBCr	f_{PZ}	References
pc-Pt	AN		0.14	—	0.73	3.9–4.0	797
pc-Pt	DMSO		0.09	—	0.69	1.9	806
Pt(100)	AN	$NaClO_4$	—	-0.51 ± 0.01	—		801
Pt(111)	AN	$NaClO_4$	—	-0.51 ± 0.01	—		801
pc-Pd	AN		0.32	—	0.91	3.3–3.4	797
pc-Pd	DMSO		0.24	—	0.84	2.0	806

[a]Ferricinium/ferrocene scale.

dielectric constant of AN in the diffuse layer (bulk value). The constancy of the potential of the minimum with the concentration of $LiClO_4$ indicates an absence of specific adsorption. No indication of diffuseness has been found in solutions of $NaClO_4$, which may be due to certain specific adsorption of the less solvated Na^+ cation. According to data for aqueous solutions, specific adsorption of cations is higher on Pt-group metals than on other metals. The potential of zero charge of Pt in AN solutions is more positive than for Hg, Bi, Ga, and In/Ga alloy.[354,353,480] The shift of $E_{\sigma=0}$ in the transition from the latter metals to Pt does not correspond to the change in Φ, which indicates strong chemisorption of AN on the Pt surface. The minimum in the *C,E* curves for Pt and Pd is retained as a small quantity of H_2O is added to AN, while $E_{\sigma=0}$ shifts to the positive direction as the amount of H_2O increases. In the presence of C_6H_6, the potential of the diffuse-layer capacitance as well as the minimum value of the capacity remain unchanged, which has been explained in terms of very weak adsorption of C_6H_6 on Pt electrodes.[797]

The potential dependence of Con Pd in AN is somewhat more marked than for Pt, and the values of *C* are somewhat higher. This has been related to different chemisorption of AN on Pt and Pd. As for Pt, the potential $E_{\sigma=0}$ of Pd shifts to positive values as the amount of H_2O in AN increases. The addition of C_6H_6 does not change the values of *C* and $E_{\sigma=0}$ for Pd.[797]

The adsorption behavior of AN on Pt has been investigated by Conway and co-workers[799,800] for both polycrystalline and single-crystal surfaces. The orientation of AN molecules at Pt single-crystal face electrodes has been studied by Fawcett and co-workers[801] using SNIFTIRS. It was found that $E_{\sigma=0}$ for Pt/AN is independent of the crystallographic structure, which has been explained by the very strong adsorption of AN at Pt single-crystal face electrodes.

At renewed Pt and Pd electrodes in AN with different additions of $(C_2H_5)_4NBF_4$, Petrii *et al.*[802] have observed a broad capacitance minimum in a wide potential range (~1 V for Pt and 0.8 V for Pd). The values of $E_{\sigma=0}$ have been observed at -0.43 ± 0.03 V for Pt and -0.30 ± 0.03 V (Ag/0.1 M AgCl in AN) for Pd. $E_{\sigma=0}$ is independent of the nature of the anion (ClO_4^-, BF_4^-). The PZ plots are linear, with $f_{PZ} \approx 1.0$. It has been found[802,803] that very small additions of Na^+ $(1 \times 10^{-6}$ M) in the dilute $LiClO_4$ + AN solutions cause the disappearance of the diffuseness of the electrical double layer at both Pt/AN and Pd/AN interfaces. Thus the activity of cations increases in the order $Li^+ < (C_2H_5)_4N^+ < Na^+$, which has been explained in terms of lower solvation energy for Na^+ than Li^+.[802-804]

The electrical double-layer structure of a Pt/DMSO interface has been investigated using the potentiostatic pulse method.[805] The value of C at E = const, as well as the potential of the diffuse layer minimum, have been found to depend on time, and this has been explained by the chemisorption of DMSO dipoles on the Pt surface, whose strength depends on time. $E_{\sigma=0}$ has been found[11] at E = –0.64 V (SCE in H_2O).

Renewed polycrystalline Pt and Pd electrodes in DMSO have been studied by impedance.[806] Pt and Pd electrodes appear to be ideally polarizable in the region of potential $-0.6 < E < +0.2$ V (SCE in H_2O) where C is independent of time. Minima in the C,E curves, caused by the diffuseness of the electrical double layer, have been found at $E_{min} = -0.15$ V for Pt and at E = 0.00 V for Pd (SCE in H_2O) in DMSO solutions of $LiClO_4$, $NaClO_4$, and $KClO_4$. E_{min} was independent of c_{el} and time, as well as the nature of the cations. The Parsons-Zobel plots at $\sigma = 0$ were linear, with $f_{PZ}(Pt) = 1.9$ and $f_{PZ}(Pd) = 2.0$.[806] The agreement between calculated and experimental C,E curves over the whole potential range has been taken to indicate the applicability of the GCSG theory to Pt/DMSO and Pd/DMSO interfaces. The dramatic difference between $E_{\sigma=0}$ obtained by the potentiostatic pulse method[805] and by impedance ($\Delta E_{\sigma=0} = 0.49$ V) has been explained in terms of slow but very strong chemisorption of DMSO molecules on Pt,[806] oriented with the positive end of the dipole toward Pt. This has been explained by strong preferential adsorption of DMSO molecules, even at negatively charged Pt and Pd surfaces. Specific adsorption of cations in DMSO is very weak compared with AN, and the adsorption activity only slightly increases in the sequence $Li^+ < Na^+ < K^+$ as the solvation energy of cations decreases.

Unlike cations, the adsorption activity of Cl^-, Br^-, and I^- at Pt electrodes is appreciable[806] and increases in the given sequence of anions. At $\sigma << 0$, the σ,E curves for $LiClO_4$, NaCl, NaBr, and NaI coincide, which indicates that complete desorption of halide ions takes place at negatively charged surfaces. The values of $E_{\sigma=0}$ for a renewed Pt electrode have been found to be –0.18, –0.24, and –0.33 V (SCE in H_2O) for NaCl, NaBr, and NaI in DMSO, respectively.

(xvi) Metal Alloys

One of the features of liquid as well as solid alloys is that their bulk and surface compositions are as a rule substantially different because one of the components is more surface active than the other.[120,807–809] In the

case of liquid alloys [e.g., In(Ga) and Tl(Ga)], a small amount of the surface-active component (In or Tl) imparts to the alloy electrode the same surface properties as the pure metal (solid In or Tl, respectively).[10,120,334-337] However, in contrast to liquid alloys, the surface composition of solid alloys can change with time as well as through surface processes (selective oxidation or dissolution, surface migration and diffusion of components, etc.),[807,808,810] as shown, for instance, by Auger spectroscopy in the case of the Sn + Pb alloy surface in a vacuum.[810]

(a) Au + Ag

Au + Ag alloys with different Ag contents (9 to 94 mol%) have been studied by Kukk and Clavilier[807] in $H_2O + NaF$ using impedance. The E_{min} was independent of c_{NaF} and time. A very small amount of Ag in the Au + Ag alloy gave a remarkable shift of E_{min} toward $E_{\sigma=0}$ for pure pc-Ag, which has been taken as an indication that Ag is surface active in the alloy. The E_{min} has been found to be sensitive to the limit of E: with increasing anodic limit, $E_{\sigma=0}$ shifts toward less negative values. This has been explained by the selective anodic dissolution of Ag.[807] Auger spectroscopy shows that the surface composition of Au + Ag alloys is very different from the bulk composition; e.g., for an alloy with 37 mol% Ag, the surface composition is 75 mol%.[810] It has been consistently found[811] that small additions of Ag to Au cause large changes in work function. The relation between bulk and surface composition of Au + Ag alloys has been the object of many discussions[812,815] and the problem of the exact surface composition of these electrodes is still open.

(b) Sn + Pb

The first studies of the electrical double-layer structure at Sn + Pb and Sn + Cd solid drop electrodes in aqueous surface-inactive electrolyte solutions were carried out by Kukk and Püttsepp.[808] Alloys with various contents of Pb (from 0.2 to 98%) were investigated by impedance.[615,643,667,816] Small amounts of Pb caused dramatic shifts of E_{min} toward more negative values. For alloys with Pb bulk content $\geq 0.2\%$, E_{min} was the same as E_{min} for pc-Pb. The E_{min} was independent of c_{KF} and frequency. C^{-1}, C_d^{-1} plots were linear, with f_{PZ} very close to unity. Thus the surface of Sn + Pb alloys behaves as if it were geometrically smooth, and Pb appears to be the surface-active component.[808]

It has been consistently found that small amounts of Pb in Sn + Pb alloys cause an appreciable decrease in the electron work function of Sn, which is in good agreement with data for liquid Sn + Pb alloys.[816–818] The surface activity of Pb has been found to increase as the temperature decreases.[817,818]

Anodically polished Sn + Pb alloys (0.5 to 98% Pb) have been studied by Khmelevaya *et al.*[809] in aqueous Na_2SO_4 by impedance. For compositions of 0.50 to 0.53% Pb, E_{min} is independent of the content of Pb and is very close to $E_{\sigma=0}$ for pure pc-Sn [-0.64 V (SCE)]. For Pb content **> 0.53%,** E_{min} shifts toward more negative E values (i.e., toward $E_{\sigma=0}$ for pure pc-Pb) and in the range 0.53 to 98%, the value of E_{min} is independent of composition. However, the value of E_{min} is approximately 40 mV less negative than that for pure pc-Pb [-0.84 V (SCE)]. The shift has been explained by the formation of a surface mixture of two solid solutions (i.e., Sn in Pb and Pb in Sn) whose compositions are 0.4% of Pb in Sn and 1.9% of Sn in Pb.[819] The mixture of two solid solutions is supposed to form the solid surface phase with crystallographic parameters differing from those of pure Sn and pure Pb. Adsorption studies of $(C_4H_5)_4N^+$ at Sn + Pb alloy electrodes with Pb > 0.55% showed splitting of the adsorption-desorption peaks in C,E curves, which is indicative of the energetic inhomogeneity of the electrode surface.[809]

Renewed Sn + Pb and Sn + Cd alloy electrodes have been studied by Safonov *et al.*[820–822] in the composition range 1 to 10% Pb and Cd, respectively. Mechanical renewal of the surface can be expected to equalize surface and bulk composition, with a subsequent drift of the electrical double-layer properties with time, reflecting the kinetics of surface composition changes. In Na_2SO_4 or NaF solutions, E_{min}, corresponding to the zero-charge potential $E_{\sigma=0}$, shifts with time in the negative direction, i.e., toward $E_{\sigma=0}$ for pure pc-Pb.[820,821] This effect has been explained in terms of slow enrichment of the Sn + Pb alloy surface with Pb as a function of time. The most significant changes in the surface composition of Sn + Pb alloys take place in the range from several minutes to several tens of minutes. Since the self-diffusion coefficient for Pb atoms is approximately 10^{-18} **cm^2 s^{-1},** the processes observed with these electrodes[820–822] are anomalously fast at room temperature.

Sn + Pb is a two-phase eutectic system in which fine crystals of Pb with a linear parameter of 0.01 to 0.02 μm are localized along the grain boundaries of large Sn crystals **(3 to 4 μm).** A comparison of experimental

data with model calculations supports the view that the time effects observed are associated with the surface diffusion of Pb atoms.[820–822]

X-ray scattering studies at a renewed pc-Ag/electrolyte interface[366,823] provide evidence for assuming that fast relaxation and diffusional processes are probable at a renewed Sn + Pb alloy surface. Investigations by secondary-ion mass spectroscopy (SIMS) of the Pb concentration profile in a thin Sn + Pb alloy surface layer show that the concentration penetration depth in the solid phase is on the order of 0.2 μm, which leads to an estimate of a surface diffusion coefficient for Pb atoms in the Sn + Pb alloy surface layer on the order of 10^{-13} to 10^{-12} cm^2 s^{-1}.[820] Chemical analysis by electron spectroscopy for chemical analysis (ESCA) and Auger of just-renewed Sn + Pb alloy surfaces in a vacuum confirms that enrichment with Pb of the surface layer is probable.[810]

Adsorption of various organic compounds (e.g., cyclohexanol, adamantanol-1, and camphor) has been studied at a renewed Sn + Pb alloy/electrolyte interface.[820–824] The time variation of the surface composition depends on the solution composition, the nature and concentration of the surface-active substance, and on E. The E^{max} of cyclohexanol for just-renewed Sn + Pb alloys shifts toward more negative E with time, i.e., as the amount of Pb at the Sn + Pb alloy surface increases.

Solid Sn + Pb alloys have been studied by Shuganova *et al.*[825] by impedance. As found by Kukk and PUttsepp,[808] E_{min} was independent of the Pb content in a wide region of alloy composition, i.e., $E_{min}^{Sn\text{-}Pb} \approx E_{\sigma=0}^{pc\text{-}Pb}$, and only at Sn content $\geq$ 95% is a marked shift of E_{min} observed. A comparison of solid and liquid alloys indicates that Pb is the surface-active component.[825]

(c) Sn + Cd

Sn + Cd alloys with compositions from 0.5 to 98% Cd in KF aqueous solutions have been studied by Kukk and Püttsepp[808] by impedance. The E_{min} was independent of c_{KF} and time. Small amounts of Cd in the alloy shift E_{min} toward a more negative E ($\Delta E_{min} \approx 0.2$ V); in the range of eutectic composition (0.5–40% Cd) $E_{min} = -0.82$ V (SCE), independent of composition. At higher Cd content, another jump of E_{min} ($\Delta E_{min} \approx -0.19$ V) to a value only slightly less negative than $E_{\sigma=0}^{pc\text{-}Cd}$ was observed. This implies that the component with the more negative $E_{\sigma=0}$ (Cd) is surface active at the Sn + Cd alloy surface.[808]

The results of Kukk and Püttsepp[808] are in good agreement with other data,[817,818] showing a correlation between the adsorption isotherm and the type of solid-state phase diagram.[819] X-ray microanalysis has shown that Sn + Cd alloys are two-phase eutectic systems with fine crystals of Cd (≈ 0.01 μm) localized along the grain boundaries of larger Sn crystals (≈ 3 to 4 μm).[818,824]

Renewed Sn + Cd alloy surfaces have been studied by Safonov and Choba[821] by impedance. The E_{min} has been found to shift toward more negative E with time, suggesting that the content of Cd at the Sn + Cd alloy surface increases with time. For the alloy with 10% Cd, the time dependence of C for adsorption of organic substances is significantly different from that for Sn + Pb alloys. At relatively short times, E^{max} shifts in the negative direction, which shows the increase of the Cd content in the Sn + Cd alloy surface layer. At longer times, an additional adsorption-desorption peak (step) has been observed, which has been explained by the formation of rather wide two-dimensional areas of Cd microcrystals at the alloy surface.[824]

The increase in the Cd content in the Sn + Cd alloy surface layer can also be deduced from the shift with time in the negative direction of polarization (log i,E) curves of $S_2O_8^{2-}$ reduction. X-ray radiation investigations of Sn + Cd alloys show that the alloy consists of Sn crystals (of average size 2 to 3 μm) and substantially smaller Cd crystals arranged along the grain boundaries.[824]

(d) Cd + Bi

Cd + Bi alloy electrodes (1 to 99.5% Bi) have been prepared by Shuganova *et al.*[825] by remelting alloy surfaces in a vacuum chamber (10^{-6} torr) evacuated many times and thereafter filled with very pure H_2. C dispersion in H_2O + KF has been reported to be no more than 5 to 7%. C at E_{min} has been found to be independent of alloy composition and time. The E_{min}, independent of the Bi content, is close to that of pc-Cd. Only at a Bi content ≥ 95% has a remarkable shift of E_{min} toward less negative E (i.e., toward $E_{\sigma=0}^{pc\text{-}Bi}$) been observed. This has been explained by the existence of very large crystallites (10^{-4} to 10^{-3} cm) at the alloy surface. Each component has been assumed to have its own electrical double layer (independent electrode model[262,263]). The behavior of Cd + Bi alloys has been explained by the eutectic nature of this system and by the surface segregation of Cd.[826,827]

(e) Cd + Pb

Anodically polished and then cathodically reduced Cd + Pb alloys have been studied by impedance in aqueous electrolyte solutions (NaF, KF, $NaClO_4$, $NaNO_2$, $NaNO_3$).[827] For an alloy with 2% Pb at $c_{NaF} \geq 0.03$ M, $E_{min} = -0.88$ V (SCE) and depends on c_{NaF}, which has been explained by weak specific adsorption of F^- anions. Surface activity increases in the sequence $F^- < ClO_4^- < NO_2^-$. The Parsons-Zobel plot at E_{min} is linear, with $f_{PZ} = 1.33$ and $C_i^{\sigma=0} = 0.31$ F m^{-2}. Since the electrical double-layer parameters are closer to those for pc-Pb than for pc-Cd, it has been concluded that Pb is the surface-active component in Cd + Pb alloys[827] (Pb has a lower interfacial tension in the liquid state).

Various pc electrode models have been tested.[827] Using the independent diffuse layer electrode model,[74,262] the value of $E_{min} = -0.88$ V (SCE) can be simulated for Cd + Pb alloys with 63% Pb if bulk and surface compositions coincide. However, large deviations of calculated and experimental *C,E* curves are observed at $\sigma << 0$. Better correspondence between experimental and calculated *C,E* curves was obtained with the common diffuse-layer electrode model,[262] if the Pb percentage in the solid phase is taken as 20%. However, the calculated C_i at $\sigma << 0$ is noticeably lower than the experimental one. It has been concluded that Pb is the surface-active component in Cd + Pb alloys, but there are noticeable deviations from electrical double-layer models for composite electrodes.[827]

(f) Other systems

Ni + Sn alloys have been studied by Lazarova and Nikolov.[828] Ni + Fe alloys have been investigated by Lazarova and Raichev.[829] pH and composition effects have been reported in both cases.

An attempt to measure the pzc of Pb + Na alloys has been reported by Kiseleva *et al.*[830] The system was studied in the context of the cathodic processes during hydrogen evolution that are believed to result in the incorporation of alkali metal atoms.

Work function measurements of Sb alloys with Sn, In, and Zn have been reported by Malov *et al.*[831]

Liquid alloys of Hg with a variety of metals (amalgams) constitute particularly complex systems in view of the potential dependence of surface composition. A detailed study of In and Tl amalgams, with

reference to the previous work, has been recently reported by Koene *et al.*[832]

(xvii) Metals in Molten Salts

Metal/molten salt interfaces have been studied mainly by electrocapillary[833–838] and differential capacitance[839–841] methods. Sometimes the estance method has been used.[842] Electrocapillary and impedance measurements in molten salts are complicated by nonideal polarizability of metals, as well as wetting of the glass capillary by liquid metals. The capacitance data for liquid and solid electrodes in contact with molten salt show a well-defined minimum in *C*,*E* curves and usually have a symmetrical parabolic form.[8,10,839–841] Sometimes inflections or steps associated with adsorption processes arise, whose nature, however, is unclear.[8,10] A minimum in the *C*,*E* curve lies at potentials close to the electrocapillary maximum, but some difference is observed, which is associated with errors in comparing reference electrode (usually Pb/2.5% $PbCl_2$ + LiCl + KCl)[840] potential values used in different studies.[8,10] It should be noted that any comparison of experimental data in aqueous electrolytes and in molten salts is somewhat questionable.

The data obtained for metal/molten salt interfaces cannot be interpreted in terms of electrical double-layer concepts[8,10,99] generally used for aqueous electrolyte solutions. A double-layer structure first pointed out by Esin,[843] involving layers of ions of alternating sign, is more probable. This conception was corroborated by Dogonadze and Chizmadjev.[844] The present state of the theory of molten salts at the interface with metals does not allow us to draw definite conclusions about the coincidence of $E_{\sigma=0}$ with E_{min} in differential capacitance curves and E_{max} in electrocapillary curves, especially for the general case in which the radii and the polarizability of cations and anions are different. Similarity between the potential of the minimum in the *C*,*E* curves, as well as the electrocapillary maximum in molten salts can be considered only as an empirically established fact. It should be noted that any comparison of electrocapillary phenomena in molten salts with electrical double-layer data at metal/aqueous electrolyte interfaces is complicated by, besides the absence of a solvent, the significant difference in temperature. According to Ukshe and Bukun,[840] the difference of $E_{\sigma=0}$ for two metals (M_1 and M_2) in aqueous electrolyte and in the molten salt (MS) is given by

$$\left(E^{M_1}_{\sigma=0} - E^{M_2}_{\sigma=0}\right)_{H_2O} - \left(E^{M_1}_{\sigma=0} - E^{M_2}_{\sigma=0}\right)_{MS}$$

$$= \Delta T \frac{\partial \Delta \Phi}{\partial T} + \left(\Delta \Phi^{M_1} - \Delta \Phi^{M_2}\right)$$

$$+ \left[\left(\Delta^{H_2O}_{M_1}\psi\right)_{\sigma=0} - \left(\Delta^{H_2O}_{M_2}\psi\right)_{\sigma=0} + \left(\Delta^{MS}_{M_2}\psi\right)_{\sigma=0} - \left(\Delta^{MS}_{M_1}\psi\right)_{\sigma=0}\right] \quad (61)$$

i.e., by the difference in the temperature dependence of the work functions for the two metals ($\Delta\Phi$), the change in the difference of the work functions due to melting of the metals (if this occurs) ($\Delta\Phi^{M_1} - \Delta\Phi^{M_2}$), and by the change in the difference of Volta potentials at the metal/molten salt interface (the last term).

In Table 25 the values of $E^{M}_{\sigma=0} - E^{Pb}_{\sigma=0}$ in molten salt (eutectic LiCl + KCl melt) are compared with $\Delta E_{\sigma=0}$ in aqueous solutions (relative to the value of $E_{\sigma=0}$ for a pc-Pb electrode in a surface-inactive aqueous electrolyte). According to these data, the difference of $\Delta E_{\sigma=0}$ in aqueous electrolytes and molten salts is not very high; to a first approximation, it can be assumed that the quantity in square brackets in Eq. (61) has the greatest

Table 25
Differences of Potentials of Zero Charge of Various Metals with Respect to Pb

Metal	$\Delta E_{\sigma=0}$/V[a] Aqueous solutions	$\Delta E_{\sigma=0}$/V[b] LiCl + KCl at 450°C	$\Delta E_{\sigma=0}$/V[b] LiCl (NaCl + KCl) at 700°C
Hg	0.41	0.44	—
Sb	0.43	—	0.56
Sn	0.21	0.27	0.30
Bi	0.22	0.27	0.30
Pb	0.00	0.00	0.00
In	−0.05	−0.05	−0.07
Ga	−0.09	0.09	0.06
Tl	−0.11	−0.11	−0.11
Cd	−0.15	−0.15	—

[a]From Table 26, this work.
[b]From Ref. 8

importance. Based on a simplified theoretical analysis, Ukshe and Bukun[840] have reached the same conclusions.

It should be noted that the possibility of a change in the work function of a metal upon melting is defined by the difference in the work functions for different single-crystal planes. Therefore, data for aqueous solutions and molten salts should be compared without changing the state of aggregation of metals, and if this condition cannot be satisfied, the data for pc samples should be used, for which the $E_{\sigma=0}$ for individual faces are averaged, so that a minimum change would be expected upon melting.[8,10] However, as shown in Section H.2(ii), E_{min} in C,E curves for pc-metal/aqueous solution interfaces do not correspond to $E_{\sigma=0}$ and probably the same is also the case for solid pc-metal/molten salt interfaces. Thus more experimental and theoretical investigations are necessary to reach more definite conclusions.

III. ANALYSIS OF THE EXPERIMENTAL DATA

1. Comparison of Compilations

Although no compilations of potentials of zero charge have appeared in this series since the chapter by Perkins and Andersen in 1969,[9] a discussion on double-layer potentials was given by Trasatti in 1980 (No. 13).[7] At the same time, a number of collections have been published in various places.[6,8,10,14,21–27] The last, however, dates back to 1986.[27]

It may be interesting to collate the more complete compilations so as to follow the developments in the measurement of the potential of zero charge. Comparisons are provided in Table 26 for polycrystalline metals as well as for the few single-crystal faces that were among the first to be investigated. Purposely, only "recommended" values are given. For this reason, in the column on Perkins and Andersen's data,[9] only the pzcs obtained with their scrape method[141,845] as well as with the immersion method[846] (in brackets, conceptually equivalent) are reported. In fact, these authors compiled a list of (at that time) available values without any selection based on some definite criteria. Although in this chapter (Section II) lists of experimental data have actually been compiled, in the first column of Table 26, only "preferred" values are given, the selection being based on criteria of reliability related to the preparation of the electrode surface and the experimental procedure.

Table 26
Chronological Arrangement of Compilations of Potentials of Zero Charge of Metals in Aqueous Solutions ($E_{\sigma=0}$ vs. SHE/V)

Metal	This work	1954[4]	1965[20]	1969[9,190]	1971[22]	1974[23]	1979[10]	1980[8]	1986[25]	1986[27]
Hg	−0.192 ± 0.001	−0.19	−0.19	(−0.193 ± 0.004)[a]	−0.19	−0.193	−0.193	−0.193	−0.192 ± 0.001	−0.193
Sb	−0.17 ± 0.01	—	—	−0.11	−0.14	−0.15	−0.15	−0.15	—	−0.15 ± 0.02
Bi	−0.38 ± 0.01	—	−0.36	−0.34	−0.39	−0.39	−0.39	−0.39	−0.39	−0.39 ± 0.02
Bi(111)	−0.41 ± 0.01			—		−0.42	−0.42	−0.42	−0.41	−0.42 ± 0.02
Sn	−0.39 ± 0.01	—	−0.46	−0.43	−0.43	−0.38	−0.38	−0.38	−0.38	−0.38 ± 0.02
Pb	−0.60 ± 0.01	−0.65	−0.64/67	—	−0.62	−0.56	−0.56	−0.56	−0.60	−0.60 ± 0.01
In	−0.65 ± 0.01	—	—	−0.65	−0.65	−0.65	−0.65	−0.65	−0.65	−0.65 ± 0.02
In(Ga)	−0.67 ± 0.01	—	—	—	—	−0.68	−0.68	−0.68 ± 0.01	−0.67	—
Tl	−0.71 ± 0.01	−0.79	−0.82	—	−0.75	−0.71	−0.71	−0.71	—	−0.71 ± 0.02
Tl(Ga)	−0.69 ± 0.01	—	—	—	—	—	—	—	−0.71	—
Ga	−0.69 ± 0.01	−0.62	−0.61	−0.63	−0.69	−0.69	−0.69	−0.69 ± 0.01	−0.69	−0.69 ± 0.02
Cd	−0.75 ± 0.01	−0.89	−0.9	—	−0.72	−0.75	−0.75	−0.75	−0.75	−0.75 ± 0.02
Zn	−0.91 ± 0.02	−0.62	—	—	−0.63	—	—	—	—	—

Ag	-0.70 ± 0.02	0.04	−0.7	−0.64	−0.44	−0.7	—	—	—	-0.70 ± 0.05
Ag(111)	-0.450 ± 0.016	—	—	(−0.18)[a]	—	−0.46	−0.46	−0.46	-0.459 ± 0.002	-0.46 ± 0.02
Ag(100)	-0.616 ± 0.015			(−0.28)[a]		−0.61	−0.61	−0.61	−0.609	-0.61 ± 0.02
Ag(110)	-0.735 ± 0.007			—		−0.77	−0.77	−0.77	-0.734 ± 0.005	-0.77 ± 0.02
Au	0.20	—	0.3	0.15	0.18	0.18	—	—	—	0.19 ± 0.01
Au(110)	0.200 ± 0.005			(0.24)[a]		0.19	0.19	0.19	0.19 ± 0.01	0.19 ± 0.02
Cu	-0.64 ± 0.05	—	0.05/07	0.073 ± 0.005[b]	0.09	0.09	—	—	—	—
Pt	0.18[c]	0.28	0.11/17	0.02	0.02	—	0.185	0.185	—	—
Ni	-0.33 ± 0.05[d]	−0.06	—	—	−0.30	—	—	—	−0.33	—
Fe	-0.70 ± 0.02[e]	—	−0.37	—	−0.35	—	—	—	−0.70	-0.70 ± 0.05

[a]Literature value: not by scrape.
[b]Immersion method.
[c]pH = 2.4.
[d]pH = 2.97.
[e]pH = 3.5.

Table 26 shows some steps in the "chronological" sequence of compilations, which are evidently related to improvements in the preparation and control of electrode surfaces. In second order, the control of the cleanliness of the electrolyte solution has to be taken into consideration since its effect becomes more and more remarkable with solid surfaces. A transfer of "emphasis" can in fact be recognized from Hg (late 1800s) to sp-metals, to sd-metals, to single-crystal faces, to d-metals, although a sharp chronological separation cannot be made.

While the pzc of Hg in F^- solution has not changed by more than 1 mV for over 70 years, marginal variations are visible for Ga, Tl, In, Cd, Bi, Sn, and Sb that are related to electrolyte effects (weak specific adsorption or disturbance of the adsorbed water layer, as for Ga).[847] Important variations can be seen, on the other hand, for polycrystalline Ag, Zn, Ni, Fe, and Cu. For all these metals a drop of the pzc to much more negative values has been recorded; this is evidently related to an improvement in the preparation of the surface with more effective elimination of surface oxides. All these metals, with the exception of Ag, are naturally sensitive to atmospheric oxygen. Values of pzc for single-crystal faces first appeared in a 1974 compilation,[23] in particular for the three main faces of Ag and for Au (110). Values for a number of other metals were reported in 1986.[25] However, for sd-metals, an exhaustive, specific compilation of available experimental data was given by Hamelin *et al*. in 1983.[24]

The metals of the Pt-group constitute a particular case. Their catalytic activity has long frustrated the determination of the pzc because of interference from adsorbed hydrogen and oxygen. Nevertheless, estimated values of pzc for polycrystalline Pt are included in all compilations in Table 26. However, after the publication by Frumkin and Petrii[14] of a summary of pzc values for Pt, Rh, Ir, and Pd, no further progress was made for about 20 years until recently UHV techniques of surface preparation have enabled pzc determinations using methods other than the traditional ones.[140]

2. Crystal-Face Specificity

Polycrystalline electrodes are still used in many electrochemical experiments. For this reason, polycrystalline metals are still included in compilations of pzc as in this chapter, although the physical significance of such a quantity is ambiguous (see Section I).

The first data on the pzc of single-crystal faces can be found in Perkins and Andersen's compilation[9] and refer to Ag and Zn in the late 1950s, as well as Au in the early 1960s. However, the disclosure of the features of the dependence of the pzc on the crystallographic orientation of a metal surface was possible only with the work of Clavilier and Hamelin and Valette[67,848,849] on single crystals of Au and Ag in the 1960s–70s. For these two metals there are now a number of pzc values for different faces (low index and stepped)[396,502] which unambiguously demonstrate the dependence of $E_{\sigma=0}$ on the surface structure.[32]

Figure 12(a) shows graphically the dependence of the pzc on the crystallographic orientation of the surface for Ag, Au, and (tentatively) Cu, all three crystallizing in the same fee system. The plots exhibit a typical pattern, with minima and maxima that fall at the same angle for all three metals, and that are correlated with the density of atoms on the given surface. In particular, the pzc is more positive for dense surfaces and more negative for open surfaces.

The dependence of $E_{\sigma=0}$ on the atomic structure of a surface is emphasized by the close correlation of $E_{\sigma=0}$ values for the same face of different metals crystallizing in the same system. Thus it has been shown[26,33] that $E_{\sigma=0}$ for Ag faces is linearly correlated with the $E_{\sigma=0}$ for Au single-crystal faces. Accordingly, both sets of $E_{\sigma=0}$ values (and tentatively also for Cu) are linearly correlated with the coordination number of surface metal atoms[32] [Fig. 12(b)].

The correct pzc of single-crystal faces of Cu was obtained[576,578,587] only after a really oxide-free surface was produced, although unsuccessful attempts are still reported.[597] The pzc values for the three main faces of Cu show the correct sequence with the crystallographic orientation, i.e., **(111) > (100) > (110).** These three values are still insufficient, however, to give definite evidence in a plot such as Fig. 12 of the characteristic pattern of the dependence on the crystallographic orientation.

Pb also crystallizes in the fee system and therefore the same dependence of $E_{\sigma=0}$ on the crystallographic orientation should be expected. Quite surprisingly, $E_{\sigma=0}$ varies in the sequence **(112) ≈ (110) > (100) > (111),**[155] i.e., exactly the other way round. Although the authors of the measurements do not remark on this apparent anomaly, a possible explanation can be sought in the surface mobility of Pb atoms at room temperature, which may lead to extensive surface reconstruction phenomena. It doesn't seem possible to clarify this aspect for the time being, since the most recent studies on the pzc of Pb single-crystal faces date back almost 20 years.

Zn and Cd both crystallize in the hcp system. The basal (0001) face is the most dense and for both metals the $E_{\sigma=0}$ of this face is more positive than for the lateral faces.[156,850] While Zn was among the first metals to be studied as single crystals, Cd has been among the last and is being actively investigated.[249]

For Sn, the variation of $E_{\sigma=0}$ with the crystal face is negligible.[621] Finally, Bi and Sb have been studied for several decades in Tartu[671] and an extensive number of different crystal faces have been investigated thus far.[28,725] Being semimetals, Bi and Sb show anomalies in the correlation of $E_{\sigma=0}$ with the surface atomic density[254] which can be explained in terms

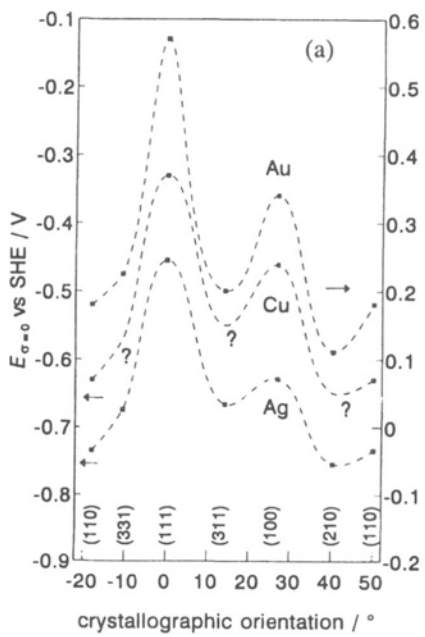

Figure 12. (a) Dependence of the potential of zero charge, $E_{\sigma=0}$, on the crystallographic orientation for the metals Cu, Ag, and Au, which crystallize in the fcc system. From Ref. 32, updated, (b) (pg. 155) Correlation between $E_{\sigma=0}$ of single-crystal faces of Cu, Ag, and Au, and the density of broken bonds on the surface of fee metals. From Ref. 32, updated.

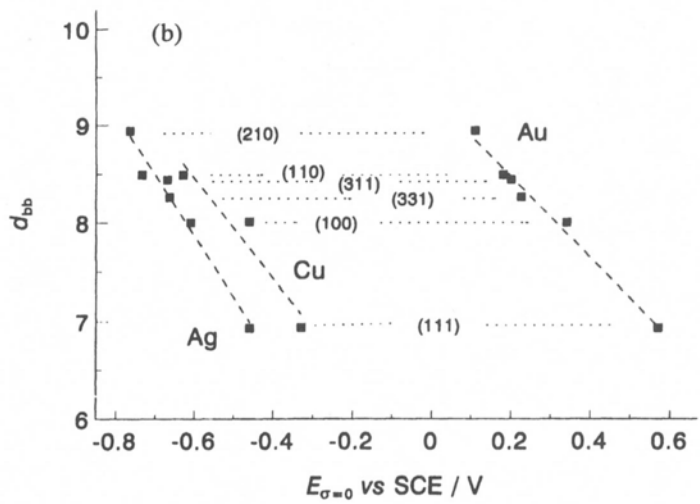

Figure 12. (continued).

of face-specific space-charge effects. Thus, while the wealth of data for Bi and Sb is invaluable for disclosing the laws governing interfacial phenomena, these elements cannot be discussed in close parallelism with other surface-heterogeneous metals such as Ag and Au.

It is evident from the data discussed above that the difference in $E_{\sigma=0}$ between the most dense and the most open surface depends on the "softness" of the metal surface, which to a first approximation can be measured by the melting point of the given metal.[63] This simple concept is proved by Fig. 13 in which $\Delta E_{\sigma=0}$ for the two extreme main faces has been plotted against the melting point of the given metal. It is clearly seen that $\Delta E_{\sigma=0}$ is highest for Au (T_f = 1063°C) and lowest for Sn (T_f = 231.9°C). According to this approach, $\Delta E_{\sigma=0} = 0$ for liquid metals at room temperature. In principle, solid Ga should exhibit a minimum of heterogeneity. Attempts to measure $E_{\sigma=0}$ for solid Ga have been reported.[851,852] In some cases, a pH-dependent pzc has been observed.[853] This usually happens with metals adsorbing H or O,[14] and is an indication that adsorbed species take part in surface equilibria. A pH dependence of the pzc of easily oxidizable metals[730,731] indicates that the measurement is not being carried out on a really bare surface, so that the measured value is questionable as a pzc.

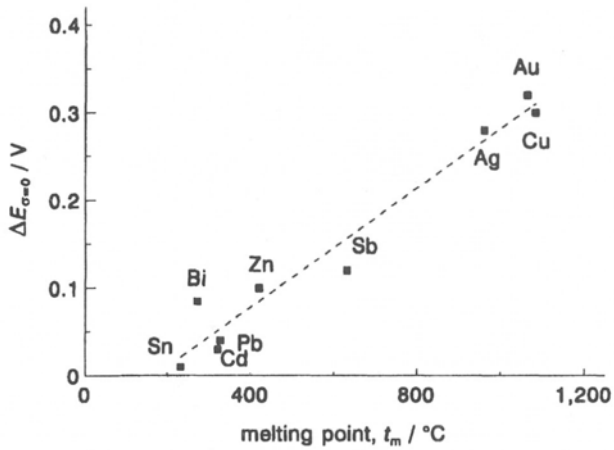

Figure 13. Correlation between the heterogeneity of a metal surface, as expressed by the maximum range of $E_{\sigma=0}$ for the main single-crystal faces, and the melting point of the given metal.

3. Potential of Zero Charge and Work Function

(i) GeneralAspects

It was shown in Section I that the potential of zero charge is related to the electron work function of the electrode metal by Eq. (27):

$$E_{\sigma=0} \text{ vs. Ref.} = \Phi + X + \text{const} \qquad (27)$$

The "interfacial parameter"[34,408] X measures the surface modifications occurring as the metal is brought in contact with the solution. The discussion of whether the difference in potential of zero charge between two metals is equal to the difference in their work function was initiated by Frumkin and Gorodetskaya[18] in 1928. The problem cannot be solved with the data for a single metal in view of the uncertainty in the values of the experimental quantities and the ignorance of the constant term. For these reasons, correlations between $E_{\sigma=0}$ and Φ have been used to gain insight into the significance and behavior of X.

$E_{\sigma=0}$ vs. Φ correlations have been examined several times in the literature. The early work has been reviewed elsewhere[6,22,104] and will not

be discussed here again. Early approaches tended to attribute the variation in $E_{\sigma=0}$ between different metals to the change in Φ. Later, a more comprehensive scrutiny of the existing data by Trasatti[22] revealed systematic deviations that are related to the metal dependence of the term X.

Since the first analysis, Trasatti has reviewed $E_{\sigma=0}$ vs. Φ correlations several times, and the reader is referred to the original papers[6,25,31,34,408] for detailed discussions. Here only a brief, general survey will be given. It is stressed that the physical picture emerging from the first paper in 1971 required only marginal modifications during the years as some of the experimental data were checked.

The main problem in $E_{\sigma=0}$ vs. Φ correlations is that the two experimental quantities are as a rule measured in different laboratories with different techniques. In view of the sensitivity of both parameters to the surface state of the metal, their uncertainties can in principle result of the same order of magnitude as ΔX between two metals. On the other hand, it is rare that the same laboratory is equipped for measuring both $E_{\sigma=0}$ and Φ. The consequence is that in many cases even the preparation of a single-crystal face is not followed by a check of its perfection by means of appropriate spectroscopic techniques. In these cases we actually have "nominal" single-crystal faces. This is probably the reason for the observation of some discrepancies between differently prepared samples with the same "nominal" surface structure. Fortunately, there have been a few cases in which both $E_{\sigma=0}$ and Φ have been measured in the same laboratory: these will be examined later. Such measurements have enabled the resolution of controversies that have long persisted because of the basic criticism of $E_{\sigma=0}$ vs. Φ plots.

More than with $E_{\sigma=0}$, the problem is with the selection (in the lack of data for the same specimen with which $E_{\sigma=0}$ is measured) of values for Φ.[32,854,855] In fact, while almost all $E_{\sigma=0}$ have been obtained recently as a consequence of the continuous improvement in the preparation of clean surfaces in electrochemistry, the measurement of Φ is rather casual in surface science at present. In particular, work functions are mostly measured for d-metals rather than for sp-metals, which are more common in electrochemical double-layer studies. As a consequence, compilations of work function values report data for sp-metals that are 20 to 30 years old.[63,856,857] This does not imply that the data are unreliable, but imparts to the situation a sense of frustration related to the immobility in one of the variables.

Twenty-five years ago the idea was discussed in the literature,[858] based on the results of Frumkin's school,[23] that while the difference in $E_{\sigma=0}$ may contain a contribution from the solvent, this should not be the case at strongly negative charges where the value of X becomes metal independent because of the effect of the strong electric field that outweighs chemical interactions. This idea was corroborated by the apparent convergence of the capacitance for different metals to the same value at strongly negative charges. The difference in potential at $\sigma << 0$ was thus taken to measure the difference in work function.[6] In this way, "electrochemical work functions" could be estimated for the metals for which reliable "physical" values were not available.

Such an approach revealed objective limitations as it became evident that the equality in the capacitance values for different metals was only a first approximation. The case of Ga is representative.[335,336,341] Ga is a liquid metal and the value of capacitance cannot depend on the exact determination of the surface area as for solid metals (i.e., the roughness factor is unambiguously =1).

For the above reasons, $E_{\sigma=0}$ vs. Φ correlations are reported in this chapter as obtained in the last review[32,33] of the situation without any attempt to make selections of new values of Φ, which would be unavoidably based on compilations reporting data evaluated several years ago. Note that the most "recent" exhaustive work devoted to work functions dates back to 1979.[65] Admittedly, there are some more recent data[66] (but mostly for single-crystal faces of d-metals); however, the method of measurement has led to values systematically higher by 0.2 to 0.3 eV. This aspect has been pointed out by Trasatti[410] in dealing with Ag single-crystal faces.

The only metal for which $E_{\sigma=0}$ and Φ refer to the same sample is Hg, because of its liquid state. However, even in this case the situation is not settled, as discussed in Section I, since Φ values obtained several years ago are regarded with suspicion by surface physicists. Nevertheless, recent measurements[46] even in ambient gases point to a reproducibility of the accepted value of Φ for Hg that cannot be simply occasional, as implied in the criticisms of "detractors." Another metal in the same situation as Hg would be Ga, but in this case its surface reactivity toward oxygen and its solid state at room temperature are complications that make its Φ value less reliable, although acceptably reproducible.

Figure 14 shows a plot of $E_{\sigma=0}$ as a function of Φ. Hg is taken as a reference surface: a straight line of unit slope is drawn through its point.

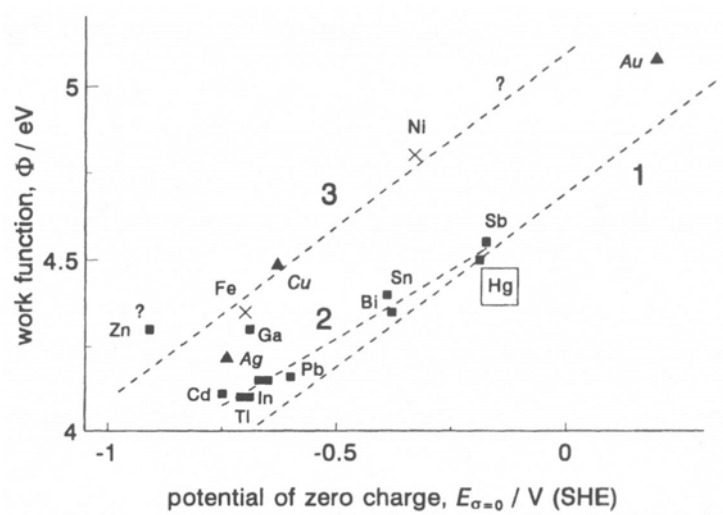

Figure 14. Plot of the potential of zero charge, $E_{\sigma=0}$ (from Table 26), against the work function, Φ, of polycrystalline metals. Hg is taken as a reference metal. (1) Straight line of unit slope through the point of Hg. (2) Linear correlation gathering most sp-metals (except Ga and Zn). The two points for In and Tl include their alloys with Ga, for which the same value of work function is presumed. (▲) sd-metals [the points refer to the (110) face]. (3) First approximation, apparent correlation for polycrystalline d-metals.

According to Eq. (27), if a metal possessed the same value of X as Hg, its point would fall on the straight line. The plot shows that all other metals lie on the left of the straight line: in terms of Eq. (27) all of them have an X term more negative than that of Hg. In other words, there are no metals on whose surface the contact with water produces a lower Φ drop than on Hg (or a positive $\Delta\Phi$).

In the plot, the sp-metals (except Ga) apparently can be gathered in a single group. There is a clear trend within the group for $E_{\sigma=0}$ to become more negative as Φ decreases. This causes ΔX to increase as Φ decreases. This trend has been questioned by two different authors starting from different positions. In one case,[854] it has been maintained that no general rule can be established since the points are rather scattered in the plot of Fig. 14. However, this remark stems from an analysis of the experimental data that was not sufficiently selective. This becomes clear as one exam-

ines the approach used by the same author in the case of single-crystal faces.[389,399]

In another case it has been claimed[343,859] that the decrease of $E_{\sigma=0}$ with Φ is not true, as manifested by correlating metals within the same group, for instance Ga, In, and T1. It has even been shown by the same authors that in DMSO $E_{\sigma=0}$ *increases as* Φ decreases (see later discussion). In water, as Fig. 14 shows, $E_{\sigma=0}$ is almost constant within the above group of metals while Φ varies up to 0.2 eV. However, the approach based on groups rather than on periods is chemically inadequate. It is of course possible to obtain any kind of correlation, depending on the points correlated. However, the choice must be based on sound arguments. In his theory on the variations of the bond strength and magnetic properties, Pauling[860] correlated the properties of metals along a period and not down a group. This is because a meaningful correlation involving electronic properties can be best followed as a given electronic shell is progressively filled and not as filled shells of core electrons are added down a group. According to the structure of the periodic table, metals in the same group possess similar chemical properties. Therefore they should not be correlated with the aim of obtaining evidence of a variation in the chemical properties.

Koene *et al.*[861] have recently measured the pzc of a number of In amalgams of different compositions and have plotted $E_{\sigma=0}$ vs. the electron work function determined in another laboratory 20 years earlier. They obtained a linear correlation of unit slope for $0.02 < x_{In} < 0.6$. However, from pure Hg to $x_{In} = 0.02$, a drop in $E_{\sigma=0}$ of 85 mV corresponds to a change in Φ of only 10 meV. For this reason it is doubtful that such a plot can be used as a typical $E_{\sigma=0}$ vs. Φ dependence. The shift in $E_{\sigma=0}$ for $0 \leq x \leq 0.02$ corresponds to almost the whole shift from pure Hg to pure In. Thus the unit slope of the plot can be interpreted as a constancy in the X term, reflecting that of an In surface. This implies that a variation of $E_{\sigma=0}$ reflects a variation in Φ (which includes a bulk term, the chemical potential of electrons, which depends on amalgam composition) rather than a surface property. Precisely for this reason, the family of In amalgams cannot be taken as representative of a continuous series of metal phases for studying the metal dependence of interfacial. properties.[408] In other words, the result with amalgams cannot be used to question the correlation found for sp-metals, but rather the latter is useful to explain the former.

If sp-metals are gathered in a single group as in Fig. 14, the straight line that best fits the data has the equation

$$E_{\sigma=0} \text{ vs. SHE/V} = 1.27\ \Phi/\text{eV} - 5.91 \quad (62)$$

This equation does not differ appreciably from that proposed by Trasatti[22] in 1971, whose slope was 1.33. However, in that plot there were metals inadequately placed, such as Ag and Au, because of the unreliability (as it was discovered later) of some data available at that time. Equation (62) shows that the deviations from the unit slope dependence are in turn linearly related to Φ (and $E_{\sigma=0}$).

The horizontal distance (along the $E_{\sigma=0}$ axis) of each metal point from the line of unit slope through Hg measure AX with respect to Hg, i.e.

$$\Delta X = X_M - X_{Hg} \quad (63)$$

ΔX measures the relative values of the cpd at the metal/water interface. The values of ΔX have been summarized in Table 27. Taking for X_{Hg} the value of–0.25 V[42,43] [see Section II.2(v)], the cpd for the other metals can be calculated. These values are also reported in Table 27.

X_M measures the changes occurring at the surfaces of a metal and water as the two phases are brought in contact to create an interface. In surface science concepts, X_M corresponds to the decrease in work function

Table 27
Relative and Absolute Interfacial Parameter for Polycrystalline Metals in Contact with Water

Metal	$-\Delta X$/V[a]	$-X(\equiv\delta\chi^M + \delta\chi^S)$/V
Hg	—	0.25
Sb	0.03	0.28
Bi	0.04	0.29
Pb	0.07	0.32
Sn	0.10	0.35
In	0.11	0.36
In(Ga)	0.13	0.38
Tl	0.12	0.37
Tl(Ga)	0.10	0.35
Cd	0.17	0.42
Ga	0.30	0.55
Fe	(0.36)	(0.61)
Ni	(0.44)	(0.69)

[a]From Fig. 14.

upon adsorption of water.[31,34] However, as pointed out earlier, sp-metals are of little relevance for surface science studies so that no directly measured values of $\Delta\Phi \equiv X_M$ are available for comparison.

ΔX results from a small difference between two large figures. Taking into account the uncertainty in the experimental quantities involved, the uncertainty in ΔX may be quite high, probably of the same order of magnitude as the quantity itself for metals with low values of ΔX. This does not detract from the validity of the approach based on the derivation of ΔX: the trend is more important than the precise value, and the trend, as shown later, is corroborated by a number of other correlations.

The separate position of Ga is not random. It cannot be related to the uncertainty in Φ or $E_{\sigma=0}$ values. The latter is known with high accuracy, while it can be ruled out that Φ can be lower by 0.3 eV. On the other hand, it has been shown in previous correlations that Zn is probably close to Ga. The point of Zn is shown[408] in Fig. 14 with a question mark because of the lack of a reliable value for Φ, but values of pzc for single-crystal faces suggest that Zn cannot fall in the main group of sp-metals. Thus, Ga and Zn have in common a much higher value of ΔX than the other sp-metals with comparable work functions. Since $X \equiv \delta\chi^M + \delta\chi^S$, the major contribution is probably in $\delta\chi^S$, but this aspect will be discussed later.

In Fig. 14 the points for Cu, Ag, and Au are also shown. In view of the large heterogeneity effect on the value of $E_{\sigma=0}$ for these metals, the points are those for the (110) face which, however, shows behavior close to that of a polycrystalline surface.[6] While these metals will be discussed in a separate plot, they are also shown here to highlight the relationship with the sp-metals.

Cu, Ag, and Au are sd-metals (the d-band is complete but its top is not far from the Fermi level, with a possible influence on surface bond formation) and belong to the same group (I B) of the periodic table. Their scattered positions definitely rule out the possibility of making correlations within a group rather than within a period. Their ΔX values vary in the sequence $Au < Ag < Cu$ and are quantitatively closer to that for Ga than for the sp-metals. This is especially the case of Cu. The values of ΔX have not been included in Table 27 since they will be discussed in connection with single-crystal faces.

Although $E_{\sigma=0}$ for d-metals is not very reliable and no substantial advances have been achieved recently, the points of Fe and Ni are included in Fig. 14 as broadly representative of d-metals. A separate discussion will

be given later for Ft because of its exceedingly high values for both Φ and $E_{\sigma=0}$.

Ni and Fe are the only d-metals for which capacitance curves displaying a nice diffuse-layer minimum have been obtained.[727,743] These minima are in reasonable agreement with values obtained with renewable surfaces.[730] However, strongly heterogeneous surfaces are expected for these metals and therefore the behavior of a pc sample can be taken as close to the most open main single-crystal face.

It has been suggested in previous correlations[6,7,22,25] that d-metals probably gather around a straight line of unit slope. If this is the case, the dashed straight line in Fig. 14 has the equation:

$$E_{\sigma=0} \text{ vs. SHE/V} = \Phi/\text{eV} - 5.09 \qquad (64)$$

This equation has been derived only as a reference for a comparative discussion of data for sd- and d-metals later on. However, the meaning of such a line is that there exists a limit to ΔX values in the sense that after a given top effect, a further increase in metal-water interaction will not produce higher ΔX values.[6,7] An indirect confirmation of this is given by the observation of a top value in the decrease of Φ upon water adsorption on d-metals from the gas phase.[35,36]

The values of ΔX for pc Ni and Fe are reported in Table 27 in brackets. Polycrystalline surfaces of these metals are still used both in surface science and in electrochemical studies. The relevance of $E_{\sigma=0}$ to the potential of initial passivation of metals has been pointed out.[862]

(ii) Single-Crystal Faces

Figure 15 shows a plot of $E_{\sigma=0}$ vs. Φ for single-crystal faces of Cu, Ag, and Au. A similar plot was reported by Trasatti for the first time in 1985[407] and several other times later.[25,26,32,408] For a discussion of the selection of Φ data, see the previous papers. It should be noted that the $E_{\sigma=0}$ and Φ data used for Fig. 15 do not refer to the same samples.

It is remarkable that each metal forms a separate group in which the faces are aligned along apparently parallel straight lines. It is intriguing that the slope of the straight lines is to a first approximation the same as that for the group of sp-metals in Fig. 14. On average, the points for the same face (the metals crystallize in the same fee system) are placed with respect to the line of mercurylike metals so that ΔX varies in the sequence

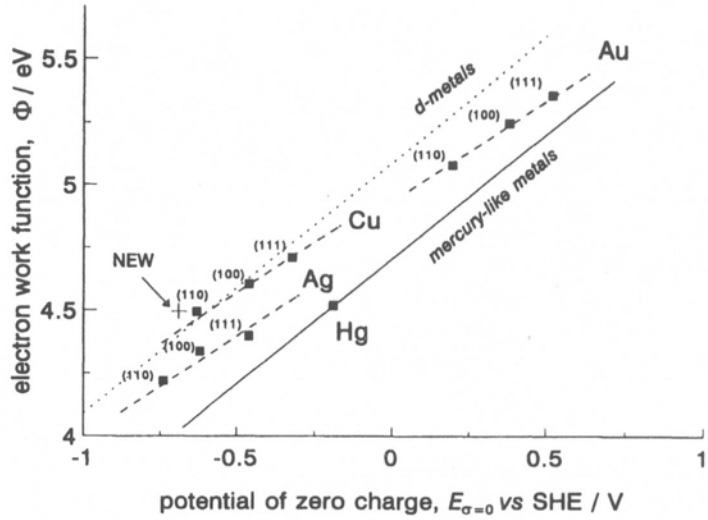

Figure 15. Plot of the potential of zero charge, $E_{\sigma=0}$, vs. the electron work function, Φ, for the main low-index faces of Cu, Ag, and Au. (——, ····) Straight lines of unit slope. (-----) parallel straight lines with the same slope as that for sp-metals in Fig. 14. (+) Ref. 587. From Ref. 32 updated.

Au < Ag < Cu and for the same metal with the crystal face **(111) < (100) < (110).**

The above sequence of faces has been questioned and the opposite order has been proposed.[389,399,863] However, Trasatti[410] has shown that a proper selection of Φ values (or still better, of Φ sequences) leads without doubt to the order of face specificity evident in Fig. 15. On the other hand, Lecoeur *et al.*[64,362] unambiguously proved that ΔX increases as $E_{\sigma=0}$ becomes more negative. They measured Φ and $E_{\sigma=0}$ using the same samples of several different plane and stepped surfaces of Au. These data are reported in Fig. 16 and show that the points definitely deviate from a straight line of unit slope toward more negative ΔX values, as in Fig. 15. The points for the (110) and the (311) faces are scattered because different surface structures (reconstruction) were present in UHV and in solution.[64] The dotted line has a slope of 1.27, the same as in Fig. 15.

While the situation of $E_{\sigma=0}$ is settled for Au and Ag, this is not yet the case for Cu. Recently, Foresti *et al.*[587] have been able to determine $E_{\sigma=0}$ for Cu(l 10). This value is shown in Fig. 15. using of course the same value

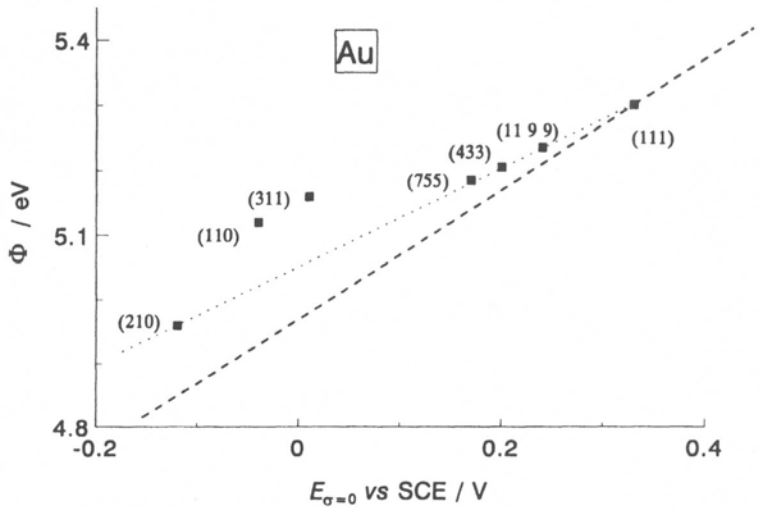

Figure 16. Plot of the potential of zero charge, $E_{\sigma=0}$, vs. the electron work function of several low-index and stepped surfaces of Au. $E_{\sigma=0}$ and Φ measured on the *same* sample. (-----) Straight line of unit slope. (····) Straight line with the same slope as that for sp-metals in Fig. 14. Data from Refs. 64 and 562.

of Φ as before. The value is close to the previous set of data, although a bit more negative, probably because it was obtained in acid solution with a really oxide-free surface. On the whole, the position of Cu in the plot is confirmed by the latest results.

Assuming that the dashed lines in Fig. 15 gather the different faces of a given metal, values of ΔX have been derived and summarized in Table 28, where the "absolute" cpd for each face is also reported based on the value of –0.25 V for Hg. As discussed in previous sections, X_M measures the drop in work function as the given crystal face is brought in contact with water. These values of ΔX are the same as those derived in previous papers[26,32] since there have been no recent developments. The new point for Cu(l 10) has not been taken into account for the derivation of ΔX since homologous values for the other faces would be necessary.

Note that the only values of ΔX of high reliability are in principle those for Au, specifically Au(111), for which "congruent" pairs of data exist for Φ and $E_{\sigma=0}$. Although the approach suggests that all faces should lie on the same line, no ΔX has been estimated for faces other than the

Table 28
Relative and Absolute Interfacial Parameter for Metal Single-Crystal Faces in Contact with Water

Metal crystal face	$-\Delta X/V^a$	$-X$ ($\equiv \delta\chi^M + \delta\chi^S$)/V
Au(111)	0.12	0.37
Au(100)	0.14	0.39
Au(110)	0.18	0.43
Ag(111)	0.19	0.44
Ag(100)	0.22	0.47
Ag(110)	0.24	0.49
Cu(111)	0.32	0.57
Cu(100)	0.35	0.60
Cu(110)	0.42	0.67

[a]From Fig. 15.

three main ones since no (even indicative) work function values are available for Cu and Ag.

For the same reasons, data on single-crystal faces for metals such as Zn, Sb, Bi, Sn, and Cd have not been plotted in Fig. 15. In order to indicate the probable position of d-metal surfaces, the line described by Eq. (64) has also been drawn in Fig. 15. It is interesting that all the points for sd-metals fall between the sp- and the d-metal groups. The crystal face specificities of $E_{\sigma=0}$ for Sb and Bi are complicated by their semimetallic nature. In any case, no data on Φ exist for a series of faces of these elements (only "electrochemical" work functions are available).[28,864]

(iii) The Case of Pt(111)

Thus far, Ft has never found a definite position in $E_{\sigma=0}$ vs. Φ correlations, more for the uncertainty in the reliability of its pzc than for its work function. On the other hand, Pt is a highly heterogeneous metal and the fact that only polycrystalline surfaces have been used in double-layer studies has not helped remove suspicions. According to Frumkin's data,[10,14] the pzc of pc-Pt is around 0.2 V(SHE) (in acidic solution). If this value is introduced into Fig. 14 (the Φ of pc-Pt is around 5.5 eV),[22,65,343,856,865,866] the point of Pt would fall far distant from the line of mercurylike metals and near the line of d-metals.

Recently, with the improvement achieved in the preparation and control of surfaces, a number of approaches have been devoted to the estimation of the pzc of pt(111).[140,197,210,211] These are summarized in Table 29 for convenience of the reader. The value recommended for pc-Pt is also reported for comparison. In three cases the pzc has been estimated indirectly and the value is strikingly close to the pzc of polycrystalline Pt. In view of the heterogeneity of Pt surfaces, this closeness is puzzling and suggests that the phenomenon used to estimate the pzc does not conform to the concept of zero charge.

The value obtained by Hamm *et al.*[140] directly by the immersion method is strikingly different and much more positive than others reported. It is in the right direction with respect to a polycrystalline surface, even though it is an extrapolated value that does not correspond to an existing surface state. In other words, the pzc corresponds to the state of a bare surface in the double-layer region, whereas in reality at that potential the actual surface is oxidized. Thus, such a pzc realizes to some extent the concept of ideal reference state, as in the case of ions in infinitely dilute solution.

It is intriguing to try to discuss such a pzc within a framework of all other metals. The first problem is the selection of a work function. A search of the recent literature[37,48,865–867] shows that there is a range of values between 5.6 and 6.4 eV, with a strong indication that 6.1 eV may be the most appropriate value.[867] Figure 17 shows a first picture of the situation where Hg (as a sp-metal) and Au(111) (as the closest sd-metal) are included. It is evident that the uncertainty in the Φ value is high enough to leave some ambiguity. However, on the whole, the point of Pt is further

Table 29
Potentials of Zero Charge of Pt(111) in Aqueous Solutions

Value	Electrolyte	Method	References
0.185 V vs. SHE ($\sigma = 0$) (poly)	0.42 M HF + KF	Titration	14
0.235 V vs. SHE ($Q = 0$)	0.42 M HF + KF		
1.1 V vs. SHE ($\sigma = 0$)	0.1 M $HClO_4$	Immersion	140
0.78 V vs. SHE ($Q = 0$)	0.1 M $HClO_4$		
0.22 V vs. RHE ($\sigma = 0$)	0.3 M HF	CV + HREELS	210
0.34 V vs. Pd/H ($Q = 0$)	0.1 M $HClO_4$	Reaction rate	197
0.35 V vs. RHE ($\sigma = 0$)	0.1 M $HClO_4$	Spectroscopy	148

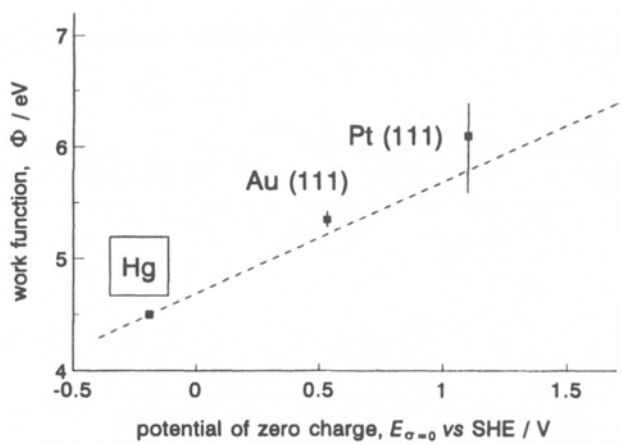

Figure 17. Plot of the potential of zero charge, $E_{\sigma=0}$, vs. the electron work function, Φ, for the (111) face of Au and Pt. (-----) Straight line of unit slope through Hg taken as a reference metal. The vertical bars indicate the range of experimental values of Φ. The point is the most probable value. Data for $E_{\sigma=0}$ from Ref. 140; Φ for Au (111) from Ref. 25; Φ for Pt (111) from Ref. 867.

away from the Hg line than Au(111), i.e., the variation of ΔX is Pt(111) > Au(111). This contrasts with the conclusions of the authors of the original paper,[140] who have opted for a Φ value of Pt(111) in the lower range of values without any specific motivation.

If the value of Φ = 6.1 eV is taken as the work function of Pt(111), some speculation is possible about the value of ΔX. This is illustrated in Fig. 18, where it is assumed that the different faces of Pt, including the pc surface, are grouped on a straight line parallel to that for the single-crystal faces of sd-metals (and sp-metals). If so, the value of $E_{\sigma=0}$ given by Frumkin[10] would imply that Φ = 5.4 eV for the pc surface of Pt, which is within the usual range of experimental data. However, there remains the puzzling aspect that while $E_{\sigma=0}$ refers to a surface with hydrogen adsorbed on it, Φ values do not include contributions from H adsorbed from the gas phase.

If, on the other hand, the pzc estimated at around 0.35 V(SHE)[197,210] is taken for Pt(111) (see Table 29), the point of Pt would be located further from the line for d-metals, with a high value of ΔX that is not justified by

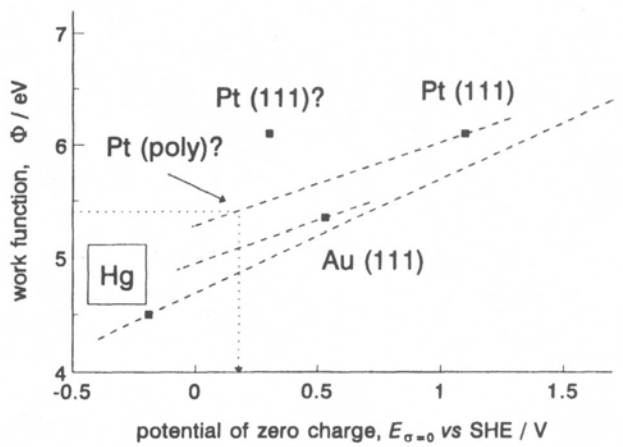

Figure 18. Tentative analysis of the plot in Fig. 17. The straight lines through Au(111) and Pt(111) are parallel to the line for sp-metals in Fig. 14. The question mark (?) indicates the hypothetical positions of Pt(poly) based on the $E_{\sigma=0}$ value given by Frumkin,[10] and of Pt(111) based on the $E_{\sigma=0}$ value proposed by Iwasita.[210]

the known behavior of the Pt surface. Therefore the value of $E_{\sigma=0}$ found by the immersion method appears to fit in well with the general picture of all other metals. The value derived for ΔX from Fig. 18 is 0.33 V, while that (extrapolated) for a polycrystalline surface is speculated to be 0.57 V.

4. UHV vs. Solution Data

As discussed in Section I.3(i), ΔX indicates the variation in the work function of a metal as an interface is created by bringing a solid and a liquid in contact. In principle, it should be possible to compare ΔX values with $\Delta\Phi$ values measured directly in gas phase experiments. This is the aim of UHV synthesis of the electrochemical double layer[868] in which the electrode interface is created molecule by molecule, starting with the bare metal surface. It is thus possible to obtain evidence of ion–water interactions that can be envisaged from electrochemical measurements but that are not directly demonstrable. Wagner[55] has given a recent comprehensive review of "electrochemical" UHV experiments.

UHV $\Delta\Phi$ and electrochemical ΔX are compared in Table 30. A quantitative comparison with reliable recent data is possible only for

Table 30
Work Function Drop Due to Metal/Water Contact

Metal	Solution/eV	Gas phase/eV	References
Ag(110)	−0.49	−0.7	37
Cu(110)	−0.67	−0.95	37
Pt(111)	−0.58	>−0.8	86
Au(110)	−0.43		
Au(111)	−0.37		
Ag(111)	−0.44		
Cu(111)	−0.57		

Ag(110), Cu(110), and Pt(111). Qualitatively, the gas phase data confirm the sequence observed electrochemically. In particular, $\Delta\Phi$ varies in the order **Au < Ag < Cu** [$\Delta\Phi$ for Au is compared with $\Delta\chi$ for the (110) face]; also, $\Delta\Phi$ forCu(110)>Pt(111).

Quantitatively, however, it is evident that directly measured $\Delta\Phi$ values are on average 0.2 to 0.3 eV higher than $\Delta\chi$ values. This shift in the "potential" scale has been discussed by Trasatti,[31–34] who has attributed such a systematic difference to the different conditions of measurement (different temperatures, nonequivalence between thin water layers and bulk water, uncompensated partial charge transfer in UHV). For a more detailed discussion, the reader is referred to the original papers.

5. "Hydrophilicity"

$\Delta\chi$ as well as $\Delta\Phi$ measure changes in the structure of the surface layers of a metal and of a solvent as the two phases are brought in contact. These changes are associated with the reorientation of solvent molecules and the redistribution of the electron tail at the surface of the metal. In principle, these are not energetic parameters, but in fact reorientation of a molecule is possible if there are orienting forces acting on it which in the absence of an electric field ($\sigma = 0$) can only be short-range chemical interactions.[15,25,26,408,869] Thus, $\Delta\chi$ can also be interpreted in terms of metal–water interaction. A high value of $\Delta\chi$ entails an appreciable modification of the surface structure as a consequence of strong interactions between the phases and vice versa. The concept of "hydrophilicity" has been

introduced[870] to deal with metal-water interactions in the double layer.[23,871]

(i) Comparison with TDS Data

While $\Delta\Phi$ values are directly comparable with $\Delta\chi$ values, metal–water interactions are better probed by thermal desorption spectroscopy (TDS) in which heat is used to detach molecules from a surface. TDS data are in parallel with $\Delta\Phi$ (and $\Delta\chi$) data. This is illustrated in Fig. 19.[35] The spectrum of Ag(110) shows only one peak at 150 K, corresponding to ice sublimation. This means that $Ag-H_2O$ interactions are weaker than H_2O-H_2O interactions (although they are still able to change the structure of the

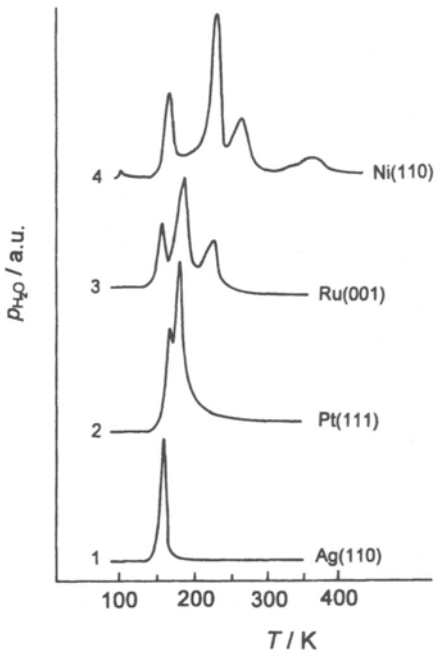

Figure 19. Thermal desorption spectra of water adsorbed on (1) Ag(110), (2) Pt(111), (3) Ru(001), and (4) Ni(110). (Reproduced from P.A. Thiel and T.E. Madey, *Surf. Sci. Reports* 7 258, Fig. 29, 1987, © 1987 with permission of Elsevier Science.)

surface region). There are TDS data for Cu(110) showing an additional peak at 175 K, which is not present on the (111) and the (100) faces; this corresponds to a weakly chemisorbed state.[872,873] These data support the conclusion based on ΔX that $M-H_2O$ interactions are stronger on Cu than on Ag.[874]

Figure 19 also shows that there is a peak at 170–175 K on the surface of Pt(111), which confirms that such a surface is more reactive than that of sd-metals. In particular, in agreement with ΔX data, the high-temperature TDS peak of Pt(111) is very close to that of Cu(l 10). More complex spectra are exhibited by Ni(110), which is known to be easily oxidized and thus tends to react strongly with water molecules.[875] In conclusion, TDS and ΔX ($\Delta\Phi$) data are qualitatively in agreement in ranking different metals and different crystal faces on a scale of metal–H_2O interaction strength. A comparison of the two sets of data also supports the view that there is a limiting value of ΔX (limiting restructuring effects) while the actual $M-H_2O$ bond strength (chemical affinity) continues to increase.

(ii) Quantum Chemical Calculations

Quantum chemical calculations, molecular dynamics (MD) simulations, and other model approaches have been used to describe the state of water on the surface of metals. It is not within the scope of this chapter to review the existing literature; only the general, qualitative conclusions will be analyzed.

The decrease in Φ at the surface of Ag(110) has been successfully reproduced by a jellium–point dipole model by assuming a disordered water structure at the interface.[876] It is intriguing that for hydrophobic surfaces, models generally predict a stronger penetration into bulk water of the disturbance of the local structure.[877,878] Thus, in the case of hydrophilic surfaces, the first layer (or two) of water is strongly oriented by the forces emanating from the surface, but the bulk structure is soon recovered in a few layers after some very disorganized layers in between. This picture confirms the model proposed by Drost-Hansen,[879] although on a larger scale (each region was composed of several layers).

MD simulations have been used for water at Pt(100) and (111),[880–882] as well as at Ag(l 11).[883] The structure of water is predicted to conform to a hexagonal pattern and the metal–water interaction is probably stronger for the (111) than the (100) surface.[882] On the basis of the extended Hückel theory, Estiù *et al.*[884,885] have reached different conclusions in favor of the

(100) face. The predicted surface potential drops are in general much higher than expected,[170] although the Monte Carlo method has given a value of 70 mV for the surface potential of water on a neutral planar surface (simulating a hydrophobic surface).[886]

Water reorientation is usually predicted by theoretical models. However, in the case of Ag(111), MD simulations[883] do not confirm the dramatic increase in water population near a charged surface claimed by Toney *et al.*[776,777] on the basis of surface X-ray scattering experiments. The same results have been claimed as indicating that water molecules are oriented with the hydrogen down on a negatively charged surface. This picture is not confirmed by far-IR spectroscopy results[887] according to which, although they change orientation with charge, water molecules always point the oxygen atom toward the solid surface.

Such a picture was proposed by Trasatti[6,7] on the basis of double-layer evidence. A reason suggested for this behavior is that water molecules do not behave as isolated monomers (as assumed in the early molecular models), but are located in a network of hydrogen-bonded molecules.[888] Rotating a bound molecule entails breaking hydrogen bonds and requires a much higher energy than rotating an isolated molecule.

The importance of the presence of other molecules for the interaction of a water molecule with a metal surface is seen clearly in calcula-

for water on a metal surface, i.e., with the lone pair directed toward the solid and the dipole tilted toward the solution. The adsorption energy calculated for H_2O on Hg is –32.2 kJ mol^{-1}, which is less than that for hydrogen bonding; therefore Hg behaves as a hydrophobic surface.[890]

Quantum chemical calculations have recently been extended to In.[891] Adsorption has been found to be nondissociative and the metal–water interaction has been proposed to be in the sequence Hg < Ag(100) < In < Cu(100). Compared with the data in Tables 27 and 28, it appears that the positions of In and Ag(100) are exchanged.

A consistently anomalous (with respect to electrochemical evidence) position of Au has been found by two different groups. According to Kuznetsov *et al.*,[437] the complete neglect of differential overlap (CNDO) method predicts for any given metal a weaker interaction on the more dense surface. Thus the predicted sequence is (111) < (100) < (110) for fcc metals such as Cu, Ag, and Au; and (0001) < (1100) for hcp metals such as Zn and Cd. However, for the most compact surfaces, the calculated sequence is Hg < Ag(111) < Cu(111) ≈ Zn(0001) < Au(111) < Cd(0001).

It is difficult to accept that Zn can be less hydrophilic than Au, and also that Au can be more reactive than Cu.

More recent calculations by a relatively new technique have in part modified the above sequence.[438] The proposed order for the (100) face is Ag < Au < Cu. This confirms the position of Cu in Table 28, but Au still appears to be more reactive than Ag. There are also other interesting aspects. The most adsorbing position has been found to be the "top" or "bridge" rather than the "hollow" site. On the other hand, the adsorption energy has been calculated to be –31.8 kJ mol^{-1} for Cu, which is the same value as that found for water on Hg by other authors.[890]

On the whole, theoretical calculations provide only a general insight into the problem of water–metal interactions, probably because not all factors are appropriately taken into account. Thus the agreement of ΔX data with $\Delta\Phi$ and TDS results is much closer than with theoretical calculations. Nevertheless, each author claims good agreement with some experimental facts, with the outcome that plenty of "hydrophilicity" scales have been suggested[23,153,352,389,399,834,870,890,892,893] based on different parameters; these have increased the entropy of the situation with a loss of clarity.

(iii) Controversies over ΔX

While contrasting results obtained by different experimental techniques as well as different theoretical methods are not surprising, internal controversies over ΔX values in electrochemistry are more serious. The controversy referred to here[32] is that about the sequence of metal–water interactions for the different faces of fcc metals. More recently, a controversy has also arisen about single-crystal faces of Cd.

The ΔX sequence (111) < (100) < (110) in Table 28 has been questioned by Valette,[389,399] who proposed (110) < (100) < (111). He also suggested[252] the sequence Ag < Au < Cu rather than Au < Ag < Cu. It happens that these two different pictures have been obtained using the same experimental values of $E_{\sigma=0}$. In particular, data for exactly the same electrodes of Ag are used to arrive at different conclusions. It is clear that the controversy issues from a different concept of selection of Φ values. Trasatti[410] has discussed this point at length and has proven that Valette's "hydrophilicity" series for Cu, Ag, and Au is based on an inadequate "choice" of work function values.

Another, more serious controversy, issues from the data of Popov *et al.*[382,443] They also claim the sequence of hydrophilicity Ag(111) > (100), but their claim is based on their own results obtained with electrodes prepared in a quite different way: grown in a Teflon capillary rather than crystallized, oriented, cut, and polished. These authors define their electrodes as "quasi-perfect" while they call the others "real." The meaning is clear: the former electrodes are considered structurally more adequate than the latter.

The puzzling point is that both sets of electrodes give the same values of $E_{\sigma=0}$. Thus, on the basis of $E_{\sigma=0}$ vs. Φ correlations, the same conclusions should be reached. However, Popov et al. do not discuss ΔX values; they arrive at their hydrophilicity scale on the basis of other parameters, which will be considered later on. If the situation is true, the two sets of electrodes can give different ΔX sequences only if different Φ values are involved. However, this would mean that surfaces of a given metal can have the same $E_{\sigma=0}$ but a different Φ. This ambiguous situation has been pointed out by Trasatti[32] in a recent paper and calls for further study.

6. Other Solvents

Results in other solvents are scanty for metals other than Hg.[81,108,109] Liquid Ga and its Tl and In liquid alloys have been studied in DMSO, DMF, NMF, AN,[343,894] MeOH[360] and EtOH.[361] Among solid metals, only Bi,[28,152] Au,[25,26,109] Al,[750,751] and Fe[729] have been investigated in a number of nonaqueous solvents. Pt and Pd have been studied in DMSO and AN.[25,802,806,895]

The general picture emerging from the pzc in aqueous solutions is that the major variation of $E_{\sigma=0}$ between two metals is due to Φ, with a minor contribution from ΔX that is governed by metal–solvent interactions. If this is also the case in nonaqueous solvents, a similar picture should be obtained. This is confirmed by Fig. 20 in which the data in DMSO are reported. As in aqueous solution, all points lie to the left of the point of Hg. Bi, In(Ga), and Tl(Ga) lie with Hg on a common line deviating from the unit slope. As in aqueous solution, Ga is further apart. Au is in the same position, relatively close to the Hg line. Finally, the point of Pt is (tentatively) much farther than all the other metals.

The same situation is also found with the other solvents, the difference being the magnitude of ΔX. Since ΔX includes a contribution from the

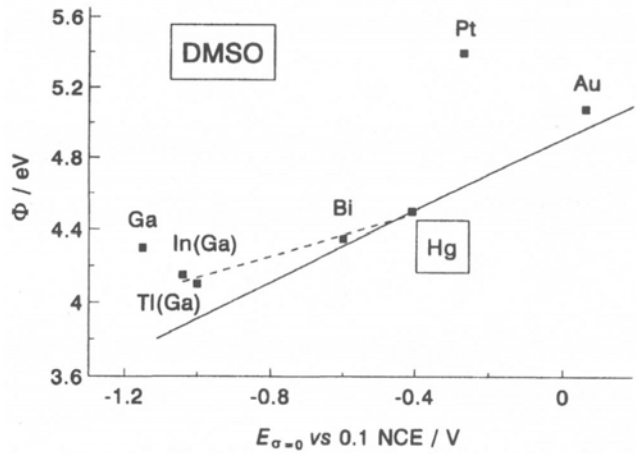

Figure 20. Plot of the potential of zero charge, $E_{\sigma=0}$, vs. the electron work function, Φ, for metals in DMSO solutions, exhibiting the same general features as for aqueous solutions (Fig. 14).

solvent, it is expected to be a function of some properties of the solvent. This point has been dealt with exhaustively by Bagotskaya *et al.*[334,343,350,894] For instance, ΔX values are higher for DMSO than for water, and these are higher than for AN. The sequence can be understood in terms of polarizability, chemical interaction, and orientation of solvent molecules. Given the scope of this chapter, no more quantitative discussion is possible since there are no data that can be used to check the ΔX values. Specific discussions of this point have been given by Trasatti elsewhere.[25,26,81]

7. Indirect Evidence of the "Interfacial Parameter" Scale

ΔX is proportional to the modifications occurring at the interface with respect to the separate phases. Therefore any events occurring at the interface should in some way be influenced by ΔX or should to some extent reflect ΔX.

(i) *Metal–Water Affinity*

Using ΔX or X makes no difference from a conceptual point of view. However, since the value of X for Hg is questioned by some authors, ΔX values will be used in the following discussion. Since X measures the impact of metal–water interactions on the value of $E_{\sigma=0}$, X should be proportional to the thermodynamic affinity of metals for water. There are no tabulated data for a hypothetical M–OH_2 compound, but since interactions are expected to take place through the oxygen atom of water molecules, Trasatti[52,869,871] suggested that the needed parameter can be $\Delta_f H°$, the enthalpy of formation of the generic oxide MO. This parameter has also been used to make thermodynamic predictions regarding the type of water adsorption on metals from the gas phase, and it has been shown[35] to work in that case as well.

Figure 21 shows a plot of ΔX against $\Delta_f H°$. As expected, the broad trend is that ΔX increases with the negative value of $\Delta_f H°$. It is even more interesting that metals can be gathered into different groups, with sp-metals in two distinct groups and sd-metals in a separate group. It is also

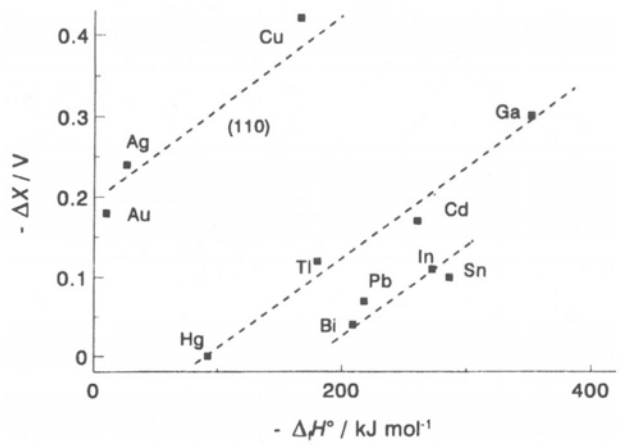

Figure 21. Correlation between the enthalpy of formation of the oxide MO and the relative value of the interfacial parameter, ΔX, derived from Fig. 14.

intriguing that in terms of $\Delta_f H°$, the sd-metals are arranged in the same sequence as ΔX, i.e., Au < Ag < Cu.

A possible objection to the use of $\Delta_f H°$ is that it refers to the formation of bulk compounds and not to adsorbate monolayers only. The $\Delta_f H°$ for bulk compounds would include metal–metal bond breaking, which is not expected to occur upon adsorption unless there is an exchange of places between the metal and the adsorbate. However, this is only partly true: as chemisorption takes place, surface electrons will be concentrated (or diluted) at the surface site where the adsorbate is placed, with delocalized effects on neighboring sites. The effect of chemisorption on surface conductivity is a practical example, the other being the difference between M–H bond strength in solution and in the gas phase.[406,896] Therefore the $\Delta_f H°$ values are very likely to be consistent with the original concepts. However, an attempt to correct the $\Delta_f H°$ values for a metal–metal surface bond by subtracting the metal sublimation heat produces[26] an intriguing arrangement of the metals, as shown in Fig. 22. The metals can still be gathered in three main groups but, quite interestingly, according to the periods of the Mendeleev table.

It is intriguing that the slopes of the straight lines tentatively drawn in Fig. 22 are now of opposite sign with respect to Fig. 21. Within a given group, the value of ΔX increases as the affinity for water decreases. Au and Ag are known to be among the very few metals that adsorb water associatively from the gas phase.[35] Nevertheless, they show a large value of ΔX. A possible explanation[897] is that in the case of Au and Ag, the polarizability of the surface electrons, as measured by $\delta\chi^M$, is more important than water reorientation as measured by $\delta\chi^S$. The quite isolated position of Hg in Fig. 22 is noteworthy. This may be primarily related to the fact that the *liquid* metal is used as a reference state for thermodynamic parameters at 25°C. In other words, the point of Hg simply cannot fit the plot of Fig. 22.

(ii) Contact (Volta) Potential Difference

The meaning attached to X is precisely that of the cpd at the metal/solution interface, i.e., X measures the change in Φ of a given metal as it is covered with a macroscopic film of solution at $\sigma = 0$. The cpd, $\Delta\Phi \equiv X$, includes a contribution from metal electrons and from solvent dipoles. While it may be difficult to compare the behavior of different metals, as Figs. 21 and 22 show, because of the lack of a parameter unambiguously

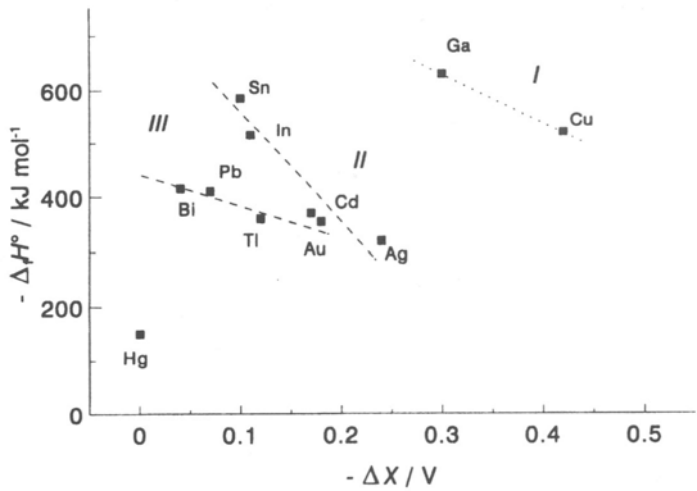

Figure 22. Correlations between the interfacial term, $\Delta\chi$, derived from Fig. 14, and the enthalpy of formation of the oxide MO, corrected for the work to break metal–metal bonds. I, II, III mean first, second, and third periods of the periodic table of elements. From Ref. 26, updated. (From R. Guidelli, ed., *Electrified Interfaces in Physics, Chemistry, and Biology*, p. 252, Fig. 3. Copyright © 1992 Kluwer Academic Publishers. Reproduced with permission.)

related to X, for a given metal in contact with different solvents $\delta\chi^{M}$ may be less important than $\delta\chi^{S}$. Thus X could probably be compared as a function of the nature of the various solvents.

Assuming the tendency of a solvent to form a bond to be measured, to a first approximation, by its donor number (DN), Trasatti[26,81] has obtained a broad correlation between $\Delta\psi_{\sigma=0}$ and DN: the higher the DN, the higher the cpd as a result of stronger metal–solvent interactions. Such a plot has been improved by Jaworski,[898] who has pointed out that as for the electronegativity of a metal, the donor–acceptor properties of solvents are more adequate than just the donicity. Jaworski has thus been able to produce a much less scattered plot (Fig. 23). Figure 23 proves that $\Delta\psi_{\sigma=0}$, i.e., X is related to the strength of the interaction between the metal surface and the solvent molecules.

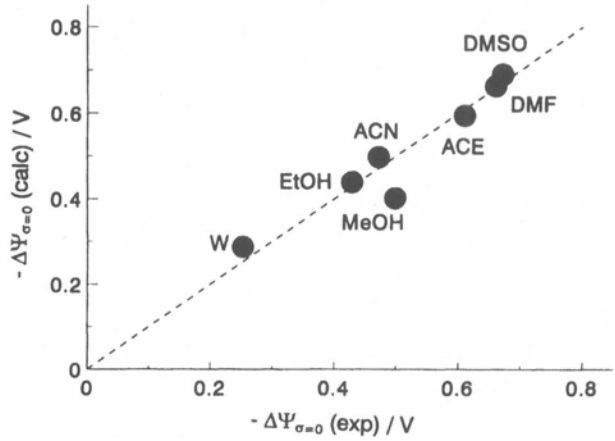

Figure 23. Plot of the experimental contact (Volta) potential difference at metal/solvent interfaces ($\sigma = 0$) vs. the values calculated by Jaworski[898] as a function of solvent donor (DN) and acceptor (AN) numbers using the equation: $\Delta\psi_{\sigma=0} = 0.007$ AN – 0.011 DN – 0.485. (Reproduced from J.S. Jaworski; *Electrochim. Acta* **34** 486, Fig. 2, 1989, Copyright © 1989 with permission of Elsevier Science.)

(iii) Interfacial Permittivity

It is an experimental fact that the capacitance of an electrode in a given solvent is a function of the nature of the metal. This was pointed out by Frumkin *et al.*[333] and has been discussed several times in the literature.[7,349,894,899,900] Trasatti[34,901] showed that the reciprocal of the differential capacitance at $\sigma = 0$ is linearly correlated with the strength of the metal–water interaction. The reader is referred to the original papers for a detailed discussion.

The idea is that X must govern in some way all properties of the interface, including the permittivity. The latter includes an electronic and a molecular term, which have been tentatively separated[7] on the basis of model approaches. In this chapter, only the correlation of the capacitance with X is relevant. The correlation between $1/C$ and ΔX has been demonstrated for eight metals in aqueous solution. It has been shown[26,34] that the correlation derived from sp-metals is fit also by single-crystal faces of sd-metals. In particular, the capacitance of Ag increases in the sequence

(111) < (100) < (110). The point for Au(100) is also located near the general correlation.[32]

The increase of C as X increases appears to be a general occurrence.[26] Since the $E_{\sigma=0}$ vs. Φ plots in nonaqueous solvent reproduce the main features of the plot in aqueous solution, Fig. 24 shows that in the same plot linear correlations of $1/C$ vs. ΔX are obtained for water and DMSO. Any attempt to extend the analysis to other solvents is frustrated by the scatter of the point for Tl(Ga). A general trend can be identified, but any systematic dependence of the slope on the nature of the solvent cannot be established.

Figure 24 shows that the values of ΔX derived from Figs. 14 and 15 are consistent with the values of C measured by Valette.[390] On the other hand, the same values of C cannot fit Fig. 24 if the values of ΔX estimated by Valette[389] are used. The same is the case for the values of C as reported by Popov *et al.*[382] for single-crystal faces grown in a Teflon capillary. These authors observed the opposite sequence, i.e., $C(111) > C(100)$, thus concluding that the (111) face is more hydrophilic than the (100) face. However, as pointed out earlier, they measured the same $E_{\sigma=0}$ as the other

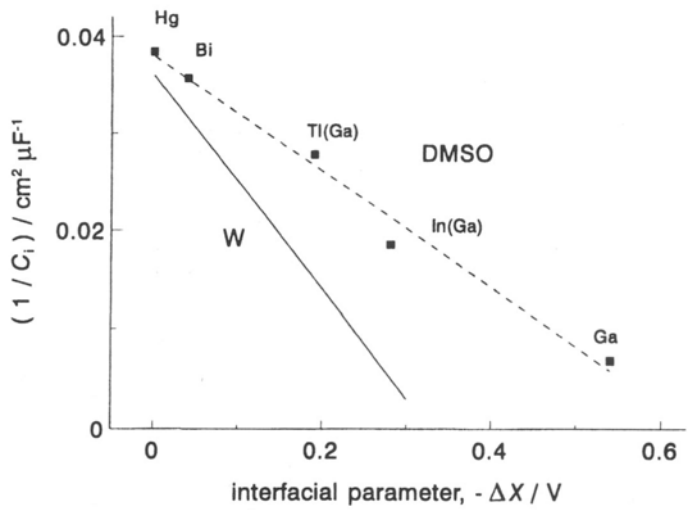

Figure 24. Linear dependence of the reciprocal of the inner-layer capacitance at $\sigma = 0$ on the interfacial parameter, ΔX. (———) Line for aqueous solutions.[901] (-----) Line for DMSO solutions.

authors and therefore the ΔX values should also be the same. This indicates that differently prepared surfaces of Ag single crystals behave not only quantitatively but also qualitatively differently.[32]

Capacitance data for various crystal faces are available for Bi and Sb.[28] As a broad trend, the faces with more negative values of $E_{\sigma=0}$ show higher values of C. Although this is qualitatively in line with the behavior of "real" Ag surfaces, the response of Bi and Sb is complicated by their semimetal nature, which gives rise to space-charge effects. For this reason it is not straightforward to compare the absolute values of C and their crystal face sequences with those of metals.

Single-crystal faces of Cd prepared in different laboratories show the same anomalies as Ag single crystals. In particular, Lust *et al.*,[249] using polished surfaces, obtained higher capacitances for the faces with the more negative pzc. On the contrary, Naneva *et al.*,[156,660,661] using surfaces grown in a Teflon capillary, have reported a reverse order of capacitances, on the basis of which these authors have assigned the higher hydrophilicity to the basal plane (0001). Thus the same situation experienced with Ag is reproduced with Cd electrodes. These results pose the problem of which of these two sets of data is more realistic.

(iv) Temperature Coefficient of the Potential of Zero Charge

The extent of perturbation brought by a change in temperature in the interfacial layer is expected to depend on the structure of the layer itself. In other words, $\partial E_{\sigma=0}/\partial T$ must depend in some way on ΔX. This point has been discussed at length by Trasatti[26,32,76] in previous papers and only some recent aspects will be illustrated here.

Values of $\partial E_{\sigma=0}/\partial T$ are usually >0. This has long been taken to be a confirmation of the orientation of water at a metal (Hg) surface, with the negative end of the dipole (oxygen) pointing to the metal.[7] However, this interpretation suffers from two limitations: (1) it rests on a simplistic model for a molecular layer of water consisting of up and down dipoles only, and (2) it totally neglects the entropic contribution of metal electrons[77] (i.e., $\partial\Phi/\partial T$). These limitations are well illustrated by the negative temperature coefficient of $E_{\sigma=0}$ for Hg in ethanol and methanol[108] even though the orientation of the solvent dipoles does not differ qualitatively from that of water.[81] The significance of $\partial E_{\sigma=0}/\partial T$ for Hg has been discussed elsewhere by Trasatti[76] and the reader is referred to the original papers.

In this chapter it is of interest to discuss the dependence of $\partial E_{\sigma=0}/\partial T$ on ΔX. Data for a number of faces of Ag and Au are available and constitute the basis for some correlations. In particular, Trasatti and Doubova[32] have shown that a common correlation exists (Fig. 25) between $\partial E_{\sigma=0}/\partial T$ and ΔX for single-crystal faces of Ag and Au in the sense that $\partial E_{\sigma=0}/\partial T$ becomes less positive as ΔX increases. As a limiting case, a negative temperature coefficient has been found[393] for Ag(110), which exhibits the highest ΔX.

A controversy exists over the interpretation of such a correlation. According to the simple two-state model for water at interfaces, the higher the preferential orientation of one of the states, the higher the value of $\partial E_{\sigma=0}/\partial T$. If the preferentially oriented state is that with the negative end of the dipole down to the surface, the temperature coefficient of $E_{\sigma=0}$ is positive (and vice versa). Thus, in a simple picture, the more positive $\partial E_{\sigma=0}/\partial T$, the higher the orientation of water, i.e., the higher the hydrophilicity of the surface. On this basis, Silva *et al.*[446] have proposed the

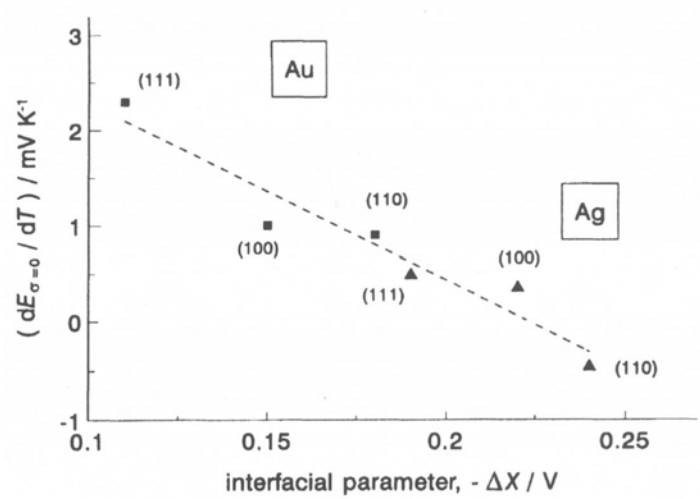

Figure 25. Plot of the temperature coefficient of the potential of zero charge for different crystal faces of Ag and Au, vs. the interfacial parameter, ΔX. From Ref. 32. (Reproduced from S. Trasatti and L.M. Donbova, *J. Chem. Soc. Faraday* Trans. **91**, 3318, Fig. 7, 1995 with permission of The Royal Society of Chemistry.)

following sequence of "hydrophilicity" for Au single-crystal faces: (111) > (100) > (110).

The interpretation based on the thermal disorganization of a dipolar layer neglects the role played by the dipole–metal interactions. If a molecule is strongly oriented, it is more weakly affected by a temperature change since the thermal energy (kT) has to overcome a chemical bond strength. Therefore a higher value of $\partial E_{\sigma=0}/\partial T$ is instead an indication of a more loosely bound dipolar layer.

More recently, Silva *et al.*[447,448] have found that the temperature coefficients of $\partial E_{\sigma=0}/\partial T$ for a number of stepped Au surfaces do not fit into the above correlation, being much smaller than expected. These authors have used this observation to support their view of the hydrophilicity sequence: the low $\partial E_{\sigma=0}/\partial T$ on stepped surfaces occurs because steps randomize the orientation of water dipoles. Besides being against common concepts of reactivity in surface science and catalysis, this interpretation implies that stepped surfaces are less hydrophilic than flat surfaces. According to the plot in Fig. 25, an opposite explanation can be offered: the small $\partial E_{\sigma=0}/\partial T$ of stepped surfaces is due to the strong chemisorption energy of water molecules on these surfaces.

The difference between smooth and stepped surfaces for Au has been discussed by Trasatti,[7] starting from the observation reported by Bond[902–904] that this metal in catalysis is surprisingly active in some morphological states. Au is certainly an sp-metal when it is negatively charged since the Fermi level is inside the sole sp band. However, inorganic chemistry suggests that Au should be regarded as a transition metal and this is certainly true since Au possesses empty d-levels in its ionic forms. Consistently, on very rough surfaces (and at stepped surfaces) it may be that at some sites Au atoms exhibit transition metal characteristics. This is particularly the case of atoms in a kink position, where the electronic smoothing effect can deprive them of the screening of the external valence electrons. Thus it is difficult to envisage a stepped surface as less reactive than a compact, smooth one.

The results of Popov *et al.*[382] are again in contrast with those above. In the case of Ag, $\partial E_{\sigma=0}/\partial T$ is higher for (100) than for the (111). In this case, on the basis of Silva's interpretation, the more hydrophilic surface would be the (100), in contrast to the conclusion of the same authors based on the value of the capacitance. In the case of Cd, Popov *et al.*[662] have found that $\partial E_{\sigma=0}/\partial T$ is higher for the (0001) face than for the polycrystal-

line surface and have concluded that the former is more hydrophilic than the latter.

Thus, two interpretations based on two different concepts of the effect of temperature on dipole orientation have been put forward. The two views clash with each other on physical as well as chemical grounds. However, the view based on the correlation of Fig. 25 introduces chemical concepts that are absent in the other, which ignores some definite facts. For instance, although a value for $\partial E_{\sigma=0}/\partial T$ is not available for Ga, the temperature coefficient of C is apparently small.[905] Ga is universally recognized as a strongly hydrophilic metal. Therefore, according to the simple model of up-and-down dipoles, the effect of temperature should be major, which is in fact not the case.

(v) Adsorption of Neutral Compounds

Adsorption at electrodes is universally considered to be a solvent replacement reaction[90,906,907]:

$$B(sol) + nH_2O(ad) \leftrightarrow B(ad) + nH_2O(sol) \qquad (65)$$

where B is an adsorbing substance replacing n water molecules on the electrode surface. Adsorption will affect the pzc since water dipoles are replaced by adsorbate dipoles.[21] However, deriving molecular parameters from adsorption potential shifts is not a simple task since the various contributions can only be separated on the basis of model assumptions.[97,98] This aspect has not yet been developed within a theory of water–metal interactions and will not be dealt with further here.

On the other hand, the adsorption Gibbs energy of a given adsorbate B can be divided into several contributions:

$$\Delta_{ad}G^{\circ}(B) = G(M - B) - G(B - S) - G(M - S) \qquad (66)$$

where S stands for solvent, G is the bond strength, and Eq. (66) simply means that in order for B to be adsorbed (this may be physical adsorption only), B must travel from the solution, breaking B–S bonds, to the metal surface, thus replacing M–S bonds. Lateral interactions are neglected in this simplified view (or better, their effects are included in the other terms).

If the same adsorbate is studied on different metals in the same solvent, then $G(B\text{-}S) \approx \text{const.}$ Furthermore, if only physical adsorption occurs, $G(M\text{-}B) \approx \text{const.}$ Under similar circumstances, $\Delta_{ad}G^{\circ}(B)$ is only a function of G(M-S), hence it is expected to be correlated with ΔX, the

interfacial parameter. In particular, $\Delta_{ad}G°(B)$ is predicted to decrease (lower adsorption) as ΔX increases.

This approach has been discussed by Trasatti[7,26,32,407,408] in several papers and the reader is referred to the original work for more quantitative discussion. In this chapter, only recent developments will be emphasized.

According to the concepts developed above, $\Delta_{ad}G°(B)$ is the only experimental parameter that probes energy terms rather than orientation effects. Therefore it is the most appropriate for describing metal–water interactions at electrodes. Figure 26 shows[32] the variation of $\Delta_{ad}G°(B)$ with ΔX for pentanol and hexanol. A nice linear correlation is observed, with $\Delta_{ad}G°$ decreasing as ΔX increases. In physical terms, as the adsorbate B enters the interface, it feels the difference between the bulk and the local structure. The higher this difference, the more difficult it is to penetrate the interface, i.e., to be adsorbed. Thus the more hydrophilic metals (or faces) adsorb less.

Two aspects are especially intriguing: (1) The slope of the correlation depends marginally on the nature of the adsorbate, i.e., it is a property of the interface. Adsorption of AN on Hg and pc-Ag[368] also conforms to the picture. (2) The correlation is valid for both polycrystalline and single-

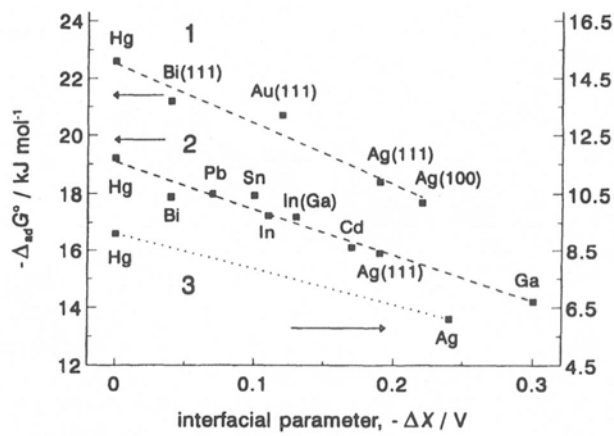

Figure 26. Plot of the Gibbs energy of adsorption of organic substances at $\sigma = 0$ vs. the interfacial parameter, ΔX. (1) 1-Hexanol, (2) 1-pentanol, and (3) acetonitrile. From Ref. 32, updated. Additional points: (1) Au(111),[910] Bi(111),[152] and (2) Ga.[916]

crystal faces, which suggests that common factors are behind this phenomenon. Lust *et al.*[908] have provided a recent comprehensive analysis.

Despite the conceptual evidence of this approach, Silva *et al.*[448] have also questioned the interpretation of Fig. 26. They maintain that a higher $\Delta_{ad}G^{\circ}$ on the (111) face of fcc metals may imply that G(M-B) and G(M-S) both change in the same direction, with the variation of G(M-B) with the crystal face prevailing over that of G(M-S). However, if the condition $G(\text{M-B}) \approx \text{const}$ is removed, then $\Delta_{ad}G^{\circ}$ cannot be related to hydrophilicity only, and any further argument becomes necessarily speculative. It is in fact necessary to *prove* that G(M-B) changes as assumed by Silva *et al.*

Afanasyev and Akulova[909] have attempted to calculate G(M-B) and G(B-S) theoretically to be able to derive G(M-S) from the experimental $\Delta_{ad}G^{\circ}$.[893] Assuming that only dispersion forces are involved in G(M-B) (this is reasonable in the case of organic adsorption if the hydrocarbon chain points to the metal surface as with aliphatic alcohols, and breaks down the hypothesis of Silva *et al.*[448]), the authors have obtained G(M-S) (relative to Hg), which increases with increasing ΔX as shown[893] schematically in Fig. 27 (even though the point of Sn is scattered). It is interesting that the metal–water bond strength is on the order of a few

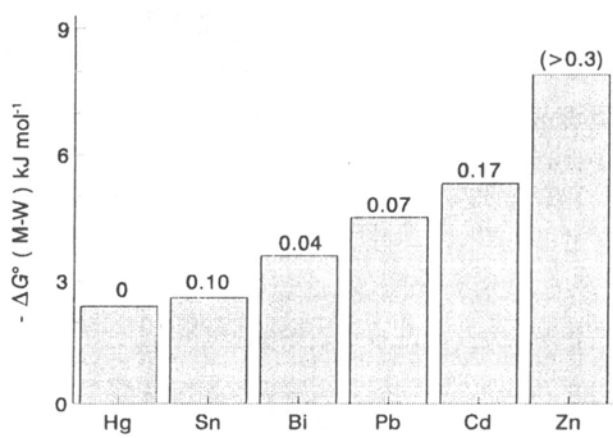

Figure 27. Gibbs energy of adsorption of water from the bulk of the solution on the given metals as calculated by Afanasyev and Akulova.[909] The figures on top of the bars are the values of the interfacial parameter, ΔX.

kilojoules mol^{-1}. Estimates on the same order of magnitude were made on the basis of the effect of water on the surface tension of Hg.[907] Thus, Figs. 26 and 27 are a direct confirmation of the view that ΔX and water–metal interaction strength are parallel. Therefore the hydrophilicity scales of Popov *et al.*, Silva *et al.*, and Valette cannot be sustained on the basis of sound experimental and theoretical arguments.

Other data support the above picture. Hexanol adsorbs very weakly on Ag(110), more weakly than expected, and in any case less than on the (100) face.[440] Such a poor adsorption on (110) faces has been explained in terms of steric hindrance caused by the superficial rails of atoms. Consistently, adsorption on the (110) face of Cu is vanishing small.[587] Predictions based on a linear regression analysis of the data for pentanol (nine metals) give a value of –12 kJ mol^{-1} for Cu(110) and about –16 kJ mol^{-1} for Au(110). No data are available for polycrystalline Au, but Au(111) is placed in the correct position in the adsorption of hexanol.[910] Thus, these data confirm the hydrophilicity sequence Hg < Au < Ag and the crystal face sequence for fcc metals (111) < (100) < (110).

The data of Popov *et al.*[443] for Ag contradict the above sequence. They found that pentanol adsorbed more strongly on Ag(100) than on Ag(111). Similarly, Cd(0001) adsorbs less strongly than pc-Cd.[661] The data for Sb and Bi are to some extent contradictory since the trend is broadly correct but with scatter, which is attributed to the crystal face specificity of space-charge effects.[153] For instance, adsorption of cyclohexanol on Bi conforms to the sequence (011) > (101) > (211) > (001) > (111), while the capacitance at $\sigma = 0$ varies in the sequence (001) > (011) > (211) > (101) > (111). Thus only the faces (001), (211), and (111) are in the expected order.[32,407] Surprisingly, the Cd data of Lust *et al.*[153] show similarities with those of Naneva *et al.*,[212] although capacitances disagree. Thus the order of cyclohexanol adsorbability is (1010) > (0001) while the capacitance varies in the order (1010) > (1120) > (0001), i.e., the other way round. In these cases one might wonder whether the G(M-B) term is really independent of face.

Another case study supporting the ΔX hydrophilicity scale is the adsorption of terminal diols. Figure 28 shows that adsorption on Au[911] is weaker than on Hg[912] as expected, while adsorption increases with the number of carbon atoms almost in parallel for the two metals. It is intriguing that the adsorption of 1,4-butanediol at the air/solution interface is weaker than on Hg[328] and is of the same order of magnitude as on Au.

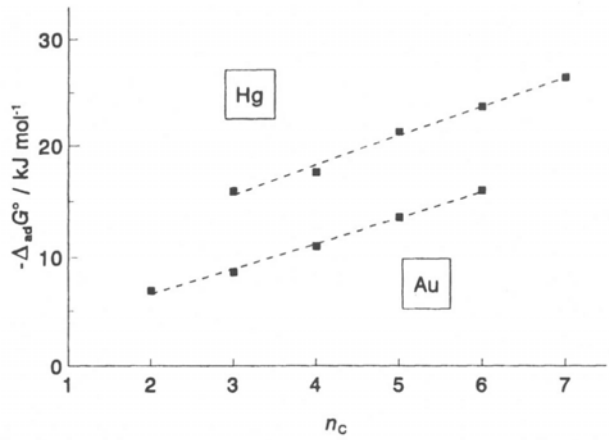

Figure 28. Dependence of the Gibbs energy of adsorption of diols on the number of carbon atoms in the molecule. Data for Hg from Ref. 912; data for Au from Ref. 911.

If the term G(M-B) is not constant, the adsorbability scale turns out to be different. In particular, for pyrazine,[913] Au(111) > Ag(111) (which is opposite to the effect of hydrophilicity); for uracils,[914] Au(100) > Au(111) > Ag(100) > Ag(111) > Hg; and for pyridine,[915] Au(311) > Ag(311) > Hg as well as Au(210) > Au(111). In all these cases the adsorbate interacts with the metal via its π-electrons. The partial d-character of Au gives to this metal the ability to form stronger bonds. The situation thus resembles that described by Silva *et al.*,[448] i.e., G(M-B) increases more rapidly than G(M-S). However, just the opposite sequence of that hypothesized by the authors is obtained.

IV. CONCLUSIONS

The analysis in this chapter has shown that during the past 10–15 years there have been only marginal modifications in our understanding of the structure of metal/solution interfaces based on the potential of zero charge. The general picture for the relative behavior of the various metals seems well established. In particular, new, more reliable data, where available, have confirmed trends already identifiable in a more ambiguous situation.

A few aspects need to be stressed, either because they are still ambiguous, or because they have been definitely clarified.

1. The potentials of zero charge considered in this chapter are those in the absence of specific adsorption of ionic as well as nonionic species. There has been no attempt to review the enormous amount of data on the effect of specific adsorption on $E_{\sigma=0}$, except for the few cases where extrapolation back to zero specific adsorption has been used as a more accurate way to determine $E_{\sigma=0}$. However, specific adsorption is difficult to relate quantitatively to the structure of interfacial water as well as to the effect of the metal.

2. The potential of zero charge measures, on a relative scale, the electron work function of a metal in an electrochemical configuration, i.e., immersed in a solution rather than in a vacuum. Converted to an "absolute value" (UHV scale) and compared with the classic electron work function of the given metal, the difference between the two quantities tells us what occurs from the local structural point of view as the metal comes in contact with the solution.

3. While the measurement of the work function is losing importance in UHV studies (because other more specific techniques have been developed), such a quantity retains its role in electrochemistry because it is intimately related to the electrode potential. A major problem is thus the dichotomy between samples for which $E_{\sigma=0}$ is known but not Φ, and vice versa. This is one of the major obstacles to the unambiguous interpretation of $E_{\sigma=0}$-Φ plots. However, this point has been recently addressed in a few cases and the outcome has allowed us to clarify some debated aspects. It is now well established that within a major group of sp- and sd-metals ΔX (the decrease in Φ as the metal comes in contact with the solution) increases as Φ decreases.

4. Conversion of $E_{\sigma=0}$ into an "absolute" (UHV) scale rests on the values of $E_{\sigma=0}$ and Φ for Hg used as a reference surface. While the accuracy of $E_{\sigma=0}$ is indisputable, the experimental value of Φ, and especially its relevance to the conditions for the determination of the contact potential difference between Hg and H_2O, are a subject of continued dispute. Efforts have been made in this chapter to try to highlight the elements of the problem. However, a *specialized* experimental approach to the measurement of Φ (and $\Delta\Phi$ upon water adsorption) of Hg would definitely remove any further ambiguity as well as any reasons not to accept certain conclusions.

5. While the picture for sp- and sd-metals is satisfactory, the situation is still ambiguous for d-metals. This is due to the difficulty of determining a reliable $E_{\sigma=0}$ free from the effects of adsorption (hydrogen and/or oxygen from water). There is some evidence that the ΔX for d-metals is probably independent of the nature of the metal (unlike sp- and sd-metals). This points to a top effect in the orientation of water molecules in contact with these metal surfaces. This view has long been sustained by Trasatti; it stems from the consideration that water molecules are hydrogen bonded to each other in a continuous network, and reorientation is possible only to the extent allowed by these bonds. It is thus inadequate to consider an "up" and "down" free (and almost symmetric) rotation of water molecules at electrode surfaces under the action of a changing electric field. Orientation with the O atom down to the surface is favored by the possibility of M–O bond formation, while orientation with the H atoms down is chemically unfavorable, thus requiring a much higher activation energy to break the structural network of water molecules in the liquid phase.

6. Pt-group metals are usually considered model electrodes for kinetic and voltammetric studies because of the possibility of controlling their surface state. Unfortunately, for precisely the same reasons, these metals are *not* polarizable model systems. Thus, the structure of their interfaces is still a mysterious object in terms of the electrical double layer because the determination of $E_{\sigma=0}$ is inhibited by interferences related to strong interactions with the solvent (water). There are now pioneering results for Pt(111) suggesting that $E_{\sigma=0}$ refers to a surface situation that does not exist in reality, i.e., a "virtual" surface state attained by extrapolation. Results for other Pt faces as well as other metals of the Pt-group would be welcome to assess the situation more comprehensively. The picture obtained with the data for Pt(111) is promising.

7. A term that is widely used (and sometimes abused) in discussions about metal–water interactions is "hydrophilicity." By this term is meant the strength of interaction between a metal surface and water molecules in contact with it, and the term usually implies chemical bond strength. However, there is a problem with the way "hydrophilicity" scales are built up. Various quantities (capacitance, adsorption energy, etc.) are used to rank the metals, and the "hydrophilicity" scale may differ for different parameters.

In this chapter it has been shown that what happens as an interface is formed is directly measured by ΔX as derived from $E_{\sigma=0}$ vs. Φ plots. ΔX

explains in electrical units all the modifications occurring at the interface with respect to the separate phases. Thus one can say that interactions are weak if ΔX is small and that they are strong if ΔX is large. Rather than "hydrophilicity," one can speak of "hardness" and "softness" with a structural meaning. Thus a large ΔX is indicative of a "hard" interface, i.e., of an interface with a structure that it is difficult to further modify by thermal, electrical, or chemical perturbations. It is therefore straightforward to understand why adsorption is weak at an interface with a large ΔX (adsorbing species penetrate the interface with difficulty), and $dE_{\sigma=0}/dT$ is small (the disorienting effect of temperature is dampened).

8. Almost all that is known about the crystal face specificity of double-layer parameters has been obtained from studies with metal single-crystal faces in aqueous solutions. Studies in nonaqueous solvents would be welcome to obtain a better understanding of the influence of the crystallographic structure of metal surfaces on the orientation of solvent molecules at the interface in relation to their molecular properties.

9. Experiments at present are concentrated on sd-metals and Pt-group metals. The sp-metals, on which theories of the double layer have been based, are somewhat disregarded. In some cases the most recent results date back more than 10 years. It would be welcome if double-layer studies could be repeated for some sp-metals, with samples prepared using actual surface procedures. For instance, in the case of Pb, the existing data manifest a discrepancy between the crystalline system and the crystal face sequence of $E_{\sigma=0}$. In other cases (e.g., Sn and Zn) the determination of $E_{\sigma=0}$ is still doubtful. For most of sp-metals, there are no recent data on the electron work function.

10. As a final point, there is the dichotomy created by the different results obtained with the same single-crystal face prepared with different procedures. This is the case for Ag but also for Cd. This is a serious point since it leads to two opposite "truths." Although the $E_{\sigma=0}$ values are the same, single-crystal faces of Ag or Cd suggest different "hydrophilicity" scales since different sequences of double-layer parameters are obtained. It is intriguing that in terms of ΔX, different hydrophilicities imply different ΔX values. If $E_{\sigma=0}$ is the same, then Φ must be different. This is easy to prove. But if $E_{\sigma=0}$ is the same, how can Φ vary? This is an interesting question since it involves the degree to which a change in Φ affects single-crystal faces and the nature of this influence.

ACKNOWLEDGMENTS

S. T. is grateful to the National Research Council (C.N.R., Rome) and the Ministry for University and Scientific and Technological Research (M.U.R.S.T., Rome) for financial support. The authors are indebted to J. M. Feliu and A. F. Silva for providing some unpublished data.

REFERENCES

[1] R. Parsons, in *Comprehensive Treatise of Electrochemistry*, Vol. 1, J. O'M. Bockris, B. E. Conway, and E. Yeager, eds., Plenum Press, New York, 1980, p. 1.
[2] A. N. Frumkin, *Phil. Mag.* **40** (1920) 363.
[3] S. Trasatti, in *Comprehensive Treatise of Electrochemistry*, Vol. 1, J. O'M. Bockris, B. E. Conway, and E. Yeager, eds., Plenum Press, New York, 1980, p. 45.
[4] R. Parsons, in *Modem Aspects of Electrochemistry*, No. 1, J. O'M. Bockris, ed., Butterworths, London, 1954, p. 103.
[5] S. Trasatti, *Pure Appl. Chem.* **58** (1986) 955.
[6] S. Trasatti, in *Advances in Electrochemistry and Electrochemical Engineering*, Vol. 10, H. Gerischer and C.W. Tobias, eds., Wiley-Interscience, New York, 1976, p. 213.
[7] S. Trasatti, in *Modem Aspects of Electrochemistry*, No. 13, B. E. Conway and J. O'M. Bockris, eds., Plenum Press, New York, 1979, p. 81.
[8] A. N. Frumkin, O. A. Petrii, and B. B. Damaskin, in *Comprehensive Treatise of Electrochemistry*, Vol. 1, J. O'M. Bockris, B. E. Conway, and E. Yeager, eds., Plenum Press, New York, 1980, p. 221.
[9] R. S. Perkins and T. N. Andersen, in *Modem Aspects of Electrochemistry*, Vol. 5, J. O.M.
[10] Bockris and B. E. Conway, eds., Plenum Press, New York, 1969, p. 203.
[11] A. Frumkin, *Zero Charge Potentials*, Nauka, Moscow, 1979.
A. Frumkin, O. Petrii, and B. Damaskin, *J. Electroanal. Chem.* **27** (1970) 81.
[12] G. Lippmann, *Pogg. Ann. Phys.* **149** (1875) 54b.
[13] A. N. Frumkin, *J. Electroanal. Chem.* **64** (1975) 247.
[14] A. N. Frumkin and O. A. Petrii, *Electrochim. Acta* **20** (1975) 347.
[15] S. Trasatti, in *Electrified Interfaces in Physics, Chemistry and Biology*, R. Guidelli, ed., Kluwer, Dordrecht, 1992, p. 229.
[16] R. Parsons, in *Advances in Electrochemistry and Electrochemical Engineering*, Vol. 1, P. Delahay and C. W. Tobias, eds., Wiley-Interscience, New York, 1961, p. 1.
[17] S. Trasatti, *Electrochim. Acta* **35** (1990) 269.
[18] A. Frumkin and A. Gorodetzkaya, *Z. Phys. Chem.* **136** (1928) 451.
[19] A. Frumkin, *Phys. Z. Sov.* **4** (1933) 239.
[20] A. N. Frumkin, *Svensk. Kem. Tidskr.* **77** (1965) 300.
[21] L. Campanella, *J. Electroanal. Chem.* **28** (1970) 228.
[22] S. Trasatti, *J. Electroanal. Chem.* **33** (1971) 351.
[23] A. Frumkin, B. Damaskin, N. Grigoryev, and I. Bagotskaya, *Electrochim. Acta* **19** (1974) 69.
[24] A. Hamelin, T. Vitanov, E. Sevastyanov, and A. Popov, *J. Electroanal. Chem.* **145** (1983) 225.
[25] S. Trasatti, in *Trends in Interfacial Electrochemistry*, A. F. Silva, ed., Reidel, Dordrecht, 1986, p. 25.
[26] S. Trasatti, in *Electrified Interfaces in Physics, Chemistry and Biology*, R. Guidelli, ed., Kluwer, Dordrecht, 1992, pp. 245.

[27]E. I. Krushcheva and V. E. Kazarinov, *Elektrokhimiya* **22** (1986) 1262.
[28]E. I. Lust, A. A.-Ya. Yanes, K. K. Lust, and Yu. I. Erlikh, *Elektrokhimiya* **32** (1996) 597.
[29]S. Trasatti, *J. Electroanal. Chem.* **52** (1974) 313.
[30]S. Trasatti, *J. Electroanal. Chem.* **139** (1982) 1.
[31]S. Trasatti, *J. Chem. Phys.* **69** (1978) 2983; *Mat. Chem. Phys.* **16** (1987) 157.
[32]S. Trasatti and L. M. Doubova, *J. Chem. Soc. Faraday Trans.* **91** (1995) 3311.
[33]S. Trasatti, *Surf. Sci.* **335** (1995) 1.
[34]S. Trasatti, *Electrochim. Acta* **36** (1991) 1659.
[35]P. A. Thiel and T. E. Madey, *Surf. Sci. Rep.* **7** (1987) 211.
[36]J. M. Heras and L. Viscido, *Catal. Rev. Sci. Eng.* **30** (1988) 281.
[37]J. K. Sass, D. Lackey, and J. Scott, *Electrochim. Acta* **36** (1991) 1883.
[38]G. Pirug, C. Ritke, and H. P. Bonzel, *Surf. Sci.* **241** (1991) 289.
[39]J.-W. He and P. R. Norton, *Surf. Sci.* **238** (1990) 95.
[40]D. M. Kolb and W. N. Hansen, *Surf. Sci.* **79** (1979) 205.
[41]Z. Samec, B. W. Johnson, and K. Doblhofer, *Surf. Sci.* **264** (1992) 440.
[42]J. E. B. Randles, *Trans. Faraday Soc.* **52** (1956) 1573.
[43]J. R. Farrell and P. McTigue, *J. Electroanal. Chem.* **139** (1982) 37.
[44]R. Gomer and G. Tryson, *J . Chem. Phys.* **66** (1977) 4413.
[45]W. N. Hansen and C. J. Hansen, *Phys. Rev. A* **36** (1987) 1396.
[46]W. N. Hansen and K. B. Johnson, *Surf. Sci.* **316** (1994) 373.
[47]E. R. Kötz, H. Neff, and K. Müller, *J. Electroanal Chem.* **215** (1986) 331.
[48]I. Villegas, R. Gómez, and M. J. Weaver, *J. Phys. Chem.* **99** (1995) 14832.
[49]J. Schneider, C. Franke, and D. M. Kolb, *Surf. Sci.* **198** (1988) 277.
[50]Z. Koczorowski, unpublished results (personal communication).
[51]Z. Samec, B. W. Johnson, M. Cappadonia, M. Jauch, and K. Doblhofer, *Sensors Actuators B* **13-14** (1993) 741.
[52]A. De Battisti and S. Trasatti, *Croat. Chem. Acta* **48** (1976) 607.
[53]D. C. Grahame, E. M. Coffin, J. I. Cummings, and M. A. Poth, *J. Am. Chem. Soc.* **74** (1952) 1207.
[54]Y C. Chen, J. E. Cunningham, and C. P. Flynn, *Phys. Rev. B* **30** (1984) 7317.
[55]F. T. Wagner, in *Structure of Electrified Interfaces,* J. Lipkowski and P. N. Ross, eds., VCH, New York, 1993, p. 309.
[56]A. Krasnopoler and E. M. Stuve, *Surf. Sci.* **303** (1994) 355.
[57]L.-W. H. Leung and D. W. Goodman, *Langmuir* **7** (1991) 493.
[58]J. K. Sass, J. Schott, and D. Lackey, *J. Electroanal. Chem.* **283** (1990) 441.
[59]L. W. Swanson and P. R. Davis, *Meth. Exp. Phys.* **22** (1985) 1.
[60]J. E. Inglesfield, *Prog. Surf. Sci.* **20** (1985) 105.
[61]T. Vitanov and A. Popov, *Trans. SAEST* **10** (1975) 5.
[62]G. A. Somorjai, *J. Phys. Chem.* **94** (1990) 1013.
[63]A. Hamelin, in *Modern Aspects of Electrochemistry,* No. 16, B. E. Conway, R. E. White, and J. O.M. Bockris, eds., Plenum Press, New York, 1985, p. 1.
[64]J. Lecoeur, J. P. Bellier, and C. Koehler, *Electrochim. Acta* **35** (1990) 1383.
[65]J. Hölzl and F. K. Schulte, *Springer Tracts Mod. Phys.* **65** (1979) 1.
[66]K. Wandelt, in *Thin Metal Films and Gas Chemisorption,* P. Wissman, ed., Elsevier, Amsterdam, 1987, p. 280.
[67]G. Valette and A. Hamelin, *J. Electroanal. Chem.* **45** (1973) 301.
[68]N. B. Grigoryev, *Dokl. Akad. Nauk SSSR* **229** (1976) 647.
[69]J. C. Riviére, in *Solid State Surface Science,* Vol. 1, M. Green, ed., Marcel Dekker, New York, 1969, p. 179.
[70]A. N. Frumkin, *J. Res. Inst. Catal., Hokkaido Univ.* **15** (1967) 61.
[71]R. W. Cahn, *Physical Metallurgy,* North-Holland, Amsterdam, 1970.
[72]R. Parsons and F. G. R. Zobel, *J. Electroanal. Chem.* **9** (1965) 333.

[73]S. Trasatti and O. A. Petrii, *Pure Appl. Chem.* **63** (1991) 711.
[74]M. A. Vorotyntsev, in *Modern Aspects of Electrochemistry,* No. 17, J. O'M. Bockris, B. E. Conway, and R. E. White, eds., Plenum Press, New York, 1986, p. 131.
[75]M. L. Foresti, R. Guidelli, and A. Hamelin, *J. Electroanal. Chem.* **346** (1993) 73.
[76]S. Trasatti, *J. Electroanal. Chem.* **82** (1977) 391.
[77]R. Guidelli, G. Aloisi, E. Leiva, and W. Schmickler, *J. Phys. Chem.* **92** (1988) 6671.
[78]J. E. B. Randles and K. S. Whiteley, *Trans. Faraday Soc.* **52** (1956) 1509.
[79]J. O'M. Bockris, M. A. V. Devanathan, and K. Müller, *Proc. R. Soc. Lond. Ser. A* **274** (1963) 55.
[80]J. R. Farrell and P. McTigue, *J. Electroanal. Chem.* **163** (1984) 129.
[81]S. Trasatti, *Electrochim. Acta* **32** (1987) 843.
[82]B. B. Damaskin and O. A. Baturina, *Elektrokhimiya* **31** (1995) 105.
[83]J. Lawrence, R. Parsons, and R. Payne, *J. Electroanal. Chem.* **16** (1968) 193.
[84]L. I. Antropov, M. A. Gerasimenko, and Yu. S. Gerasimenko, *Elektrokhimiya* **7** (1971) 1524.
[85]M. Bacchetta, S. Trasatti, L. Doubova, and A. Hamelin, *J. Electroanal. Chem.* **200** (1986) 389.
[86]H. P. Bonzel and G. Pirug, in *The Chemical Physics of Solid Surfaces and Heterogeneous Catalysis,* Vol. 6, D. A. King and D. P. Woodruff, eds., Elsevier, Amsterdam, 1992.
[87]D. E. Grider, K. Bange, and J. K. Sass, *J. Electrochem. Soc.* **130** (1983) 246.
[88]K. Bange, B. Straehler, J. K. Sass, and R. Parsons, *J. Electroanal. Chem.* **229** (1987) 87.
[89]S. Trasatti, in *Trends in Interfacial Electrochemistry,* A. F. Silva, ed., Reidel, Dordrecht, 1986, p. 1.
[90]S. Trasatti, *Electrochim. Acta* **37** (1992) 2137.
[91]A. N. Frumkin, B. B. Damaskin, and A. A. Survila, 7. *Electroanal. Chem.* **16** (1968) 493.
[92]A. Daghetti, S. Trasatti, I. Zagórska, and Z. Koczorowski, *J. Electroanal. Chem.* **129** (1981) 253.
[93]A. Frumkin and B. Damaskin, *Pure Appl. Chem.* **15** (1967) 263.
[94]N. S. Polyanovskaya and B. B. Damaskin, *Elektrokhimiya* **16** (1980) 531.
[95]A. Daghetti, S. Trasatti, I. Zagórska, and Z. Koczorowski, *Electrochim. Acta* **33** (1988) 1705.
[96]A. N. Frumkin and B. B. Damaskin, in *Modern Aspects of Electrochemistry,* No. 3, J. O'M. Bockris and B. E. Conway, eds., Butterworths, London, 1964, p. 149.
[97]Z. Koczorowski, S. Kurowski, and S. Trasatti, *J. Electroanal. Chem.* **329** (1992) 25.
[98]P. Nikitas and A. Pappa-Louisi, *J. Electroanal. Chem.* **385** (1995) 257.
[99]D. C. Grahame, *Chem. Rev.* **41** (1947) 441.
[100]J. O'M. Bockris and S. U. M. Khan, *Surface Electrochemistry. A Molecular Level Approach,* Plenum Press, New York, 1993.
[101]J. O'M. Bockris and K. Reddy, *Modern Electrochemistry,* Plenum Press, New York, 1970.
[102]J. O'M. Bockris and M. A. Habib, *J. Electroanal. Chem.* **68** (1976) 367.
[103]A. N. Frumkin, N. Polianovskaya, N. Grigoryev, and I. Bagotskaya, Electrochim. Acta **10** (1965) 793.
[104]A. Frumkin, B. Damaskin, I. Bagotskaya, and N. Grigoryev, Electrochim. Acta **19** (1974) 75.
[105]B. B. Damaskin and O. A. Petrii, *Vvedenie* v *elektrokhimicheskuyu kinetiku,* Vyshaya Shkola, Moscow, 1975.
[106]S. Trasatti, *J. Electroanal. Chem.* **64** (1975) 128; **130** (1981) 319.
[107]R. Parsons, *Chem. Rev.* **90** (1990) 813.
[108]Z. Borkowska, *J. Electroanal. Chem.* **244** (1988) 1.
[109]Z. Borkowska and G. Jarzabek, *J. Electroanal. Chem.* **353** (1993) 1.
[110]W. Lorenz, *Z. Phys. Chem.* **218** (1961) 272.
[111]K. J. Vetter and J. W. Schultze, *Ber. Bunsenges. Phys. Chem.* **76** (1972) 920.

[112]D. C. Grahame, *J. Am. Chem. Soc.* **74** (1952) 1207.
[113]B. E. Conway, *J. Electroanal. Chem.* **123** (1981) 81.
[114]B. E. Conway, *Theory and Principles of Electrode Processes,* Ronald Press, New York, 1965, p. 25.
[115]L. Antropov, *Theoretical Electrochemistry,* Mir, Kiev, 1972, p. 764.
[116]R. M. Reeves, in *Modem Aspects of Electrochemistry,* No. 10, R. E. White, J. O'M. Bockris, and B. E. Conway, eds., Plenum Press, New York, 1974, p. 239.
[117]J. R. Macdonald, *J. Chem. Phys.* **22** (1954) 1857.
[118]J. R. Macdonald and C. A. Barlow, *J. Chem. Phys.* **36** (1962) 3062.
[119]N. F. Mott and R. J. Watts-Tobin, *Electrochim. Acta* **4** (1961) 79.
[120]I. A. Bagotskaya, in *Itogi Nauki i Tekhniki. Elektrokhimiya,* Vol. 23, Yu. M. Polukarov, ed., Nauka, Moscow, 1986, p. 60.
[121]W. R. Fawcett, S. Levine, R. M. de Nobriga, and A. C. Macdonald, *J. Electroanal. Chem.* **111** (1980) 163.
[122]S. Amokrane and J. P. Badiali, in *Modern Aspects of Electrochemistry,* No. 22, R. E. White, J. O'M. Bockris, and B. E. Conway, eds., Plenum Press, New York, 1991, p. 1.
[123]J. Goodisman, *Electrochemistry: Theoretical Foundations,* Wiley, New York, 1987.
[124]W. Schmickler, *Chem. Phys. Lett.* **99** (1983) 135.
[125]M. A. Vorotyntsev, *Itogi Nauki i Tekhniki. Elektrokhimiya,* Vol. 21, Nauka, Moscow, 1984, p. 3.
[126]M. A. Vorotyntsev and A. A. Kornyshev, *Elektrokhimiya* **20** (1984) 3.
[127]Z. Borkowska and W. R. Fawcett, *Can. J. Chem.* **59** (1981) 710.
[128]G. Gouy, *J. Chim. Phys., J. Phys. et Radium* **9** (1910) 457.
[129]D. Chapman, *Phil. Mag.* **25** (1913) 475.
[130]G. Gouy, *Ann. Chim. Phys.* **29** (1903) 145.
[131] A. N. Frumkin, *Electrocapillary Phenomena and Electrode Potentials* (in Russ.), Odessa, 1919.
[132]F. O. Koening, *J. Phys. Chem.* **38** (1934) 111.
[133]S. R. Croxford, O. Gatty, and J. Philpot, *Phil. Mag.* **19** (1935) 965.
[134]D. C. Grahame and R. B. Whitney, *J. Am. Chem. Soc.* **64** (1942) 1548.
[135]R. Parsons and M. A. Devanathan, *Trans. Faraday Soc.* **49** (1953) 404.
[136]P. R. Couchman and C. R. Davidson, *J. Electroanal. Chem.* **85** (1977) 407.
[137]D. M. Mohilner and R. J. Beck, *J. Phys. Chem.* **83** (1979) 1160.
[138]O.J. Murphy and J. S. Wainright. *Langmuir* **5** (1989) 519.
[139]V. Endrašic, *J. Electroanal. Chem.* **22** (1969) 157.
[140]U. W. Hamm, D. Kramer, R. S. Zhai, and D. M. Kolb, *J. Electroanal. Chem.* **414** (1996) 85.
[141]T. M. Andersen, R. S. Perkins, and H. Eyring, *J. Am. Chem. Soc.* **86** (1964) 4496.
[142]N. Balashova and V. E. Kazarinov, in *Electroanalytical Chemistry,* Vol. 3, A. Bard, ed., Marcel Dekker, New York, 1969, p. 135.
[143]G. Horanyi, E. M. Rizmayer, and P. Joo, *J. Electroanal. Chem.* **154** (1983) 281.
[144]M. Vorsina and A. N. Frumkin, *Compt. Rend. Acad. Sci. USSR* **24** (1939) 918.
[145]V. Voropaeva, B. Deryagin, and B. Kabanov, *Dokl. Akad. Nauk SSSR* **128** (1959) 981.
[146]Chen Jin-Hua, Si Shi-Hui, Nie Li-Hua, and Yao Shou Zhuo, *Electrochim. Acta* **42** (1997) 689.
[147]Chen Jin-Hua, Nie Li-Hua, and Yao Shou Zhuo, *J. Electroanal. Chem.* **414** (1996) 53.
[148]T. Agladze and A. Podobayev, *Electrochim. Acta* **36** (1991) 859.
[149]L. Doubova and S. Trasatti, *Electrochim. Acta* **42** (1997) 785.
[150]G. Valette, *J. Electroanal Chem.* **269** (1989) 191.
[151]T. Vitanov, A. Popov, and E. S. Sevastyanov, *J. Electroanal. Chem.* **142** (1982) 289.
[152]E. J. Lust, K. K. Lust, and A. A.-J. Jänes, *Elektrokhimiya* **31** (1995) 876.
[153]E. Lust, A. Jänes, K. Lust, and M. Väärtnõu, *Electrochim. Acta* **42** (1997) 771.

[154]V. V. Batrakov and B. B. Damaskin, *J. Electroanal. Chem.* **65** (1975) 361.
[155]L. P. Khmelevaya, A. V. Chizhov, and B. B. Damaskin, *Elektrokhimiya* **14** (1978) 1304.
[156]R. Naneva, V. Bostanov.O. Popov, andT. Vitanov, *J. Electroanal. Chem.* **274** (1989) 179.
[157]J. Butler, *J. Phys. Chem.* **69** (1965) 3817.
[158]C. A. Smolders and E. M. Duyvis, *Recl. Trav. Chim. Pays-Bas* **80** (1961) 635.
[159]V. I. Melik-Gaikazyan, V. V. Voronchikhina, and E. A. Zakharova, *Elektrokhimiya* **4** (1968) 479.
[160]G. Kuãera, *Ann. Phys.* **11** (1903) 52; **11** (1903) 698.
[161]R. G. Barradas, F. M. Kimmerle, and E. M. L. Valeriote, *J. Polarog. Soc.* **13** (1967) 30.
[162]V. G. Levich, *Physicochemical Hydrodynamics* (in Russ.), 2nd ed., Fizmatgiz, Moscow, 1959, p. 581.
[163]B. E. Conway and S. Colledan, *J. Electroanal. Chem.* **301** (1991) 53.
[164]L. G. M. Gordon, J. Helpern, and B. E. Conway, *J. Electroanal. Chem.* **21** (1969) 3.
[165]H. Vos, J. Wiersma, and J. M. Los, *J. Electroanal Chem.* **52** (1974) 27.
[166]F. Pachen, *Ann. Phys.* **41/42** (1890) 177; **43** (1891) 585.
[167]D. Jenkins and R. Newcombe, *Electrochim. Acta* **7** (1962) 685.
[168]A. Ya. Gokhstein, *Surface Tension of Solids and Adsorption*, Nauka, Moscow, 1976, p. 382.
[169]P. R. Couchman, D. H. Ewerett, and W. A. Jesser, *J. Colloid Interface Sci.* **52** (1975) 410.
[170]R. Fredlein and J. O'M. Bockris, *Surf. Sci.* **46** (1989) 519.
[171]O. J. Murphy and J. S. Wainright, *J. Electrochem. Soc.* **135** (1988) 138.
[172]G. Sauerbery, *Z. Phys.* **155** (1959) 906.
[173]K. E. Heusler and G. Lang, *Electrochim. Acta* **42** (1997) 747.
[174]G. Lang and K. E. Heusler, *J. Electroanal. Chem.* **377** (1995) 1.
[175]L. Jaeckel, G. Lang, and K. E. Heusler, *Electrochim. Acta* **39** (1994) 1081.
[176]I. O. Efimov and K. E. Heusler, *J. Electroanal. Chem.* **414** (1996) 75.
[177]V. G. Levich, B. I. Khaikin, and B. M. Grafov, *Dokl. Akad. Nauk. SSSR* **153** (1963) 1374.
[177a]F. Veggini, S. Trasatti, and L. M. Doubova, *J. Electroanal. Chem.* **378** (1994) 125.
[178]A. G. Zelinski and B. Ya. Pirogov, *Elektrokhimiya* **19** (1983) 1267.
[179]E. Lust, A. Jänes, and K. Lust, unpublished results.
[180]V. V. Elkin, V. N. Alekseyev, L. L. Knots, and D. I. Leikis, *Dokl. Akad. Nauk. SSSR* **199** (1971)638.
[181]V. Ya. Mishuk, E. A. Solomatin, V. V. Elkin, and L. L. Knots, *Elektrokhimiya* **11** (1975) 1897.
[182]B. Jakuszewski and Z. Kozlovski, *Roczn. Chem.* **36** (1962) 1873.
[183]B. Jakuszewski, Z. Koslovski, S. Partyka, M. Pshasnyski, and S. Romanovski, *Elektrokhimiya* **7** (1971) 804.
[184]J. M. Czajkowski, T. Blaszczyk, and D. Kazmierczak, *Electrochim. Acta* **29** (1984) 439.
[185]J. Sokolowski, J. M. Czajkowski, and M. Turowska, *Electrochim. Acta* **35** (1990) 1393.
[186]J. Clavilier, R. Faure, G. Gainet, and R. Durand, *J. Electroanal. Chem.* **107** (1980) 205.
[187]D. M. Kolb, *Ber. Bunsenges Phys. Chem.* **92** (1988) 1175.
[188]D. M. Kolb, in *Structure of Electrified Interfaces*, J. Lipkowski and P. N. Ross, eds., VCH, New York, 1993, p. 65.
[189]D. Bode, T. Andersen, and H. Eyring, *J. Phys. Chem.* **71** (1967) 792.
[190]T. N. Andersen, J. L. Anderson, and H. Eyring, *J. Phys. Chem.* **73** (1969) 3562.
[191]H. Noninski and E. Lazarova, *Elektrokhimiya* **11** (1975) 1103.
[192]A. G. Zelinskii and R. Yu. Bek, *Elektrokhimiya* **21** (1985) 66.
[193]E. M. Lazarova, *Elektrokhimiya* **17** (1981) 871.
[194]E. M. Lazarova, *Elektrokhimiya* **17** (1981) 868.
[195]V. A. Safonov, B. B. Damaskin, and M. A. Choba, *Elektrokhimiya* **25** (1989) 1432.
[196]J. Clavilier, R. Albalat, R. Gómez, J. M. Orts, J. M. Feliu, and A. Aldaz, *J. Electroanal. Chem.* **330** (1992) 489.

[197]G. A. Attard and A. Ahmadi, *J. Electroanal. Chem.* **389** (1995) 175.
[198]J. O'M. Bockris and R. Parry-Jones, *Nature* **171** (1953) 930.
[199]P. A. Rebinder and E. K. Wenstrom, *Acta Physicochem.* **19** (1944) 39.
[200]J. O'M. Bockris and S. D. Argade, *J. Chem. Phys.* **50** (1969) 1622.
[201]J. O'M. Bockris and R. Sen, *Surf. Sci.* **30** (1972) 232.
[202]G. Barker, A. Gadner, and D. Sammon, *J. Electrochem. Soc.* **113** (1966) 1182.
[203]A. Brodsky and Yu. Gurevich, *Electrochim. Acta* **13** (1968) 1245.
[204]A. Brodsky, Yu. Gurevich, and S. Sheberstov, *J. Electroanal Chem.* **20** (1971) 353.
[205]A. Brodsky and Yu. Pleskov, in *Progress in Surface Science,* Vol. 2, S. Davidson, ed., Pergamon, Oxford, 1972, p. 2.
[206]T. Iwasita and F. C, Nart, in *Advances in Electrochemical Science and Engineering,* Vol. 4, H. Gerisher and C. W. Tobias, eds., VCH, Weinheim, 1995, p. 123.
[207]R. Nichols, in *Adsorption of Molecules at Metal Electrodes,* J. Lipkowski and P. N. Ross, eds., VCH, Weinheim, 1992, p. 347.
[208]*Spectroelectrochemistry. Theory and Practice,* R. J. Gale, ed., Plenum Press, New York, 1988.
[209]J. J. Calvente, N. S. Marinkovic, Z. Kovácová, and W. R. Fawcett, *J. Electroanal. Chem.* **421** (1997) 49.
[210]T. Iwasita and X. Xia, *J. Electroanal. Chem.* **411** (1996) 95.
[211]F. T. Wagner and T. E. Moylan, *Surf. Sci.* **206** (1988) 187.
[212]M. Janda and O. Stefan, *Thin Solid Films* **112** (1984) 127.
[213]J. Clavilier and C. Nguyen Van Huong, *Compt. Rend., Ser. C* **269** (1969) 736.
[214]R. E. Malpas, R. A. Fredlein, and A. T. Bard, *J. Electroanal. Chem.* **98** (1979) 171.
[215]R. E. Malpas, R. A. Fredlein, and A. T. Bard, *J. Electroanal. Chem.* **98** (1979) 339.
[216]M. Seo, T. Makino, and N. Sato, *J. Electroanal. Chem.* **133** (1986) 1138.
[217]K. M. Dickinson, K. E. Hanson, and R. A. Fredlein, *Electrochim. Acta* **37** (1992) 139.
[218]R. C. Salvarezza and A. J. Arvia, in *Modern Aspects of Electrochemistry,* No. 28, R. E. White. J. O'M. Bockris, and B. E. Conway, eds., Plenum Press, New York, 1995. p. 289.
[219]B. B. Damaskin and U. V. Palm, in *Itogi Nauki i Tekhniki. Elektrokhimiya,* Vol. 12, Yu. M. Polukarov, ed., VINITI, Moscow, 1977. p. 99.
[220]T. I. Borissova, B. V. Ershler, and A. N. Frumkin, *Zh. Fiz. Khim.* **22** (1948) 925.
[221]T. I. Borissova and B. V. Ershler, *Zh. Fiz. Khim.* **24** (1950) 337.
[222]N. Hampson and D. Larkin, *J. Electrochem. Soc.* **114** (1967) 933.
[223]D. I. Leikis, K. V. Rybalka, and E. S. Sevastyanov, in *Double Layer and Adsorption at Solid Electrodes,* A. N. Frumkin and B. B. Damaskin, eds., Nauka, Moscow, 1972, p. 5.
[224]D. Leikis, K. Rybalka, E. Sevastyanov, and A. Frumkin, *J. Electroanal. Chem.* **46** (1973) 161.
[225]E. S. Sevastyanov, V. K. Chubarova, and M. N. Ter-Akopyan, *Elektrokhimiya* **24** (1988) 834.
[226]A. J. Bard, *Anal. Chem.* **33** (1961) 11.
[227]F. G. Will and C. A. Knorr, *Z. Elektrochem.* **64** (1960) 258.
[228]M. Breiter, K. Hoffmann, and C. Knorr, Z. *Elektrochem.* **61** (1957) 1168.
[229]H. Siegenthaler and K. Jüttner, *J. Electroanal. Chem.* **163** (1984) 327.
[230]V. E. Kazarinov, D. Horani, Yu. B. Vasilyev, and V. N. Andreyev, in *Itogi Nauki i Tekhniki. Elektrokhimiya,* Vol. 22, Yu. M. Polukarov, ed., VINITI, Moscow, 1985, p. 97.
[231]R. H. Burshtein, *Elektrokhimiya* **3** (1967) 349.
[232]B. V. Tilak, C. G. Rader, and S. K. Rangarajan, *J. Electrochem. Soc.* **124** (1977) 1879.
[233]K. Micka and I. Rousar, *Electrochim. Acta* **32** (1987) 1387.
[234]R. Sonnenfeld, J. Schneir, and P. K. Hansma, in *Modern Aspects of Electrochemistry,* No. 21, R. E. White, J. O'M. Bockris, and B. E. Conway, eds., Plenum Press, New York, 1990, p. 1.

[235]P. Lustenberger, H. Röhrer, R. Cristoph, and H. Siegenthaler, *J. Electroanal. Chem.* **243** (1988) 225.
[236]M. P. Soriaga, D. A. Harrington, J. L. Stickney, and A. Wieckowski, in *Modern Aspects of Electrochemistry*, No. 28, R. E. White, J. O'M. Bockris, and B. E. Conway, eds., Plenum Press, New York, 1996, p. 1.
[237]L. Bai, L. Gao, and B. E. Conway, *J. Chem. Soc. Faraday Trans.* **89** (1993) 235.
[238]R. K. Schofield, *Nature* **160** (1974) 480.
[239]A. Kozava, *J. Electrochem. Soc.* **106** (1959) 552.
[240]S. Brunauer, P. H. Emmett, and E. Teller, *J. Am. Chem. Soc.* **60** (1938) 309.
[241]J. L. Lemaitre, P. G. Menon, and F. Delannay, in *Characterization of Heterogeneous Catalysis*, F. Delannay, ed., Marcel Dekker, New York, 1984.
[242]S. J. Cregs and K. S. W. Sing, *Adsorption, Surface Area and Porosity*, Academic Press, London, 1982.
[243]A. W. Adamson, *Physical Chemistry of Surfaces*, 5th ed., Wiley, New York, 1970.
[244]J. M. Thomas and W. J. Thomas, *Introduction to the Principles of Heterogeneous Catalysis*, Academic Press, London, 1967.
[245]A. J. Salkind, in *Techniques of Electrochemistry*, Vol. 1, J. Salkind and E. Yeager, eds., Wiley, New York, 1972.
[246]A. J. Arvia and R. C. Salvarezza, *Electrochim. Acta* **39** (1994) 1481.
[247]A. Hamelin and L. Stoicoviciu, *J. Electroanal. Chem.* **236** (1987) 267.
[248]A. Hamelin and L. Stoicoviciu, *J. Electroanal. Chem.* **271** (1989) 15.
[249]E. Lust, K. Lust, and A. Jänes, *J. Electroanal. Chem.* **413** (1996) 111.
[250]A. Hamelin, M. L. Foresti, and R. Guidelli, *J. Electroanal. Chem.* **346** (1993) 251.
[251]G. Valette, *J. Electroanal. Chem.* **260** (1989) 425.
[252]G. Valette, *J. Electroanal. Chem.* **255** (1988) 215.
[253]E. J. Lust and U. V. Palm, *Elektrokhimiya* **21** (1985) 1256.
[254]E. J. Lust, K. K. Lust, and A. A.-J. Jänes, *Elektrokhimiya* **26** (1990) 1627.
[255]A. P. Korotkov, E. B. Bezlepkina, B. B. Damaskin, and E. F. Kolov, *Elektrokhimiya* **22** (1985) 1298.
[256]J. Clavilier and C. Nguyen Van Huong, *J. Electroanal. Chem.* **80** (1977) 101.
[257]A. Hamelin, X. Gao, and M. J. Weaver, *J. Electroanal. Chem.* **323** (1992) 361.
[258]J. Lecoeur, J. P. Bellier, and R. Cherrak, *J. Electroanal. Chem.* **218** (1987) 319.
[259]Yu. P. Ipatov, V. V. Batrakov, and V. V. Salaginov, *Elektrokhimiya* **12** (1976) 286.
[260]U. V. Palm, M. P. Pärnoja, and N. B. Grigoryev, *Elektrokhimiya* **13** (1977) 1074.
[261]A. G. Zelinsky, R. Yu. Beck, A. L. Makurin, and S. D. Abdubov, *Elektrokhimiya* **14** (1975) 1740.
[262]I. A. Bagotskaya, M. D. Levi, and B. B. Darnaskin, *J. Electroanal. Chem.* **115** (1980) 189.
[263]M. A. Vorotyntsev, *J. Electroanal. Chem.* **123** (1981) 379.
[264]E. J. Lust and U. V. Palm, *Elektrokhimiya* **22** (1986) 565.
[265]E. J. Lust, M. A. Salve, and U. V. Palm, *Elektrokhimiya* **23** (1987) 561.
[266]E. J. Lust and U. V. Palm, *Elektrokhimiya* **24** (1988) 557.
[267]M. A. Vorotyntsev, in *Double Layer and Adsorption at Solid Electrodes. Proc. 6th Symp.*, Tartu University Press, Tartu, Etonia, 1981, p. 59.
[268]J. R. Macdonald, *Impedance Spectroscopy Emphasizing Solid Materials and Systems*, Wiley, New York, 1987.
[269]M. Sluyters-Rehbach, *Pure Appl. Chem.* **66** (1994) 1831.
[270]W. R. Fawcett, Z. Kovacova, A. J. Motheo, and C. A. Ross Jr., *J. Electroanal. Chem.* **326** (1992)91.
[271]E. S. Sevastyanov and V. K. Chubarova, *Elektrokhimiya* **24** (1988) 1578.
[272]E. S. Sevastyanov, V. K. Chubarova, and M. N. Ter-Akopyan, *Elektrokhimiya* **25** (1989) 558.

[273]A. J. Motheo, J. R. Santos Jr., A. Sadkowski, and A. Hamelin, *J. Electroanal. Chem.* **397** (1995) 331.
[274]T. Pajkossy, *J. Electroanal. Chem.* **364** (1994) 14 and references therein.
[275]B. B. Mandelbrot, *The Fractal Geometry of Nature*, Freeman, San Francisco, 1982.
[276]L. I. Daikhin, A. A. Kornyshev, and M. A. Urbakh, *Phys. Rev. E* **53** (1996) 6192.
[277]L. I. Daikhin, A. A. Kornyshev, and M. A. Urbakh, *Proceedings of the Baltic Conference on Interfacial Electrochemistry*, 1996, p. 57.
[278]L. I. Daikhin, A. A. Kornyshev, and M. A. Urbakh, *Electrochim. Acta* **42** (1997) 2853.
[279]S. L. Carnie and D. Y. C. Chan, *J. Chem. Phys.* **73** (1980) 2349.
[280]L. Blum and D. Henderson, *J. Chem. Phys.* **74** (1981) 1902.
[281]L. Blum, D. Henderson, and R. Parsons, *J. Electroanal Chem.* **161** (1984) 389.
[282]W. Schmickler and D. Henderson, *J. Chem. Phys.* **85** (1986) 1650.
[283]A. A. Kornyshev and J. Ulstrup, *J. Electroanal. Chem.* **183** (1985) 387.
[284]A. A. Kornyshev, J. Ulstrup, and M. A. Vorotyntsev, *Thin Solid Films* **75** (1981) 105.
[285]V. A. Koslov, V. S. Vilinskaya, and G. A. Tedoradze, *Elektrokhimiya* **18** (1982) 234.
[286]D. C. Grahame, *J. Am. Chem. Soc.* **76** (1954) 4819.
[287]R. Payne, *J. Electroanal. Chem.* **7** (1964) 343.
[288]D. J. Schiffrin, *Trans. Faraday Soc.* **67** (1971) 3318.
[289]A. Daghetti, S. Romeo, M. Usuelli, and S. Trasatti, *J. Chem. Soc. Faraday Trans.* **89** (1993) 187.
[290]B. M. Grafov and B. B. Damaskin, *J. Electroanal. Chem.* **416** (1996) 25.
[290a]A. Daghetti and S. Trasatti, *J. Electroanal. Chem.* **162** (1984) 327.
[290b]A. Daghetti and S. Trasatti, *Can. J. Chem.* **59** (1981) 1925.
[291]Z. Borkowska, W. R. Fawcett, and S. Anantawan, *J. Phys. Chem.* **84** (1980) 2769.
[292]Z. Borkowska, *J. Electroanal. Chem.* **79** (1977) 206.
[293]Z. Borkowska and W. R. Fawcett, *Can. J. Chem.* **60** (1982) 1787.
[294]Z. Borkowska and J. Stafiej, *J. Electroanal. Chem.* **170** (1984) 289.
[295]R. Payne, in *Advances in Electrochemistry and Electrochemical Engineering*, Vol. 7, P. Delahay and C. W. Tobias, eds., Wiley-Interscience, New York, 1970, p. 1.
[296]R. Parsons, *Electrochim. Acta* **21** (1976) 681.
[297]W. R. Fawcett, *Israel J. Chem.* **18** (1979) 3.
[298]B. B. Damaskin and R. V. Ivanova, *Usp. Khim.* **68** (1979) 1747.
[299]R. Parsons, *Trans. Soc. Adv. Electrochem. Sci. Technol.* **13** (1978) 239.
[300]S. K. Rangarajan, *Specialist Periodical Reports. Electrochemistry*, Vol. 7, Chemical Society, London, 1980, p. 203.
[301]W. R. Fawcett, B. M. Ikeda, and J. G. Sellan, *Can. J. Chem.* **57** (1979) 2268.
[302]Huu Cuong Nguyen, A. Jenard, and H. D. Hurwitz, *J. Electroanal. Chem.* **103** (1979) 399.
[303]Z. Borkowska, R. N. de Nobriga, and W. R. Fawcett, *J. Electroanal. Chem.* **124** (1981) 263.
[304]Z. Borkowska and J. Stafiej, *J. Electroanal. Chem.* **226** (1987) 283.
[305]D. C. Grahame, *J. Am. Chem. Soc.* **79** (1957) 2093.
[306]B. B. Damaskin and Yu. M. Povarov, *Dokl. Akad. Nauk SSSR* **140** (1961) 394.
[307]W. R. Fawcett and O. R. Loutfy, *J. Electroanal Chem.* **39** (1972) 185.
[308]R. Parsons, *J. Electroanal. Chem.* **59** (1975) 229.
[309]W. R. Fawcett, *J. Phys. Chem.* **82** (1978) 1385.
[310]Z. Borkowska and W. R. Fawcett, *Elektrokhimiya* **16** (1980) 1092.
[311]W. R. Fawcett and R. N. de Nobriga, *J. Phys. Chem.* **80** (1982) 371.
[312]R. Payne, *J. Phys. Chem.* **71** (1967) 1548.
[313]G. J. Hills and R. M. Reeves, *J. Electroanal. Chem.* **41** (1973) 213.
[314]W. R. Fawcett and Z. Borkowska, *J. Phys. Chem.* **87** (1983) 4861.
[315]J. A. Harrison, J. E. B. Randies, and D. J. Schiffrin, *J. Electroanal. Chem.* **48** (1973) 359.

[316]N. H. Cuong, C. V. D'Alkaine, A. Jennard, and D. H. Hurwitz, *J. Electroanal. Chem.* **51** (1974) 377.
[317] W. R. Fawcett, R. C. Rocha Filho, and L. Doubova, *J. Chem. Soc. Faraday Trans.* **87** (1991) 2967.
[318]W. R. Fawcett and R. C. Rocha Filho, *J. Chem. Soc. Faraday Trans.* **88** (1992) 1143.
[319]L. Blum and W. R. Fawcett, *J. Phys. Chem.* **96** (1992) 408.
[320]E. N. Protskaya, V M, Gerovich, B. B. Damaskin, V. Ya. Rosolovskii, and D. O. Lemesheva, *Elektrokhimiya* **16** (1980) 526.
[321] V. A. Chagelishvili, J. I. Japaridze, and B. B. Damaskin, *Elektrokhimiya* **13** (1977) 1300.
[322]J. I. Japaridze, V. A. Chagelishvili, and Zh. A. Khutzishvili, *Elektrokhimiya* **23** (1987) 1342.
[323]J. I. Japaridze, Zh. A. Khutzishvili, V. A. Chagelishvili, G. Borghesani, A. De. Battisti, C. Locatelli, and S. Trasatti, *J. Electroanal. Chem.* **257** (1988) 123.
[324]W. R. Fawcett and M. D. Mackey, *J. Chem. Soc. Faraday Trans.* **69** (1973) 634.
[325]E. Wilhelm and R. Battino, *J. Chem. Phys.* **55** (1971) 4012.
[326]R. Guidelli, *J. Chem. Phys.* **92** (1990) 6152.
[327]I. Nikitas, *Can. J. Chem.* **64** (1986) 1286.
[328]I. Zagórska, Z. Koczorowski, and S. Trasatti, *J. Electroanal. Chem.* **366** (1994) 211.
[329]C. M. Criss and M. Salomon, in *Physical Chemistry of Organic Solvent Systems,* A. K. Covington, and T. Dickinson, eds., Plenum Press, New York 1973, p. 286.
[330]M. Jurkiewicz-Herbich, *J. Electroanal. Chem.* **119** (1981) 275.
[331]T. Blaszczyk, B. Jakuszewski, and J. M. Czajkowski, *Electrochim. Acta* **28** (1983) 675.
[332]R. Meynczyk, Z. Figaszewski, and Z. Koczorowski, *Pol. J. Chem.* **57** (1983) 1011.
[333]A. Frumkin, I. Bagotskaya, and N. Grigoryev, *Z. Phys. Chem. N.F.* **98** (1975) 3.
[334]M. D. Levi, A. V. Slepakov, B. B. Damaskin, and I. A. Bagotskaya, *J. Electroanal. Chem.* **138** (1982) 1.
[335]I. A. Bagotskaya, V. V. Yemets, V. G. Boitsov, and V. E. Kazarinov, *Elektrokhimiya* **27** (1991) 291.
[336]G. Pezzatini, M. R. Moncelli, M. L. Foresti, F. Pergola, and R. Guidelli, *J. Electroanal. Chem.* **196** (1985) 429.
[337]G. Pezzatini, M. L. Foresti, M. Innocenti, and R. Guidelli, *J. Electroanal. Chem.* **295** (1990) 265.
[338] M. Innocenti, G. Pezzatini, M. L. Foresti, and R. Guidelli, *J. Electroanal. Chem.* **349** (1993) 113.
[339]J. N. Butler and M. L. Meehan, *J. Phys. Chem.* **70** (1966) 3582.
[340]T. S. Horanyi and M. Takas, *J. Electroanal. Chem.* **215** (1986) 83.
[341] L. Doubova, A. De Battisti, and S. Trasatti, *Electrochim. Acta* **31** (1986) 881.
[342]I. A. Bagotskaya and A. V Shlepakov, *Elektrokhimiya* **18** (1982) 462.
[343]I. A. Bagotskaya and V. E. Kazarinov, *J. Electroanal. Chem.* **329** (1992) 225.
[344]N. B. Grigoryev, S. A. Fateev, and I. A. Bagotskaya, *Elektrokhimiya* **8** (1972) 1525.
[345] N. B. Grigoryev, I. A. Gedvillo, and N. G. Bardina, *Elektrokhimiya* **8** (1972) 409.
[346]N. B. Grigoryev and V. A. Bulavka, *Elektrokhimiya* **12** (1976) 1103.
[347]N. B. Grigoryev, V. A. Bulavka, and Yu. M. Loshkaryev, *Elektrokhimiya* **11** (1975) 1404.
[348]S. Amokrane, J. *Electroanal. Chem.* **361** (1993) 1.
[349]I. A. Bagotskaya, B. B. Damaskin, and V. E. Kazarinov, *Elektrokhimiya* **30** (1994) 293.
[350]V. V. Emets, B. B. Damaskin, and V. E. Kazarinov, *Elektrokhimiya* **31** (1995) 117.
[351]V. V. Emets, B. B. Damaskin, and V. E. Kazarinov, *Elektrokhimiya* **31** (1995) 787.
[352]V. V. Emets, B. B. Damaskin, and V. E. Kazarinov, *Elektrokhimiya* **32** (1996) 1146.
[353]B. B. Damaskin and V. A. Safonov, *Electrochim. Acta* **42** (1997) 737.
[354] I. A. Bagotskaya, S. A. Fateyev, N. B. Grigoryev, and A. N. Frumkin, *Elektrokhimiya* **9** (1973) 1676.
[355]I. A. Bagotskaya and A. M. Kalyuzhnaya, *Elektrokhimiya* **12** (1976) 1043.

[356]I. A. Bagotskaya and L. M. Dubova, *Elektrokhimiya* **14** (1978) 1373.
[357]I. A. Bagotskaya and L. M. Dubova, *Elektrokhimiya* **14** (1978) 1264.
[358]I. A. Bagotskaya V. V. Emets, V. G. Boitsov, and V. E. Kazarinov, *Elektrokhimiya* **24** (1988) 1145.
[359]V. V. Emets, V. E. Kazarinov, and I. A. Bagotskaya, *Elektrokhimiya* **32** (1996) 1157.
[360]V. V. Emets, *Elektrokhimiya* **33** (1997) 1183.
[361]V. V. Emets, *Elektrokhimiya* **33** (1997) 1189.
[362]V. V. Emets, B. B. Damaskin, and V. E. Kazarinov, *Elektrokhimiya* **33** (1997) 1104.
[363]D. I. Leilas, *Dokl. Akad Nauk SSSR* **135** (1960) 1429.
[364]G. Valette, *Compt. Rend., Ser. C* **275** (1972) 167.
[365]G. Valette, *Compt. Rend., Ser. C* **274** (1972) 2046.
[366]A. G. Zelinsky and R. Yu. Beck, *Elektrokhimiya* **14** (1978) 1825.
[367]E. S. Sevastyanov, M. N. Ter-Akopyan, and V. K. Chubarova, *Elektrokhimiya* **16** (1980) 432.
[368]L. M. Doubova, S. Trasatti, and S. Valcher, 7. *Electroanal. Chem.* **349** (1993) 187.
[369]Q. X. Zha, *Introduction of Electrode Process Kinetics,* 2nd ed., Science Press, Beijing, 1987.
[370]J. O'M. Bockris, S. D. Argade, and E. Gileadi, *Electrochim. Acta* **14** (1969) 1259.
[371]R. L. Sobocinski and J. E. Pemberton, *Langmuir* **6** (1990) 43.
[372]R. L. Sobocinski and J. E. Pemberton, *Langmuir* **8** (1992) 2049.
[373]S. L. Joa and J. E. Pemberton, *Langmuir* **8** (1992) 2301.
[374]J. E. Pemberton, S. L. Joa, A. Shen, and K. J. Woelfel, *J. Chem. Soc. Faraday Trans.* **92** (1996) 3683.
[375]R. Truu, P. Kippasto, and E. Lust, *Proc. Baltic Conf. on Interfacial Electrochemistry*, 1996, p. 232.
[376]E. Sevastyanov and T. Vitanov, *Elektrokhimiya* **3** (1967) 402.
[377]E. S. Sevastyanov, T. Vitanov, and A. Popov, *Elektrokhimiya* **8** (1972) 412.
[378]T. Vitanov, A. Popov, and E. Budevski, *J. Electrochem. Soc.* **121** (1974) 207.
[379]T. Vitanov, A. Popov, and E. S. Sevastyanov, *Elektrokhimiya* **12** (1976) 582.
[380]T. Vitanov and A. Popov, *Dokl. Akad. Nauk SSSR* **226** (1976) 373.
[381]T. Vitanov and A. Popov, *J. Electroanal. Chem.* **159** (1983) 437.
[382]A. Popov, O. Velev, T. Vitanov, and D. Tonchev, *J. Electroanal Chem.* **257** (1988) 95.
[383]A. Hamelin, *Elektrokhimiya* **18** (1982) 1413.
[384]A. Hamelin and G. Valette, *Compt. Rend., Ser. C* **269** (1969) 1020.
[385]G. Valette and A. Hamelin, *Compt. Rend., Ser. C* **272** (1971) 602.
[386]G. Valette and A. Hamelin. *Compt. Rend., Ser. C* **279** (1974) 295.
[387]G. Valette, *J. Electroanal. Chem.* **122** (1981) 285.
[388]G. Valette, *J. Electroanal. Chem.* **138** (1982) 37.
[389]G. Valette, *J. Electroanal. Chem.* **178** (1984) 179.
[390]G. Valette, *J. Electroanal. Chem.* **244** (1987) 285.
[391]A. Hamelin, in *Trends in Interfacial Electrochemistry*, A. F. Silva, ed., Reidel, Dordrecht, The Netherlands, 1986, p. 83.
[392]A. Hamelin, L. Doubova, D. Wagner, and H. Schirmer, *J. Electroanal. Chem.* **220** (1987) 155.
[393]M. Bacchetta, A. Francesconi, L. Doubova, A. Hamelin, and S. Trasatti *J. Electroanal. Chem.* **218** (1987) 355.
[394]A. Popov, *Electrochim. Acta* **40** (1995) 551.
[395]G. Valette, *J. Electroanal. Chem.* **132** (1982) 311.
[396]A. Hamelin, L. Stoicoviciu, L. Doubova, and S. Trasatti, *Surf. Sci.* **201** (1988) L 498.
[397]A. Hamelin, L. Doubova, L. Stoicoviciu, and S. Trasatti, *J. Electroanal. Chem.* **244** (1988) 133.

[398]L. Doubova, A. Hamelin, L. Stoicoviciu, and S. Trasatti, *J. Electroanal. Chem.* **325** (1992) 197.
[399]G. Valette, *J. Electroanal. Chem.* **230** (1987) 189.
[400]M. Lopez, J. R. Vilche, and A. I. Arvia, *J. Electwanal. Chem.* 162 (1984) 207.
[401]G. Valette, A. Hamelin, and R. Parsons, *Z. Phys. Chem.* **113** (1978) 71.
[402]R. Waser and K. G. Weil, *J. Electroanal. Chem.* **150** (1983) 89.
[403]B. Wichman, J. P. van der Eerden, H. Meekes, and J. Gerritsen, *Electrochim. Acta* **32** (1992) 2331.
[404]J.-S. Chen, T. M. Devine, D. F. Ogletree, and M. Salmeron, *Surf. Sci.* **258** (1991) 346.
[405]S. Trasatti, *J. Chem. Soc. Faraday Trans.* **170** (1974) 1752.
[406]S. Trasatti, *Electrochim. Acta* **28** (1983) 1083.
[407]S. Trasatti, *Mater. Chem. Phys.* **12** (1985) 507.
[408]S. Trasatti, *Croat. Chem. Acta* **60** (1987) 357.
[409]S. Trasatti, *J. Electroanal. Chem.* **172** (1984) 27.
[410]S. Trasatti, *J. Electroanal. Chem.* **329** (1992) 237.
[411]S. Trasatti, *Elektrokhimiya* **31** (1995) 777.
[412]R. Adzic, in *Modern Aspects of Electrochemistry*, No. 21, R. E. White, J. O'M. Bockris, and B. E. Conway, eds., Plenum Press, New York, 1990, p. 163.
[413]P. N. Ross, in *Structure of Electrified Interfaces*, J. Lipkowski, and P. N. Ross, eds., VCH, New York, 1992, p. 35.
[414]S. Amokrane and J. P. Badiali, *J. Electroanal. Chem.* **266** (1989) 21.
[415]S. Amokrane, V. Russier, and J. P. Badiali, *Surf. Sci.* **210** (1989) 251.
[416]R. Christoph, H. Siegenthaler, H. Rohrer, and H. Wiese, *Electrochim. Acta* **34** (1989) 259.
[417]M. Hottenhues, M. Mickers, J. Gerritzen, and J. P. van der Eerden, *Surf. Sci.* **206** (1989) 259.
[418]J. P. van der Eerden, M. Mickers, J. Gerritzen, and M. Hottenhues, *Electrochim. Acta* **34** (1989) 1141.
[419]V. Bostanov and W. Obretenov, *Electrochim. Acta* **34** (1989) 1193.
[420]M. Höptner, W. Obretenov, K. Jüttner, W. J. Lorenz, G. Staikov, V. Bostanov, and E. Budevski, *Surf. Sci.* **248** (1991) 225.
[421]W. Obretenov, M. Höptner, W. J. Lorenz, E. Budevski, G. Staikov, and H. Siegenthaler, *Surf. Sci.* **271** (1992) 191.
[422]R. R. Adzic, M. E. Hanson, and E. B. Yeager, *J. Electrochem. Soc.* **131** (1984) 1730.
[423]E. B. Budevski, in *Comprehensive Treatise of Electrochemistry*, Vol. 7, B. E. Conway, J. O'M. Bockris, E. Yeager, S. U. M. Khan, and R. E. White, eds., Plenum Press, New York, 1983, p. 339.
[424]V. Bostanov, A. Kotzeva, and E. Budevski, *Bull. Inst. Chem. Phys*., *Bulg. Acad. Sci.* **6** (1967) 33,
[425]E. Budevski, V. Bostanov, T. Vitanov, Z. Stoynov, A. Kotzeva, and R. Kaischev, *Electrochim. Acta* **11** (1966) 1697.
[426]R. De Levie, *J. Electroanal. Chem.* **280** (1990) 179.
[427]E. Budevski, V. Bostanov, and G. Staikov, *Ann. Rev. Mater. Sci.* **10** (1980) 85.
[428]E. Leiva and W. Schmickler, *J. Electroanal. Chem.* **205** (1986) 323.
[429]E. Leiva and W. Schmickler, *J. Electroanal. Chem.* **229** (1987) 39.
[430]J. P. Badiali, M. L. Rosinberg, and J. Goodisman, *J. Electroanal. Chem.* **130** (1981) 31.
[431]J. P. Badiali, M. L. Rosinberg, and J. Goodisman, *J. Electroanal. Chem.* **143** (1983) 73.
[432]W. Schmickler, *J. Electroanal. Chem.* **150** (1983) 19.
[433]A. A. Komyshev, M. B. Partensk, and W. Schmickler, Z. *Naturforsch* **39a** (1984) 1122.
[434]W. Schmickler and D. Henderson, *J. Chem. Phys.* **80** (1984) 3381.
[435]D. Henderson and W. Schmickler, *J. Chem. Phys.* **82** (1985) 2825.
[436]An. Kuznetsov and J. Reinhold, Z. *Phys. Chem.* **267** (1986) 824.

[437]An. M. Kuznetsov, R. R. Nazmutdinov, and M. S. Shapnik, *Electrochim. Acta* **34** (1989) 1821.
[438]A. Ignaczak and J. A. N. F. Gomes, *J. Electroanal. Chem.* **420** (1997) 209.
[439]R. R. Nazmutdinov and M. S. Shapnik, *Electrochim. Acta* **41** (1996) 2253.
[440]M. L. Foresti, M. Innocenti, and R. Guidelli, *J. Electroanal. Chem.* **376** (1994) 85.
[441]L. M. Doubova, S. Valcher, and S. Trasatti, *J. Electroanal Chem.* **376** (1994) 73.
[442]T. Vitanov and A. Popov, *Elektrokhimiya* **12** (1976) 319.
[443]A. Popov, O. Velev, and T. Vitanov, *J. Electroanal. Chem.* **256** (1988) 405.
[444]T. Vitanov, A. Popov, M. Ter-Akopyan, and E. Sevastyanov, *J. Electroanal. Chem.* **171** (1984)331.
[445]M. Klaua and T. E. Madey, *Surf. Sci.* **136** (1984) L 42.
[446]F. Silva, M. J. Sottomayor, and A. Hamelin, *J. Electroanal. Chem.* **294** (1990) 239.
[447]F. Silva, M. J. Sottomayor, and A. Martins, *J. Electroanal. Chem.* **360** (1993) 199.
[448]F. Silva, M. J. Sottomayor, and A. Martins, *J. Chem. Soc. Faraday Trans.* **92** (1996) 3693.
[449]D. M. Kolb and C. Franke, *Appl. Phys. A* **49** (1989) 373.
[450]C. Franke, G. Piazza, and D. M. Kolb, *Electrochim. Acta* **34** (1984) 67.
[451]G. C. Aers and H. E. Inglesfield. *Surf. Sci.* **217** (1989) 367.
[452]R. Kötz, D. M. Kolb, and J. K. Sass, *Surf. Sci.* **69** (1977) 359.
[453]G. L. Richmond, H. M. Rojhantalab, J. M. Robinson, and V. L. Channon, *J. Opt. Soc. Am.* **4** (1987) 228.
[454]F. Chao, M. Costa, J. Lecoeur, and J. P. Bellick, *Electrochim. Acta* **34** (1989) 1627.
[455]F. Chao, M. Costa, and J. Lecoeur, *Electrochim. Acta* **36** (1991) 1839.
[456]F. Chao, M. Costa, and A. Tadjeddine, *J. Electroanal. Chem.* **329** (1992) 313.
[457]M. Petit, C. Nguyen Van Huong, and J. Clavilier, *Compt. Rend., Ser. C* **266** (1968) 300.
[458]J. Clavilier and C. Nguyen Van Huong, *Compt. Rend., Ser. C* **267** (1968) 207.
[459]J. Clavilier and C. Nguyen Van Huong, *Compt. Rend., Ser. C* **270** (1970) 982.
[460]J. Clavilier and C. Nguyen Van Huong, *Compt. Rend., Ser. C* **273** (1971) 902.
[461]C. Nguyen Van Huong and J. Clavilier, *Compt. Rend., Ser. C* **273** (1971) 1404.
[462]J. Clavilier and C. Nguyen Van Huong, *J. Electroanal. Chem.* **41** (1973) 193.
[463]C. Nguyen Van Huong, J. Clavilier, and M. Bonnemay, *J. Electroanal. Chem.* **65** (1975) 531.
[464]C. Nguyen Van Huong, C. Hinnen, J. P. Dalbera, and R. Parsons, *J. Electroanal. Chem.* **125** (1981) 177.
[465]A. Hamelin, *J. Electroanal. Chem.* **165** (1984) 167.
[466]A. Hamelin, A. Katayama, G. Picq, and P. Vennereau, *J. Electroanal. Chem.* **113** (1980) 293.
[467]A. Hamelin, in *Nanoscale Probes of the Solid/Liquid Interface,* A. G. Gewirth and H. Siegenthaler, eds., Kluwer, Dordrecht, 1995, p. 285.
[468]R. Yu. Beck, N. V. Makurin, and A. G. Zelinsky, *Elektrokhimiya* **11** (1975) 1607.
[469]A. G. Zelinsky and R. Yu. Beck, *Elektrokhimiya* **16** (1980) 39.
[470]S. D. Abdulov, A. G. Zelinsky, and R. Yu. Beck, *Elektrokhimiya* **16** (1980) 655.
[471] A. G. Zelinsky and B. P. Tolochko, in *Double Layer and Adsorption at Solid Electrodes, Proc. 6th Symp.,* Tartu University Press, Tartu, Estonia, 1981, p. 139.
[472]S. Romanovski and G. Sholl, *Elektrokhimiya* **16** (1980) 1184.
[473]G. Jarzabek and Z. Borkowska, *J. Electroanal. Chem.* **226** (1987) 295.
[474]G. Jarzabek and Z. Borkowska, in *Electrocatalysis,* P. Novac, A. Pomianowski, and J. Sobkowski, eds., P. A. N., Krakow, 1987.
[475]E. V. Petyarv and U. V. Palm, *Elektrokhimiya* **12** (1976) 814.
[476]A. Yu. Alekseyeva, V. A. Safonov, and O. A. Petrii, *Elektrokhimiya* **20** (1984) 945.
[477]Z. Borkowska and A. Hamelin, *J. Electroanal. Chem.* **241** (1988) 373.
[478]D. Dickertman, F. D. Koppitz, and J. W. Schultze, *Electrochim. Acta* **21** (1986) 967.
[479]I. A. Bagotskaya, *Elektrokhimiya* **16** (1980) 216.

[480]E. Petyarv and U. Palm, in *Double Layer and Adsorption at Solid Electrodes, Proc. 4th Symp.,* Tartu University Press, Tartu, Estonia, 1975, p. 242.
[481]C. Nguyen Van Huong, *J. Electroanal. Chem.* **194** (1985) 131.
[482]M. Brzostowska-Smolska and S. Minc, *Pol. J. Chem.* **106** (1983) 1005.
[483]H. D. Hurwitz, *J. Electroanal. Chem.* **10** (1965) 35.
[484]E. Dutkiewic and R. Parsons, *J. Electroanal. Chem.* **11** (1966) 100.
[485]X. Gao, G. J. Edens, A. Hamelin, and M. J. Weaver, *Surf. Sci.* **318** (1994) 1.
[486]A. Hamelin, *J. Electroanal. Chem.* **142** (1982) 299.
[487]D. M. Kolb and J. Schneider, *Surf. Sci.* **162** (1985) 764.
[488]D. M. Kolb and J. Schneider, *Electrochim. Acta* **31** (1986) 929.
[489]A. Hamelin, *Electrochim. Acta* **31** (1986) 937.
[490]A. Hamelin, *J. Electroanal Chem.* **210** (1986) 303.
[491]A. Hamelin, L. S. Stoicoviciu, and F. Silva, *J. Electroanal. Chem.* **229** (1987) 107.
[492]A. Hamelin and S. Rottgermann, *Electrochim. Acta* **32** (1987) 723.
[493]H. Angerstein-Kozlowska, B. E. Conway, A. Hamelin, and L. Stoicoviciu, *Electrochim. Acta* **31** (1986) 1051.
[494]A. Hamelin S. Rottgermann, and W. Schmickler, *J. Electroanal. Chem.* **230** (1987) 281.
[495]A. Hamelin and L. Stoicoviciu, *J. Electroanal. Chem.* **234** (1987) 93.
[496]E. Dutkiewicz, P. Skoluda, and A. Hamelin, *J. Electroanal. Chem.* **248** (1988) 209.
[497]E. Dutkiewicz, P. Skoluda, and A. Hamelin, *J. Electroanal. Chem.* **240** (1988) 291.
[498]A. Hamelin, *J. Electroanal. Chem.* **255** (1988) 281.
[499]F. Silva, C. Moura, and A. Hamelin, *Electrochim. Acta* **34** (1989) 1665.
[500]A. Hamelin, S. Morin, J. Richer, and J. Lipkowski. *J. Electroanal Chem.* **272** (1984) 241.
[501]X. Gao, G. J. Edens, and M. J. Weaver, *J. Electroanal. Chem.* **376** (1994) 21.
[502]A. Hamelin and J. Lecoeur, *Surf. Sci.* **57** (1976) 771.
[503]F. Silva, M. J. Sottomayor, A. Hamelin, and L. Stoicoviciu, *J. Electroanal. Chem.* **295** (1990)301.
[504]X. Gao, A. Hamelin, and M. J. Weaver, *Phys. Rev. B* **44** (1991) 10983.
[505]X. Gao, A. Hamelin, and M. J. Weaver, *Phys. Rev. Lett.* **67** (1991) 618.
[506]X. Gao, A. Hamelin, and M. J. Weaver, *J. Chem. Phys.* **95** (1991) 6993.
[507]X. Gao, S.C. Chang, X. Jiang, A. Hamelin, and M. J. Weaver, *J. Vac. Sci. Techn. A* **10** (1992) 2997.
[508]A. Hamelin, *J. Electroanal. Chem.* **329** (1992) 247.
[509]B. M. Ocko, G. Helgesen, B. Schardt, J. Wang, and A. Hamelin, *Phys. Rev. Lett.* **69** (1992) 3350.
[510]X. Gao, A. Hamelin, and M. J. Weaver, *Phys. Rev. B* **46,** (1992) 7096.
[511]X. Gao, A. Hamelin, and M. J. Weaver, *Surf. Sci. Lett.* **274** (1992) L 588.
[512]S. Strbac, A. Hamelin, and R. R. Adzic, *J. Electroanal. Chem.* **362** (1993) 47.
[513]X. Gao, G. J. Edens, A. Hamelin, and M. J. Weaver, *Surf. Sci.* **296** (1993) 333.
[514]A. Hamelin, L. Stoicoviciu, G. J. Edens, X. Gao, and M. J. Weaver, *J. Electroanal. Chem.* **365** (1994) 47.
[515]W. R. Fawcett, M. Fedurco, and Z. Kovácová, *J. Electrochem. Soc.* **141** (1994) L 30.
[316]A. Hamelin, *J. Electroanal. Chem.* **386** (1995) 1.
[517]A. Hamelin, *J. Electroanal. Chem.* **407** (1996) 1.
[518]A. Hamelin and A. M. Martins, *J. Electroanal. Chem.* **407** (1996) 13.
[519]J. Wang, B. M. Ocko, A. J. Davenport, and H. S. Isaacs, *Phys. Rev. B* **46** (1992) 10321.
[520]B. M. Ocko, D. M. Magnussen, R. R. Adzic, J. X. Wang, Z. Shi, and J. Lipkowski, *J. Electroanal. Chem.* **376**(1994) 35.
[521]B. Pettinger, J. Lipkowski, and S. Mirwald, *Electrochim. Acta* **40** (1995).
[522]I. M. Tidswell, N. M. Markovic, C. A. Lucas, and P. N. Ross, *Phys. Rev. B* **47** (1993) 16542.
[523]K. M. Robinson and W. E O'Grady, *Rev. Sci. Inst.* **64** (1993) 1061.

[524]J. Wang, G. M. Watson, and B. M. Ocko, *Physica A* **200** (1993) 751.
[525]J. J. Calvente, Z. Kováèová. R. Andreu, and W. R. Fawcett, *J. Electroanal. Chem.* **401** (1996)231.
[526]M. A. van Hove, R. J. Koestner, P. C. Stair, J. P. Siberian, L. L. Kesmodel, I. Bartos, and C. A. Somorjai, *Surf. Sci.* **103** (1981) 189.
[527]G. A. Somorjai and M. A. van Hove, *Prog. Surf. Sci.* **30** (1989) 201.
[528]K. Takayanagi, *Ultramicroscopy* **8** (1982) 145.
[529]A. T. Hubbard, *Chem. Rev.* **88** (1988) 633.
[530]G. Binning , H. Rohrer, C. Gerber, and E Weibel, *Surf. Sci.* **131** (1983) L 379.
[531]G. A. Somorjai, *Chemistry in Two Dimensions: Surfaces,* Cornell Univ. Press, Ithaca, NY, 1991.
[532]V. Heine and L. D. Marks, *J. Electron Spectrosc.* **38** (1986) 229.
[533]C. L. Fuanel and K. M. Ho, *Phys. Rev. Lett.* **63** (1989) 1617.
[534]D. M. Kolb, *Prog. Surf. Sci.* **51** (1996) 109.
[535]B. M. Ocko and J. Wang, in *Synchroton Techniques in Interfacial Electrochemistry,* C. A. Melendcres, and A. Tadjeddine, eds., Kluwer, Dordrecht, The Netherlands, 1994, p. 127.
[536]B. M. Ocko, G. M. Watson, and J. Wang, *J. Phys. Chem.* **98** (1994) 897.
[537]B. M. Ocko, O. M. Magnussen, J. X. Wang, and R. R. Adzic, in *Nanoscale Probes of the Solid/Liquid Interface,* A. A. Gewirth and H. Siegenthaler, eds., Kluwer, Dordrecht, The Netherlands, 1995, p. 103.
[538]D. M. Kolb, A. S. Dakkouri, and N. Batina, in *Nanoscale Probes of the Solid/Liquid Interface,* A. A. Gewirth, and H. Siegenthaler, eds., Kluwer, Dordrecht, 1995, p. 263.
[539]X. Gao, G. J. Edens, Fon-Chen Liu, A. Hamelin, and M. J. Weaver, *J. Phys. Chem.* **98** (1994) 8086.
[540]A. Friedrich, B. Pettinger, D. M. Kolb, G. Lüpke, R. Steinhoff, and G. Marowsky, *Chem. Phys. Lett.* **163** (1989) 123.
[541]N. Batina, A. S. Dakkouri, and D. M. Kolb. *J. Electroanal. Chem.* **370** (1994) 967.
[542]O. M. Magnussen, J. Hotlos, R. J. Behm, N. Batina, and D. M. Kolb, *Surf. Sci.* **296** (1993) 310.
[543]D. M. Kolb, G. Lehmpfuhl, and M. S. Zei, *J. Electroanal. Chem.* **179** (1984) 289.
[544]J. Scheneider and D. M. Kolb, *Surf. Sci.* **193** (1988) 579.
[545]R. R. Adzic, A. V. Tripkovic, and N. M. Markovic. *J. Electroanal. Chem.* **150** (1983) 79.
[546]A. Hamelin, M. J. Sottomayor, F. Silva, Si Shung Cang, and M. J. Weaver, *J. Electroanal. Chem.* **295** (1990) 291.
[547]R. C. Newman and G. T. Burstein, *J. Electroanal. Chem.* **129** (1981) 343.
[548]H. Angerstein-Kozlowska, B. E. Conway, B. Barnett, and J. Mozota, *J. Electroanal. Chem.* **100** (1979) 185.
[549]C. Nguyen Van Huong , C.Hinnen, and J. Lecoeur, *J. Electroanal. Chem.* **106** (1980) 185.
[550]J. Desilvestro and M. J. Weaver, *J. Electroanal. Chem.* **209** (1986) 377.
[551]H. Angerstein-Kozlowska, B. E. Conway, A. Hamelin, and L. S. Stoicoviciu, *J. Elec-troanal. Chem.* **228** (1987) 429.
[552]Z. Borkowska and U. Stimming , *J. Electroanal. Chem.* **312** (1991) 237.
[553]A. Hamelin and P. Dechy, *Compt. Rend., Ser. C* **276** (1973) 33.
[554]A. Hamelin and J. P. Bellier, *Compt. Rend., Ser. C* **279** (1974) 371.
[555]A. Hamelin, S. Morin, J. Richer, and J. Lipkowski, *J. Electroanal. Chem.* **285** (1991) 249 Appendix.
[556]H. Ibach, *J. Vac. Sci. Technol. A* **12** (1994) 267.
[557]W. Haiss and J. K. Sass, *J. Electroanal. Chem.* **386** (1995) 267.
[558]A. Hamelin, L. Stoicoviciu, and F. Silva, *J. Electroanal. Chem.* **236** (1987) 283.
[559]J. Lecoeur, J. Andro, and R. Parsons, *Surf. Sci.* **114** (1982) 320.
[560]R. Smoluchowski, *Phys. Rev.* **60** (1941) 661.
[561]J. Lecoeur, J. P. Bellier, and C. Koelher, *J. Electroanal. Chem.* **337** (1992) 197.

[562]J. Lecoeur, J. P. Bellier, and C. Koehler, *J. Electroanal. Chem.* **375** (1994) 117.
[563]A. A. Kornyshev and I. Vilfan, *Electrochim. Acta* **40** (1995) 109.
[564]L. Ya. Egorov and I. M. Novosel'ski, *Elektrokhimiya* **6** (1970) 521; **6** (1970) 869.
[565]L. Ya. Egorov and I. M. Novosel'ski, *Elektrokhimiya* **7** (1971) 988.
[566]D. Armstrong, N. A. Hampson, and R. J. Latham, *J. Electroanal. Chem.* **23** (1969) 361.
[567]V. V. Batrakov, Yu. Dittrich, and A. Popov, *Elektrokhimiya* **8** (1972) 640.
[568]I.M. Novosel'ski, N. I. Konevskih, and L. Ya. Egorov, *Elektrokhimiya* **8** (1972) 1480.
[569]I. M. Novosel'ski, N. I. Konevskih, and L. Ya. Egorov, in *Double Layer and Adsorption at Solid Electrodes, Proc. 3rd Symp.,* Tartu University Press, Tartu, Estonia, 1972, p. 195.
[570]G. J. Clark, T. N. Andersen, R. S. Valentine, and A. Eyring, *J. Electrochem. Soc.* **121** (1974)618.
[571]M. A. Evseeva, G. A. Kitaev, and O. S. Lebedeva, in *Double Layer and Adsorption at Solid Electrodes, Proc. 6th Symp..*, Tartu University Press, Tartu, Estonia, 1981, p. 131.
[572]I. M. Novosel'ski, N. I. Maksimyuk, and L. Ya. Egorov, *Elektrokhimiya* **9** (1973) 1518.
[573]N. I. Maksimyuk and L. Ya. Egorov, in *Double Layer and Adsorption at Solid Electrodes, Proc. 6th Symp.,* Tartu University Press, Tartu, Estonia, 1975, p. 177.
[574]V. V. Batrakov and H. Hennig , *Elektrokhimiya* **13** (1977) 259.
[575]N. I. Maksimyuk, in *Double Layer and Adsorption at Solid Electrodes, Proc. 5th Symp.,* Tartu University Press, Tartu, Estonia, 1978, p. 148.
[576]H. Hennig and V. V. Batrakov, *Elektrokhimiya* **15** (1979) 1833.
[577]N. I. Maksimyuk and I. M. Novosel'ski, in *Double Layer and Adsorption at Solid Electrodes, Proc. 6th Symp.,* Tartu University Press, Tartu, Estonia, 1981, p. 233.
[578]J. Lecoeur and J. P. Bellier, *Electrochim. Acta* **30** (1985) 1027.
[579]G. V. Korshin, Ph. D. Thesis, Kazan Stale Technological University, Kazan, SSSR 1983.
[580]E. Lazarova and Ts. Nikolov, *Elektrokhimiya* **22** (1986) 121.
[581]L. M. Rice-Jackson, G. Horanyi, and A. Wieckowski, *Electmchim. Acta* **36** (1991) 753.
[582]G. M. Brown and A. Hope, *J. Electroanal. Chem.* **382** (1995) 179.
[583]M. Turowska and J. Sokolowski, *Elektrokhimiya* **28** (1992) 298.
[584]R. O. Loutfy, *Electrochim. Acta* **18** (1973) 227.
[585]V. I. Naumov, T. V. Sazontéva, and Yu. M. Tyurin, *Electrokhimiya* **24** (1988) 1455.
[586]D. N. Staikopolus, *J. Electrochem. Soc.* **108** (1961) 900.
[587]M. L. Foresti, G. Pezzatini, and M. Innocent, *J. Electroanal. Chem.* **434** (1997) 191.
[588]B. B Damaskin and V V. Batrakov, *Elektrokhimiya* **10** (1974) 140.
[588a]E. J. Lust, unpublished results.
[589]S. Romanowski, *Elektrokhimiya* **24** (1988) 1612; **25** (1989) 945.
[590]H. Niehus, *Surf. Sci.* **130**(1983)41.
[591]E. K. L. Wong, K. A. Friedrich, J. M. Robinson, R. A. Bradley, and G. L. Richmond, *J. Vac. Sci. Technol. A* **10** (1992) 2985.
[592]B. J. Cruickshank, D. D. Sneddon, and A. A. Gewirth, *Surf. Sci. Lett.* **281** (1993) L 308.
[593]J. R. LaGraff and A. A. Gewirth, in *Nanoscale Probes of the Solid/Liquid Interface,* A. A. Gewirth and H. Siegenthaler, eds., KJuwer Academic, Dordrecht, The Netherlands 1995, p. 83.
[594]I. Villegas, C. B. Enters, and J. L. Stickney, *J. Electrochem. Soc.* **137** (1990) 3143.
[595] M. Pourbaix, *Atlas of Electrochemical Equilibria in Aqueous Solutions,* Pergamon, Oxford, 1966, p. 384.
[596]F. Besenbachek and J. K. Norskov, *Prog. Surf. Sci.* **44** (1993) 5.
[597]S. Hartinger and K. Doblhofer, *J. Electroanal. Chem.* **380** (1995) 185.
[598]G. Horanyi, *J. Electroanal. Chem.* **55** (1974) 287.
[599]K. V. Rybalka and D. I. Leikis, *Elektrokhimiya* **3** (1967) 383.
[600]K. V. Rybalka, *Elektrokhimiya* **7** (1971) 242.
[601]N. B. Grigoryev and D. N. Machavaariani, *Elektrokhimiya* **6** (1970) 89.

[602]J. P. Carr, N. A. Hampson, S. N. Holley, and R. Taylor, *J. Eltctroanal. Chem.* **32** (1971) 345.
[603]L. P. Khmelevaya, A.V. Chizhov, B. B. Damaskin, and T. I. Vainbiat, *Elektrokhimiya* **16** (1980)257.
[604]L. P. Khmelevaya, B. B. Damaskin, and A. I. Sidnin, *Elektrokhimiya* **17** (1981) 436.
[605]T. H. Pütsepp, V. E. Past and U. V. Palm, in *Double Layer and Adsorption at Solid Electrodes, Proc. 6th Symp*., Tartu University Press, Tutu, Estonia 1981, p. 297.
[606]V.Ya Ya. Mishuk, E.A. Solomatin, and V. V. Elkin, *Elektrokhimiya* **14** (1978) 1135.
[607]E. S. Sevastyanov, V. K. Chubarova, N. A. Morozova, and E. V. Pekar, *Elektrokhimiya* **28** (1992) 720.
[608]Z. N. Ushakova and V. F. Ivanov, in *Double Layer and Adsorption at Solid Electrodes, Proc. 6th Symp*., Tartu University Press, Tartu, Estonia, 1975, p. 321.
[609]Z. N. Ushakova and V. F. Ivanov, *Elektrokhimiya* **12** (1976) 485.
[610]V. A. Panin, K.V. Rybalka, and D. I. Leikis, *Elektrokhimiya* **8** (1972) 1507.
[611]K. V. Rybalka and V. A. Panin, in *Double Layer and Adsorption at Solid Electrodes, Proc. 3rd Symp.,* Tartu University Press, Tartu, Estonia, 1972, p. 217.
[612]Z. N. Ushakova and V. F. Ivanov, *Elektrokhimiya* **12** (1972) 1880.
[613]N. A. Hampson and D. Larkin, *J. Electrochem. Soc.* **115** (1968) 612.
[614]F. I. Danilov, V. V. Orlenko, and R. D. Sukhomlin, *Elektrokhimiya* **5** (1969) 634.
[615]V. Ya. Bartenev, E. S. Sevastyanov, and D. I. Leikis, *Elektrokhimiya* **6** (1970) 1868.
[616]T. Erlikh, Yu. Kukk, and V. Past, *Trans. Tartu Univ.* **289** (1971) 9.
[617]N. B. Grigoryev, V. P. Kuprin, and Yu. M. Loshkarev, *Elektrokhimiya* **9** (1973) 1842.
[618]V. P. Kuprin, N. B. Grigoryev, Yu. M. Loshkarev, and R.V. Malaya, *Eleklrokhimiya* **11** (1975) 638.
[619]V. P. Kuprin and N. B. Grigoryev, *Elektrokhimiya* **16** (1980) 383.
[620]V. Ya. Bartenev, Phd. Thesis, Moscow State University, Moscow, 1969, p. 17.
[621]L. P. Khmelevaya and B. B. Damaskin, *Elektrokhimiya* **17** (1981) 1721; L. P. Khmelevaya, Thesis, Moscow State University, Moscow, 1982, p. 4.
[622]V. L. Heyfets and B. S. Krassikov, *Dokl. Akad. Nauk SSSR,* **109** (1956) 586.
[623]P. Caswell, N.A. Hampson, and D. Larkin, *J. Electroanal. Chem.* **20** (1964) 335.
[624]A. Marshall and N.A. Hampson, *J. Electroanal. Chem.* **53** (1974) 133.
[625]V. V. Batrakov and A. I. Sidnin, *Elektrokhimiya* **8** (1972) 122.
[626]B. Krasikov and V. Sisoeva, *Dokl. Akad. Nauk SSSR* **114** (1957) 826.
[627]Tza Chuan-Sin and Z. Iofa, *Dokl. Akad. Nauk SSSR* **131** (1960) 137.
[628]A. I. Danilov, V. Batrakov, and V. A. Safonov, *Elektrokhimiya* **16** (1980) 100.
[629]A. N. Frumkin, V. V Batrakov, and A. I. Sidnin, *J. Electroanal. Chem.* **39** (1972) 225.
[630]V. V. Batrakov, B. B. Damaskin, and Yu.P. Ipatov, *Elektrokhimiya* **10** (1974) 144.
[631]V. V Batrakov and A. I. Sidnin, *Elektrokhimiya* **8** (1972) 743.
[632]V. V. Batrakov, A. N. Frumkin, and A.I. Sidnin, *Elektrokhimiya* **10** (1974) 216.
[633]V. V. Batrakov and A. I. Sidnin, *Elektrokhimiya* **10** (1974) 1757.
[634]Yu. P. Ipatov and V. V. Batrakov, *Elektrokhimiya* **11** (1975) 1717.
[635]Yu. P. Ipatov and V. V. Batrakov, *Elektrokhimiya* **16** (1980) 624.
[636]Yu. P. Ipatov and V. V. Batrakov, *Elektrokhimiya* **16** (1980) 630.
[637]V. Ya. Bartenev, E. S. Sevastyanov, and D. I. Leikis, *Elektrokhimiya* **5** (1969) 1491.
[638]V. Ya. Bartenev, E .S. Sevastyanov, and D. I. Leikis, *Elektrokhimiya* **5** (1969) 1502.
[639]D. I. Leikis, V. A. Panin, and K. V. Rybalka. *J. Electroanal. Chem.* **40** (1972) 9.
[640]N. A. Hampson and R. Latham, *J. Electroanal. Chem.* **34** (1972) 247.
[641]V. A. Panin, D. I. Leikis, and L. A. L'vova, *Elektrokhimiya* **8** (1972) 280.
[642]G. V. Pankina, D. I. Leikis, and E. S. Sevastyanov, *Elektrokhimiya* **16** (1980) 213.
[643]V. Ya. Bartenev, E. S. Sevastyanov, and D. I. Leikis, *Eleklrokhimiya* **4** (1968) 745.
[644]A. V Shlepakov and E. S. Sevastyanov, *Elektrokhimiya* **14** (1978) 287.
[645]V. B. Obrastsov, Yu. A. Partenov, and F. I. Danilov, *Elektrokhimiya* **27** (1991) 980.

[646]V. B. Obrastsov, Yu. A. Partenov, and F. I. Danilov, *Elektrokhimiya* **29** (1993) 699.
[647]V. A. Panin, K. V. Rybalka, and D. I. Leikis, *Elektrokhimiya* **8** (1972) 310.
[648]K. V. Rybalka and V. A. Panin, *Elektrokhimiya* **9** (1973) 172.
[649]D. Leikis, V. Panin, and K. Rybalka, *J. Electroanal. Chem.* **40** (1972) 9.
[650] N. B. Grigoryev, in *Double Layer and Adsorption at Solid Electrodes. Proc. 4th Symp*., Tartu University, Press Tartu, Estonia, 1975, p. 79.
[651]E. S. Sevastyanov, V. K. Chubarova, and M. N. Ter-Akopyan, *Elektrokhimiya* **26** (1990) 586.
[652]J. P. G. Farr and N. A. Hampson, *Trans. Faraday Soc.* **62** (1966) 3494.
[653]D. I. Leikis and B. N. Kabanov, *Trans. Institut Fiz Khimii AN SSSR* **2** (1957) 5.
[654]G.O. Karbasov, K. T. Tikhonov, and P. M. Vyacbeslavov, *Elektrokhimiya* **16** (1980) 1273.
[655] K. I. Tikhonov, B. G. Karbasov, B. A. Ravdel, and A. L. Rotinyan, in *Double Layer and Adsorption at Solid Electrodes, Proc. 6th Symp.,* Tartu University Press, Tartu, Estonia, 1981, p. 330.
[656]G. I. Ikrannikova, V. A. Golovin, and G. A. Dobrenkov, *Elektrokhimiya* **22** (1986) 1683.
[657] V. A. Golovin, L.T. Guseva, and G.I. Ikrannikova, *Double Layer and Adsorption at Solid Electrodes,* Vol. VI, 1981, p. 83.
[658]W. H. Moulder and J. H. Sluyters, *Electrochim, Acta* **33** (1988) 313.
[659]I. A. Abdullin, V. A. Golovin, and N. V. Gudin, in *Double Layer and Adsorption at Solid Electrodes, Proc. 2nd Symp*., Tartu University Press, Tartu, Estonia 1970, p. 52.
[660]R. Naneva, T. Vitanov, N. Dimitrov, V. Bostanov, and A. Popov, *J. Electroanal. Chem.* **328** (1992)287.
[661]R. Naneva, N. Dimitrov, A. Popov, T. Vitanov, and V. Bostanov, *J. Electroanal. Chem.* **362** (1993)281.
[662]A. Popov, N. Dimitrov, R. Naneva, and T. Vitanov, *J. Electroanal. Chem.* **376** (1994) 97.
[663]B. B. Damaskin, *J. Electroanal. Chem.* **75** (1977) 359.
[664]E. Lust and J. Ehrlich, in *Double Layer and Adsorption at Solid Electrodes, Proc. 9th Symp*., Tartu University Press, Tartu, Estonia, 1991, p. 112.
[665]E. Lust, A. Jänes, K. Lust, and M. Salve, *Trans. Tartu Univ.* **966** (1993) 63.
[666]U. V. Palm, V. E. Past, and R. J. Pullerits, *Elektrokhimiya* **2** (1966) 604.
[667]U. Palm, V. Past, and R. Pullerits, *Trans. Tartu Univ.* **219** (1968) 63.
[668]K. Palts, U. Palm, V. Past, and R. Pullerits, *Trans. Tartu Univ.* **235** (1969) 57.
[669]K. Palts, U. Palm, V. Past, and R. Pullerits, *Trans. Tartu Univ.* **235** (1969) 64.
[670]M. Salve and U. Palm, *Trans. Tartu Univ.* **322** (1974) 71.
[671]U. Palm and V. Past, *Usp. Khim.* **44** (1975) 2035.
[672]B. B. Damaskin, U. V. Palm, and M. A. Salve, *Elektrokhimiya* **12** (1976) 232.
[673]B. B. Damaskin and A. N. Frumkin. *Electrochim. Acta* **19** (1974) 173.
[674]A. S. Bluvstein, N. V. Syrchina, G. N. Marsurov, A. Z. Zaindenberg, A. M. Brodsky, A. M. Skundin, and O. A. Petrii, *J. Electmanal. Chem.* **260** (1989) 25.
[675]V. Ya. Mishuk, M. A. Amatunov, and V. V. Elkin, *Elektrokhimiya* **30** (1994) 1176.
[676]V. Ya. Mishuk, V. V. Elkin, and D. I. Leikis, *Elektrokhimiya* **16** (1980) 945.
[677]E. Petyarv, K. Kolk, and U. Palm, *Trans. Tartu Univ.* **289** (1971) 22.
[678]E. Petyarv, K. Kolk, and U. Palm, *Elektrokhimiya* **8** (1972) 100.
[679]E. Petyarv and U. Palm, *Elektrokhimiya* **9** (1973) 1836.
[680]E. Petyarv and U. Palm, *Elektrokhimiya* **12** (1976) 806.
[681]E. Petyarv, R. Jaanisoo. and U. Palm, *Trans. Tartu Univ.* **378** (1976) 44.
[682]E. J. Lust, *Elektrokhimiya* **27** (1991) 424.
[683]U. Palm, M. Väärtnõu, and E. Petjärv, *Elektrokhimiya* **11** (1975) 1849.
[684]M. Väärtnõu, E. Petjärv, and U. Palm, *Trans. Tartu Univ.* **378** (1976) 36.
[685]M. Väärtnõu and U. Palm, *Elektrokhimiya* **13** (1977) 1211.
[686]U. Palm, M. Väärtnõu, and M. Salve, *J. Electroanal. Chem.* **86** (1978) 35.
[687]M. Väärtnõu and U. Palm, *Elektrokhimiya* **15** (1979) 1568.

[688]M. Väärtnõu and U. Palm, *Elektrokhimiya* **15** (1979) 1719.
[689]M. Väärtnõu and U. Palm, *Elektrokhimiya* **16** (1980) 179.
[690]M. Väärtnõu and U. Palm, *Elektrokhimiya* **16** (1980) 183.
[691]M. Väärtnõu and U. Palm, *Elektrokhimiya* **14** (1978) 311.
[692]M. Väärtnõu and U. Palm, *Elektrokhimiya* **16** (1980) 1877.
[693]M. Väärtnõu and U. Palm, *Elektrokhimiya* **15** (1979) 591.
[694]M. Väärtnõu and U. Palm, in *Double Layer and Adsorption at Solid Electrodes Proc. 6th Symp*., Tartu University Press, Tartu, Estonia, 1981, p. 66.
[695]U. V. Palm, M. G. Väärtnõu, and M. A. Salve, *Elektrokhimiya* **19** (1983) 310.
[696]M. G. Väärtnõu and U. V Palm, Elektrokhimiya **24** (1988) 553.
[697]V. A. Chagelishvili, M. Väärtnõu, U. V. Palm, and Dzh.I. Dzhaparidze, *Elektrokhimiya* **14** (1978) 890.
[698]D. C. Grahame and B. A. Soderberg, *J. Chem. Phys.* **22** (1954) 22.
[699]J. M. Party and R. Parsons, Tram. *Faraday Soc.* **59** (1963) 241.
[700]R. V. Ivanova, B. B. Damaskin, and L. F. Maiorova, *Elektrokhimiya* **6** (1970) 382.
[701]B. B. Damaskin, U. V. Palm, R. V. Ivanova, and M. A. Salve, *Elektrokhimiya* **21** (1985) 1262.
[702]B. Damaskin, I. Pankratova, U. Palm, K. Anni, and M. Väärtnõu, *J. Electroanal. Chem.* **234** (1987)31.
[703]J. I. Japaridze and V. A. Chagelishvili, *Elektrokhimiya* **8** (1972) 1837.
[704]A. N. Frumkin, M. P. Pärnoja, N. B. Grigoryev, and U. V. Palm, *Elektrokhimiya* **10** (1974) 1130.
[705]U. V. Palm, M. P. Pärnoja, and M. A. Salve, *Elektrokhimiya* **13** (1977) 873.
[706]W. B. Pearson, *The Crystal Chemistry and Physics of Metals and Alloys*, Wiley-Interscience, New York, 1972, p. 280.
[707]P. M. Platzman and P. A. Wolf, *Waves and Interactions in Solid State Plasmas. Solid State Physics,* Suppl. 13, Academic Press, New York, 1973.
[708]V. S. Edelman, *Usp. Fiz. Nauk* **129** (1972) 257.
[709]T. A. Raud, T. H. Silk, and U. V. Palm, *Eletrokhimiya* **24** (1988) 344.
[710]U. Palm, T. Silk, and T. Raud, *Chemistry and Physics of Electrified Interfaces Solid/Electrolyte and Biological Systems. Ext. Abstr. Int. Conf.,* 1988, p. 103.
[711]T. A. Raud, M. M. Lepik, T. H. Silk, and U. V. Palm, in *Double Layer and Adsorption at Solid Electrodes, Proc. 8th Symp*., Tartu University Press, Tartu, Estonia, 1988, p. 334.
[712]K. L. Anni, M. G. Väärtnõu, and U. V. Palm, *Elektrokhimiya* **24** (1988) 846.
[713]K. L. Anni, M. G. Väärtnõu, and U. V. Palm, *Elektrokhimiya* **22** (1986) 992.
[714]E. Lust and K.Anni, in *Double Layer and Adsorption at Solid Electrodes, Proc. 9th Symp*, Tartu University Press, Tartu, Estonia, 1991, p. 109.
[715]P. Pärsimägi, K. Anni, M. Väärtnõu, and E. Lust, in *Double Layer and Adsorption at Solid Electrodes, Proc. 9th Symp.,* Tartu University Press, Tartu, Estonia, 1991, p. 144.
[716]M. Väärtnõu, P. Pärsimägi, and E. Lust, *J. Electroanal. Chem.* **385** (1995) 115.
[717]M. Väärtnõu P. Pärsimagi, and E Lust, *J. Electroanal. Chem.* **407** (1996) 227.
[718]V. Past, U. Palm, K. Palts, R. Pullerits, and M. Haga, in *Double Layer and Adsorption at Solid Electrodes, Proc 1st Symp.,* Vol. I, Tartu University Press, Tartu, Estonia, 1968, p. 114.
[719]M. Haga and V. Past, *Elektrokhimiya* **5** (1969) 618.
[720]M. Haga and V. Past, *Trans. Tartu Univ.* **235** (1969) 47.
[721]R. Pullerits, M. Moldau, and V. Past, *in Double Layer and Adsorption at Solid Electrodes, Proc. 4th Symp.,* Tartu University Press, Tartu, Estonia, 1975, p. 257.
[722]R. Pullerits, M. Moldau and V. Past, in *Double Layer and Adsorption at Solid Electrodes, Proc. 5th Symp.,* Tartu University Press, Tartu, Estonia, 1978, p. 20.
[723]R. Pullerits, M. Moldau, and V. Past, in *Double Layer and Adsorption at Solid Electrodes, Proc. 6th Symp.,* Tartu University Press, Tartu, Estonia, 1981, p. 293.

[724]V. Past, R. Pullerits, and M. Moldau, *Trans. Tartu Univ.* **755** (1986) 140.
[725]E. J. Lust and A. A.-J. Jänes, *Elektrokhimiya* **28** (1992) 802.
[726]E.J. Lust and A. A.-J. Jänes, *Elektrokhimiya* **30** (1994) 357.
[727]L. E. Rybalka and D. I. Leikis, *Elektrokhimiya* **11** (1975) 1619.
[728]L. E. Rybalka, D. I. Leikis, and A. G. Zelinskii, *Elektrokhimiya* **12** (1976) 1340.
[729]V. A. Safonov, L. Yu. Komissarov, and O. A. Petrii, *Electrochim. Acta* **42** (1997) 675.
[730]E. M. Lazarova, *Elektrokhimiya* **14** (1978) 1300.
[731]M. Turowska and J. Sokolowski, *Elektrokhimiya* **30** (1994) 821.
[732]V. A. Safonov, L. Yu. Komissarov, and O. A. Petrii, *Zash. Met.* **22** (1986) 292.
[733]L. Yu. Komissarov, V. A. Safonov, and O. A. Petrii, *Vesti MGU. Khimiya,* Moscow, 1986, p. 21.
[734]V. A. Safonov, B. B. Damaskin, L. Yu. Komissarov, and O. A. Petrii, in *Double Layer and Adsorption at Solid Electrodes, Proc 7th Symp*., Tartu University Press, Tartu, Estonia, 1985, p. 292.
[735]V. A. Safonov, *IV Japan-USSR Corrosion Seminar. Extended Abstracts,* Tokyo, JSCE, 1985, p. 126.
[736]V. A. Safonov, L. Yu. Komissarov, O. A. Petrii, and V. M. Gravovoch, *Elektrokhimiya* **23** (1987) 1375.
[737]E. I. Mikhailova and Z. A. Joffa, *Elektrokhimiya* **6** (1970) 231.
[738]V. A. Safonov, K. Jackovska and O. A. Petrii, *Elektrokhimiya* **11** (1975) 1628.
[739]V. V. Batrakov and N. I. Naumova, *Elektrokhimiya* **13** (1979) 551.
[740]V. L. Kheifets and L. S. Reishakhrit, *Uch Zap. Leningr. Gas. Univ. 169, Ser. Khim. Nauk* **13** (1953) 173.
[741]T. Ohmori, *J. Electroanal. Chem.* **157** (1983) 159.
[742]Yu. M. Tyurin, T. V. Sazonntyeva, and V. I. Naumiva, *Elektrokhimiya* **30** (1994) 1320.
[743]J. Arold and J. Tamm, *Elektrokhimiya* **25** (1989) 1417.
[744]H. Yang and J. L. Whitten, *Surf. Sci.* **223** (1989) 131.
[745]M. Grodzicki and O. Kühnholz, *Mol. Struct.* **174** (1988) 65.
[746]Yu. F. Zhukovski, E. P. Smimov, and A. K. Lokenbakh, *Zh Fiz. Khim.* **64** (1990) 1825.
[747]B. Jakuszewski and Z. Kozlowski, *Rocz. Chem.* **38** (1964) 93.
[748]B. Jakuszewski and Z. Kozlowski, *Soc. Sci. Lodz Acta Chim.* **10** (1965) 5.
[749]V. A. Safonov, S. A. Sokolov, and V. M. Gerowich, *Dokl. Akad. Nauk SSSR,* **299** (1988) 1438.
[750]V. A. Safonov and S. A. Sokolov, in *Double Layer and Adsorption at Solid Electrodes, Proc. 8th Symp*., Tartu University Press, Tartu, Estonia, 1988, p. 253.
[751]V. A. Safonov and S. A. Sokolov, *Elektrokhimiya* **27** (1991) 1317.
[752]B. I. Podlovchenko and N. A. Epshtein, *Elektrokhimiya* **8** (1972) 1522.
[753]K. Al Jaaf-Golze, D. M. Kolb, and D. Scherson, *J. Electroanal. Chem.* **200** (1986) 353.
[754]J. Clavilier, K. El Achi, and A. Rodes, *J. Chem. Phys.* **141** (1990) 1.
[755]A. Rodes and J. Clavilier, *J. Electroanal. Chem.* **344** (1993) 269.
[756]J. Clavilier and A. Rodes, *J. Electroanal. Chem.* **348** (1993) 247.
[757]S. Thomas, Y.-E. Sung, H. S. Kirn, and A. Wieckowski, *J. Phys. Chem.* **100** (1986) 11726.
[758]V. L. Heifets and B. S. Krasikov, *Zh. Fiz Khim.* **31** (1957) 1992.
[759]A. N. Frumkin, N. Balashova, and V. Kazarinov, *J. Electroanal. Chem.* **113** (1966) 1011.
[760]E. Gileadi, S. Argade, and J. O'M. Bockris, *J. Phys. Chem.* **70** (1966) 2044.
[761]M. Rosen, O. Flinn, and S. Schuldiner, *J. Electroanal. Chem.* **116** (1969) 1112.
[762]D. Flinn, M. Rosen, and S. Schuldiner, *Coll. Czech. Chem. Comm.* **36** (1971) 454.
[763]O. A. Petrii and A. V. Ushmaev, *Elektrokhimiya* **17** (1981) 1154.
[764]B. I. Podlovchenko and E. A. Kolyadko, *Elektrokhimiya* **24** (1988) 1138.
[765]B. I. Podlovchenko, E. A. Kolyadko, and V. I. Naumov, *J. Electroanal. Chem.* **309** (1991) 49.
[766]E. A. Kolyadko, V. 1. Naumov, and B. I. Podlovchenko, *Elektrokhimiya* **27** (1991) 409.

[767]E. M. Lazarova, *Elektrokhimiya* **18** (1982) 1654.
[768]F. T. Wagner and P. N. Ross, *J. Electroanal. Chem.* **250** (1988) 301.
[769]K. Itaya, S. Sugawara, K. Sashikaat, and I. Furneya, *J. Vac. Sci. Technol.* **48** (1990) 515.
[770] A.Rodes, E. Pastor, and T. Iwasita, *J. Electroanal. Chem.* **376** (1994) 109.
[771]T. Iwasita, A. Rodes, and E. Pastor, *J. Electroanal. Chem.* **383** (1995) 181.
[772]J. M. Orts, R. Gómez, J. M. Feliu, A. Aldaz, and J. Clavilier, *Electrochim. Acta* **39** (1994) 1519.
[773]J. Clavilier, D. Armand, S. G. Sun, and M. Petit, *J. Electroanal. Chem.* **205** (1986) 267.
[774]B. A. Sexton, *Surf. Sci.* **94** (1980) 435.
[775]H. Ogasanea, J. Yoshinubu, and M. Kaway, *Chem. Phys. Lett.* **231** (1994) 188.
[776]M. F. Toney, J. N. Howard, J. Richer, G. L. Borges, J. G. Gordon, O. R. Melroy, D. G. Wiesler, D. Yee, and L. B. Soerensen, *Nature* **368** (1994) 188.
[777]J. G. Gordon, O. R. Melroy, and M. F. Toney, *Electrochim. Acta* **40** (1995) 3.
[778]T. Solomun, *J. Electroanal. Chem.* **255** (1988) 163.
[779]J. Clavilier, *J. Electroanal. Chem.* **107** (1980) 211.
[780]J.Clavilier, A. Rodes, K. El Achi, and M. A. Zamakhchari, J. Chem. *Phys.* **88**(1991) 1291.
[781]W. Ranke, *Surf. Sci* **209** (1994) 1555.
[782]M. Kiskinova, G. Pirug, and H. P. Bonzel, *Surf. Sci.* **150** (1985) 319.
[783]G.B. Fisher and J. L. Gland, *Surf Sci.* **94** (1980) 446.
[784]J. M. Feliu, J. M. Orts, R. Gómez, A. Aldaz, and J. Clavilier, *J. Electroanal. Chem.* **372** (1994)265.
[785]H. Ebert, R. Parsons, G. Ritzoulis, and T. Vandemoot, *J. Electroanal. Chem.* **264** (1989) 181.
[786]A. Ahmadi, E. Bracey, R. W. Evans, and G. Attard, *J. Electroanal. Chem.* **350** (1993) 297.
[787]G. Attard, R. Price, and Al Al-Akl, *Electrochim. Acta* **39** (1994) 1525.
[788]N. M. Markovic, S. T. Sarraf, H. A. Gasteiger, and P. N. Ross, *J. Chem. Soc. Faraday Trans.* **92** (1996) 3719.
[789]J. Sobkowski, A. Wieckowski, P. Zelanay, and A. Czerwinski, *J. Electroanal. Chem.* **100** (1979) 781.
[790]N. Hoshi, H. Ito, T. Suzuki, and Y. Hori, *J. Electroanal. Chem.* **395** (1995) 309.
[791]N. Hoshi, T. Mizumuka, and Y. Hori. *Electrochim. Acta* **40** (1995) 883.
[792]N. Hoshi, T. Uchida, T. Mizumuka, and Y. Hori, *J. Electroanal. Chem.* **381** (1995) 261.
[793]A. Bewick, C. Gutiérrez, and G. Larramona, *J. Electroanal. Chem.* **332** (1992) 155.
[794]E. Herrero, J. M. Feliu, A. Wieckowski, and *J.* Clavilier, *Surf. Sci.* **325** (1995) 131.
[795]V. Climent, R. Gómez, J. M. Orts, A. Aldaz, and J. M. Feliu, in *Electrochemical Double Layer,* B. E. Conway and C. Korzeniewski, eds., Vol. 97-17, Electrochemical Society, Pennington, NJ, 1997, p. 222.
[796]R. Gómez, J. M. Orts, and J. M. Feliu, in Solid/*Liquid Electrochemical Interfaces,* G. Jerkiewicz, M. P. Soriaga, K. Uosaki, and A. Wieckowski, eds., American Chemical Society, Washington, DC, 1997, p. 156.
[797]O. A. Petrii and I. G. Khomchenko, *J. Electroanal Chem.* **106** (1980) 277.
[798]F. Magno and G. Bontempelli, *J. Electroanal. Chem.* **39** (1972) 489.
[799]B. E. Conway, H. Angerstein-Kozlowska, and B. R. MacDougall, *J. Electroanal. Chem.* **39**(1972)287.
[800]S. Morin and B. E. Conway, *J. Electroanal. Chem.* **376** (1994) 135.
[801]N. S. Marincovic, M. Hecht, T. S. Loring, and W. R. Fawcett, *Electrochim. Acta* **41** (1996) 641
[802]O. A. Petrii, I. G. Khomchenko, and A. G. Zelinsky, *Elektrokhimiya* **15** (1979) 400.
[803]I. G. Khomchenko and O. A. Petrii, *Elektrokhimiya* **19** (1983) 1544.
[804]C. Bernard, C. Tarby, and G. Robert, *Electrochim. Acta* **25** (1980) 435.
[805] T. P. Agladze, *Itogi nauki i tekhniki. Korroziya i zashchita ot korrozii.* Vol. 9, Moscow, VINITI, 1982, pp. 36–47.

[806]E. Yu. Alakseyeva, V. A. Safonov, and O. A. Petrii, *Elektrokhimiya* **20** (1984) 945.
[807]Yu. A. Kukk and J. Clavilier. *Elektrokhimiya* **13** (1977) 841.
[808] Yu. A. Kukk and T. H. Püttsepp, in *Double Layer and Adsorption at Solid Electrodes, Proc. 5th Symp*., Tartu University Press, Tartu, Estonia, 1978, p. 124.
[809]L. P. Khmelevaya, B. B. Damaskin, and T. I. Vainblat, *Elektrokhimiya* **18** (1982) 1141.
[810]R. P. Frankenthal and D. J. Siconolfi, *Surf. Sci.* **119** (1982) 331.
[811]S. C. Fain Jr. and J. M. McDavid, *Phys, Rev. B* **9** (1974) 5099.
[812]R. Bouwman, L. H. Toneman, M. A. Boersma, and R. A. van Santen, *Surf. Sci.* **38** (1976) 318.
[813]S. H. Orenbury and G. A. Somorjai, *Surf. Sci.* **55** (1976) 909.
[814]G. C. Nelson, *J. Colloid Interface Sci.* **55** (1976) 289.
[815]A. Bewick and J. Robinson, *J. Electroanal. Chem.* **60** (1975) 383.
[816]V. A. Korolkov, Yu. I. Malov, and A. A. Markov, *Fizicheskaya khimiya granits razdela kontaktiruyushchih faz,* Naukova Dumka, Kiev, 1976, p. 128.
[817]J. W. Taylor, *Acta Metall.* **4** (1965) 460.
[818]N. L. Pokrovski and H. I. Iebragimov, *Physical Chemistry of the Alloys Surfaces,* Metshniereba, Tbilisi, Georgia, 1977, p. 30.
[819]T. B. Massalski, ed., *Binary Alloy Phase Diagrams,* Vol. 1, 1985, p. 682; Vol. 2, 1985, p. 1848, American Soc. Metals, Metals Park, Ohio.
[820]V. A. Safonov, M. A. Choba, L. G. Toshchevikov, and D. V. Kireev, *Elektrokhimiya* **27** (1991) 1323.
[821]V. A. Safonov and M. A. Choba, *Elektrokhimiya* **29** (1993) 1131.
[822]V. A. Safonov, M. A. Choba, and Ya. D. Seropegin, *Electrochim. Acta* **42** (1997) 2907.
[823]G. A. Zelinski and R. Yu. Beck, *Elektrokhimiya* **21** (1985) 66.
[824]V. A. Safonov, M. A. Choba, and Yu. D. Seropegin, *Surf. Sci.* **119** (1982) 331.
[825]M. I. Shuganova, G. V. Birjukova, and V. A. Kuznetsov, in *Double Layer and Adsorption at Solid Electrodes, Proc. 6th Symp*., Tartu University Press, Tartu, Estonia, 1975, p. 334.
[826]M. I. Shuganova, R. A. Alekseyeva, and V. A. Kuznetsov, *Elektrokhimiya* **16** (1980) 924.
[827]P. A. Morozova, E. V. Pekar, E. S. Sevastyanov, and V. K. Chubarova, *Elektrokhimiya* **27** (1991) 1307.
[828]E. M. Lazarova and Ts. Nikolov, *Elektrokhimiya* **16** (1980) 1231.
[829]E. M. Lazarova and R. G. Raichev, *Elektrokhimiya* **16** (1980) 191.
[830]I. G. Kiseleva, D. I. Leikis, and B. N. Kabanov, *Elektrokhimiya* **8** (1972) 250.
[831]Yu. I. Malov, A. A. Markov, and V. A. Korolkov, *Elektrokhimiya* **12** (1976) 1740.
[832]L. Koene, M. Sluyters-Rehbach, and J. H. Sluyters, *Elektrokhimiya* **31** (1995) 802.
[833]G. Luggin, Z. *Phys. Chem.* **16** (1985) 677.
[834]G. V. Hevesy and R. Lorenz, Z. *Phys. Chem.* **74** (1910) 443.
[835]S. V. Korpatshoff and A. G. Stromberg, *Zh. FIZ, Khim.* **18** (1944) 47.
[836]V. A. Kuznetsov, L. C. Zagaynova, A. A. Dyakova, and A. A. Kotegova, *Elektrokhimiya* **1** (1965) 676.
[837] M. V. Smirnov, *Elektrodnye potentsyaly v rasplavlennykh kloridakh,* Nauka, Moscow, 1973.
[838]V. B. Stepanov, *Interfacial Phenomena in Ionic Salt Melts.* Ekaterinburg Science, 1993 (in Russian).
[839]J. E. B. Randels and J. L. White, *Trans. Faraday Soc.* **51** (1995) 185.
[840]E. Ukshe and N. Bukun, *Itogi nauki i tekhnild. Rastvory* **2** (1975) 140.
[841] Yu. Delimansky, *Issledovaniya v oblasti elektrokhimii ionnykh rasplavov,* Naukova Dumka, Kiev, Ukraine, 1971.
[842]Yu. G. Pastukhov and V. P. Stepanov, *Dokl. Akad. Nauk. SSSR* **307** (1989) 648.
[843]O. Esin, *Zh. Fiz Khim.* **30** (1956) 3.
[844]R. Dogonadze and Yu. Chizmadjev, *Dokl. Akad. Nauk. SSSR* **157** (1964) 944.

[845]R. S. Perkins, R. Livingston, T. N. Andersen, and H. Eyring, *J. Phys. Chem.* **69** (1965) 3329.
[846]B. Jakuszewski and Z. Koczorowski, Roczn. Chem. **36** (1962) 1873.
[847]I. A. Bagotskaya, A. M. Morozov, and N. B. Grigoryev, *Electrochim. Acta* **13** (1968) 873.
[848]J.Clavilier, A. Hamelin, and G. Valette, *Compt. Rend. Ser. C* **265** (1967) 221.
[849]A. Hamelin and J. Lecoeur, *Coll. Czech. Chem. Commun.* **36** (1971) 714.
[850]Yu. P. Ipatov and V. V. Batrakov, *Elektrokhimiya* **12** (1976) 1174.
[851]D. I. Leikis and E. S. Sevast'yanov, *Dokl. Akad. Nauk SSSR* **144** (1962) 1320.
[852]N. B. Grigor'ev, S. A. Fateev, and I. A. Bagotskaya, *Elektrokhimiya* 7 (1971) 1852; 8 (1972)311.
[853]E. M. Lazarova and Yu. I. Kuyumdzhieva, *Elektrokhimiya* **15** (1979) 1204.
[854]G. Valette, *J. Electroanal. Chem.* **139** (1982) 285.
[855]I. A. Bagotskaya, V. G. Boitsov, and V. E. Kazarinov, *Elektrokhimiya* **25** (1989) 111.
[856]D. R. Lide, ed., *Handbook of Chemistry and Physics,* 76th ed. CRC Press, Boca Raton, FL, 1995.
[857] H. B. Michaelson, *J. Appl. Phys.* **48** (1977) 4729.
[858]S. Trasatti, *J. Electroanal. Chem.* **54** (1974) 19.
[859]I. A. Bagotskaya, C, N. Hai, V. G. Boitsov, and V. E. Kazarinov, *Elektrokhimiya* **24** (1988) 265.
[860]L. Pauling, *Phys. Rev.* **54** (1938) 899; *J. Am. Chem. Soc.* **69** (1947) 542; *Proc. Roy. Soc. Lond. Ser. A* **A196** (1949) 343.
[861]L. Koene, M. Sluyters-Rehbach, and J. H. Sluyters, *J. Electroanal. Chem.* **398** (1995) 569.
[862]V. P. Grigor'ev, O. N. Necheva, and V. E. Goielik, *Elektrokhimiya* **27** (1991) 1418.
[863]G. Valette, *J. Electroanal. Chem.* **255** (1988) 225.
[864]E. Lust, *Elektrokhimiya* **27** (1991) 104.
[865]B. E. Nieuwenhuys, *Thin Solid Films* **50**(8) (1978) 257.
[866]R. Vanselow and X. Q. D. Li, *Sur. Sci. Lett.* **264** (1992) L200.
[867]G. N. Derry and Z. Ji-Zhong, *Phys. Rev. B* **39** (1989) 1940.
[868]J. K. Sass, N. V. Richardson, H. Neff, and D. K. Roe, *Chem. Phys. Lett.* **73** (1980) 209.
[869]S. Trasatti, *J. Electroanal. Chem.* **54** (1974) 437.
[870]N. S. Razutikhina and A. N. Efremova, *Elektrokhimiya* **19** (1983) 1439.
[871]S. Trasatti, *J. Chim. Phys.* **72** (1975) 561.
[872]A. Spitzer and H. Lüth, *Surf. Sci.* **160**(1985) 353.
[873]A. Spitzer, A. Ritz, and H. Lütz, *Surf. Sci.* **152/153** (1985) 543.
[874]A. F. Carley, P. R. Davies, M. W. Roberts, and K. K. Thomas, *Surf. Sci. Lett.* **238** (1990) L467.
[875]B. W. Callen, K. Griffiths, U. Memmert, D. A. Harrington, S. J. Bushby, and P. R. Norton, *Surf. Sci.* **230** (1990) 159.
[876]M. I. Rojas and E. P. M. Leiva, *Surf. Sci. Lett.* **227** (1990) L121.
[877]J. R. Grigeva and S. G. Kalko, *Langmuir,* **12** (1996) 154.
[878]I. I. Vaisman, F. K. Brown, and A. Tropsha, *J. Phys. Chem.* **98** (1994) 5559.
[879]W. Drost-Hansen, *Ind. Eng. Chem.* **61** (1969) 10.
[880]K. Heinzinger, *Pure Appl. Chem.* **63** (1991) 1733.
[881]E. Spohr. *J. Phys. Chem.* **93** (1989) 6171.
[882]K. Raghavan. K. Foster, and M. Berkowitz, *Chem. Phys. Lett.* **177** (1991) 426.
[883]K. J. Scweighofer, X. Xia, and M. L Berkowitz, *Langmuir*, **12** (1996) 3747.
[884]G. Estiù. S. A. Maluendes, E. A. Castro, and A. J. Arvia, *J. Phys. Chem.* **92** (1988) 2512.
[885]G. Estiù, S. A. Maluendes, E. A. Castro, and A. J. Arvia, *J. Electroanal. Chem.* **284** (1990) 289.
[886]G. Aloisi, R. Guidelli, R. A. Jakson, S. M. Clark, and P. Barnes, *J. Electroanal. Chem.* **206**(1986)131.
[887]A. E. Russell, A. S. Lin, and W. E. O'Grady, *J. Chem. Soc. Faraday Trans.* **89** (1993) 195.

[888]G. Aloisi and R. Guidelli, *J. Electroanal. Chem.* **260** (1989) 259.
[889]R. R. Nazmutdinov, *Elektrokhimiya* **29** (1993) 384.
[890]R. R. Nazmutdinov, M. Probst, and K. Heinzinger, *J. Electroanal. Chem.* **369** (1994) 227.
[891]R. R. Nazmutdinov, M.S. Shapnik, and O. I. Malyucheva, *Elektrokhimiya* **27** (1991) 1275.
[892]I. A. Bagotskaya and A. V. Shlepakov, *Elektrokhimiya* **16** (1980) 565.
[893]B. N. Afanas'ev and Yu. P. Akulova, *Elektrokhimiya* **30** (1994) 1357.
[894]V. E. Kazarinov and I. A. Bagotskaya, *Elektrokhimiya* **32** (1996) 1221.
[895]I. G. Khomchenko and O. A. Petrii, *Elektrokhimiya* **19** (1983) 1122.
[896]S. Trasatti. Z. *Phys. Chem. N. F.* **98** (1975) 75.
[897]S. Trasatti, *J. Electroanal. Chem.* **138** (1982) 449.
[898]J. S. Jaworski, *Electrochim. Acta* **34** (1989) 485.
[899]V. V. Emets, B. B. Damaskin, and V. E. Kazarinov, *Elektrokhimiya* **32** (1996) 1424.
[900]V. E. Kazarinov and I. A. Bagotskaya, *Elektrokhimiya* **33** (1997) 327.
[901]S. Trasatti, *J. Electroanal. Chem.* **91** (1978) 293.
[902]G. C. Bond, *Gold Bull.* **5** (1971) 115.
[903]G. C. Bond and P. A. Sermon, *Gold Bull.* ***6*** (1973) 102.
[904]G. C. Bond, P. A. Sermon, G. Webb, D. A. Buchanan, and P. B. Wells, *J. Chem. Soc. Chem. Commun.* (1973) 444.
[905]N. B. Grigoryev, S. A. Fateev, and I. A. Bagotskaya, *Elektrokhimiya* **8** (1972) 1633.
[906]S. Trasatti. *J. Electroanal. Chem.* **53** (1974) 335.
[907]S. Trasatti, *J. Electroanal. Chem.* ***65*** (1975) 815.
[908]E. Lust, A. Jänes, K. Lust, and R. Pullerits, *J. Electroanal. Chem.* **431** (1997) 183.
[909]B. N. Afanasyev and Yu. P. Akulova, *Elektrokhimiya* **30** (1994) 1397.
[910]A. Paulo Ferreira, M. J. Sottomayor, and A. F. Silva, unpublished results (personal communication).
[911]T. Luczak, M. Beltowska-Brzezinska, and R. Holze, *Electrochim. Acta* **38** (1993) 717.
[912]M. R. Moncelli and R. Guidelli, *J. Electroanal. Chem.* **295** (1990) 239.
[913]U. W. Hamm, V. Lazarescu, and D. M. Kolb, *J. Chem. Soc. Faraday Trans.* **92** (1996) 3785.
[914]Th. Wandlowski, *J. Electroanal. Chem.* **395** (1995) 83.
[915]J. Lipkowski, L. Stolberg. D.-F. Yang. B. Pettinger, S. Mirwald, F. Henglein, and D. M. Kolb, *Electrochim. Acta* **39** (1994) 1045.
[916]G. Pezzatini, M. R. Moncelli, M. Innocenti, and R. Guidelli, *J. Electroanal. Chem.* **295** (1990) 275.